

Reducing Braking Distance by Control of Semi-Active Suspension

Reducing Braking Distance by Control of Semi-Active Suspension

Vom Fachbereich Maschinenbau der
Technischen Universität Darmstadt
zur Erlangung des Grades eines
Doktor-Ingenieurs (Dr.-Ing.)
genehmigte

Dissertation

vorgelegt von

Dipl.-Ing. Tobias Niemz
aus Frankfurt am Main

Erstreferent: Prof. Dr. rer. nat. Hermann Winner

Korreferent: Prof. Dr.-Ing. Horst Peter Wölfel

Tag der Einreichung: 31. Oktober 2006

Tag der mündlichen Prüfung: 19. Dezember 2006

Darmstadt, 2006

Vorwort

Die vorliegende Arbeit entstand während der Zeit meiner Anstellung als wissenschaftlicher Mitarbeiter am Fachgebiet Fahrzeugtechnik der Technischen Universität Darmstadt (FZD). Die Inhalte der Dissertation wurden in einem von mir geleiteten, auf drei Jahre angelegten Forschungsprojekt, welches von der ZF Sachs AG in Schweinfurt in Auftrag gegeben und mit ihr zusammen durchgeführt wurde, erarbeitet.

Dem Leiter von FZD, Prof. Dr. rer. nat. Hermann Winner – mein Doktorvater und der Referent dieser Arbeit –, danke ich sehr für die hervorragende Betreuung. Prof. Winner hat durch die ihm eigene Art der Entfaltung von Autorität – durch seine herausragenden intellektuellen Fähigkeiten mehr denn durch autoritäres Auftreten – viele Denkprozesse bei mir in Gang gesetzt, die mich in dem von mir bearbeiteten Projekt, bei der Dissertation, insbesondere aber persönlich viele Schritte vorangebracht haben. Hierfür und für sein Bestreben, die von ihm betreuten Doktoranden zu selbständig handelnden und unvoreingenommen denkenden Menschen zu erziehen, und für die in jeder Hinsicht von ihm gewährte Unterstützung möchte ich mich herzlich bedanken.

Der Gründer und vormalige Leiter von FZD, Prof. em. Dr.-Ing. Bert Breuer, ließ mich stets bereitwillig von seiner jahrzehntelangen Erfahrung im Bereich der Fahrzeugtechnik profitieren, indem er auch über den Besuch meiner Doktorandenseminare hinaus in Fachgesprächen meine Forschungsfortschritte kritisch mit mir diskutierte. Seine Hinweise, das große Ganze ob des Grübelns über einem speziellen Problem nicht aus den Augen zu verlieren, waren immer hilfreich. Hierfür möchte ich ihm herzlich danken und hoffe, daß Prof. Breuer noch vielen FZD-Assistentengenerationen beratend zur Seite stehen wird.

Herrn Prof. Dr.-Ing. Horst Peter Wölfel danke ich für die Übernahme des Korreferats meiner Arbeit. Schon während meiner Studienzeit beeindruckte und prägte mich seine kritische und stets klar strukturierte Denk- und Argumentationsweise. Durch ihn und seine Lehrveranstaltungen wurde mein Interesse an Problemen der Dynamik geweckt. Auch während des Entstehens dieser Arbeit erhielt ich von ihm wertvolle Anregungen, die zum Gelingen derselben beigetragen haben.

Der Alltag bei FZD ist geprägt durch das freundschaftliche Miteinander der Kollegen und durch die große Bereitschaft jedes Einzelnen, Verantwortung zu übernehmen und Dinge zu gestalten. Das gesamte Team einschließlich der Sekretärinnen und der Werkstattmitarbeiter zeichnet sich durch ein hohes Maß an Kollegialität und Hilfsbereitschaft aus. Allen FZD-Mitarbeitern möchte ich für die vielen schönen Erinnerungen und den moralischen Beistand in jeder Lebenssituation danken. Das Musizieren in der fast schon legendären FZD-Band wird mir lange in Erinnerung bleiben. Frau Dipl.-Wirtsch.-Ing. Gabriele Wolf und Herr Dipl.-Ing. Thomas Degenstein waren mir immer verlässliche Stützen, auch bei der Korrektur dieser Arbeit, wofür ich mich herzlich bedanke.

Der ZF Sachs AG danke ich dafür, das von mir bearbeitete Industrieprojekt finanziert und mir somit die Möglichkeit zur Arbeit an einem spannenden wissenschaftlichen Thema gegeben zu haben. Konkret möchte ich allen Mitarbeitern der ZF Sachs AG danken, die mir im Laufe der Bearbeitungszeit des Kooperationsprojektes bei der Lösung allerlei Probleme halfen und mir stets mit ausgesprochener Hilfsbereitschaft und Freundlichkeit zur Seite standen. Besonders erwähnen möchte ich Herrn Dipl.-Ing. Eberhard Hees, der stets mit großem Engagement und mit großer Verlässlichkeit für mich da war.

Den vielen von mir während meiner Zeit bei FZD betreuten Studierenden, sei es im Rahmen ihrer Studien-, Diplomarbeit oder Master Thesis oder durch die Anstellung als Hilfswissenschaftler, gebührt ebenfalls großer Dank. Ohne ihren unermüdlichen Einsatz und ihre zahlreichen guten Ideen und Vorschläge wäre das Projekt nicht durchführbar gewesen und die vorliegende Dissertationsschrift hätte nicht entstehen können. Besonders danken möchte ich meinem guten, langjährigen Freund Dipl.-Ing. Raphael Stahl, der mich während einer längeren Abwesenheit vom Fachgebiet in jeder Hinsicht hervorragend vertrat.

Meiner Familie bin ich dankbar für die Gewißheit, in jeder Situation und zu jeder Zeit Beistand erhalten zu können. Dieser sichere Rückhalt ließ mich viele schwierige Situationen unbeschwerter angehen. Meinen Eltern danke ich im Speziellen dafür, mir eine hervorragende Ausbildung ermöglicht zu haben.

Tobias Niemz

Darmstadt, im Oktober 2006

Der Unterschied zwischen Theorie und Praxis
ist in der Praxis weit höher als in der Theorie.

The difference between theory and practice
is by far greater in practice than in theory.

Ernst Ferstl

Contents

List of Abbreviations	ix
List of Symbols and Indices	x
Abstract	xv
1 Introduction	1
1.1 Classification of Suspension Systems	1
1.2 State of the Art	3
1.3 Research Objectives	11
1.4 Methodology	12
2 Fundamentals of Vehicle Dynamics	14
2.1 Coordinate Systems	14
2.2 The Braking Process	16
2.2.1 The Quality of a Braking Process	23
2.2.2 Parameters that Influence the Braking Distance	24
2.3 Possibilities to Influence the Braking Force	26
2.3.1 Influence via Braking Torque—ABS	30
2.3.2 Influence via Wheel Load—Active Shock Absorbers	34
2.4 Conclusions	35
3 Tools and Research Environment	36
3.1 Active Shock-Absorbers	36
3.2 Testing Vehicle	38
3.2.1 Testing Vehicle Specifications	39
3.2.2 Testing Vehicle Measurement System	39
3.2.3 Measuring Rim	44
3.2.4 Indirect Measurands	45
3.3 4-Post Test Rig	52
3.4 Test Tracks	53
3.4.1 Test Track ‘Defined Obstacles’	53
3.4.2 Test Track ‘Standard Road’	55
3.5 Conclusions	59

4	Vertical Dynamics	60
4.1	Definitions	61
4.2	Possibilities to Influence Wheel Load	62
4.3	Quarter-Car Model and Simulation	64
4.4	Wheel Load-Controller—MiniMax-Controller	74
4.4.1	Artificial Characteristic Lines	76
4.4.2	Lowering and Lifting of the Vehicle’s Body	78
4.5	Test Drives on a Typical German Autobahn	81
4.6	Test Rig Experiments	86
4.6.1	Method	86
4.6.2	Results	91
4.6.3	Comparison of Simulation and Experiment	102
4.7	Conclusions	107
5	Longitudinal Dynamics	109
5.1	Definitions	109
5.2	Connecting Wheel Load and Braking Slip/Braking Force	114
5.2.1	Theoretical Approach	114
5.2.2	Test Drives to Validate the Connection Between Wheel Load and Braking Force/Braking Slip	117
5.3	Slip Controller	123
5.3.1	Demands on the Actuator in the Time Frame	126
5.3.2	Demands on the Actuator in the Magnitude Frame	127
5.4	Reducing the Braking Distance	127
5.4.1	Experimental Setting	128
5.4.2	Results for Uncontrolled Shock Absorbers	129
5.4.3	Results for Controlled Shock Absorbers	132
5.5	Conclusions	141
6	Discussion and Outlook	143
6.1	Results	143
6.2	Transferability of Results	144
6.3	Relevance of Results for Other Systems	145
6.4	Outlook	146
7	Summary	148
	Bibliography	150
	Student Research Work Advised	161
	Own Publications	164

List of Abbreviations

Abbreviation Description

ABC	Active Body Control
ABS	Antilock Braking System
BMC	Brake master cylinder
CDC	Continuous Damping Control
CG	Center of gravity
DIN	Deutsches Institut für Normung (German Standardization Bureau)
DP	Data processing
ECU	Electronic Control Unit
EDC	Electronic Damper Control
EPS	Electric Power Steering
ERM	Electro-Rheological Magnetic fluids
ESP	Electronic Stability Program
FZD	Fachgebiet Fahrzeugtechnik der Technischen Universität Darmstadt (Chair of Automotive Engineering at TU Darmstadt)
GCC	Global Chassis Control
IDS-plus	Interactive Driving System-plus
LMS	Least mean square
PC	Pitching center
PDC	Pneumatic Damping Control
PSD	Power spectral density
RMS	Root mean square
SAE	Society of Automotive Engineers
TEMS	Toyota Electronic Modulated Suspension
TSC	Traction Slip Control
TTC	Time to collision
VDI	Verein deutscher Ingenieure (Society of German Engineers)

List of Symbols and Indices

Symbol	Unit	Description
a	kg	Threshold that separates $F_{z,\text{req}} = -1$ from $F_{z,\text{req}} = +1$ for the slip controller
A_e	Ns	Effect Magnitude with respect to Delta Wheel Load
$A_{e,\text{tot}}$	Ns	Total Effect Magnitude with respect to Delta Wheel Load
$a_{B,i}$	m/s ²	Vertical body acceleration above the i -th wheel
$a_{W,i}$	m/s ²	Vertical acceleration of the i -th wheel
a_x	m/s ²	Longitudinal acceleration of the vehicle
$c_{B,i}$	N/m	Stiffness of the body spring at the i -th wheel
$c_{W,i}$	N/m	Stiffness of the tire spring at the i -th wheel
d_B	m	Braking distance, measured via the integral of longitudinal velocity from t_{BB} to t_{BE}
$d_{B,\text{corr}}$	m	Braking distance, corrected by the failure of initial velocity
$E_{e,\text{tot}}$	Ns	Total Effect Magnitude with respect to Delta Braking Force
F	N	Force
$F_{B,i}$	N	Braking force applied at the i -th wheel
$\Delta F_{B,i}$	N	Delta Braking Force applied at the i -th wheel
$F_{c_{B,i}}$	N	Force of the body spring at the i -th wheel due to its deflection
$F_{c_{W,i}}$	N	Force of the wheel spring at the i -th wheel due to its deflection
f_e	Hz	Excitation frequency of a seismic excitation
f_{e1}	Hz	First undamped eigenfrequency of the quarter-car model
f_{e2}	Hz	Second undamped eigenfrequency of the quarter-car model
FI^{bound}	Ns	Threshold for Delta Wheel Load Integral whose crossing determines the Effect Time t_e
FI_i	Ns	Integral of dynamic wheel load at the i -th wheel
ΔFI_i	Ns	Integral of Delta Wheel Load at the i -th wheel
$F_{k_{B,i}}$	N	Force of the body damper at the i -th wheel due to its velocity
$F_{k_{W,i}}$	N	Force of the wheel damper at the i -th wheel due to its velocity
f_s	Hz	Sampling rate
$F_{z,i}$	N	Wheel load at the i -th wheel
$\Delta F_{z,i}$	N	Delta Wheel Load at the i -th wheel
$\Delta F_{z,\text{bi}}$	N	Wheel load difference between non-braking and braking situations due to weight transfer
$F_{z,\text{bi},i}$	N	Body induced wheel load at the i -th wheel
$F_{z,\text{dyn},i}$	N	Dynamic wheel load at the i -th wheel
$F_{z,\text{dyn},B,i}$	N	The part of dynamic wheel load at the i -th wheel that leads to an acceleration of the body

$F_{z,\text{dyn},W,i}$	N	The part of dynamic wheel load at the i -th wheel that leads to an acceleration of the wheel
$F_{z,\text{req},i}$	-	Request of wheel load at the i -th wheel, either one or minus one
$F_{z,\text{stat},i}$	N	Static wheel load at the i -th wheel
g_{switch}	-	
$h(x)$	m	Longitudinal profile of a test track
$i_{p_{B,M_B,i}}$	Nm/bar	Factor to transfer braking pressure into braking torque at the i -th axle
j	-	Imaginary $j = \sqrt{-1}$
J	kg m ²	Mass moment of inertia
J_B	kg m ²	Mass moment of inertia of the vehicle's body with respect to the y-axis
$J_{W,i}$	kg m ²	Mass moment of inertia of the i -th wheel with respect to the y-axis
$k_{B,i}$	Ns/m	Damping coefficient of the body damper at the i -th wheel
$k_{W,i}$	Ns/m	Damping coefficient of the tire damper at the i -th wheel
l	m	Vehicle's wheel base, distance from front to rear axle
l_f	m	Longitudinal distance from front axle to the vehicle's center of gravity
l_r	m	Longitudinal distance from rear axle to the vehicle's center of gravity
m	kg	Mass
m_B	kg	Mass of the vehicle's body (overall mass minus the sum of all unsprung masses)
$M_{B,i}$	Nm	Braking torque applied at the i -th wheel
m_V	kg	Gross mass of the vehicle
$m_{W,i}$	kg	Mass of the i -th wheel
N	-	Number of a set of test drives of the same kind
$p_{\text{ABS},i}$	-	ABS action at the i -th wheel, value is either -1, 0, or +1, standing for decreasing, holding, and increasing the braking pressure at the i -th wheel
$p_{B,i}$	bar	Pressure at the i -th wheel braking cylinder
$\dot{p}_{B,\text{inc}}$	bar/s	Gradient with which braking pressure is increased by the ABS
$p_{B,\text{MC}}$	bar	Pressure at the main braking cylinder
$\dot{p}_{B,\text{rel}}$	bar/s	Gradient with which braking pressure is relieved by the ABS
$p_{T,i}$	bar	Tire inflation pressure of the i -th wheel
$r_{\text{eff},i}$	m	Effective radius of the i -th wheel
$s_{\text{hs},C,i}$./.	Ratio between linearized hard and soft damping factor for compression of the shock absorber at the i -th wheel
$s_{\text{hs},R,i}$./.	Ratio between linearized hard and soft damping factor for rebound of the shock absorber at the i -th wheel
$s_{p,i}$	m	Displacement of the 4-post test rig's post at the i -th wheel
$s_{\text{RC},i}$./.	Ratio between linearized damping factor for rebound and compression of the shock absorber at the i -th wheel
$s_{S,i}$	m	Displacement of the projected spring at the i -th wheel, equals $z_{B,i} - z_{W,i}$

List of Symbols and Indices

$\Delta s_{S,i}$	m	Delta Spring Displacement at the i -th wheel
$s_{S,i}^{\text{real}}$	m	Displacement of the actual spring at the i -th wheel,
s_x	m	Traveled distance in longitudinal direction, counted from the beginning of braking t_{BB}
t	s	Time
T_{B}	$^{\circ}\text{C}$	Temperature of the braking disc at the front left wheel
Δt_{B}	s	Duration of the braking process, equals $t_{\text{BE}} - t_{\text{BB}}$
t_{BB}	s	Time at which the braking process begins, defined via a threshold for the braking pressure at the front left wheel
t_{BE}	s	Time at which the braking process ends, defined via a threshold for the vehicle's longitudinal velocity
t_{BI}	s	Time at which the braking process is initiated, meaning the time at which the braking machine is triggered
t_{C}	s	Time at which the clutch is decoupled during a braking process, per definition at 1,000 revolutions
t_e	s	Effect Time, first time at which the integral of Delta Wheel Load crosses a threshold
$t_{e,\text{total}}$	s	Total Effect Time, first time after Effect Time at which Delta Wheel Load crosses zero
T_{P}	$^{\circ}\text{C}$	Temperature of the pavement
t_s	s	Switching time, time at which the shock absorber is switched from one to another constant setting
$T_{\text{T},i}$	$^{\circ}\text{C}$	Temperature of the i -th wheel's tire
$t_{90\%}$	s	Time that it takes for the spring displacement to establish 90 % of the total Delta Spring Displacement after switching the strategy from $F_{z,\text{req}} = +1$ to $F_{z,\text{req}} = -1$ or vice versa
U_{P}	m^2	Unevenness of a pavement, negative slope of the double-logarithmical plotted spectrum of the pavement over the wave number
$v_{\text{D},i}$	m/s	Velocity of the projected shock absorber at the i -th wheel, equals $\dot{z}_{\text{B},i} - \dot{z}_{\text{W},i}$
$v_{\text{D},i}^{\text{real}}$	m/s	Velocity of the actual shock absorber at the i -th wheel
$v_{\text{D},s,i}$	m/s	Velocity of the projected shock absorber at the i -th wheel at the time of switching the damper from hard to soft or vice versa
$v_{\text{diff},i}$	km/h	Longitudinal velocity of the vehicle minus longitudinal velocity of the i -th wheel, equals $\lambda_{\text{B},i} v_x$
VI	m^3/s^2	Integral of the square of the vehicle speed with respect to the traveled distance
$v_{\text{W},i}$	km/h	Longitudinal velocity of the i -th wheel, equals $\omega_{\text{W},i} r_{\text{eff},i}$
v_x	km/h	Longitudinal velocity of the vehicle
$v_{x,0}$	km/h	Initial longitudinal velocity of the vehicle
$v_{x,0}^{\text{des}}$	km/h	Desired initial longitudinal velocity of the vehicle
W	m^3	Unevenness of a pavement, negative slope of the PSD of the pavement over the wave number
$z_{\text{B},i}$	m	Vertical body displacement above the i -th wheel
$z_{\text{W},i}$	m	Vertical displacement of the i -th wheel

$z_{0,i}$	m	Seismic excitation at the i -th wheel
α	-	Weighting factor
α_s	-	Level of significance
β	-	Weighting factor
ε_f	rad	Brake supporting angle of the front axle
ε_r	rad	Brake supporting angle of the rear axle
$\varepsilon_f^{\text{opt}}$	rad	Optimal brake supporting angle of the front axle
$\varepsilon_r^{\text{opt}}$	rad	Optimal brake supporting angle of the rear axle
λ	1/(100 m)	Wave number, number of vertical waves on a pavement per 100 m in longitudinal direction
$\lambda_{B,i}$./.	Braking slip at the i -th wheel
$\Delta\lambda_{B,i}$./.	Delta Braking Slip at the i -th wheel
$\lambda_{B,\text{opt},i}$./.	Optimal braking slip at the i -th wheel, $\mu(\lambda_{B,\text{opt}}) = \mu_{\text{max}}$
ϑ_B	rad	Angular displacement of the vehicle's body around the global y-axis
$\varphi_{W,i}$	rad	Angular displacement of the i -th wheel around the wheel's y-axis
μ	./.	Braking coefficient, ratio between braking force and wheel load
μ_{max}	./.	Maximum braking coefficient
μ_{PD}	./.	Friction coefficient between braking pad and braking disc
$\rho_{x,y}$	-	Correlation coefficient between the two variables x and y
$\sigma(\bullet)$	like \bullet	Standard deviation of a quantity
$\Delta\tau_{F_z}$	s	Time delay between the real wheel load and the signal of the measuring rim
Ω	rad/s	Excitation frequency of a seismic excitation
$\omega_{W,i}$	rad/s	Angular velocity of the i -th wheel around the wheel's y-axis
[]		An interval that includes its boundaries
()		An interval that excludes its boundaries
{ }		A set
\bullet	like \bullet	Amplitude of a sinusoidal oscillating quantity, can be either real or complex
$\dot{\bullet}$	like \bullet/s	First derivative with respect to time
$\ddot{\bullet}$	like \bullet/s^2	Second derivative with respect to time
$\bar{\bullet}$	like \bullet	Mean value of a quantity
\bullet^*	like \bullet	A distinguished value for variable \bullet
\bullet^{eff}	like \bullet	RMS on a quantity with respect to time
bold		A vector or a matrix

Index	Description
B	Concerning a quantity of the vehicle's body
c	A quantity that takes its course in case of controlled damping
f	Concerning a quantity of the front axle
fl	Concerning the front left wheel
fr	Concerning the front right wheel
h	A quantity that takes its course in case of hard damping ($I_D = 0$ A)
m	A quantity that takes its course in case of medium damping ($I_D = 0.8$ A)
r	Concerning a quantity of the rear axle
rl	Concerning the rear left wheel
rr	Concerning the rear right wheel
s	A quantity that takes its course in case of soft damping ($I_D = 1.6$ A)
W	Concerning a quantity of one of the vehicle's wheels
w	A quantity that takes its course with switching the damper
w/o	A quantity that takes its course without switching the damper
x	A quantity that acts in x-direction
y	A quantity that acts in y-direction
z	A quantity that acts in z-direction

Abstract

This thesis presents a control algorithm for semi-active suspensions to reduce the braking distance of passenger cars. Active shock absorbers are controlled and used to influence the vertical dynamics during ABS-controlled full braking. In today's series cars the active shock absorbers are switched to a passive damping—usually hard damping—during ABS-braking. Several approaches to reduce oscillations of vertical dynamic tire forces are known, implemented and some of them tested in non-braking situations (refer to Yi¹, Valášek², and Nouillant³).

The approach presented in this paper goes a step further by connecting the vertical with the longitudinal dynamics. To influence the vertical dynamics a switching control logic, called MiniMax-controller, is used. It is named after the fact that it changes only from soft to hard damping and vice versa. A control quantity was identified that connects the vertical dynamics with the longitudinal dynamics: the integral of dynamic wheel load. The control algorithm is implemented in a compact class passenger car. Simulations with a quarter-car model have been undertaken as well as tests on a 4-post-test rig, driving tests with defined excitations (like defined obstacles), and test drives on a real road, using a braking machine for reproducibility reasons.

It could be shown that it is possible to reduce the braking distance by affecting on the vertical dynamics of a passenger car in general. The amount of reduction depends on the elevation profile of the chosen testing track and on the initial velocity. On a road with an unevenness comparable to the one that is found on a typical German Autobahn a reduction of typically 1–2 %, compared to the best passive damping, was achieved.

¹Yi/Wargelin/Hedrick (1992): Dynamic Tire Force Control by Semi-Active Suspensions.

²Valášek et al. (1998): Pergamon—Control Engineering Practice.

³Nouillant/Moreau/Oustaloup (2001): Hybrid Control of a Semi-Active Suspension System.

1 Introduction

1.1 Classification of Suspension Systems

In automotive engineering the suspension system serves several purposes: First of all it must carry the weight of the car. In combination with the other demands on the suspension system this is not the trivial task that it might seem to be. Due to changing loads the weight of the car can vary considerably. This change in weight should influence the ride and the handling performance as little as possible, because a driver does not accept a substantial change of his vehicle's behavior.

Secondly the suspension system has to guarantee a high handling performance, which is usually measured in terms of a low value of RMS on dynamic wheel load¹. This is based on the assumption that the lower the amount of oscillations in the vertical tire forces, the higher is the overall force transmission in horizontal direction.

Finally the suspension systems should serve a high passenger riding comfort, which is usually measured in terms of vertical acceleration of the car's body. Basically, the lower the RMS on vertical body acceleration, the higher the riding comfort.

All those demands on the suspension system—looked at each of them individually—lead to different solutions both in terms of construction and in terms of sets of optimal parameters for a given construction. This means that with a passive suspension system, for which parameters cannot be changed during operation after being defined once, the solution will always be a compromise. As for the parameters, the most common ones to change are the body spring stiffness c_B and the body damping k_B . For linear passive systems those parameters are constant and positive, for nonlinear passive systems they only depend on the spring displacement s_S , respectively on the damper velocity v_D , where the damping factor can depend on both: $c_B = c_B(s_S) > 0 \forall t$ and $k_B = k_B(v_D, s_S) > 0 \forall t$.

To solve the upper mentioned conflict of objectives in a better manner, adaptive suspension systems have been introduced. Their parameters can be adjusted during the life cycle of the vehicle, in some of them parameters can even be adjusted while driving. The time period of the adjustment in adaptive suspension systems is rather long. It differs from a few hours (if the suspension needs to be dismantled for changing the parameters) down to a couple of seconds. Some of the adaptive suspension systems introduced were not controlled electronically, but they changed their damping characteristics being controlled mechanically². Examples for those systems are adjustable torsion spring suspensions, shock absorbers with different damper states, or air suspensions for heavy trucks. Adaptive suspension systems serve to adjust the suspension parameters to slowly differing surroundings. In case of a heavy truck the level can be adjusted while loading, in case of a sports car the damping can be lowered for long highway drives in order to increase the

¹Wheel load is the vertical component of the tire force, the force that acts between pavement and tire.

For a definition of dynamic wheel load and the RMS on this quantity please refer to section 4.1.

²N.N. (1995b): ATZ Automobiltechnische Zeitschrift 97 [1995].

riding comfort, etc. For heavy trucks it is also known to combine adaptive air springs with adaptive shock absorbers. In the case of Pneumatic Damping Control (PDC) the damping coefficient is adjusted to the actual loading situation³. This system is another example for an adaptive suspension that is controlled mechanically without making use of electronic sensors or actuators.

All adaptive suspension systems have in common that they are not suitable for high frequency purposes above approximately 0.5 Hz. Those are the frequencies that need to be reached when controlling transient handling and riding effects. For example, if one wants to react to a bump on the road, this can only be assured if the time delay between switching the suspension parameters and its taking effect is very short.

This led to the development of semi-active suspension systems, in which the parameters can be changed in a rather small time frame. Frequencies that can be served by semi-active suspensions lie between zero and approximately 30 Hz for passenger cars. This is because the eigenfrequencies of passenger cars lie at approximately 1–3 Hz for body motions (vertical and pitching) and approximately 15 Hz for vertical wheel motions. With those systems it is possible not only to adjust damping and stiffness to the needs of a given road, but also to react on this particular road's small scale bumps and holes. Examples for semi-active suspension systems are electro-⁴ or magneto-rheologic shock absorbers⁵, or CDC-dampers⁶.

In the 1980s some BMW 635 CSi were equipped with shock absorbers that are adjustable in three different damping stages⁷, the system being called Electronic Damper Control (EDC). Toyota developed its Toyota Electronic Modulated Suspension (TEMS) system already in 1983 and in the early 1990s a control algorithm was introduced that made use of wheel stroke sensors to measure body rolling and pitching and to prevent it by changing the shock absorbers to their hardest setting (refer to Kojima⁸). Adaptive and semi-active suspension systems have in common that for them the stiffness c_B and the damping k_B do not only depend on the spring displacement s_S and the damper velocity v_D , but they are also time-variant: $c_B = c_B(s_S, t) > 0 \forall t$ and $k_B = k_B(v_D, s_S, t) > 0 \forall t$. Still c_B and k_B are positive for all times, which means that those systems can only dissipate or conserve energy.

In active suspension systems energy can not only be dissipated or conserved, but it can rather be brought into the system. For this purpose hydraulic or pneumatic actuators are used. Active suspension systems are characterized by the fact that their stiffness c_B and damping k_B coefficients do not only depend on the spring displacement s_S , the damper velocity v_D , and the time t , but they can also adopt negative values: $c_B = c_B(s_S, t)$ and $k_B = k_B(v_D, s_S, t)$. By means of such systems it is possible to let the vehicle's body follow a given path, e. g. to keep the body horizontal while driving a curve. The disadvantage of active suspension systems compared to semi-active ones is the enormous amount of power

³Causemann (2001): Kraftfahrzeugstoßdämpfer pp. 64–65.

⁴N.N. (1995a): ATZ Automobiltechnische Zeitschrift 97 [1995].

⁵Petek et al. (1999): Demonstration of an Automotive Semi-Active Suspension Using Electrorheological Fluid.

⁶Irmscher/Hees/Kutsche (1999): A Controlled Suspension System with Continuously Adjustable Damping Force.

⁷Hennecke/Jordan/Ochner (1987): ATZ Automobiltechnische Zeitschrift 89 [1987].

⁸Kojima et al. (1991): Development of New Toyota Electronic Modulated Suspension—Two Concepts for Semi-Active Suspension Control.

that is needed to fulfill its purpose. An example of an active suspension system is the Active Body Control (ABC) by Mercedes-Benz⁹. New developments could lead to systems in which the energy that usually is dissipated by the suspension is stored in batteries, high-caps, or other energy storages to use it at times when putting energy into the suspension is needed. Tonoli¹⁰ and Zádor¹¹ suggest shock absorbers on basis of electric generators, the Bose Corporation in 2004 presented a suspension system where electric motors work as actuators and generators at the same time¹².

To reduce the amount of power needed for the active suspension, in most of the cases a conventional spring-damper-system supports the static weight of the vehicle's body. The active elements only control displacements from the static equilibrium. Still, even active suspensions have to face the problem that every boost in wheel load automatically leads to a rising vehicle's body. The only exception is if due to the over-determinedness of the system (four wheels = four vertical supporting points) wheel load is increased at the diagonally lying wheels and decreased at the other two wheels. Then and only then the additional wheel load will not lead to a lifting of the body but to a distortion of it. But neglecting this very special case, the amount of possible wheel load increase is limited by the spring travel, which can be even more limiting than the lack of energy supply in case of semi-active suspensions. While it is relatively easy to control the body movement, since the vehicle's body can lean on the wheels and therefore on the unmoveable pavement, there are more limitations for the control of wheel load. The wheels can only lean on the vehicle's body, which is not fixed, but rather moves up- or downwards if a force is applied to it.

Summarizing, the need to control the suspension parameters led to the development of first slowly, later rapidly adjustable semi-active suspensions, and to active suspensions in which an external power supply is necessary. Figure 1.1 shows the classification of suspension systems described. All those new technologies provide a tool to purposefully influence the vertical dynamics of a vehicle, which was not possible before those technologies had been introduced. This tool at hand can be applied to either influence the upper part of the suspension strut—the movement of the vehicle's body—, or to influence the lower part of the suspension strut—the wheel and its vertical force applied to the ground.

1.2 State of the Art

Control of Horizontal Dynamics in Today's Series Cars

The control of the horizontal dynamics of passenger cars—whether longitudinal or lateral dynamics—is well known in today's series applications. Electronic vehicle dynamics control systems are widespread from subcompact-sized cars up to the luxury class.

The Antilock Braking System (ABS), developed by Robert Bosch GmbH and introduced in the Mercedes-Benz S-Class in 1978, can be found nowadays in almost every new au-

⁹Wolfsried/Schiffer (1999): Active Body Control (ABC) – das neue aktive Federungs- und Dämpfungssystem des CL-Coupés von DaimlerChrysler.

¹⁰Tonoli et al. (2006): Electromagnetic Shock Absorbers for Automotive Suspensions: Electromechanical Design.

¹¹Zádor/Falvy/Palkovics (2006): Electro-mechanical Suspension Actuator with Energy Recuperative Feature.

¹²Bose Corporation (2004): Bose Suspension System.

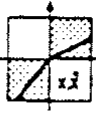
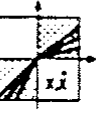
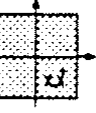
	Forces	Switching Frequency	Energy Consumption	Model
passive		—	—	
adaptive		smaller than the body natural frequency	little	
semi-active		larger than the body natural frequency	medium	
active		larger than the body natural frequency	high	

Figure 1.1: Classification of suspension systems by Redlich¹³.

tomobile in the European Union. This system acts on the longitudinal dynamics of the vehicle only, by modulating the braking torque and with this the braking slip and braking force (for a more detailed explanation refer to section 2.3.1). It has no explicit coupling to the vertical or the lateral dynamics implemented. The maximum braking pressure at a wheel (and connected to it: the maximum braking torque) that can be applied by the ABS is limited by the one in the main braking cylinder. This one is preset by the driver. If the driver is not braking at all the ABS is disabled¹⁴.

Another system that can be found in more and more new automobiles is the so called Electronic Stability Program (ESP). Developed by Robert Bosch GmbH and introduced in 1995 in the Mercedes-Benz S-Class, it goes a step further by connecting the longitudinal with the lateral dynamics. It brakes at least one wheel automatically (i.e. without the driver's intention) if the vehicle comes close to an unstable situation. The decision if a situation is unstable or not is based on the comparison of the desired course, calculated by means of the driver's inputs steering angle and vehicle speed, with the actual course, measured by means of the yaw-rate and the lateral acceleration. By braking one wheel in case of the vehicle approaching an unstable situation, a longitudinal force—the braking force of the braked wheel—is used to influence the lateral dynamics—the yaw-rate and the sideslip angle.

Thus, ESP is a system that connects the control of longitudinal tire forces with the effect on lateral tire forces. Although the vertical dynamics play a role in the sense that

¹³Redlich/Wallentowitz (1999): Vehicle Dynamics with Adaptive or Semi-Active Suspension Systems Demands on Hardware and Software p. 437

¹⁴Robert Bosch GmbH (1999): Kraftfahrtechnisches Taschenbuch p. 662.

the lateral and the longitudinal dynamics are influenced by the vertical dynamics, this connection is not implemented in the control algorithms of the ESP. Research is ongoing to develop ESP II, a system that should combine the control of the braking system, the active steering, and the semi-active suspension, in order to enhance both handling and riding performance. Schwarz^{15,16} and Trächtler¹⁷ show the way on this road. The main idea is that the functional level and the level of actuators are separated from each other.

Connecting Vertical and Horizontal Dynamics

As for the vertical dynamics, several ways are possible how the vertical tire forces can be influenced and controlled in general. Every part of the transmission path from vertical tire force over the tire itself, the rim, the wheel carrier, the suspension strut, and the strut mounting are possible positions in general to place an active or semi-active element to have an influence on the vertical tire force. The most efficient way, however, to actually influence this tire force is to apply a semi-active or an active element into the suspension strut, first for construction reasons, second simply because the stroke is largest in this part of the transmission path. This means that with rather small forces a high amount of energy can be converted.

Now that the position where the vertical dynamics should be influenced is determined, there is still the question what the control objective should be. The controller could act only in the vertical dynamics, without ‘knowing’ anything about its influence on the longitudinal or lateral dynamics. In this case the control objective is usually to reduce the oscillations of vertical tire forces. Or, the controller could connect the vertical with the horizontal dynamics. The control objective in this case is more difficult to define, because modeling the connection between vertical and horizontal tire forces is very complex, and if the modeling is successful, the model outputs depend strongly on the tire parameters. Pacejka’s magic formula for example includes six independent parameters¹⁸, each of which having a strong influence on the transmission path from wheel load to horizontal tire forces. Thus, because the customer can change the tires or the tires can alter their parameters due to aging, a controller to connect vertical and horizontal tire forces needs to be parameter invariant. This and the fact that semi-active suspensions are not widespread might be reasons why in today’s series cars this connection between vertical and horizontal tire forces is not explicitly established yet. As for the control of semi-active suspensions, the focus lies on the vertical dynamics.

Semi-Active Suspension in Today’s Series Cars

In today’s series cars most of the semi-active suspension systems come with adjustable damping coefficients. Two ways to adjust the damping ratio are known: Either to change it via the opening condition of an electro-magnetic valve or by making use of the changing viscosity of the damping fluid. The damping fluid usually is an oil, but solutions to damp with air are also known and implemented in the BMW HP2 Enduro motorbike¹⁹ for example.

¹⁵Schwarz et al. (2003a): ATZ Automobiltechnische Zeitschrift 105 [2003].

¹⁶Schwarz et al. (2003b): ATZ Automobiltechnische Zeitschrift 105 [2003].

¹⁷Trächtler (2005): at – Automatisierungstechnik.

¹⁸Pacejka (2002): Tire and Vehicle Dynamics pp. 173.

¹⁹Müller et al. (2005): ATZ Automobiltechnische Zeitschrift 107 [2005].

As for the adjustable damping, on the German market the electro-magnetic solution prevails all other solutions. It is just recently that the Audi AG came out with the new TT-model, which can be ordered with the so called Magnetic-Ride system, in which the shock absorbers work with magneto-rheological fluids²⁰. Mantled there is an active shock absorber from Delphi Corporation. On the US market Delphi's MagnetRide suspension control system was introduced in 2002 in the Cadillac Seville STS for the first time²¹.

Those semi-active components are mainly used to enhance the riding comfort, which means that they are only acting on the vertical dynamics. Some side effects are used that if one wheel starts to flatter and vibrate heavily, the damping coefficient is set to hard in order to reduce this undesirable vibration. Accelerometers are used to measure the vertical body and the vertical wheel oscillations and to calculate the damper velocity from their signals. In order to increase the riding comfort, the semi-active suspension is controlled in most of the cases by a so called skyhook-controller. This controller models a virtual damper that is thought to be attached between the vehicle's body and a virtual skyhook. The damper control in this case follows the objective to model the virtual, perfect skyhook damper with the real damper attached between wheel and body in the best possible manner²². To implement the skyhook-controller it is necessary to know the characteristic diagram of the shock absorber, the actual damper velocity, and the damping coefficient of the virtual skyhook damper must be defined. Irmscher²³ showed how the actual damper force is distributed in the characteristic diagram of an active shock absorber for the case of skyhook-controlled damping. Identifying the characteristic damper diagram and finding the best way to determine the damper velocity—those are tuning steps that are undertaken in series cars that feature active shock absorbers.

A system was introduced in the Opel Astra H of the lastest generation in 2004, showing the way in the direction of Global Chassis Control (GCC). The system is called IDS-plus and includes active shock absorbers. Those are controlled mainly with the skyhook approach. By the driver's choice between a sport and standard setting the average damping coefficient can be set to harder. At the same time the Electric Power Steering (EPS) and the accelerator are switched into a more sporty setting. So the vertical (via shock absorbers), the longitudinal (via accelerator), and the lateral dynamics (via EPS) are connected by the IDS-plus. The driver is the coupling part of this connection, because he is the one who decides if the connection is suitable or not. The systems are not connected via electronic signals with each other.

Another system in which a semi-active suspension in form of active shock absorbers is applied is the Mercedes-Benz S-Class with the so called Airmatic System. There an air spring is combined with active shock absorbers. The same combination of systems can be found in the Volkswagen Touareg²⁴. Furthermore, almost every automobile of the luxury class can be ordered with a semi-active suspension.

²⁰Jungmann (2006): Audi magnetic ride im neuen TT – all4engineers.

²¹Shutto/Toscano (2006): Magnetorheological Fluid Technology for Vehicle Applications.

²²Kutsche/Raulf (1998): Optimierte Fahrwerksdämpfung für Pkw und Nkw.

²³Irmscher/Hees/Kutsche (1999): A Controlled Suspension System with Continuously Adjustable Damping Force p. 459.

²⁴Jungmann (2003): So viel Continental steckt im Touareg – all4engineers.

Active Suspension in Today's Series Cars

Active suspension systems are used e.g. in the BMW 5 and 7 series²⁵. The system is called Dynamic Drive. By means of an active anti-roll bar the rolling during driving in a curve with lateral acceleration can be reduced, and by adjusting the stiffness of the front and the rear anti-roll bar relatively to each other, the sideslip angle can also be influenced. The main purpose of this system lies on the control of the lateral dynamics of the vehicle. Concerning the braking performance this system is not used to reduce the braking distance. It could be used in such a way that for μ -split conditions the wheel load on the front wheel that drives on the high- μ track is increased by distorting the vehicles body. This would lead to a decreasing wheel load at the front wheel of the low- μ track. The sum of braking forces would therefore increase, because the wheel load gained at the high- μ track leads to a higher increase in braking force than the reduced wheel load at the low- μ track leads to a decline in braking force.

Other active suspension systems like the ABC of Mercedes-Benz are mainly used to control the vertical body oscillations in the frequency range up to 5Hz. It is not of the author's knowledge that the ABC is also used to control the vertical tire forces in such a sense that by their means the braking distance is reduced.

The main problem for active suspension systems is that the high amount of power needed for lowering and lifting the vehicle's body does not necessarily help to increase the wheel load significantly. Of course the lifting of the vehicle's body helps to increase wheel load temporarily, but the problem remains the same for active suspensions as for every other kind of suspension: Increasing the wheel load always leads to a lifting of the vehicle's body, and this lifting is limited by the maximum spring displacement. So, even if with an active suspension forces can be applied that act within the moving direction of the body, the wheel load cannot be increased longer than it takes for the body to reach its maximum upward velocity (refer to Winner²⁶).

Research on Connecting Controls for Chassis Systems

It is not of the author's knowledge that the interaction between adjustable damping coefficient and wheel load and/or braking force is purposefully implemented in series cars. In research this is slightly different. Many authors have been working on control algorithms for semi-active and active suspensions, in most cases in order to reduce the oscillations of vertical tire forces—measured in RMS on dynamic wheel load (for the definition of RMS refer to equation 4.7 on page 62). It is assumed that if the RMS on dynamic wheel load is decreased this gives a better basis for systems that act in the horizontal plane, like ABS and ESP. Several research projects have been undertaken to improve the handling performance of vehicles by means of semi-active suspension.

Smakman suggested a control algorithm to control the lateral tire slip by means of active suspension²⁷ to improve the lateral dynamics. Trächtler suggested to decouple local actuator functions from global objectives to be able to use the provided actuators in a global network for more than only one purpose²⁸. All this research has been theoretical

²⁵Konik et al. (2000): Dynamic Drive - das neue aktive Wankstabilisierungssystem der BMW Group.

²⁶Winner et al. (2006): Die Bremse im mechatronischen Fahrwerk p. 368.

²⁷Smakman (2000): Functional Integration of Slip Control with Active Suspension for Improved Lateral Vehicle Dynamics.

²⁸Trächtler (2005): at – Automatisierungstechnik.

without application to the real world.

Reducing the braking distance has also already been investigated; the Continental AG executed a project with the objective to come up with a real car that has a braking distance from an initial velocity of 100 km/h of 30 m or less²⁹. The testing vehicle used was a Volkswagen Golf. In 2000 the Continental AG eventually was able to reduce the braking distance (which usually lies around 40 m) down to the set target of 30 m. Many different control systems and their applications were involved in this project. The vehicle was also equipped with active shock absorbers. But the main focus did not lie on controlling the vehicle's damping. This was just one additional point amongst many others. The main part of the braking distance reduction was achieved by using high-performance tires and by modifying the braking system such that the full braking pressure was applied very quickly. Furthermore, all components of the vehicle dynamics control were adjusted to each other and they were working in an integrated network. Global chassis control (GCC) was the main issue in this project. Only because all components of the control of the vehicle dynamics were adjusted to each other was it possible to reduce the braking distance by such a high amount.

Anyway, the active shock absorber controller used in the 30 m-car project cannot directly be transferred to the controller of this thesis, because all braking tests were executed on an ideally even pavement. This means that the excitation of vertical tire force oscillations came only from the fact that the braking forces applied cause a weight transfer from rear to front axle. No seismic excitation was causing oscillations in vertical tire forces. In this thesis the possibility to reduce the braking distance on a road with a typical unevenness is investigated. Therefore the control approach used in this thesis differs significantly from the one of the 30 m-car.

Research on Semi-Active Shock Absorber Control

State-of-the-art in research concerning the control of active shock absorbers is the knowledge that ride on the one hand and handling on the other hand can be improved by the control of active shock absorbers. On the handling side this is mainly based on simulation results or results of quarter- or 2D-car physical models. Only few test drives with real cars have been published. It holds true that handling performance can be improved if it is measured and assumed to be measurable in terms of RMS on dynamic wheel load, without actually using a measurand of the lateral or longitudinal dynamics. The possibility to improve the vertical counting measurand RMS on dynamic wheel load has been shown for passenger cars as well as for other land-based vehicles (such as trucks or tanks) in simulations. For an exceptional example refer to Choi³⁰ who reduced the vertical body accelerations of a tracked vehicle (a tank) by means of active shock absorbers in simulation. The steering stability could be kept constant at the same time.

Pinkos³¹ was able to reduce the rolling of a real testing vehicle by means of rotational acting active shock absorbers which are based on electro-rheological magnetic fluids (ERM). He suggested that electro-rheological based shock absorbers exceed electro-magnetic solu-

²⁹Becker/Huinink/Rieth (2001): Maßnahmen zur Verkürzung des Anhaltewegs in Notbremsituationen – das 30m Auto.

³⁰Choi/Park/Suh (2002): Journal of Dynamic Systems—Measurement and Control 124 [2002].

³¹Pinkos/Shtarkman/Fitzgerald (1994): An Actively Damped Passenger Car Suspension System with Low Voltage Electro-Rheological Magnetic Fluid.

tions with a faster response to changes of the demand of damper forces. This is probably not the case, because the main time delay comes from the fact that the pressure difference in upper and lower chamber needs to establish in order to provide a damper force. This is the case for any active shock absorber, no matter if controlled electro-magnetically or electro-rheologically.

Not talking about driving safety in general, but rather about the RMS on dynamic wheel load in particular, this quantity is known as reducible by making use of active shock absorbers. This field has widely been researched mainly in simulation models.

Redlich³² showed in 1994 on a quarter-car model that the RMS on wheel load and the RMS on vertical body acceleration can be reduced at the same time by means of active shock absorbers. His approach is to determine the actual frequency with which the vehicle oscillates and then to set the damping to the best value for this given frequency in order to reduce both wheel load and body oscillations. He furthermore deduced the demands on the hardware and the software when using such a semi-active suspension system. Alberti³³ also proposed in 1991 that with active shock absorbers it is possible to enhance riding and handling at the same time. He investigated this topic with a quarter-car model and focused on the effect of different road roughnesses on his results. Both showed the fundamental potential for an enhancement of the vertical dynamics by means of active shock absorbers.

Several experiments in the real world have been undertaken with quarter- or half-car models. Yi in 1992 reduced the dynamic tire forces in experiments with a half-car model test rig³⁴. He used a bilinear observer approach to reduce both the vertical body acceleration as well as the dynamic tire forces.

A main problem for all researchers in the field of semi-active suspension when applying the theoretical models to the real world is the uncertainty of parameters and the uncertainty whether the structure of the simple dynamical models map the vehicle behavior in the right manner. Lauwerys suggested in 2002³⁵ and again in 2004³⁶ that due to the complexity of a passenger car and the changing parameters during a life cycle it might be advantageous to do the control without complex dynamical models of the vehicle, but to rather adjust parameters of neural networks to a less complicated model. Neural networking is a control strategy that was also widely applied to the topic of semi-active suspension. Moran³⁷ could decrease the RMS on vertical body acceleration by means of such a control algorithm. Other authors, like Yeh³⁸, worked on fuzzy-control logics to improve riding and handling. Yeh based his work on a quarter-car model and showed in simulation results that an adaptive control strategy can improve the performance. The controller is adaptive in the sense that it changes control parameters by reacting on the pseudo-noise seismic excitation of the simulated pavement. Yoshimura³⁹ also implemented a fuzzy-controller into a quarter-car model with which he was able to suppress vertical body accelerations by a high amount.

³²Redlich/Wallentowitz (1994): Vehicle Dynamics with Adaptive or Semi-Active Suspension Systems Demands on Hardware and Software.

³³Alberti (1991): Adaptive Fahrwerksdämpfung.

³⁴Yi/Wargelin/Hedrick (1992): Dynamic Tire Force Control by Semi-Active Suspensions.

³⁵Lauwerys/Swevers/Sas (2002): Linear Control of Car Suspension Using Nonlinear Actuator Control.

³⁶Lauwerys/Swevers/Sas (2004): Model Free Control Design for a Semi-Active Suspension of a Passenger Car.

³⁷Moran/Hasegawa/Nagai (1999): Continuously Controlled Semi-Active Suspension Using Neural Networks.

³⁸Yeh/Lu (1999): A Genetic Algorithm Based Fuzzy System for Semi-Active Suspension System Design.

³⁹Yoshimura/Takagi (2004): Journal of Zhejiang University SCIENCE 5 [2004].

Another control approach which makes use of a 2D-model of a vehicle is to use the front axle as a sensor. By the signals that are obtained at this axle—which always passes road disturbances before the rear axle when driving forwards—the performance of the controller for the rear axle can be improved. Araki⁴⁰ implemented such a preview controller in his 4-degrees-of-freedom model and obtained an improved pitching behavior (smaller pitching angles) by this feed-forward compensation. In fact, he modeled an active suspension system. The limits for implementing such a control algorithm in a real car are once again the high model and parameter uncertainties.

As for real test drives, Valàšek was able to reduce the RMS on dynamic wheel load in the case of a heavy truck. In earlier work he developed control strategies to reduce the RMS on dynamic wheel load⁴¹. His main objective was to reduce the road damage, which can be measured in terms of a derivate of the RMS on dynamic wheel load. Valàšek used a so called groundhook-controller which is similar to the skyhook approach. In case of the groundhook a virtual shock absorber is thought to be attached between ground and the wheel's spinning axis. This is because if this damper was there for real it would lead to a reduced vertical oscillation of the wheel. Similar to the skyhook approach, this virtual shock absorber is than tried to be represented with the real active shock absorber in the best possible manner. But only controlling the vertical oscillations of the wheel will lead to an increasing deflection of the vehicle's body in the long run. This is why Valàšek went a step further and introduced a so called hybrid-controller which combines the sky- and the groundhook approach by applying two virtual dampers—one attached between sky and body and one between wheel and ground. With this control scheme Valàšek was able to reduce the RMS on dynamic wheel load in simulations. Applying this kind of controller to the real world is rather difficult, because several control parameters need to be defined and adjusted to reality. For real test drives with a truck Valàšek used a Fuzzy-control algorithm that is more parameter independent⁴². With this approach he was able to reduce the RMS on dynamic wheel load in real test drives on a stochastic road on an airfield.

All the literature sources mentioned have in common that they build the fundament for controlling active shock absorbers for the case that the RMS on dynamic wheel load should be reduced, for the case that this is the control objective. The question arises whether this is in fact the control objective in order to reduce the braking distance. Reichel⁴³ therefore started to execute test drives with controlled active shock absorbers in braking situations. He introduced a control mechanism whose control objective is to keep the wheel load constant. This objective cannot be obtained completely by a semi-active suspension, and even for an active suspension it is only possible to keep the wheel load constant if the amplitudes of the vertical excitation are small enough. Nevertheless, the control objective can still be to keep the wheel load constant, even if it is not possible to achieve this goal. It is the benchmark and shows the direction.

Reichel executed his test drives with constant velocity. The rear axle of the testing vehicle was driven while the front axle was braked. Thus, the influence of the vertical dynamics—controlled by active shock absorbers—on the braking torque and braking force could be investigated without having to consider the weight transfer and a reduced vehicle's speed

⁴⁰Araki/Oya/Harada (1994): Preview Control of Active Suspension Using Disturbance of Front Wheel.

⁴¹Valàšek/Novák (1996): Ground hook for semi-active damping of truck's suspension.

⁴²Valàšek et al. (1997): Vehicle System Dynamics.

⁴³Reichel (2003): Untersuchungen zum Einfluss stufenlos verstellbarer Schwingungsdämpfer auf das instationäre Bremsen von Personenzügen.

having an influence on the results. Reichel was able to reduce the RMS on dynamic wheel load when passing a sinusoidal obstacle for vehicle speeds up to 50 km/h. He furthermore showed that for low vehicle speeds up to 50 km/h his shock absorber controller leads to better performance for longitudinal vehicle dynamics measurands, like braking torque and braking slip. His conclusion was that due to the reduction of RMS on dynamic wheel load the longitudinal dynamics were influenced positively.

Summarizing, the analysis of the state-of-the-art of the control of semi-active and active suspension systems shows that the area has been widely investigated by researchers all over the world. Many concepts to control the vertical dynamics in order to enhance the ride and the handling of a vehicle have been presented since the early 1980s. The vast majority use quarter-car models to enhance ride and handling and measure those two quantities in terms of RMS on vertical body acceleration and RMS on dynamic wheel load. In simulations on those quarter-car models it could be shown that both RMS-values are reducible by means of active shock absorbers. Test rig trials on physical models have also been undertaken. Here the results from simulations could be verified in general. As for implementations of the results on research side to the real world only few experimental research projects have been undertaken. It is not of the author's knowledge that the connection between vertical and horizontal dynamics has been established in series applications. The main problem when it comes to this connection is to define the control objective. The RMS on dynamic wheel load might not be the only and not the best quantity to serve as control objective.

1.3 Research Objectives

The results of former researchers show the possibility to purposefully influence the RMS on dynamic wheel load by means of active shock absorbers. Using this knowledge, two more aspects are added in this thesis: Firstly, not only the response of the system in the long run is measured and acted on, but rather the transient response is treated as an essential factor as well. This means that the RMS on dynamic wheel load is only one measurand beside others. By means of RMS the response of the vehicle in the long run—e. g. for the whole braking process—can be measured. As an integrative measurand it does not give information about how one single switching process of the shock absorbers influences the course of wheel load, braking slip or braking force. In this sense it is comparable to the braking distance, which also is an integrative measurand. The braking distance itself gives information about how good the braking performance for a given braking process was, compared to others. It cannot give information about the course of all the quantities that influence the final result, like braking slip or braking force.

Secondly, the connection between vertical and horizontal tire forces is drawn—and thus between vertical and horizontal tire force controllers—in this thesis. It is not of the author's knowledge that this connection has been implemented with a measurable objective in mind (like reducing the braking distance) so far. Reducing the braking distance is not only an objective worth to desire because of the shorter braking distance alone. If a system that has the ability to reduce the braking distance, assuming a constant deceleration, is applied to a car, it also reduces the longitudinal velocity of the vehicle at every point in time and—in this context even more important—at every point in the distance domain. If a driver applies full-braking this is usually done to prevent a collision. In case the time to collision (TTC) is too short to prevent the collision completely, it is still the desire of the

driver to slow down the vehicle as much as possible. Since the kinetic energy depends on the square of the velocity, the vehicle's speed at the time of the impact plays a big role in damage reduction. A system that is meant to reduce the braking distance thus helps in two ways: By preventing collisions and—probably more often—by reducing the speed at the time of the unpreventable collision and thus the potential damage.

The objective of this thesis therefore is to determine if and to which amount there is a potential to reduce the braking distance by means of a vertical dynamics controller on a conventional pavement—and more specific, by means of active shock absorbers. Sub-targets on this way are to define an experimental setting that allows to measure the braking distance such that the influence of the driver and all other parameters that influence the braking distance besides the vertical dynamics are not relevant.

Furthermore, it needs to be checked whether the given general doctrine that the lower the RMS on wheel load, the higher the handling performance holds true for the special case of braking procedures as well. A control objective needs to be defined with which the connection between the vertical and the longitudinal dynamics of a vehicle can be established. This control objective does not necessarily has to be to reduce the RMS on wheel load. A concept ought to be developed which allows to purposefully connect vertical and longitudinal dynamics.

The interaction with the Antilock Braking System (ABS) is part of the investigation as well. By means of the ABS it is also the objective to reduce the braking distance by braking as close to the optimum braking slip as possible. Since a today's ABS does not get information about the vertical tire forces, which influence the braking slip in the same manner as the braking force and the braking torque do, it cannot reach the objective of keeping the braking slip constant at the optimal level. Both tire and type of pavement influence the course of the μ -slip curve and therefore of the value of optimal braking slip. Not knowing which type of tire is attached to the vehicle and which road conditions the system has to deal with are two other main reasons why the optimal slip cannot be achieved. Simply because it is not known in advance what the value of the optimal slip actually is.

In this thesis the ABS should therefore be supported in its trying to keep the braking slip at its optimal level. A measurand has to be found that connects the vertical tire forces with the longitudinal ones, that connects the vertical dynamics with the braking slip. All results and conclusions of this thesis should be representative for typical roads that can be found in real life, e. g. highways with a typical unevenness.

1.4 Methodology

To reach the objectives the following methodology is used:

First of all, the vertical dynamics of a quarter-car—a reduced car that only includes one wheel, one suspension strut, and a part of the vehicle's total body mass—is investigated in a simulation model. The effect of switching the active shock absorber on the course of the wheel load is investigated with this model and a wheel load control algorithm is introduced. Both the model and the control algorithm are validated in test rig trials on a 4-post test rig with a real car. The control algorithm investigated in simulation models is implemented in a real car and braking tests are executed.

An emphasis is put on the reproducibility of the braking test. Since many different parameters influence the braking distance, it is important to keep as many of them constant

as possible, to be able to measure the influence of the developed controller of vertical dynamics on the braking distance. A braking machine is used to initiate the braking process, in order to exclude the driver's influence on the results. The braking machine delivers the gradient of braking pressure as well as the position on the testing track where the braking is executed in a high reproducibility.

Furthermore, the results of this thesis should be transferable to what one can expect in the real world, meaning on a conventional German Autobahn or comparable other road. Thus, a testing track is chosen that is comparable to a road with a roughness that is typical for German highways.

The main focus of this thesis lies on deepening the understanding of what happens if there is an intervention in the vertical dynamics of a vehicle with respect to the longitudinal dynamics. To make the results transferable to other types of vehicles the developed controller is independent of most vehicle parameters as masses, stiffness, or damping coefficients. It is developed in such a way that it makes use of the principle of the vertical dynamics that is inherent to every ground based vehicle, that is, that the wheel load can be increased (decreased) by applying an additional (subtractional) force to the suspension strut at this very wheel.

2 Fundamentals of Vehicle Dynamics

2.1 Coordinate Systems

In automotive engineering the standard coordinate system is a right oriented system as shown in Figure 2.1. The x-coordinate lies in the vehicle's longitudinal direction, pointing forwards. The y-coordinate is perpendicular to the x-coordinate and points to the left (in driving direction). The z-coordinate points upwards and is perpendicular to the x-y-plane¹. The origin of this standard coordinate system usually is identical to the center of gravity (CG) of the total vehicle, and that is how it is defined in this thesis as well. Movements along the three translatory degrees of freedom are called 'longitudinal' (x), 'lateral' (y), and 'vertical' movements. Angular movements along the three rotational degrees of freedom are called 'roll' (φ , around x-axis), 'pitch' (ϑ , around y-axis), and 'yaw' (ψ , around z-axis).

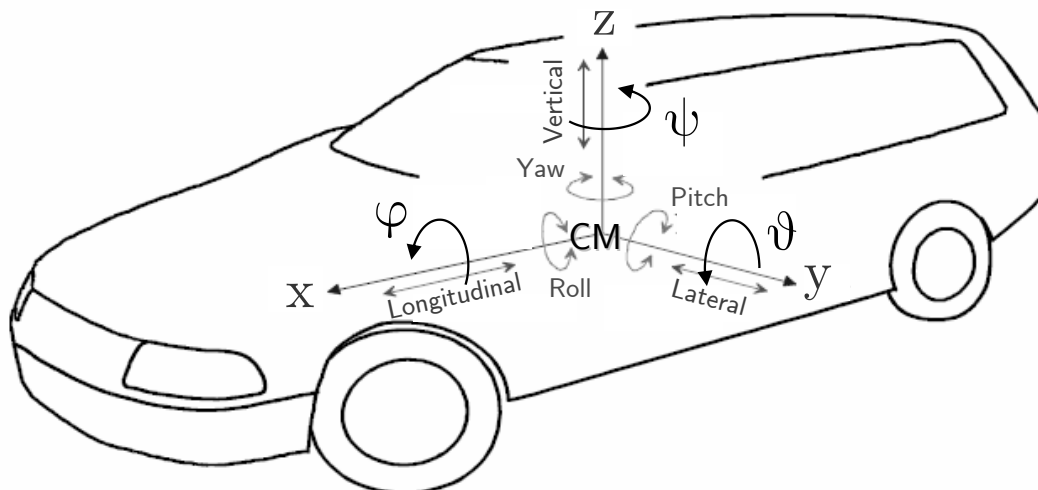


Figure 2.1: Global coordinate system of a vehicle's dynamics and naming of the possible movements².

Those are the global degrees of freedom and coordinates of the vehicle as a whole. As for the single wheels and the suspension at a wheel the coordinates are defined in Figure 2.2. In this figure the principle of a typical suspension of a front and a rear wheel are shown. For clarity reasons the springs are neglected in this figure and only the shock absorbers are drawn, but since only geometric calculus is done the conclusions are the same for either shock absorber or spring.

Measuring the shock absorbers' velocity and the springs' displacement, it must be taken into account that neither of them is aligned with the vertical coordinates $z_{B,i}$ and $z_{W,i}$

¹This definition of the coordinate system conforms to the definition in the German norm DIN 70000. It differs from the SAE-definition in the way that in this American definition the z-axis points downwards and therefore the y-axis points to the right.

²Breuer (2001): Kraftfahrzeuge II p. 2

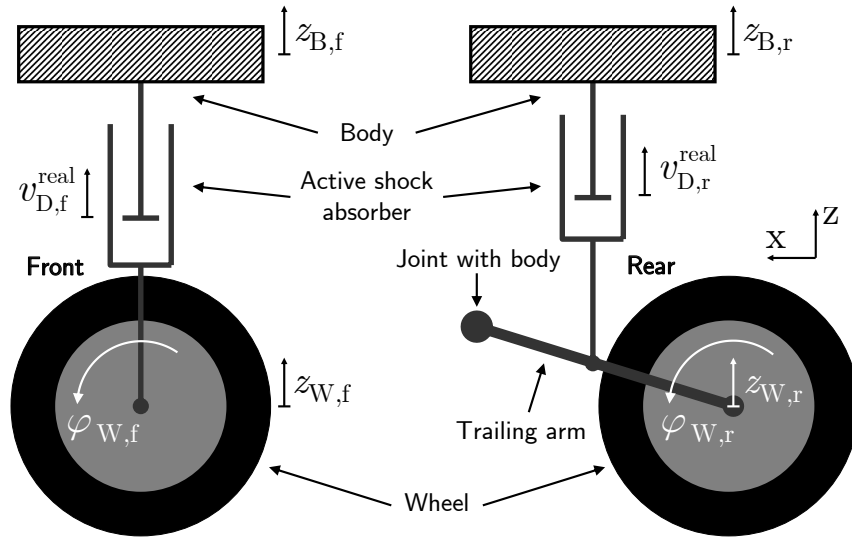


Figure 2.2: Coordinate systems for an aligned and a displaced suspension. The structures of the suspensions shown correspond with the testing vehicle's real structures.

in general. For the testing vehicle used for all experimental settings in this thesis (for a detailed description refer to section 3.2), the shock absorber as well as the spring at a rear axle's wheel are in fact displaced both with respect to each other and with respect to $z_{B,r}$ and $z_{W,r}$.

For the front axle both shock absorber and spring can be assumed to be aligned with $z_{B,f}$ and $z_{W,f}$, because the angles between their axes and the vertical axis are very small and both are directly connected with the rotational center of the wheel.

The measurands

$$v_{D,i} = \dot{z}_{B,i} - \dot{z}_{W,i} \quad (2.1)$$

and

$$s_{S,i} = z_{B,i} - z_{W,i} \quad (2.2)$$

are introduced as the projected shock absorber velocity and the projected spring displacement. The coordinate system of the model in section 4.3 always refers to those projected quantities. They do not necessarily reflect the real velocity $v_{D,i}^{\text{real}}$ and the real displacement $s_{S,i}^{\text{real}}$ of the actual shock absorber and the actual spring. The factors with which the real and the projected velocities and displacements are connected are called $i_{D,i}$ and $i_{S,i}$. This means that

$$v_{D,i}^{\text{real}} = i_{D,i} v_{D,i} \quad (2.3)$$

and

$$s_{S,i}^{\text{real}} = i_{S,i} s_{S,i}. \quad (2.4)$$

For the values of the factors $i_{D,i}$ and $i_{S,i}$ of the testing vehicle used for this thesis refer to Table 3.1 on page 40. All parameters of the testing vehicle are calculated in terms of projected quantities. If the spring stiffness, the damping coefficient, or any other parameter is mentioned, it *always* refers to the projected degree of freedom rather than to the real physical values of spring and shock absorber.

The angular displacement around the i -th wheel's y -axis is defined as φ_W .

2.2 The Braking Process

If the longitudinal acceleration of a vehicle is negativ, the car is braking. Its kinetic energy $E_{\text{kin}} = 1/2 m_V v^2$ is decreasing. This negative acceleration—or deceleration—can be caused by either body forces or by contact forces. Body forces act on the car due to the gravitational acceleration, which causes the car to decelerate if driving an inclining slope. Contact forces can be either friction forces applied in the contact zone of tire and pavement or area forces due to the wind resistance of the car.

A car which is assumed to drive on a horizontal plane is therefore not subject to any body forces but only to contact forces. As for the type of braking it can be differed between a braking procedure whose main purpose is to decelerate the vehicle, a braking procedure which is meant to bring the vehicle down to the same velocity as the preceding car, and full-brake.

In this thesis only the full-brake situation is chosen, because only when the maximum deceleration is desired by the driver a system to reduce the braking distance is of any use. In all other cases the driver can control the deceleration and therefore the braking distance himself. If the driver is not using the maximum friction coefficient possible, he can act as controller and increase or decrease the braking pressure. The deceleration will follow, because it can follow. If the driver desires a higher deceleration than is possible by using the maximum braking coefficient, the uncontrolled wheel will tend to lock. In this case the driver does not have the possibility to control the desired longitudinal acceleration, because the friction factor which would be necessary to fulfill the driver's demand simply cannot be delivered by the tire/pavement interaction.

In Figure 2.3 a passenger car with optimal brake supporting angles is shown. The angles $\varepsilon_{B,f}$ and $\varepsilon_{B,r}$ uniquely define the position of the pitching center PC. Now if braking forces are applied to the front and the rear axle, those forces together with the height of the center of gravity form a moment that lets the wheel load at the front axle increase and the wheel load at the rear axle decrease.

$$F_{B,\text{total}} h_{CG} = (F_{B,f} + F_{B,r}) h_{CG} = \Delta F_{z,bi} l, \quad (2.5)$$

where $\Delta F_{z,bi}$ is the weight transfer from rear to front axle. The static wheel load is neglected in these thoughts. Now if the wheel load increases by $\Delta F_{z,bi}$ at the front and decreases by $\Delta F_{z,bi}$ at the rear axle, this additional respectively less vertical force in the tire contact zone in stationary (quasi-static) condition has to be supported by the vehicle's body.

If the direction of action of the resulting force of $\Delta F_{z,bi}$ and $F_{B,f}$ at the front axle, $F_{\text{res},f}$, goes through the pitching center, no moment around the front suspension is present and therefore the front axle will not deflect, neither bound nor rebound. The same holds true for the rear axle. This means that in the configuration given in Figure 2.3, the vehicle's

body will not pitch when braking forces are applied at the tires. The additional wheel load at the front axle is then only transmitted via the suspension links, the suspension spring is not deflected.

Figure 2.3 also shows that this only holds true if the braking forces at front and rear axle are in the optimal ratio such that the resulting forces of front and rear axle point directly at the PC. If one or more of the named parameters differ from the optimal configuration, the vehicle's body will pitch. This happens until the sum of forces transmitted through the suspension links and the spring forces of the front and rear axles' body springs times the wheel base balance with the torque that is made of braking force times height of center of gravity.

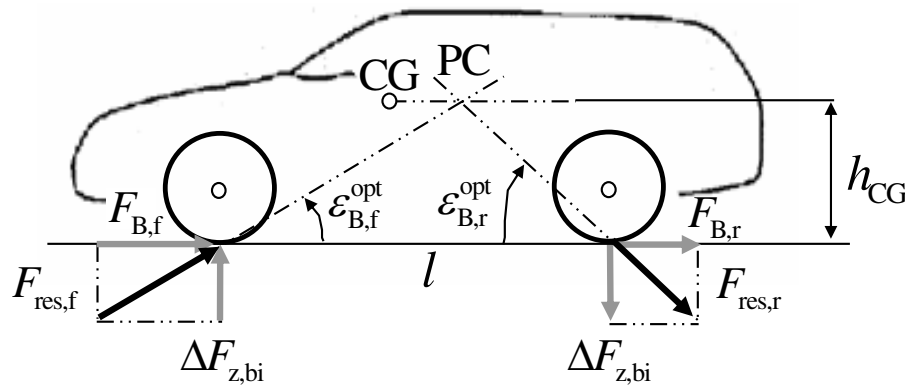


Figure 2.3: Optimal brake support angles for a passenger car³.

Theoretically speaking, this can also mean that the vehicle's body moves upwards at the front of the vehicle and downwards at its back—in case the PC lies above the CG. But this is a configuration that cannot be found in today's series cars—as the reader knows by inspection. Today's cars pitch by moving the body down at the front and up at the back.

Usually cars do not have the PC at the same height as the CG, in fact it lies much lower (e. g. $h_{PC} \approx 0.14\text{ m}$ $h_{CG} \approx 0.52\text{ m}$ for the testing vehicle, refer also to Table 3.1 on page 40). Thus, due to the fact that the PC lies below the CG, if a car is braked it is also excited to pitching oscillations. This is important to mention, because this mechanism is one source of wheel load oscillation and it is the main reason for shock absorber deflections. The other source of wheel load oscillations is the roughness of the road, which causes the wheel to bounce.

In Figure 2.4 the courses of dynamic wheel load for different heights of the pitching center are shown for a braking procedure on a vehicle with 2 axles and no seismic excitation. The deceleration increases to its stationary value in form of a ramp and is then constant during the whole braking procedure.

If PC lies at the elevation of the pavement, the oscillations of wheel load—which are only due to the angular oscillation of the vehicle's body—have the greatest amplitudes. In case of a PC at the height of the CG in combination with optimal brake supporting angles there are no oscillations of wheel load at all. The weight transfer simply leads to a higher wheel load at the front and a lower one at the rear axle, but no transient response occurs. The assumption is that the suspension bushings are infinitely stiff. Then the weight transfer is completely proportional to the amount of deceleration.

³Winner (2006): Kraftfahrzeuge II p. 144

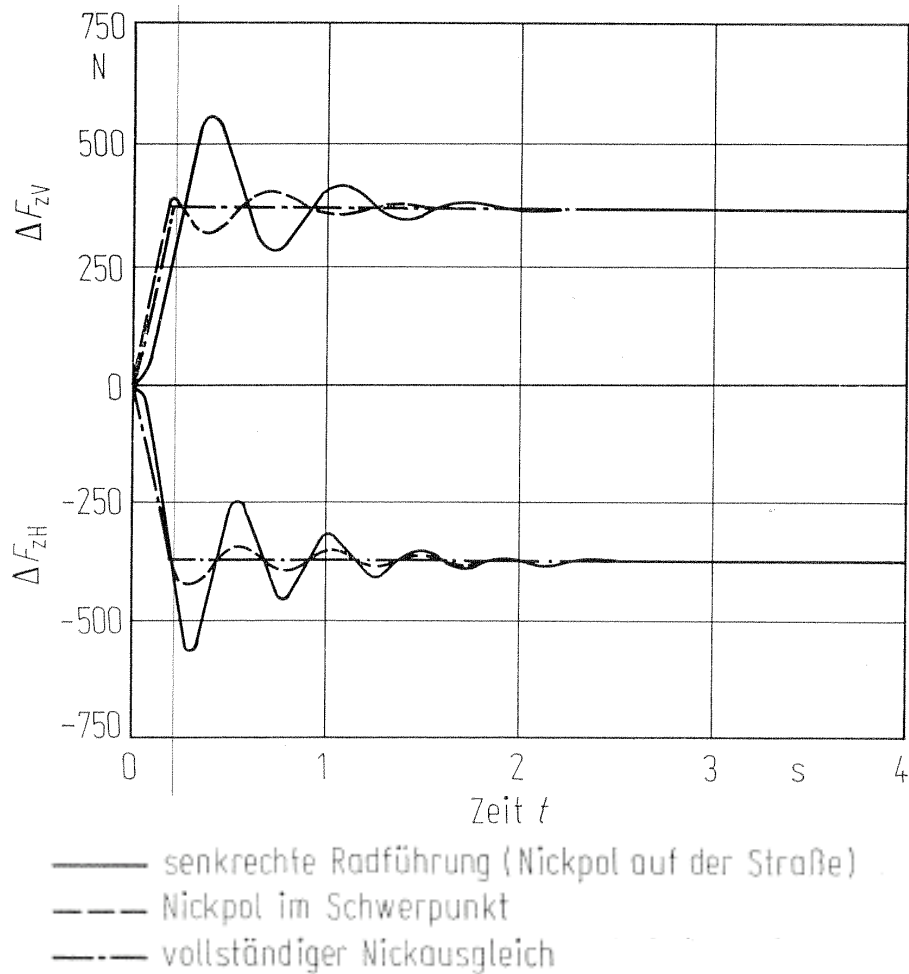


Figure 2.4: Wheel load distribution due to weight transfer between front and rear axle for different heights of the pitching center h_{PC} ⁴. Senkrechte Radführung (Nickpol auf der Straße) = vertical wheel control (pitching center on the elevation of the pavement), Nickpol im Schwerpunkt = pitching center at the same position as the center of gravity, Vollständiger Nickausgleich = optimal brake supporting angles, $\Delta F_{z,v} = \Delta F_{z,bi}$, $\Delta F_{z,h} = -\Delta F_{z,bi}$.

As was shown in the former passages, the distribution of braking force between front and rear axle, as well as the position of PC relative to CG, has an effect on the pitching of the vehicle's body. But what would the optimal braking force distribution be if there was no pitching, if the wheel load at front and rear axle would be assumed to be constant during the braking procedure as the dash-dotted line in Figure 2.4 suggests, in order to gain the shortest possible braking distance?

E. g., if only the front axle is braked, this will clearly not lead to the shortest braking distance, because the front axle can only transmit a limited amount of braking force to the ground and this does not increase if the rear axle is not braked. Quite the contrary will happen, it would rather decrease because the additional wheel load caused by the weight transfer would be missing at the front axle.

Looking at it this way and assuming that the tires at front and rear axle have the same

⁴Mitschke (1984): Dynamik der Kraftfahrzeuge, Band B – Schwingungen p. 154

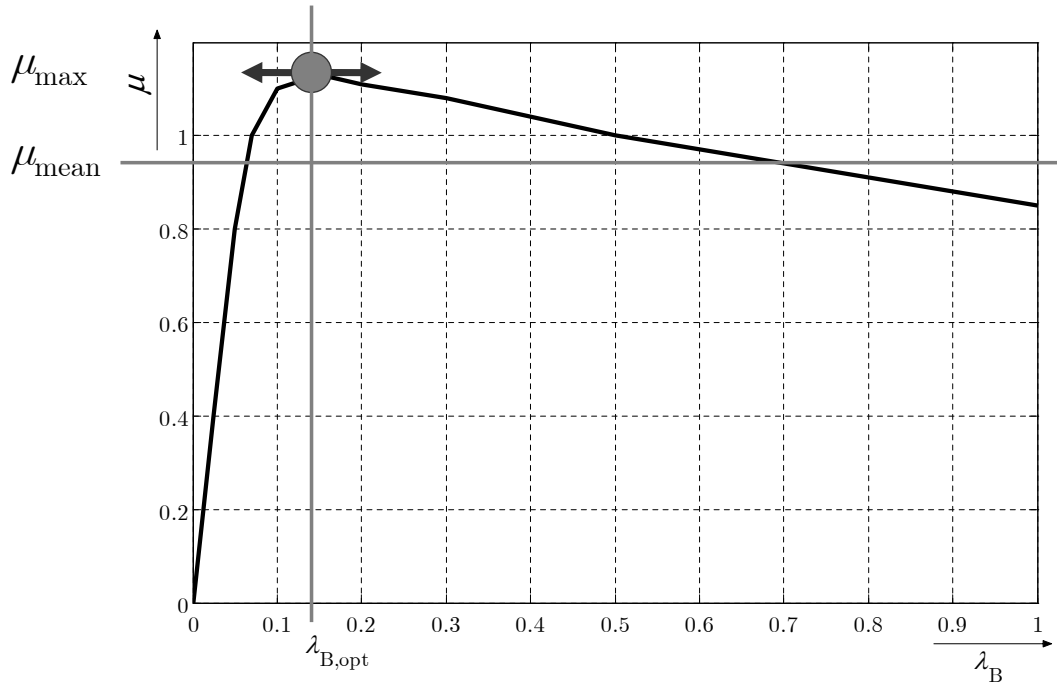


Figure 2.5: Typical μ -slip curve for a standard summer tire. The curve as seen has been used for simulations. $\mu = F_B/F_z$, $\lambda_B = 1 - v_W/v_x$.

properties, and furthermore that the μ -slip curve⁵ will not change with changing wheel loads, the braking slip at front and rear axle should be the same in order to achieve the shortest braking distance possible. Because only if every wheel is at the maximum of braking force applicable to it (or: at the optimal braking slip $\lambda_{B,opt}$) the overall braking force is at its maximum as well.

These thoughts lead to the so called brake force distribution diagram shown in Figure 2.6. This diagram shows that there is only one distribution of braking force between front and rear axle which is optimal for shortening the braking distance. In the diagram it is assumed that the wheel loads at front and rear axle are constant and have the values of the body induced wheel load. These assumptions—as can be seen in Figure 2.4—do not necessarily hold true in a real car. But since the braking force distribution is applied in a real car according to the diagram in Figure 2.6, it makes sense to try to reduce dynamic wheel load oscillations—to reduce the RMS on dynamic wheel load—in order to shorten the braking distance.

During a braking procedure the vehicle's speed is decreased by the sum of the braking forces acting on all wheels. This sum of braking forces $F_{B,total}$ causes a longitudinal acceleration in negative x-direction. During the braking procedure, $F_{B,total}$ does not have the same importance at all times. Of course, the higher the mean braking force, the shorter the braking distance. But this holds true only for two courses of braking force that are similar and only differ by a proportional factor. In fact, it is not only the mean value of braking force that effects the braking distance, but also the distribution of braking force in time during the braking procedure.

⁵A typical μ -slip curve is shown in Figure 2.5. It shows the braking coefficient $\mu = F_B/F_z$ vs. the braking slip λ_B .

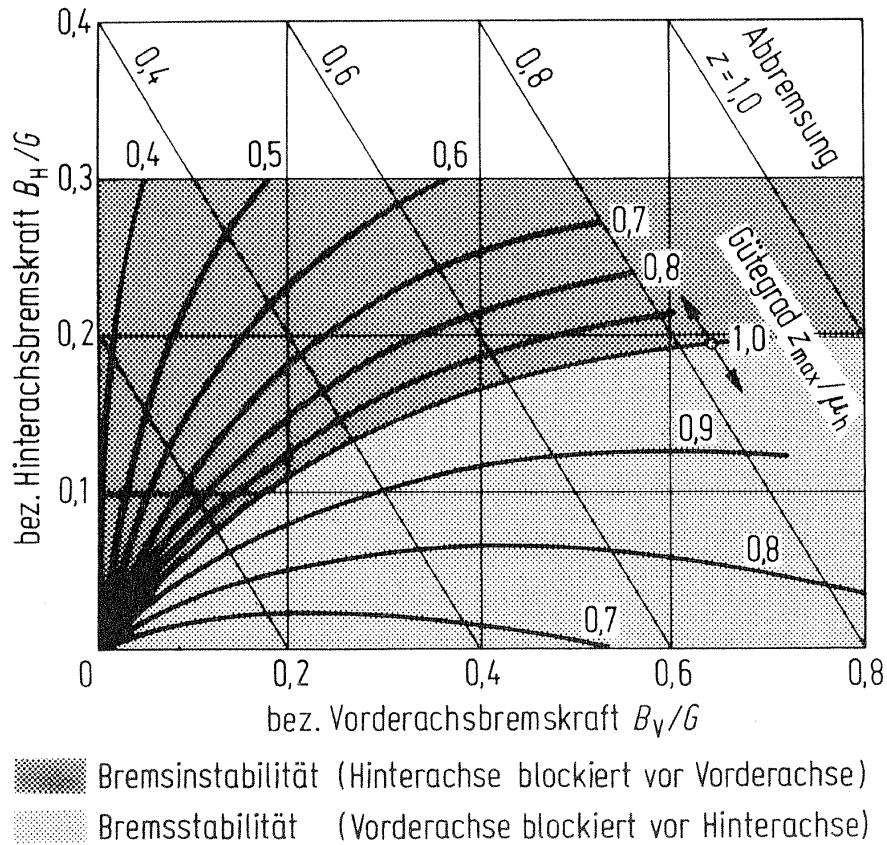


Figure 2.6: Brake force distribution diagram⁶. Bez. Hinterachsbremskraft = braking force at rear axle per weight of the car, bez. Vorderachsbremskraft = braking force at front axle per weight of the car, Bremsinstabilität = braking instability (rear axle locks before front axle locks), Bremsstabilität = braking stability (front axle locks before rear axle locks), Abbremsung = braking ratio, Gütegrad = quality of the braking ratio.

At the beginning of a braking procedure a loss in braking force is worse than the same amount of loss at later times. Why is this so? First of all, the braking duration Δt_B is constant for the mean value of the total braking force $\bar{F}_{B,\text{total}}$ with respect to time being constant (comparing two different braking procedures). Why does the braking duration Δt_B not depend on the distribution of braking force over time but only on its mean value? The acceleration of the vehicle in longitudinal direction, referring to it as a rigid mass, is given by the following equation:

$$m_V a_x(t) = -F_{B,\text{total}}(t), \quad (2.6)$$

where m_V is the total vehicle mass. The longitudinal velocity of the vehicle v_x can be determined by integrating this equation:

$$v_x(t) = \int_{t_{BB}}^t a_x(\tau) d\tau + v_{x,0} = - \int_{t_{BB}}^t \frac{F_{B,\text{total}}(\tau)}{m_V} d\tau + v_{x,0}, \quad (2.7)$$

where t_{BB} is the beginning of braking and $v_{x,0}$ is the initial velocity. At the time of the

end of braking, t_{BE} , the longitudinal velocity must be zero. This leads to:

$$v_{x,0} m_V = \int_{t_{BB}}^{t_{BE}} F_{B,total}(t) dt \quad (2.8)$$

Dividing both sides by $t_{BE} - t_{BB} = \Delta t_B$ leads to:

$$\frac{v_{x,0} m_V}{\Delta t_B} = \frac{1}{\Delta t_B} \int_{t_{BB}}^{t_{BE}} F_{B,total}(t) dt \quad (2.9)$$

Realizing that the right hand side of this equation is the mean value of the total braking force with respect to time leads to:

$$\frac{v_{x,0} m_V}{\Delta t_B} = \bar{F}_{B,total} \quad (2.10)$$

This means that the braking duration can be calculated by

$$\Delta t_B = \frac{v_{x,0} m_V}{\bar{F}_{B,total}} \quad (2.11)$$

This means that as long as the mean value of braking force stays constant, the duration of braking is the same for any braking procedure, no matter how the course of braking force looks like with respect to time. The braking duration only depends on the mean value of braking force, not on its distribution with respect to time.

For the braking distance this looks slightly different. Assuming that the braking force with respect to time can be distributed by adding two linear functions, one of which decreases from $2\bar{F}_{B,total}$ at t_{BB} down to zero at t_{BE} , and one of which increases from zero at t_{BB} up to $2\bar{F}_{B,total}$ at t_{BE} , the total braking force can be written down as:

$$F_{B,total}(t) = \alpha F_{B,1}(t) + \beta F_{B,2}(t), \quad (2.12)$$

with

$$F_{B,1}(t) = 2\bar{F}_{B,total} \left(1 - \frac{t}{t_{BE}}\right), \quad (2.13)$$

$$F_{B,2}(t) = 2\bar{F}_{B,total} \frac{t}{t_{BE}}, \quad (2.14)$$

$$\alpha \wedge \beta \in [0, 1] \quad (2.15)$$

and

$$\alpha + \beta = 1 \quad (2.16)$$

⁶Mitschke/Wallentowitz (2004): Dynamik der Kraftfahrzeuge p. 202

The braking distance can be calculated by integrating the longitudinal velocity with respect to time:

$$d_B = \int_{t_{BB}}^{t_{BE}} v_x(t) dt \quad (2.17)$$

The longitudinal velocity again is the integral of the longitudinal acceleration. Applying this leads to:

$$d_B = \int_{t_{BB}}^{t_{BE}} \left[\int_{t_{BB}}^t a_x(\tau) d\tau + v_{x,0} \right] dt \quad (2.18)$$

Applying equation 2.6 and integrating:

$$d_B = v_{x,0} \Delta t_B - \frac{1}{m_V} \int_{t_{BB}}^{t_{BE}} \int_{t_{BB}}^t F_{B,\text{total}}(\tau) d\tau dt \quad (2.19)$$

With equation 2.12 this gives:

$$d_B = v_{x,0} \Delta t_B - \frac{2 \bar{F}_{B,\text{total}}}{m_V} \int_{t_{BB}}^{t_{BE}} \int_{t_{BB}}^t \alpha + \frac{\tau}{t_{BE}} (\beta - \alpha) d\tau dt \quad (2.20)$$

Together with equation 2.16 one eventually ends up with

$$d_B = \frac{v_{x,0}^2 m_V}{3 \bar{F}_{B,\text{total}}} (2 - \alpha) \quad (2.21)$$

Equation 2.21 shows that the braking distance does not depend on the average braking force applied to the tires during a braking procedure only—precisely, it is a reciprocal dependency there—, but also depends on the distribution of braking force over time. The greater α , the shorter the braking distance. The shortest braking distance possible with the given assumptions is gained if $\alpha = 1$. In this case $\beta = 0$ and the braking force would therefore linearly decrease with time until it reaches the value zero at the end of the braking procedure. In this optimal case the braking distance would be

$$d_B = \frac{1}{3} \frac{v_{x,0}^2 m_V}{\bar{F}_{B,\text{total}}}, \quad (2.22)$$

whereas for a completely uniform distribution of braking force over time ($\alpha = 0.5 \wedge \beta = 0.5$) the braking distance would be much longer:

$$d_B = \frac{1}{2} \frac{v_{x,0}^2 m_V}{\bar{F}_{B,\text{total}}}, \quad (2.23)$$

This means that the earlier the braking force reaches large values during the braking procedure, the shorter the braking distance will be. Therefore it is useful to weight the braking force with the longitudinal velocity in order to build a quantifying parameter. The same holds true for every quantifying parameter which shall be used to rate the quality of

the braking procedure. This is why the weighted value is introduced which shall be defined for any quantity $X(t)$ as:

$$X^{v_x}(t) = X(t) \frac{v_x(t)}{\bar{v}_x}, \quad (2.24)$$

where

$$\bar{v}_x = \frac{1}{\Delta t_B} \int_{t_{BB}}^{t_{BE}} v_x(t) dt \quad (2.25)$$

is the mean value of longitudinal velocity during a braking procedure.

Summarizing, this means that there are two different ways how the braking distance can be shortened in general: First of all—most obvious—by increasing the mean value of braking force during the braking procedure, and secondly by distributing the braking force to the very beginning of the braking procedure. The higher the weighted mean value of braking force is, the shorter the braking distance will be. As for the first aspect, the braking force can in fact only be increased by increasing the average value of the friction coefficient

$$\mu_{\text{mean}} = \bar{\mu} = \frac{1}{\Delta t_B} \int_{t_{BB}}^{t_{BE}} \mu(t) dt, \quad (2.26)$$

because the mean value of wheel load cannot be increased in the long run. Thus, it can only be the braking coefficient that gives a potential to increase the mean value of braking force. As for the second aspect, it is important to weight control quantities higher the earlier (at higher longitudinal velocity) they are measured during the braking procedure. This is what is done in chapter 5. Furthermore, the necessity to reach higher braking forces at a high velocity also leads to the necessity to reach higher wheel loads at a high velocity, because there is a roughly proportional dependency between braking force and wheel load. The wheel load should therefore also be shifted from later to earlier times if possible.

2.2.1 The Quality of a Braking Process

Usually the quality of a braking process is measured by means of the braking distance. The shorter this quantity, the better the braking procedure in terms of driving safety.

Another way of measuring if the braking procedure is good in the sense of an improved driving safety is to look at the distribution of driving speed over the traveled distance. Supposed that an arbitrary full-braking procedure might be initiated in order to avoid a collision, and furthermore assuming that this collision cannot be prevented anymore, because the distance to the collision partner is smaller than the braking distance, how should then the velocity profile look like in order to be best in the sense of a high safety? Since *ceteris paribus*⁷, with an increasing amount of kinetic energy that has to be converted when a collision occurs, the amount of damage also increases, a good braking procedure is one that has a low kinetic energy (conterminous to a low vehicle speed) as early as possible.

⁷“*Ceteris paribus* is a Latin phrase, literally translated as ‘with other things being the same,’ and usually rendered in English as ‘all other things being equal.’” Source: Wikipedia

This is why the measurand ‘quadratic velocity profile integral’ VI in addition to the braking distance d_B itself is introduced in section 5.1. Integrating the square of the vehicle’s longitudinal velocity with respect to the traveled distance gives a measurand that indicates the distribution of kinetic energy (which is proportional to the square of the vehicle speed) over the traveled distance. The smaller this measurand, the better the distribution of kinetic energy, because the integral becomes small if during the braking procedure the kinetic energy is low early (with respect to traveled distance). This means the damage caused by a possible crash which occurs during the full-braking is also smaller.

2.2.2 Parameters that Influence the Braking Distance

Several parameters influence the braking distance of a passenger car. In this thesis a division into three groups is made: those parameters that act in the long-run, medium-term run, and those that act in the short-run. This is done to determine which parameters are responsible for the actual outcome of braking distance for a given braking procedure.

Parameters which influence the braking distance in the long-run are those that do not change significantly during one braking process or even during a couple of braking procedures during a day. They change their values in the long-run, meaning a couple of hours or for some parameters even days and weeks. Examples for those parameters are the tire profile, the filling status of the vehicle’s tank, or the surrounding air pressure. During one testing day those parameters can be assumed constant.

In contrary, parameters that influence the braking distance in the short-run are those that in fact change significantly during one single braking process. Examples for those parameters are the braking pressure, the local maximum friction factor between tire and pavement, or the course of vertical tire forces, which can be influenced by the vertical damping of the vehicle.

Furthermore, there are those parameters that act in the medium-term run. Those are the ones that can change from one braking process to another or from one block of braking procedures to another. During one braking process they are assumed to be constant.

Besides the classification in the time domain, there is yet another way to classify the parameters that affect the braking distance: A classification that values the controllability of the parameters. Again, there are three groups amongst which the parameters can be distributed.

First of all, the parameters that can be measured and controlled. Secondly, those that can only be measured but not controlled. Thirdly, those that can neither be measured nor controlled. Not being measurable does not necessarily mean that the quantity discussed is not measurable in general, but it means that it is not measurable in the given context with the tools provided. The same holds true for the meaning of not controllable.

An example for a parameter which can be measured and controlled is the tire inflation pressure. An example for an only measurable quantity is the temperature of the pavement.

⁸The tire temperature is controllable in the sense that before a braking procedure that should be measured is executed, there are as many braking procedures executed in advance as are necessary to obtain a stationary tire temperature such that it always has the same value at the beginning of a braking process. During braking the tire temperature will always increase, while between two braking processes the tire will cool down again. Stationary means that the amount of energy that is put into the tire during braking equals the amount of emitted heat between to braking processes.

⁹The same as for the tire temperature holds true.

Table 2.1: Parameters that influence the braking distance. Classification in the time domain and in the domain of controllability.

	Measurable and Controllable	Only Measurable	Neither Measurable nor Controllable
Short Run	<ul style="list-style-type: none"> • Time at which the clutch is uncoupled t_C • Settings of the active shock absorbers I_D • Course of wheel load 	<ul style="list-style-type: none"> • Course of steering wheel angle • Actions of the ABS-controller $p_{ABS,i}$ 	<ul style="list-style-type: none"> • Variations of local friction factor μ
Medium-term Run	<ul style="list-style-type: none"> • Initial velocity $v_{x,0}$ • Tire temperature T_T⁸ • Gradient of braking pressure at the beginning of the braking procedure • Braking disc temperature T_B⁹ • Slope of the road • Gear in which a braking procedure is executed 	<ul style="list-style-type: none"> • Wind direction • Wind speed 	
Long Run	<ul style="list-style-type: none"> • Tire inflation pressure p_T 	<ul style="list-style-type: none"> • Surrounding air pressure • Surrounding air density • Road condition (dry, wet) • Type of road (cobblestone, asphalt, ...) • Pavement temperature t_P 	<ul style="list-style-type: none"> • Vehicle's mass distribution

And an example for a quantity that can neither be measured nor controlled is the actual local friction coefficient between tire and pavement.

Other parameters, such as the drag coefficient, are assumed to be constant for all times. Though they have an influence on the absolute value of the braking distance, they do not vary and therefore do not influence the braking distance differently from one braking procedure to another.

In the experimental setup for full-braking tests all those parameters that can be controlled are kept constant. The other parameters influence the braking distance in a stochastic way. Their influence cannot be eliminated, thus they must be treated statistically by using methods of statistics.

2.3 Possibilities to Influence the Braking Force

In Figure 2.7 forces and torques at a spinning, braked wheel are shown. In the following the quantities used shall be introduced and defined.

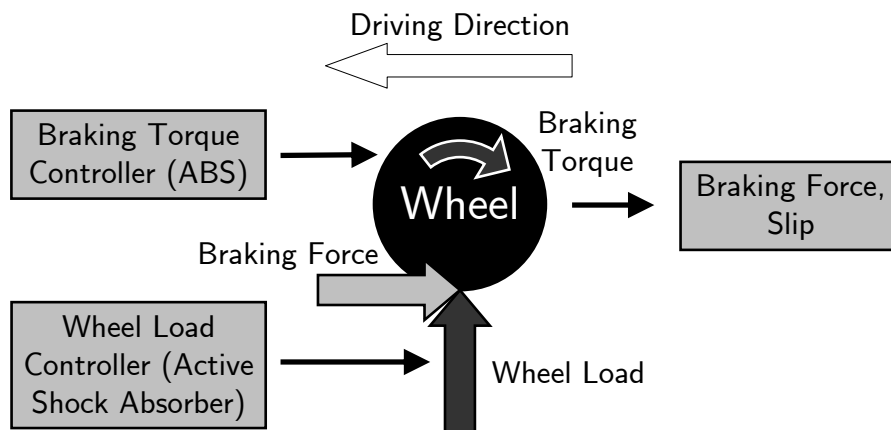


Figure 2.7: Possibilities to influence the braking force by either a braking torque or a wheel-load controller. As for the braking torque controller the ABS is state-of-the-art, as for the wheel-load controller active shock absorbers are used in this thesis.

Braking Force F_B

The braking force at a wheel is the longitudinal part of the tire force in the contact zone of tire and pavement. The braking force causes the vehicle to decelerate and the wheel at which it is applied to accelerate.

Braking Torque M_B

The braking torque at a wheel is the torque around the wheel's y-axis that causes the wheel to decelerate.

Braking Slip λ_B

The braking slip at a wheel is defined as the difference of vehicle's longitudinal speed v_x and wheel speed v_w per v_x . If the wheel locks, the braking slip equals one. If the wheel is

completely free spinning, the braking slip equals zero.

$$\lambda_B(t) = \frac{v_x(t) - v_W(t)}{v_x(t)} = 1 - \frac{\omega_W(t) r_{\text{eff}}}{v_x(t)} \quad (2.27)$$

Braking Coefficient μ

The braking coefficient μ at a wheel is defined as ratio of braking force F_B at the wheel and wheel load F_z at the same wheel (for the definition of wheel load refer to section 4.1). Its maximum value μ_{max} is reached if at a given level of wheel load the braking force cannot be increased anymore.

$$\mu(t) = \frac{F_B(t)}{F_z(t)} \quad (2.28)$$

$$\mu_{\text{max}} = \left. \frac{F_{B,\text{max}}}{F_z} \right|_{F_z=\text{const.}} \quad (2.29)$$

Applying the principle of angular momentum to the spinning wheel leads to:

$$J_W \ddot{\varphi}_W(t) = F_B(t) r_{\text{eff}} - M_B(t), \quad (2.30)$$

where J_W is the mass moment of inertia of the wheel, $\ddot{\varphi}_W$ is the angular acceleration of the wheel, and r_{eff} is the wheel's effective radius. The braking force and the wheel load are connected via equation 2.28, where μ again is a function of the braking slip λ_B .

$$\mu = \mu(\lambda_B) \quad (2.31)$$

The braking slip is defined in equation 2.27. In its definition the rotational speed of the wheel is involved, which means that the loop is closed back to equation 2.30.

From those simple considerations it becomes clear that the angular dynamics of the wheel and with it the dynamics of the braking force have two inputs: Braking torque and wheel load. Even though there are several parameters which do influence the braking performance via their influence on the braking force (refer to section 2.2.2), generally speaking there are those two parameters to influence the braking force on a braked wheel which can be controlled by a car-internal system. The braking force can either be manipulated by controlling the braking torque or by controlling the wheel load. Both are inputs for the wheel-system. Their values together with other uncontrollable parameters determine the braking slip and the braking force.

If there is a braking torque applied to a wheel, the wheel will slow down. This means that then the wheel spins slower than it ought to spin in order to hold the same longitudinal speed as the vehicle does. The slowing down of the wheel together with the constant longitudinal velocity of the vehicle leads to a braking slip at the wheel. This means that in the tire contact area there are longitudinal forces acting between pavement and tire, because there is a gap in speeds of vehicle and wheel/tire.

A slipping wheel is slightly different from standard rubber friction. In the case of standard rubber friction as it is shown in Figure 2.8, two main processes lead to a friction force: hysteresis and adhesion. While hysteresis is due to the unevenness of the pavement

and is therefore only effected little by changing friction coefficient of the pavement-tire-connection, adhesion strongly depends on this friction coefficient. Adhesion is therefore much smaller for wet roads than for dry ones, while hysteresis is almost not effected by such changes. Both effects need little amounts of deformation of the rubber in longitudinal direction to have an effect.

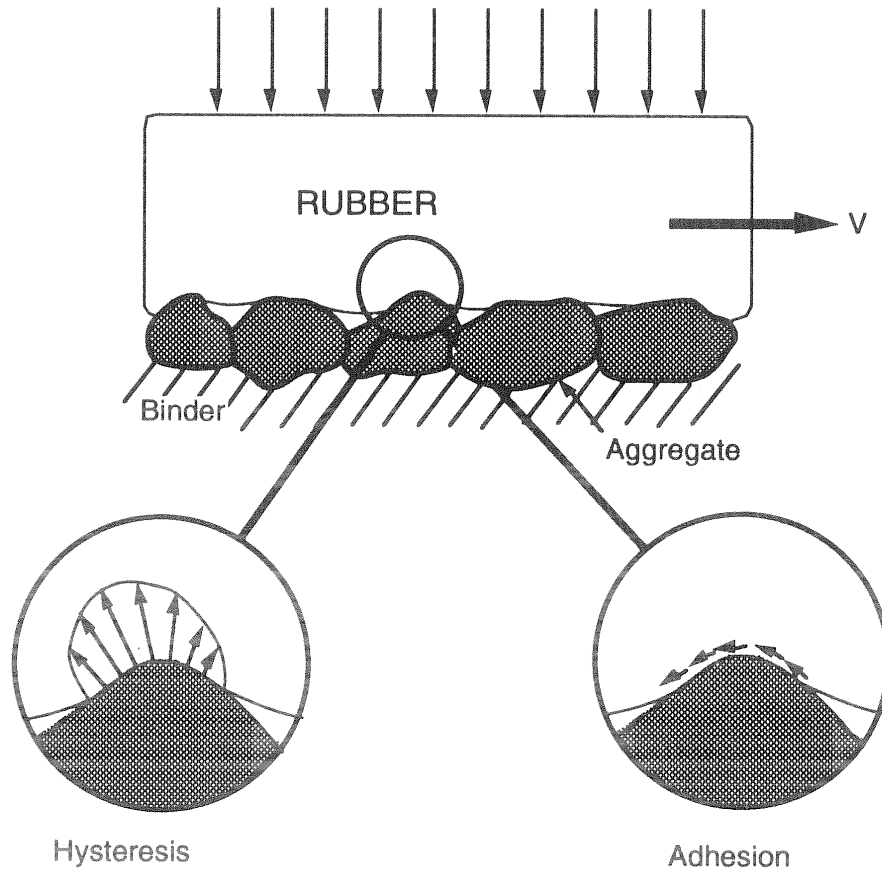


Figure 2.8: Mechanisms of rubber friction¹⁰.

Anyways, if the maximum applicable friction coefficient is exceeded, the rubber in Figure 2.8 begins to slide. The same holds true in case of a spinning tire with braking torque applied.

The difference is that the total tire contact zone can be divided into different contact areas, and depending on the amount of braking torque applied more or less of those areas have slipping tread elements. A tread element at the very beginning of the contact zone is undeformed. As it enters the contact zone it gets deformed. This deformation is caused by the friction force between pavement and tire. The friction force again occurs because there is a velocity difference of the tread elements of the tire and the pavement, which is caused by the deceleration of the wheel due to the braking torque applied. The further the tread element goes to the center of the tire contact zone the more deformation is applied to it.

¹⁰cp. Meyer/Kummer (1962): Mechanism of force transmission between tire and road p.18 according to Gillespie (1992): Fundamentals of Vehicle Dynamics p. 54

At high braking levels there are areas of the total contact zone in which the adhesion forces of the tread element cannot stand the deformation anymore and the respective elements begin to slip. In those areas the friction force is decreasing.

Figure 2.9 shows the described process. The vertical load, the friction force, and the relative slip are shown. The integrals over the total tire contact zone of those three quantities give the total wheel load, the total braking force, and the total braking slip of the wheel. Therefore, the whole deformation and relaxation process finally leads to the braking force of the wheel that leads to the deceleration of the vehicle.

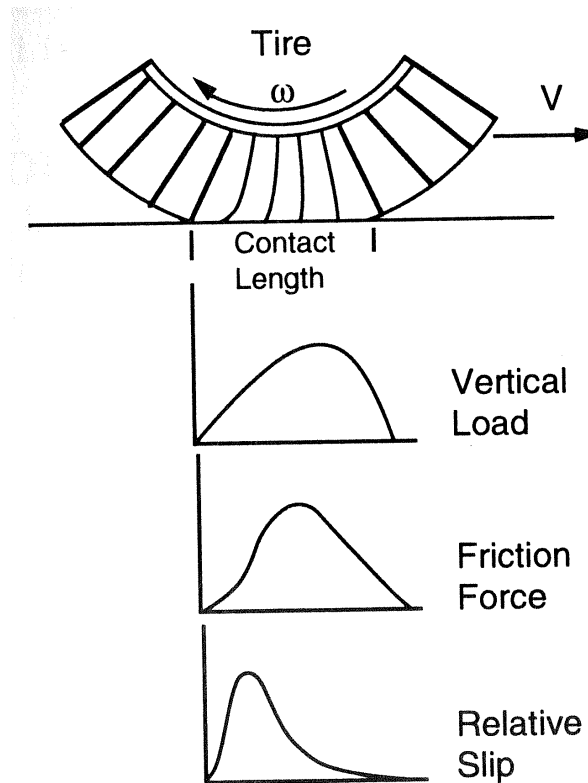


Figure 2.9: Deformation of the tire in its contact zone due to braking torque and braking force applied in a braking situation¹¹.

It also becomes clear that if and only if a braking slip occurs a braking force can be applied to the ground. Furthermore, the maximum braking force is applied at braking slip levels in the lower part of the spectrum from zero to one and not if the wheel locks. In this locked case every single tread element slides over the ground. Since friction forces are greater for friction of rest than for sliding friction, the maximum braking force applicable is the greater the less contact areas do slide.

In the best case (maximum braking force) the tread elements are all close to sliding but do not totally slide and sliding is limited to local areas. The reasoning given also explains why for bold tires the optimal braking slip is lower than for brand-new tires. The shorter the deformable tread elements, the stiffer they are. This means that the same amount of longitudinal force causes less deformation. Also the maximum braking force just before the tread element slips is reached at lower deformation levels. That is why the braking slip has smaller values the shorter the tread elements are.

¹¹Gillespie (1992): Fundamentals of Vehicle Dynamics p. 55

2.3.1 Influence via Braking Torque—ABS

The braking torque—which is the reason for the deceleration of the wheel and the existence of the braking force—can be applied to a wheel in several different ways, e.g. by electromagnetic forces or by frictional forces. In any case the braking torque times the angular velocity of the wheel delivers the part of total braking power at a wheel that is converted by the brake. The other part of the total braking power is converted in the tire contact zone. This part is calculated by the velocity difference of longitudinal velocity v_x and wheel speed $v_W = \omega_W r_{\text{eff}}$ times the braking force at the respective wheel.

The ratio of the part of the total braking power converted in the tire contact zone and the total braking power itself equals the braking slip. In case of a locked wheel, i.e. 100% braking slip, the entire braking power is converted in the tire-pavement-zone.

In case that the braking torque is applied by a frictional force, the frictional partners (e.g. braking disc and braking pads) have to be compressed by a normal force. This normal force together with the actual friction coefficient leads to the actual friction force. The normal force again can be generated in different ways, e.g. hydraulically, mechanically, or pneumatically. In today's series passenger cars the hydraulic solution predominates all other solutions by far.

Figure 2.10 shows the principle layout of an Antilock Braking System (ABS) within a hydraulic braking system. The force applied by the driver at the braking pedal increases the braking pressure in the brake master cylinder (BMC). This pressure is transmitted via the brake lines to the wheel-brake cylinders. If the pressure applied by the driver is low, the ABS will not control, the vehicle brakes as if the ABS was not there. This means the inlet valves are opened, the outlet valves at every wheel are closed.

If the braking slip at a wheel becomes too large, the respective inlet valve is closed in order to disconnect the BMC and the high pressure from the respective wheel-brake cylinder. If the slip is still too large or is even increasing, the outlet valve is opened. By this the braking pressure at the critical wheel is released and with it the braking torque. The ABS therefore has three possible settings for every wheel: inlet valve open and outlet valve closed, inlet valve closed and outlet valve closed, inlet valve closed and outlet valve opened. The variable $p_{\text{ABS},i}$ is introduced, which can take values of -1, 0, and +1, depending on the ABS' current action at the i -th wheel. These three settings shall be named as:

- Increase braking pressure = inlet valve opened and outlet valve closed: $p_{\text{ABS}} = +1$
- Hold braking pressure = inlet valve closed and outlet valve closed: $p_{\text{ABS}} = 0$
- Release braking pressure = inlet valve closed and outlet valve opened: $p_{\text{ABS}} = -1$

The ABS implemented in the testing vehicle also works on the hydraulic basis with a system similar to the one shown in Figure 2.10. The signals of the wheel-speed sensors are used to calculate the actual velocity v_x of the car and to decide if one of the wheels is about to lock or not.

The algorithm of deciding between increasing, holding, or decreasing braking pressure is shown in Figure 2.11. It shows a control cycle of a today's ABS for high friction conditions (friction between pavement and tire). The increase of braking pressure leads to a decreasing velocity v_x and an also decreasing angular velocity ω_W of the wheel.

¹²Robert Bosch GmbH (1999): Kraftfahrtechnisches Taschenbuch p. 665

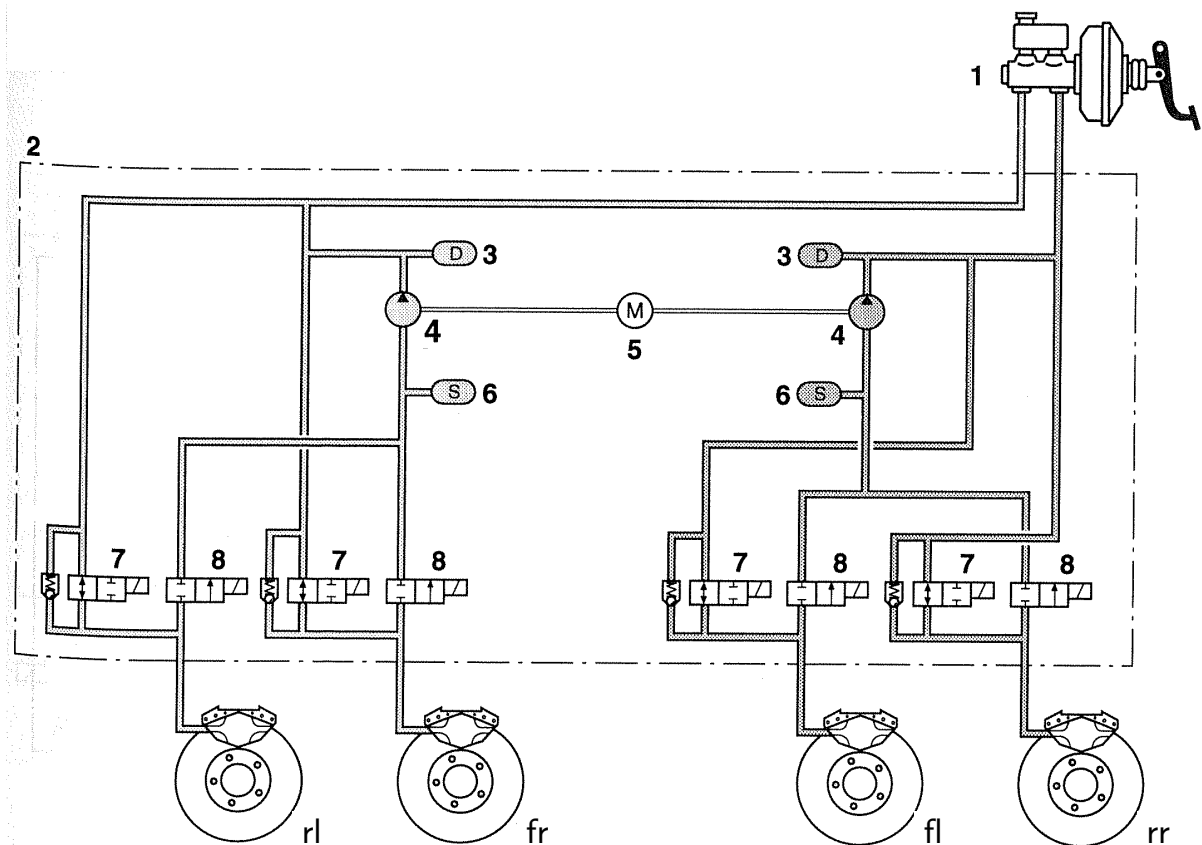


Figure 2.10: Setup of an Antilock Braking System (ABS) that is similar to the one installed in the testing vehicle¹². 1: Brake master cylinder (BMC), 2: Hydraulic unit, 3: Damping chamber, 4: Return pump, 5: Motor, 6: Reservoir, 7: Inlet valves, 8: Outlet valves.

The angular acceleration of the wheel $\dot{\omega}_W$ is negative and stays at a more or less constant level while the braking force and therefore the braking slip is increasing. If the maximum of the μ -slip curve is reached (refer to Figure 2.5), $\dot{\omega}_W$ drops dramatically. This happens because at the maximum of the μ -slip curve a further increase in braking torque cannot be compensated by an increase in braking force anymore. It must therefore lead to an angular acceleration of the wheel which will finally make it lock—if the braking pressure and with it the braking torque is not lowered in time. This sudden drop of wheel angular acceleration is detected by the ABS. Once the threshold ($-a$) is passed, the braking pressure is kept constant (hold braking pressure). The wheel speed at the time of passing the threshold a is memorized and named $v_{\text{reference}}$. Due to the negative angular acceleration of the wheel, the wheel speed will also drop. If the wheel speed referred to $v_{\text{reference}}$ drops below a slip threshold λ_1 , the braking pressure is released ($p_{\text{ABS}} = -1$), in order to prevent the wheel to lock and to keep the braking slip close to the optimal braking slip with the highest friction coefficient possible.

An important point to keep in mind is that, due to the ignorance of the ABS about the type of tire used, the ABS needs to determine where the optimal braking slip lies for every braking process newly. Thus, the first drop in wheel angular acceleration and in wheel speed can never be prevented. It is rather a necessary part of the ABS control algorithm.

This first drop in angular acceleration happens shortly before the maximum of the μ -slip curve is reached. Because of the degressive curvature of the μ -slip curve close to its maximum, an increase in braking torque does not lead to an increase in braking force in the same dimension anymore—this is what happens in the linear part of the μ -slip curve. Hence, because the ABS waits for the angular acceleration to drop below the threshold ($-a$) and the first drop happens close to the maximum of the μ -slip curve, this waiting can be treated as determining the maximum of the μ -slip curve¹³.

Due to releasing the braking pressure, the angular acceleration of the wheel will increase again. Once it crosses the threshold ($-a$)—this time from below—, the braking pressure is kept constant again. If this constant level of braking pressure is such low that the wheel will spin up more and more, the braking pressure can be increased again. This happens if the angular acceleration of the wheel crosses the threshold A . If this very threshold is crossed from above again, the braking pressure is kept constant. It increases even further once $\dot{\omega}_W$ crosses the threshold $+a$. Then the control cycle starts from its beginning. The whole process is meant to find the optimal braking slip and to adjust the actual braking slip to it.

¹³Robert Bosch GmbH (1999): Kraftfahrtechnisches Taschenbuch p. 662.

¹⁴Robert Bosch GmbH (2000): Automotive Handbook p. 662

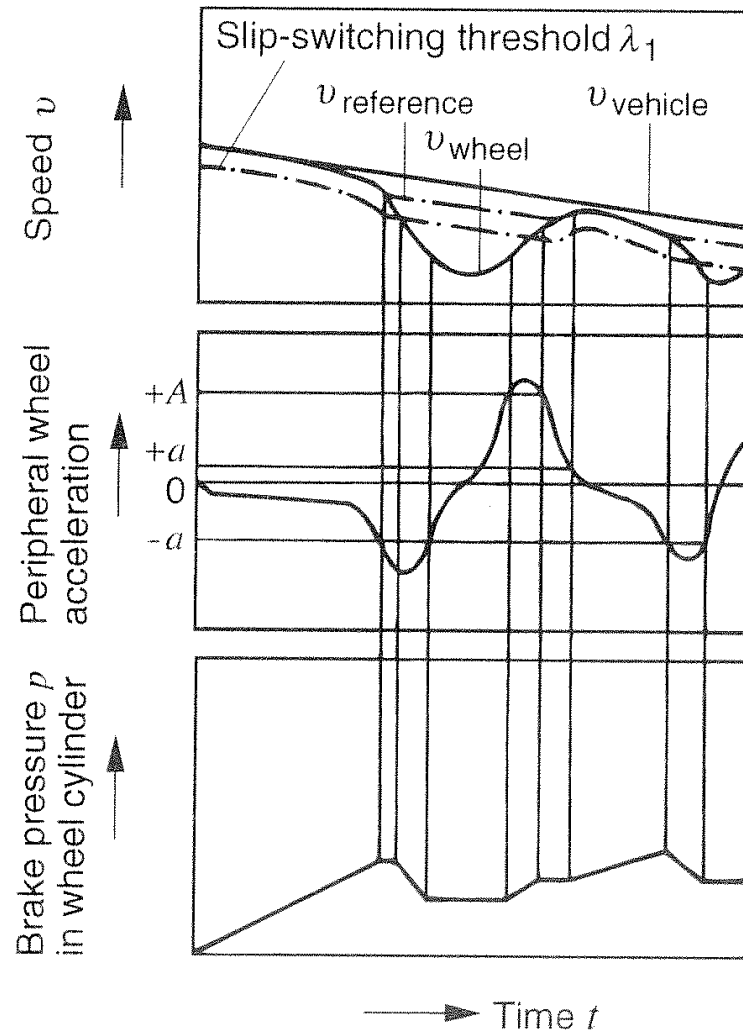


Figure 2.11: ABS control cycle for large friction coefficients¹⁴. $v_{wheel} = v_W$, $v_{vehicle} = v_x$.

2.3.2 Influence via Wheel Load—Active Shock Absorbers

For two reasons the ABS cannot completely reach the goal of keeping the braking slip constant at the optimal level: Firstly, information about the actual μ -slip curve is not present. The ABS has to estimate it. Secondly, and this is even more limiting, the ABS has no influence on the vertical tire force: the wheel load. But this force is the second input for the angular dynamics of the wheel (refer to Figure 2.7). In the same manner as the braking torque does, the wheel load also influences the rotational dynamics of the wheel.

The only difference is that a changing wheel load has to be transferred into a changing braking force before it causes an angular acceleration of the wheel. Here a time delay appears: If an additional wheel load is applied, the tread elements of the tire have to deform first before the additional wheel load leads to an additional braking force. The time that it takes for this additional braking force to establish lies in the scale frame of a couple of milliseconds. In later chapters (refer to 5.5) this connection between wheel load and braking force is investigated. Similar thoughts hold true for the connection between a lowered wheel load and the decreasing braking force. In this direction the effect should establish faster. This assumption cannot be falsified by the results shown in Figure 5.5 on page 123, but it also cannot be verified, due to too high amounts of noise and deviations of wheel load.

But a thought experiment makes the direction of thinking clear: A drastic example for the influence which wheel load has on the rotational dynamics of a wheel is a completely lifted wheel. In this case no braking force can be applied at all and the wheel will be slowed down by a braking torque present very quickly. If the wheel is lifted, the braking force breaks down immediately. In the other direction, if the wheel is set back on the pavement again, it takes some amount of time for the tread elements to deform and to carry the braking force. This extreme example makes clear that the effect which a changing wheel load has on the braking force is assumably faster in the one direction than in the other.

The best thing in the sense of an optimal braking performance would be if each wheel was slowed down such that the braking slip is constant at the optimal braking slip for all times. This is because in this case $\mu = \mu(\lambda_{B,opt}) = \mu_{max}$ would be highest. If the wheel should be slowed down in such a way, this means that—assuming a constant deceleration of the vehicle—the angular acceleration of the wheel would have to be constant as well.

A constant angular acceleration of the wheel implies a constant torque acting on this wheel. That means the difference of braking torque and braking force times effective wheel radius needs to be constant, because those two quantities sum up to the total torque on the wheel. A fluctuation in braking torque should therefore always be compensated by a fluctuation of braking force in the other direction. This change in braking force can only be caused by a corresponding change in wheel load.

Furthermore, referring to section 2.2, the wheel load can provide yet another tool: By trying to increase wheel load at earlier times of the braking procedure and reducing it at later times, the braking force will also be increased at earlier times, which eventually leads to a shorter braking distance. Doing all these considerations it must always be kept in mind that the mean value of total wheel load with respect to time over a whole braking procedure can neither be in- nor decreased. It is always equal to the total static wheel load. For a single wheel of the front (rear) axle, the mean value over a braking procedure equals the static wheel load plus (minus) the wheel load due to the weight transfer from rear to front axle.

2.4 Conclusions

In this chapter the fundamentals of vehicle dynamics which are relevant for this thesis were introduced. The braking process in general and the possibilities to influence the braking force in particular were presented.

Concerning the braking procedure it was noticed that the braking distance can be reduced in two different ways:

- Increasing the time-average of the braking force
- Distributing braking force from later to earlier times of the braking procedure

The possibility to increase the time-averaged braking force is given by the fact that due to slip oscillations the maximum friction coefficient is not fully utilized in today's braking procedures.

Furthermore, besides the braking distance itself another measurand was introduced: The quality of the braking procedure, measured by means of the integral of the squared vehicle's velocity VI . This quantity indicates the possible damage in case a collision cannot be prevented anymore. The smaller VI , the better.

Depending on the distance of the center of mass and the pitching center, a braking procedure more or less leads to oscillations in the vertical tire force (the greater the distance, the more oscillations), even on an ideally even road. Those oscillations influence the braking behavior.

Two possible ways were introduced that are feasible to influence the braking distance: Either the control of braking torque or the control of wheel load. In this thesis the latter is investigated.

3 Tools and Research Environment

3.1 Active Shock-Absorbers

Shock absorbers in passenger car suspensions serve two different purposes: Firstly, they have to guarantee the passengers' riding comfort. Secondly, they have to care for a high handling performance. Both demands have in common that for their fulfillment it is necessary to reduce vibrations in the suspension system. This is done by dissipating energy in the shock absorbers.

For riding comfort purposes the focus lies on the vibrations of the vehicle's body, for an improved handling it lies on the oscillations of the vertical tire force—namely the wheel load. Shock absorbers as a part of the vehicle's suspension usually are mantled between wheel and body. They produce forces opposing the vibratory motion. Shock absorbers usually produce a higher damper force in rebound than in compression for the same damper velocity¹. This is due to the fact that in compression the damper velocity can be much higher than in rebound, because if the vehicle is passing an obstacle that is similar to a step input, the wheel must be accelerated upwards very quickly in order to follow the step. The vehicle's body with its inertia standing against the damper force is also accelerated upwards. If the damping coefficient in compression was very large, the potentially very large damper velocity in compression would lead to a strongly accelerated vehicle body. This would bring unwanted oscillations into the system and could cause damages due to huge damper forces.

In the other direction, passing a step input with negative height or a hole, the damper velocity is only as large as the wheel is accelerated downwards by the spring force. There is no boundary restriction that implies that the wheel must be accelerated by a very high amount. Therefore, it does not do any harm if the damping coefficient is high in rebound. In fact, the rebound phase can be used to dissipate as much energy as possible. This is why the damping coefficient usually is approximately two times greater in rebound than in compression.

The same principle holds true in case of active shock absorbers. There, the rebound is harder than the compression stage (refer to Figure 4.3 on page 66), too. Active shock absorbers are characterized by the fact that their damping coefficients can be adjusted within a short amount of time. They do not only have one fixed characteristic line but rather—in case of continuously adjustable shock absorbers—an infinite number of characteristic lines. The two extreme characteristic lines shall be called 'hard' and 'soft' in this thesis (refer to Figure 4.12 on page 77).

The shock absorber that is used for all experimental testings is a so called CDC-shock absorber². Its characteristic lines can be adjusted by an electromagnetic valve. The construction of this kind of shock absorber is shown in Figure 3.1. Here, via the opening

¹Dixon (1999): The Shock Absorber Handbook p. 250.

²Continuous Damping Control by ZF Sachs AG

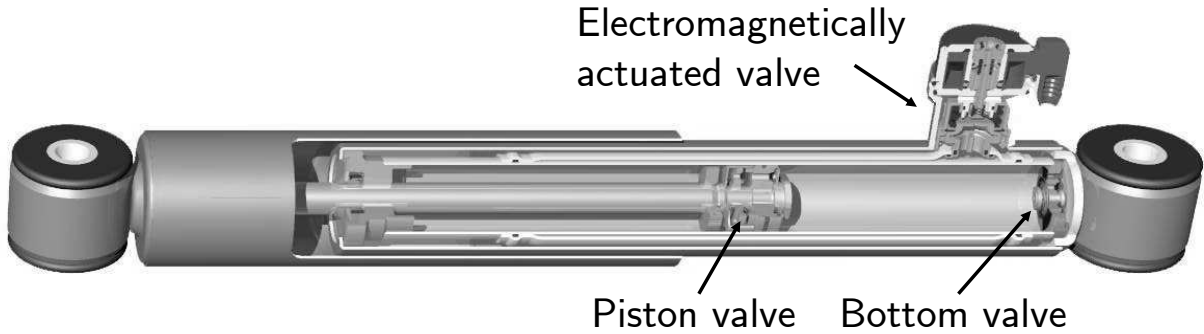


Figure 3.1: Example for an active shock absorber with external proportional and electromagnetically actuated valve. Source: ZF Sachs AG.

condition of an outlying electromagnetically actuated valve the damping ratio is changed. Constructions where the electromagnetically actuated valve is inside the shock absorber, integrated in the piston valve, are also known³. For the shock absorbers used in this thesis the hard damping is achieved by setting the current of the electromagnet to $I_D = 0$ A. The soft damping is set by a damper current of $I_D = 1.6$ A. Both characteristic lines (soft and hard) for the shock absorbers of the front and the rear axle can be seen in Figures 4.3 and 4.4 on pages 66 and 67. The reason for having the shock absorber in its hardest stage with no damper current present is that in case of a system failure the shock absorbers should not be soft but rather hard. This is because harder damping is supposedly better in the sense of a higher handling performance and is therefore safer.

In Figure 3.2 the functional principle of active shock absorbers that are controlled by an electromagnetically actuated valve is shown. The two functional principles are an inlying active valve (A) and an outlying active valve (B). In case (A) the hydraulic oil that is pushed away by the piston rod in compression is pressed through the bottom valve into the intercepting chamber. At the same time the oil from below the active piston valve is pressed through this valve into the chamber above it. Both valves, bottom and active one, deliver part of the damping. In rebound, the oil streams back from the intercepting chamber into the piston chamber through the second bottom valve, whose damping factor can differ from the one of the bottom valve which is responsible for the damping in compression. Furthermore, the oil is pressed from the lower to the upper piston chamber through the active valve. In both stages (compression and rebound) part of the damping is delivered by the active valve. Thus, the damping coefficient can be influenced by changing the opening condition of this valve.

In case of an outlying active valve the same considerations hold true in general. The difference here is that the oil streams through the active valve always in the same direction. In compression, oil is passing through the piston and the active valve, in rebound, it is the bottom and the active valve which provide the damping.

For any shock absorber (no matter if active or not) the rebound/compression damping factor ratio s_{RC} shall be defined as the ratio between linearized damping coefficient in rebound and the linearized damping coefficient in compression:

$$s_{RC} = \frac{k_{B,R}}{k_{B,C}} \quad (3.1)$$

³Causemann (2001): Kraftfahrzeugstoßdämpfer p. 60.

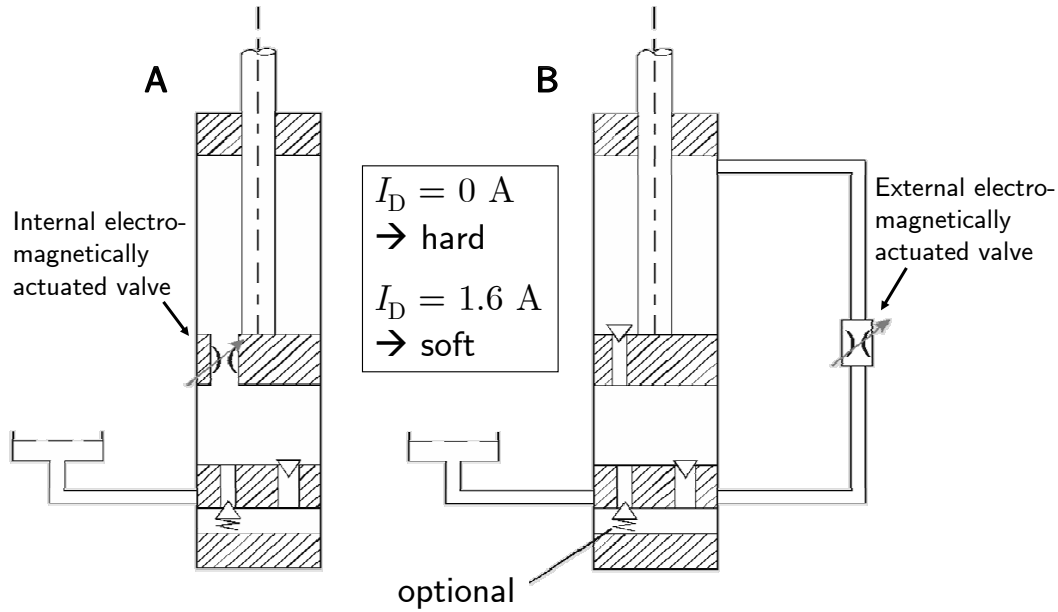


Figure 3.2: Principle of the function of active shock absorbers⁴. A: Internal electromagnetically actuated valve. B: External electromagnetically actuated valve.

For a passive shock absorber this factor is constant and—as already mentioned above—it usually has a value of approximately two. For active shock absorbers this ratio depends on the setting of the shock absorber for rebound and compression. If the shock absorber is set to hard in rebound and soft in compression, the ratio is largest. If it is set to soft in rebound and hard in compression, the ratio is smallest.

For an active shock absorber the spreading with respect to the characteristic lines for hard and soft damping s_{hs} shall be defined as the ratio between linearized damping coefficient in rebound or compression for hard damping and the linearized damping coefficient in rebound or compression for soft damping.

$$s_{hs,R} = \frac{k_{B,R}^h}{k_{B,R}^s} \quad (3.2)$$

$$s_{hs,C} = \frac{k_{B,C}^h}{k_{B,C}^s} \quad (3.3)$$

3.2 Testing Vehicle

The testing vehicle being used for all experimental investigations is an Opel Astra of the latest generation, called Astra H. It is equipped with the so called Interactive Driving System-plus (IDS-plus), which includes Continuous Damping Control (CDC) by ZF Sachs AG, Germany. In series applications this semi-active suspension system mainly is controlled by a skyhook control algorithm which reduces the vertical oscillations of the body in order to improve the riding comfort. If a critical driving situation occurs, the control of this car's active shock absorbers is switched off, meaning that the dampers are

⁴Causemann (2001): Kraftfahrzeugstoßdämpfer p. 56

in their hardest possible setting. This means that during an ABS-braking—which is considered to be a critical situation—the shock absorbers are not controlled and are therefore in the hard setting. Figure 3.3 shows the testing vehicle on the testing track ‘Standard Road’, which is an airfield that belongs to Technische Universität Darmstadt and is not in use for regular air traffic anymore.



Figure 3.3: The testing vehicle which is used for all experimental testings Opel Astra H 2.0i 16v Turbo on the testing track ‘Standard Road’.

The IDS-plus system, besides the active shock absorbers, comes with several additional equipment that cannot be found in the standard series Astra without IDS-plus. These are namely five accelerometers to measure vertical wheel and body accelerations and an Electronic Control Unit (ECU) to handle the signals and calculate the damper current for each wheel individually. In Figure 3.4 the spring-and-shock-absorber unit of a front wheel of the testing vehicle is shown. The main components and their configuration in the car can be seen. The damper velocity is calculated from the signals of the accelerometers that provide the vertical wheel and body acceleration.

3.2.1 Testing Vehicle Specifications

The testing vehicle’s specifications can be found in Table 3.1. The fact that the vehicle is a standard car that can be found in large numbers in the streets is important for the relevance and the transferability of the results gained from investigating the shock absorber controller.

3.2.2 Testing Vehicle Measurement System

Figure 3.5 shows the testing vehicle with its series configuration. Active shock absorbers are included in the series car as well as accelerometers at the front axle (wheels and body) and one accelerometer at the body above the rear axle. In the series application these sensors are connected to an Electronic Control Unit (ECU), which also includes the power amplifier for providing the damper current. The necessary damper current is calculated within the ECU for every wheel individually. It depends on the damper velocity v_D , which is calculated from the acceleration signals at the front axle and on the desired body movements (usually the control objective is to damp the body oscillations against a virtual

Table 3.1: Specifications of the testing vehicle. Sources: N.N. (2006c): Website – Opel Ireland, ZF Sachs AG, and own measuring. Own measuring are in bold.

Property	Specification
Make	Opel
Model	Astra 2.0i 16v Turbo
Engine capacity	1998 cm ³
Maximum power	125 kW at 5,400 min ⁻¹
Maximum torque	250 Nm at 1,950 min ⁻¹
Gross vehicle weight (fl+fr+rl+rr)	1,700 kg = 2 · 480 kg + 2 · 370 kg (fueled, including measurement equipment, driver and one passenger)
Front suspension	McPherson struts, Anti-roll bar, Sub frame, Hydraulic bushings $i_{D,f} = \mathbf{1}$ $i_{S,f} = \mathbf{1}$ $\varepsilon_f = 3.5^\circ$
Rear suspension	Torsion beam, Displaced shock absorbers and coil springs $i_{D,r} = \mathbf{0.68}$ $i_{S,r} = \mathbf{0.88}$ $\varepsilon_r = 26^\circ$
Shock Absorbers	Interactive Driving System-plus (IDS-plus) with Continuous Damping Control (CDC)
Tires	Pirelli P6000, 205/55 R16 91W $r_{\text{eff}} = \mathbf{0.304...0.307 m}$ Standard inflation pressure $p_T = \mathbf{2.3 bar}$
Mass moments of inertia	$J_{W,f} = \begin{cases} \mathbf{1.3 kg m^2} \pm \mathbf{0.1 kg m^2} & \text{for neutral position} \\ \mathbf{3.1 kg m^2} \pm \mathbf{0.1 kg m^2} & \text{for third gear} \\ \mathbf{6.3 kg m^2} \pm \mathbf{0.2 kg m^2} & \text{for second gear} \end{cases}$ $J_{W,r} = \mathbf{0.95 kg m^2} \pm \mathbf{0.08 kg m^2}$ $J_B = 1870 kg m^2$
Rims	Steel rims, 6.5"x16" ET 37
Transmission	Front-wheel drive Six-speed manual gearbox
Braking system	Front ventilated disk brakes (280 mm diameter) Rear disc brakes (264 mm diameter) Friction factor between braking pads and braking disc $\mu_{PD} \approx 0.4$ Factor to transfer braking pressure into braking torque front $i_{p_B 2M_B, f} \approx 24 \text{ Nm/bar}$ Factor to transfer braking pressure into braking torque rear $i_{p_B 2M_B, r} \approx 10 \text{ Nm/bar}$ Anti-lock Braking System (ABS) with Electronic Brake Force Distribution (EBD) Gradient with which braking pressure is relieved by the ABS $\dot{p}_{B, \text{rel}} = \mathbf{-1,000 bar/s}$ Gradient with which braking pressure is increased by the ABS $\dot{p}_{B, \text{inc}} = \mathbf{+250 bar/s}$
Dimensions	Wheel base $l = 2.614 \text{ m}$ Distance from front axle to center of gravity $l_f = \mathbf{1.13 m}$ Distance from rear axle to center of gravity $l_r = \mathbf{1.48 m}$ Height of center of gravity $h_{CG} = \mathbf{0.52 m}$

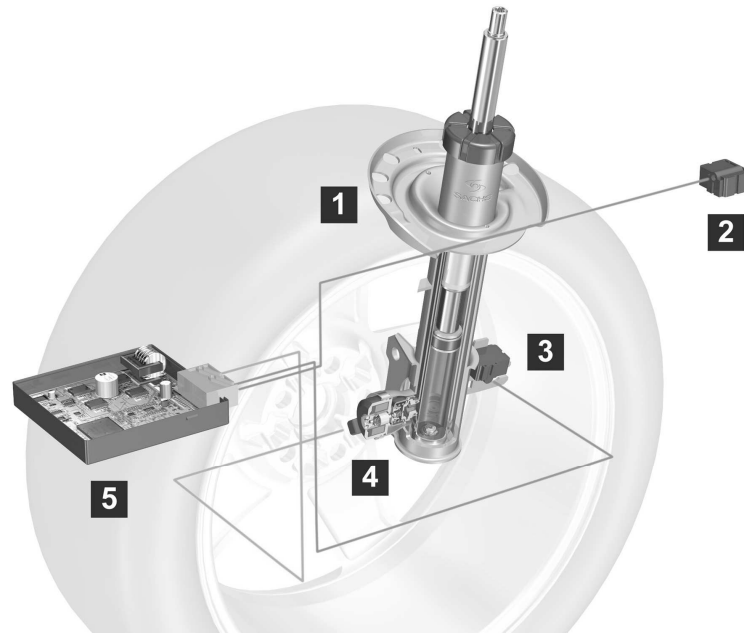


Figure 3.4: Spring-and-shock-absorber unit of a front wheel of the testing vehicle. 1: CDC-shock absorber, 2: Accelerometer for vertical body accelerations, 3: Accelerometer for vertical wheel accelerations, 4: Electromagnetically actuated valve, 5: Electronic Control Unit (ECU). Source: ZF Friedrichshafen AG.

sky-hook). The focus is put on the front axle (it is only there that wheel accelerometers are applied in series application), because the front axle supports 57% of the total wheel load and for series applications it can furthermore be assumed that the vertical excitation at the rear axle will with a phase shift which is reciprocal to the vehicle's speed be the same as at the front axle.

The standard components of the series vehicle are extended by several additional measuring equipment and by an active element, a braking machine. Table 3.2 gives an overview of the measuring equipment.

The measurement system used in the testing vehicle uses analog as well as digital signals. All quantities which are relevant for a braking procedure and which are vehicle internal quantities can be measured. An external quantity e.g. would be the friction coefficient between pavement and tire. This one cannot be measured with the measurement system presented. The core of the measuring and controlling system is a dSpace Autobox which measures all signals, calculates the optimal damper current, and gives this as an output to the active shock absorbers. All data is gained with a sampling rate of $f_s = 2,000$ Hz, in order to be able to measure effects that take place in the time frame of milliseconds.

All quantities measured can be divided into two subsections: First, those measurands that are measured to objectively value the braking procedure and to monitor the parameters that influence the braking distance. These sensor signals are not used to actually influence the braking distance by using them as inputs for a controller, but they are rather stored to be treated off-line, after the test drive is finished. For those measurands it is not critical if their signal is slightly noisy or if there is an offset. Noise and offsets usually

⁵The accelerometers of the body have an integrated high-pass filter of first order with a cutting frequency of 0.5 Hz.

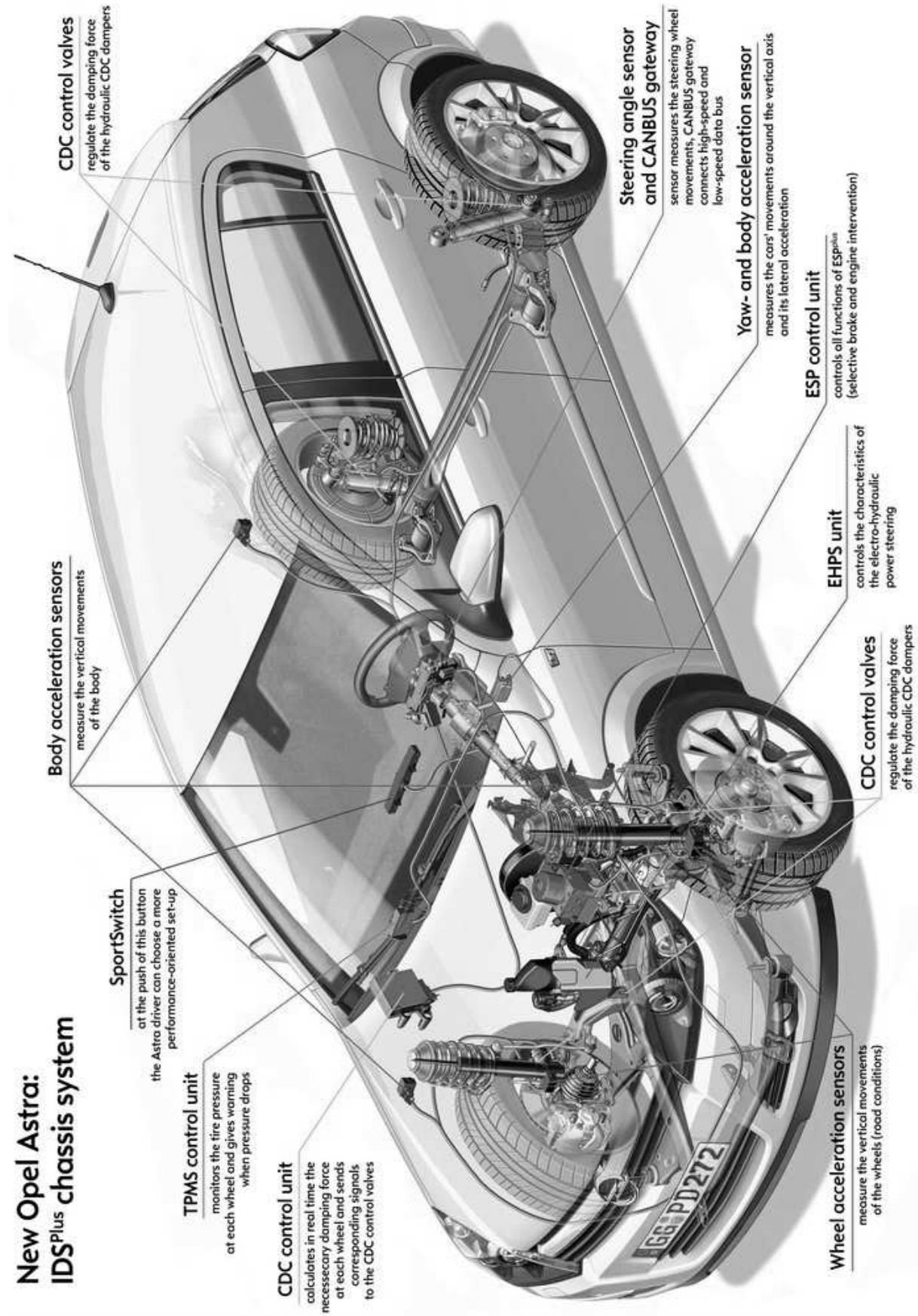


Figure 3.5: The testing vehicle with its series equipment. Source: N.N. (2006a): Website – all4engineers.

Table 3.2: Sensors and actuators in the testing vehicle

Physical Quantity	Sensor	Position	DP
Pressure	Piezo-electric sensor	Wheel braking cylinder fl, fr, rl, rr, and main braking cylinder	analog
Opening condition of ABS-valves	Digital information from the ECU of the ABS	Wheel fl, fr, rl, rr	binary
Displacement	ASM position sensor, potentiometer	Wheel to body fl, fr, rl, and rr	analog
Velocity	Datron Correvit, optical sensor	Rear bumper, longitudinal	analog
Angular velocity	Series sensors	Wheel fl, fr, rl, and rr	CAN
Acceleration	Piezo-electric sensor, same sensor-model as used in the production-model of the Opel Astra ⁵	Wheel fl, fr, rl, and rr, vertical, Body fl, fr, rl, and rr, vertical at suspension strut mounting, Body, longitudinal	analog
Force and torque	Kistler 6-components measuring rim, piezo-electric	Wheel load fl, braking force fl, and braking torque fl	analog
Temperature	Thermocouple Typ K	Brake disc fl	analog
Light intensity	Light barrier sensor	Rear bumper	analog
	Actuator	Position	DP
	Braking machine, electric motor	Attached to the braking pedal	analog
	Magnetic coils	Active shock absorbers fl, fr, rl, and rr	CAN

can be handled off-line with a minimum of loss in signal accuracy. As for the noise, this is because the relevant frequencies lie way below the typical noise frequencies in automotive applications (20–30 Hz compared to 100 Hz and more).

The other group of measurands are more crucial with respect to their realtime computability. It is those measurands which deliver the inputs for the controller—that is why they need to be computed in realtime while driving and braking. The vertical accelerometers provide the signals from which the dynamic wheel load is computed, the position sensors provide the signals from which the damper velocity is determined. Thus, for the vertical accelerations an offset correction is undertaken at the beginning of every test day.

For the position sensors the offset can be neglected, because the damper velocity is the derivative of their signals, and a possible offset therefore does not play a role in the calculation of the desired signal. But by taking the derivative, high-frequency noise is amplified. Hence, filtering is necessary for this signal, which leads to a phase shift. Since the relevant frequencies in the signal of the damper velocity are much lower than the necessary cutting frequency (refer to 5.9 on page 132 for the frequencies of the damper velocity during full-braking, the cutting frequency lies at 40 Hz), this phase shift influences the course of damper velocity in a time frame of a couple of milliseconds. Though there is this additional time delay on top of all other time delays, this one is small compared to the others.

Another crucial sensor whose signal needs to be present in realtime is the light barrier attached to the rear bumper. With this sensor not only the braking procedure is initiated, but also the determination of the longitudinal velocity is verified for every test drive. It is for every test drive that five meters before the light barrier reflector whose signal initiates the braking procedure another light barrier reflector is placed. Thus, knowing this distance of five meters during which the velocity of the vehicle is still constant, the signal from the so called Correvit sensor can be verified and, if necessary, calibrated.

3.2.3 Measuring Rim

A 6-component measuring rim is used for test drives on defined obstacles to determine the wheel load and the braking force at the front left wheel (refer to section 5.2.2 for these test drives). A wheel of the front axle is chosen to mount the measuring rim at, because the front axle is responsible for more than 3/4 of the overall braking force.

Figure 3.6 shows this measuring rim installed at the front left wheel of the testing vehicle. The actual measuring element is connected with the rim well via two rigid adapters. The purpose of using the measuring rim is to measure the wheel load—the vertical tire force in the contact zone of tire and pavement. But between the measurand ‘real wheel load’ F_z and the place of measuring, where the force $F_{z,\text{rim}}$ is captured, lies the tire, which cannot be treated as a rigid body. Thus, $F_{z,\text{rim}}$ only represents F_z with high precision at frequencies that are such low or such high that the tire can be assumed to be rigid. Evers and Reichel investigated this topic in detail for a measuring rim mounted to a 1999 BMW 5 series passenger car on a 4-post test rig⁶.

Figure 3.7 shows the transfer function from the force that is measured by the test rig described in section 3.3 and that is representing F_z in high precision to the force $F_{z,\text{rim}}$

⁶Evers et al. (2002): Radkraft-Dynamometer (RWD/FWD) als Entwicklungswerkzeug für Felge und Rad-aufhängung.

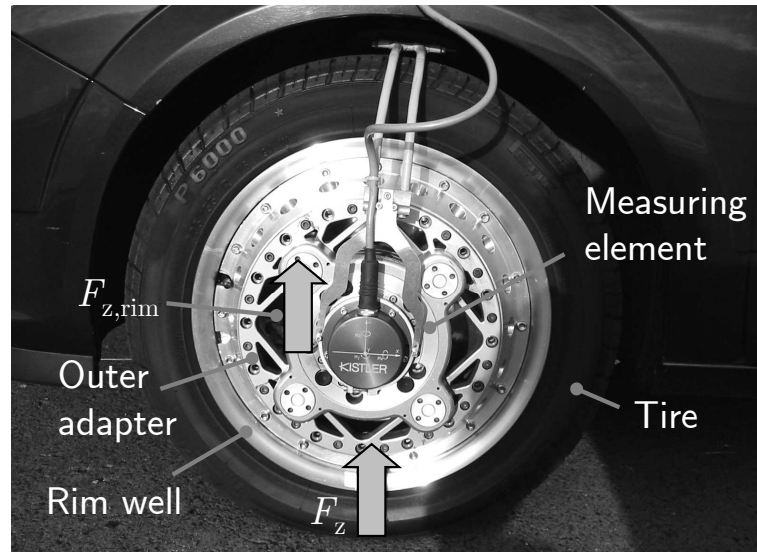


Figure 3.6: Measuring rim installed at the front left wheel of the testing vehicle.

which is measured by the measuring rim. This figure shows that on amplification level the measuring rim represents the real wheel load for frequencies up to 5–12 Hz, depending on the damper setting. The data was gained in test rig trials with the testing vehicle Opel Astra.

For soft damping it starts at 5 Hz that the measuring rim captures a signal that is smaller than the real wheel load. The amplification is approximately 1.5 throughout the frequency band from 5–20 Hz. For hard damping it starts at 12 Hz that the amplification increases and also reaches a value of 1.5 at approximately 20 Hz. On phase level it can be seen that there is almost no phase shift between F_z and $F_{z,rim}$ up to 8 Hz. Starting from there, the phase shift for soft damping decreases linearly, for hard damping it increases slightly but stays bounded to a maximum of 0.1π . The linearly decreasing phase shift for soft shock absorbers implies that there is a constant time delay in the transfer function from real wheel load F_z to rim force $F_{z,rim}$. Calculated from the data in Figure 3.7, this time delay $\Delta\tau_{F_z} \approx 5$ ms.

It is contrary to expectation that the transfer function depends on the damper setting, because the shock absorber is mounted behind the point at which the rim force $F_{z,rim}$ is measured—viewed from tire perspective—and should therefore not influence the considered transfer function. An explanation for this phenomenon cannot be given, but nevertheless the observed time delay can be considered when looking at results when using the measuring rim. For low frequencies up to 5 Hz the signals from the rim can be considered to represent the real wheel load. For higher frequencies the previous considerations must be taken into account.

3.2.4 Indirect Measurands

Several quantities which are needed for the controller or for measuring purposes cannot be measured directly. These have to be determined by calculus from actual direct measurands. Examples for such quantities are the dynamic wheel load, the damper velocity, or the braking slip. The dynamic wheel load, the wheel load integral, and the damper velocity

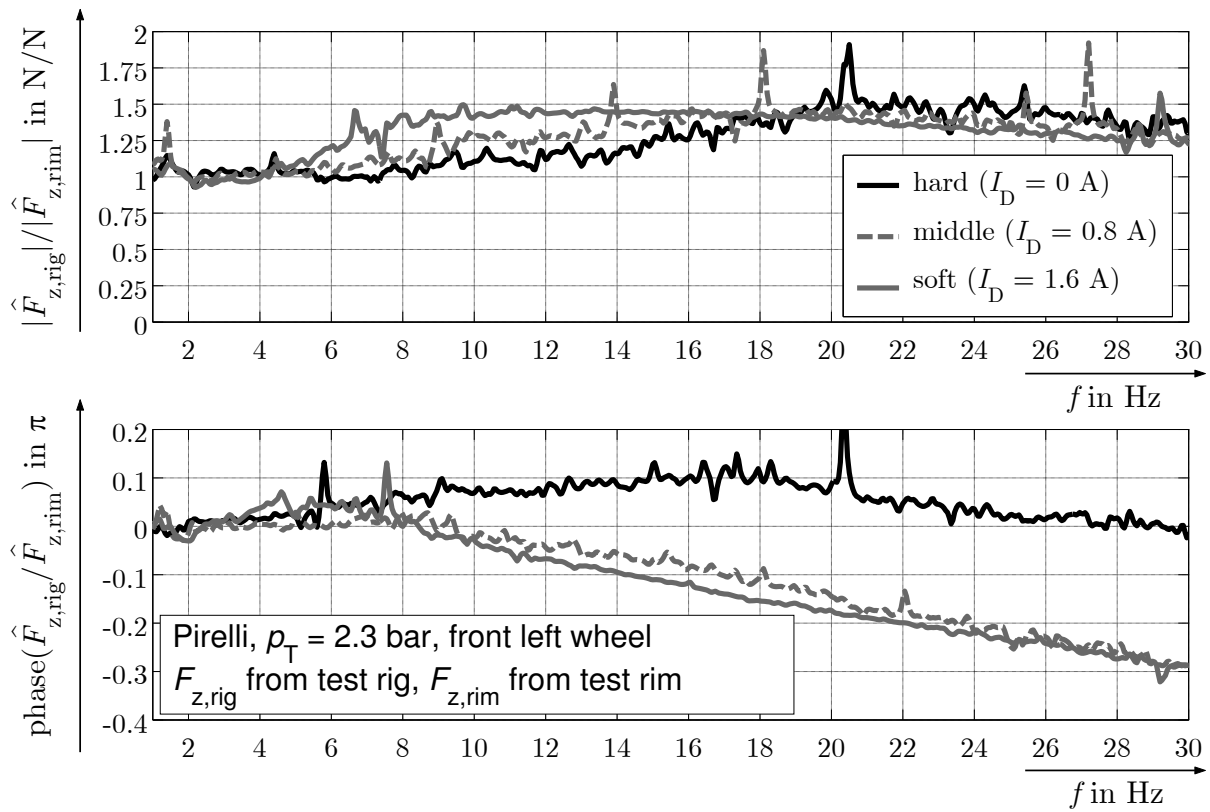


Figure 3.7: Transfer function from wheel load measured by the measuring rim to wheel load measured by the test rig.

take a special place in the list of those non-measurable quantities, because they are essential for the control algorithm. For this reason, these three quantities shall be introduced in more detail.

Dynamic Wheel Load

The dynamic wheel load $F_{z,\text{dyn}}$ is determined by a deviation of the so called Aachen procedure⁷. In the Aachen procedure it is assumed that the vehicle can be modeled with a quarter-car model, where pitching and rolling is neglected. This holds true for constant horizontal forces (constant de- or acceleration or constant lateral forces). In case of transient braking (changing braking forces, beginning of braking), the vehicle cannot be modeled in such a simple way anymore, because the pitching and rolling influences the values of the dynamic wheel load at each wheel. This alone would not make the Aachen procedure unserviceable for determining the dynamic wheel load if those influences of pitching and rolling were completely measurable by means of only the two vertical accelerations of the respective wheel and the respective part of the body. This is not the case, for the wheel load at a given wheel leads not only to accelerations at this very wheel, but at other vehicle corners as well.

Accelerometers are used to calculate the dynamic wheel load on every wheel. In fact, the dynamic wheel load has its highest influence on the vertical acceleration of the respective wheel and on the vertical acceleration of the body directly above this wheel. Moreover, there is an influence on the vertical accelerations of the rest of the vehicle's body with descending strength in the following order:

- The vertical acceleration of the vehicle's body above the second wheel at the same axle
- The vertical acceleration above the second wheel at the same track
- The vertical acceleration of the vehicle's body above the diagonal opposing wheel

The right and left track, and the front and rear axle are coupled via the so called coupling mass. This means that a vertical force at the front (rear) axle leads not only to a vertical acceleration at the front (rear) axle but also at the rear (front) axle. The same holds true for the coupling between right and left track. A vertical force at the right (left) track leads not only to a vertical acceleration at the right (left) but also at the left (right) track. This is because the mass matrices of the vehicle model which explain oscillations in the x-y-plane and in the x-z-plane are both completely filled.

In Figure 3.8 a rigid mass with a mass m and moment of inertia J is shown that shall explain the effect of the coupling mass for a vehicle, both with respect to angular oscillations around the x- and the y-axis. The motion of the mass can be described completely by either making use of the set of coordinates z_1 and z_2 , or by making use of the set of coordinates z and ϑ . Both coordinate systems are a basis for the mass' motion. The mass is forced by an external force at the coordinate z_1 . The mass and its inertia shall stand for half of the mass of the vehicle's body and its inertia around either the x- or the y-axis.

It stands for half of the mass because with this model the coupling along one axle (angular motions around the x-axis) as well as along one track (angular motions around

⁷Winner (2006): Kraftfahrzeuge II p. 95.

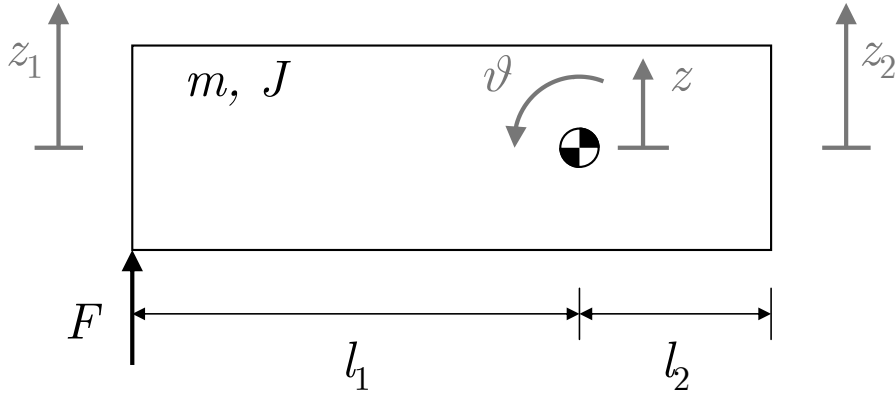


Figure 3.8: Rigid body with mass m , mass moment of inertia J and a force F applied to the coordinate z_1 .

the y -axis) is investigated. The external force stands for the force that is applied at one suspension strut, it might be the damper force that is applied additionally due to switching of the shock absorber. The system of equations that describes the motion of such a mass with an external force is given by:

$$\begin{bmatrix} m & 0 \\ 0 & J \end{bmatrix} \begin{bmatrix} \ddot{z} \\ \ddot{\vartheta} \end{bmatrix} = \begin{bmatrix} F \\ -F l_1 \end{bmatrix} \quad (3.4)$$

Assuming that $\vartheta \ll 1$, the transformation matrix

$$\mathbf{A} = \begin{bmatrix} \frac{l_2}{l_1+l_2} & \frac{l_1}{l_1+l_2} \\ -\frac{l_1}{l_1+l_2} & \frac{l_1}{l_1+l_2} \end{bmatrix} \quad (3.5)$$

can be formed. This matrix connects the two different coordinate systems.

$$\begin{bmatrix} z \\ \vartheta \end{bmatrix} = \mathbf{A} \begin{bmatrix} z_1 \\ z_2 \end{bmatrix} \quad (3.6)$$

Transforming the system of equations presented in equation 3.4 into the coordinate system z_1 and z_2 leads to:

$$\mathbf{A}^T \begin{bmatrix} m & 0 \\ 0 & J \end{bmatrix} \mathbf{A} \begin{bmatrix} \ddot{z} \\ \ddot{\vartheta} \end{bmatrix} = \mathbf{A}^T \begin{bmatrix} F \\ -F l_1 \end{bmatrix} \quad (3.7)$$

which is equivalent to

$$\frac{l_1 l_2}{(l_1 + l_2)^2} \begin{bmatrix} m \frac{l_2}{l_1} + \frac{J}{l_1 l_2} & m - \frac{J}{l_1 l_2} \\ m - \frac{J}{l_1 l_2} & m \frac{l_1}{l_2} + \frac{J}{l_1 l_2} \end{bmatrix} \begin{bmatrix} \ddot{z}_1 \\ \ddot{z}_2 \end{bmatrix} = \begin{bmatrix} F \\ 0 \end{bmatrix} \quad (3.8)$$

This means that if $m - \frac{J}{l_1 l_2}$ equals zero, the two equations are decoupled. For all other values of $m - \frac{J}{l_1 l_2}$ the two equations are coupled. $m - \frac{J}{l_1 l_2}$ is the so called coupling mass m_c . The coupling mass is a virtual point mass that cannot be measured in the sense of a real mass. It can also have negative values. The rest of the total mass m is distributed to the virtual masses m_1 and m_2 . These are point-masses that are assumed to lie at the coordinates z_1 and z_2 respectively. Keeping in mind that the three virtual masses must sum up to the total mass, that the position of the center of gravity should not be effected

by introducing those three masses, and that the total mass moment of inertia around the center of gravity of the virtual masses has to equal J , the virtual masses are determined by:

$$m_1 = \frac{J}{l_1(l_1 + l_2)} \quad (3.9)$$

$$m_2 = \frac{J}{l_2(l_1 + l_2)} \quad (3.10)$$

$$m_c = m - \frac{J}{l_1 l_2} \quad (3.11)$$

What can the introduction of the coupling mass help to do? It shows that if a force is applied at coordinate z_1 , this causes not only an acceleration at this very coordinate, but also at coordinate z_2 . This acceleration at coordinate z_2 is negative if the coupling mass is negative, it is positive if the coupling mass is positive, and it is zero if and only if the coupling mass equals zero. The coupling mass sets into relation the mass moment of inertia J and the mass m . If J is very large, much greater than $m l_1 l_2$, the coupling between z_1 and z_2 is not only strong, but also negative. On the contrary, if $m l_1 l_2$ is much greater than J , the coupling is also strong, but positive.

Beside the coupling via the vehicle's body, there is also a direct coupling between two wheels of the same axle for the testing vehicle. At the front axle this is due to the anti-roll bar, at the rear axle the torsion-beam acts in a similar way. Hence, the wheels of one axle are connected via a rotational spring. In both cases a positive (negative) vertical deflection of a wheel on the one side causes a force that accelerates the wheel on the other side upwards (downwards). The wheel load on one wheel therefore not only causes a vertical acceleration of the wheel where it is applied, but also on the wheel of the opposite track.

Thus, the dynamic wheel load for the i -th wheel can be calculated by the following equation, making use of the fact that the dynamic wheel load causes vertical accelerations of the respective wheel, the opposite wheel, and of the body in the previously described manner.

$$F_{z,\text{dyn},i} = p_{1,i} \ddot{z}_{W,i} + p_{2,i} \ddot{z}_{B,i} + p_{3,i} \ddot{z}_{B,j} + p_{4,i} \ddot{z}_{B,k} + p_{5,i} \ddot{z}_{W,j} \quad (3.12)$$

In this equation $\ddot{z}_{W,i}$ is the vertical acceleration of the wheel whose wheel load should be determined, $\ddot{z}_{B,i}$ is the vertical acceleration of the body above this wheel, $\ddot{z}_{B,j}$ is the vertical acceleration of the body above the wheel of the opposite track on the same axle, $\ddot{z}_{B,k}$ is the vertical acceleration of the body above the wheel of the same track but on the other axle, and $\ddot{z}_{W,j}$ is the vertical acceleration of the wheel of the opposite track on the same axle. The coefficients $p_{1,i}$ to $p_{5,i}$ can physically be interpreted as the masses of the respective quantities but are not completely similar to them, because it is not only the respective mass that is represented, but also the coupling of this mass with the considered wheel. The parameters $p_{1,i}$ to $p_{5,i}$ used for all test drives are shown in Table 3.3.

The determination of these parameters was verified in test rig experiments, where the real dynamic wheel load could be measured in high precision, and in braked test drives, where the signal of a 6-component measuring rim minus the weight transfer was used to validate the calculated wheel load at the front left wheel.

Table 3.3: Parameters that are used for the so called extended Aachen procedure to calculate the dynamic wheel load on every wheel.

$\begin{smallmatrix} \text{all } p \\ \text{in kg} \end{smallmatrix}$	$p_{1,i}$	$p_{2,i}$	$p_{3,i}$	$p_{4,i}$	$p_{5,i}$
f	36	377	76	44	20
r	22	297	24	44	20

Wheel Load Integral

The integral of dynamic wheel load, or wheel load integral, FI is introduced because it is the main control variable for the active shock absorber controller (refer to section 5.3). For the exact definition of the wheel load integral refer to section 4.1. It is gained by integrating the dynamic wheel load introduced in the previous section. This quantity has the property that due to the filtering behavior of the integral its frequency spectrum is shifted to lower frequencies than that for the dynamic wheel load. Due to the fact that higher frequencies are suppressed by the integral, the distribution of importance of the five coefficients changes. The wheel of the same axle on the opposing track for example has almost no influence on the wheel load integral anymore, because wheel accelerations take place at rather high frequencies above 10 Hz. To determine to which amount the parameters $p_{1,i}$ to $p_{5,i}$ change their relevance, a parameter influence analysis is executed.

Figures 3.9 and 3.10 show the results of parameter variations for the wheel load determining parameters with respect to their influence on the wheel load integral. The data in these figures are gained from a full-braking procedure. The wheel load integral is once measured by means of the test-rim minus the weight transfer and once by integrating the dynamic wheel load calculated in equation 3.12. Then the parameters which determine the dynamic wheel load are varied one by one. The variation is plotted on the x-axis (a value of 1.05 here means that the respective parameter has been increased by 5%). The change in wheel load integral that is caused by the change of the respective parameter is plotted on the y-axis. It can be seen that the wheel load integral reacts most sensitive on parameter $p_{2,i}$ for both hard and soft damping.

Other parameters, especially the parameter $p_{5,i}$, which connects the wheel load of the front left wheel with the acceleration of the right left wheel, do not influence the wheel load integral by much. This implies that with respect to the wheel load integral the body movement of the wheel for which the wheel load integral should be determined is most relevant. The wheel load integral is therefore by big parts influenced by the pitching of the body. Wheel oscillations do not have a great influence on the wheel load integral. It can furthermore be seen that for soft damping the wheel load integral has a much higher influence on the front right wheel and on the front right body acceleration than for hard damping. This is due to the fact that for soft damping the rolling of the vehicle is stronger than for hard damping. Therefore more acceleration on the opposing track is measurable for the same wheel load integral in case of soft damping than in case of hard damping.

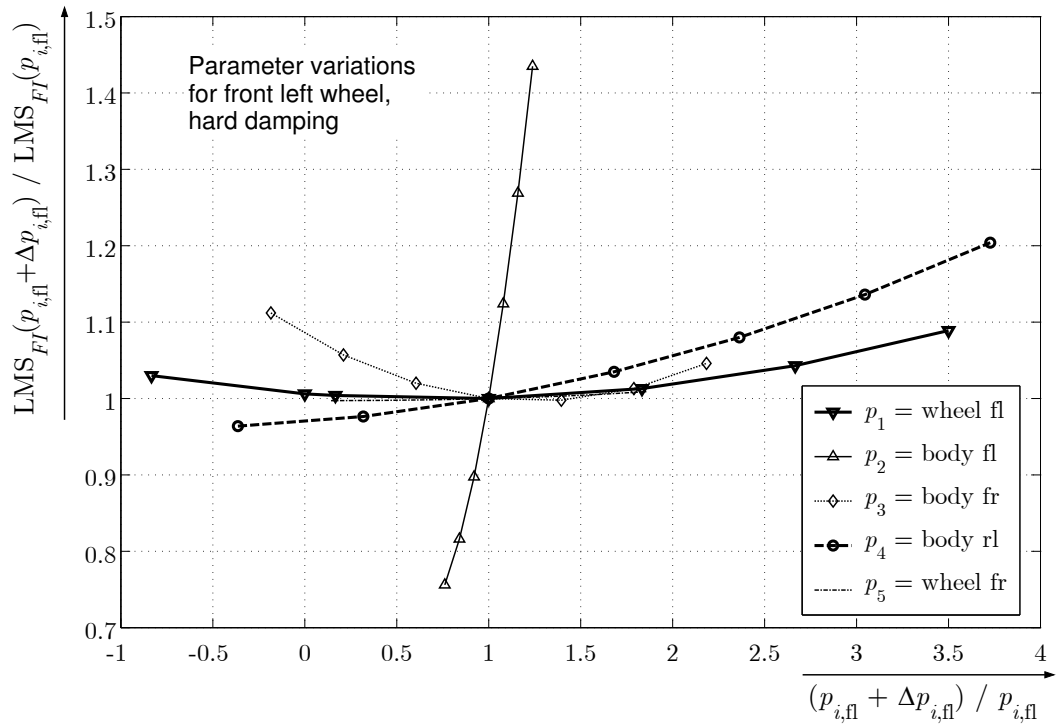


Figure 3.9: Parameter variations of the wheel load determining parameters and their influence on the wheel load integral for hard damping.

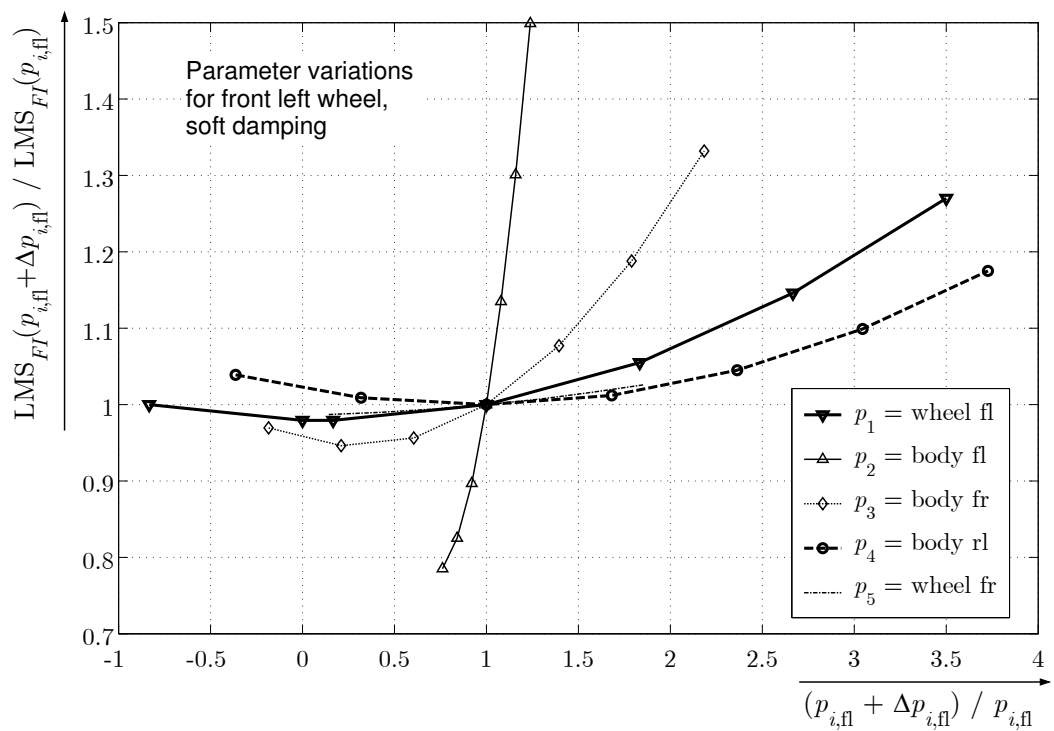


Figure 3.10: Parameter variations of the wheel load determining parameters and their influence on the wheel load integral for soft damping.

Damper Velocity

The damper velocity v_D is, beside the wheel load integral, the second input for the MiniMax-controller introduced in section 4.4. The information needed to be obtained is firstly the direction of the damper's moving, either compression or rebound, and secondly the strength of the moving, the absolute value of v_D , because a switching of the damper at high damper velocities causes a larger effect than at low damper velocities.

v_D cannot be measured directly in the testing vehicle, as no velocity sensors are implemented in the struts. In series application the damper velocity is therefore calculated by integrating the difference of body and wheel acceleration. This works fine as long as the car is not decelerated. In case of deceleration the frequency spectrum of the damper velocity is shifted down to low frequencies (due to the body pitching motion). This causes problems in the calculation of the damper velocity from accelerometer signals, for the accelerometers include high-pass filter that suppress low frequencies.

Furthermore, in case of deceleration the accelerometers of the body not only measure the vertical body acceleration anymore (which they ought to do), but they rather measure the very low-frequency longitudinal acceleration of the vehicle as well, because the body and with it the body accelerometers are pitching. This is a second reason why the signals of the accelerometers are not suitable in the given context to measure the damper velocity.

Since the low-frequency body motions are of high interest in the given context, because the wheel load integral strongly correlates with those motions, the damper velocity is calculated from the signals of the spring deflection sensors on every wheel. From their signals the derivative has to be taken of, which leads to a noisy signal which needs to be filtered by a low-pass filter. This again leads to a time delay in online testing. Nevertheless, since the time delay of the filter used is in the dimension of 10 ms or less and the important frequencies lie below 5 Hz, to filter the derivative of s_S is a much better choice to determine the damper velocity than to integrate $\ddot{z}_B - \ddot{z}_W$.

This has been investigated in test rig trials and in real test drives. The damper velocity was determined off-line, the phase-shift was adjusted, and the realtime damper velocity signals from both the spring deflection sensors and the accelerometers were compared with the off-line reference. This shows that especially for low frequencies below 2 Hz the determination of damper velocity from the accelerometers is much worse than from deflection sensors.

3.3 4-Post Test Rig

For investigation of the testing vehicle's vertical dynamics a 4-post test rig is used. This one allows to apply a seismic excitation at every wheel independently from each other. The actual wheel load $F_{z,i}$ at the i -th wheel and the stroke of the i -th hydraulic post $s_{p,i}$ can be measured. The range of the posts' stroke reaches from $\min(s_{p,i}) = -125$ mm to $\max(s_{p,i}) = 125$ mm. The test rig can supply a maximum force of 40 kN per post. The wheels are not bound in lateral direction, which means that lateral tire forces, which would influence the vertical oscillation, are not present. The seismic excitations applied at each wheel are free to be chosen within the limitations due to the hydraulic power of the test rig. Pseudo-noise seismic excitations can be applied as well as a sinusoidal or a chirp signal. Figure 3.11 shows the testing vehicle standing on the 4-post test rig.

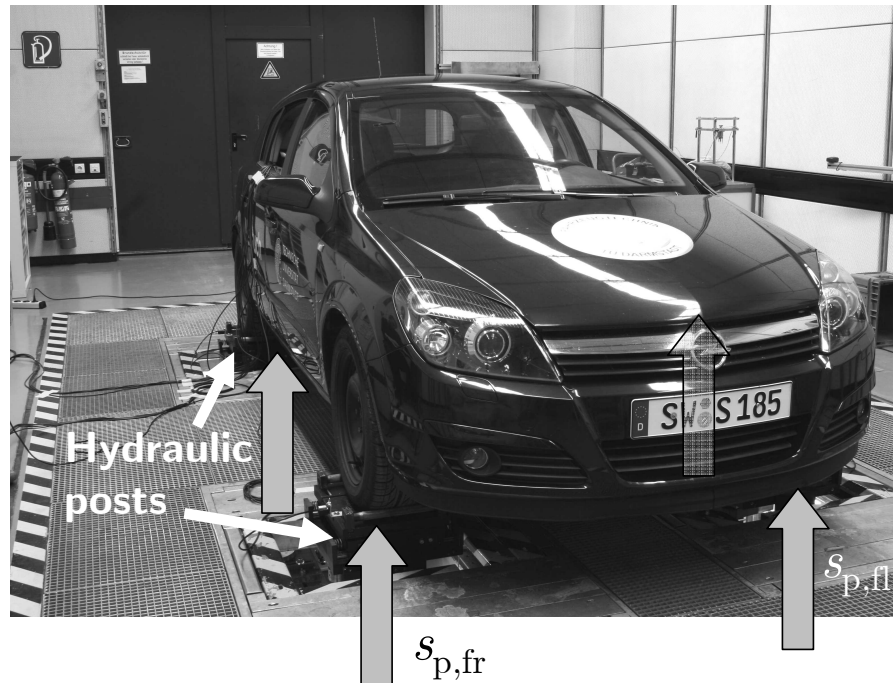


Figure 3.11: Testing vehicle on the 4-post test rig of ZF Sachs AG in Schweinfurt. A seismic excitation can be applied to every wheel independently.

The test rig is used to investigate the vertical dynamics of the vehicle and in particular to investigate the effect of switching the shock absorbers on wheel load. The advantage of using a test rig is the high reproducibility of the signals measured. E. g., the seismic excitation can be preset in high accuracy on a test rig, which is not possible on a regular pavement. The driver plays no role when testing on the test rig. Neither does the weather condition nor the heating of the tires and the brakes when executing real test drives. Using the test rig has the disadvantage, however, that only the vertical dynamics can be investigated and even there, that the coupling between longitudinal and vertical dynamics cannot be looked at. No effect on the vertical oscillation of the vehicle which is caused by lateral or longitudinal forces can be investigated.

3.4 Test Tracks

To avoid the problems of missing coupling between horizontal and vertical dynamics in the test rig experiments, real test tracks have been defined that allow to investigate the vehicle's behavior with the wheel spinning and the braking system braking.

3.4.1 Test Track 'Defined Obstacles'

When it comes to real test drives there is always the problem of reproducibility. It is hard to guarantee it on a normal road with standard kind of excitation amplitudes. For many investigations this can be dealt with by either executing many tests and/or looking at measurands that are highly integrative. But some test drives demand a very high reproducibility in the short time-scale, e. g. if the effect on wheel load, braking force or

braking slip of one single switching process should be investigated. In such cases it is useful to make use of defined obstacles. Those should have a given shape that is known and the excitation caused by them should be rather high so that it clearly can be differed between the response to the excitation of the obstacles and the response to the standard pavement (which is not very reproducible). In this thesis two cosine-shaped obstacles (cosine waves) have been used (refer to Figure 3.12). Their elevation profile is governed by the following equation:

$$h_{CW}(x) = \hat{h}_{CW} \left[1 - \cos \left(\frac{2\pi}{l_{CW}} x \right) \right], \quad (3.13)$$

where the length of the cosine waves is $l_{CW} = 2$ m and their maximum elevation from the ground is $2\hat{h}_{CW} = 0.04$ m (refer to Figure 3.13). Both are oriented parallelly in driving direction.

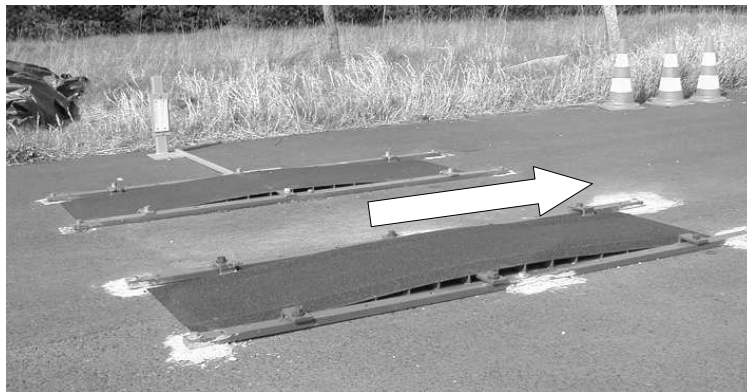


Figure 3.12: Cosine-shaped obstacles that are used for test drives to cause reproducible and high-magnitude oscillation responses of the testing vehicle⁸.

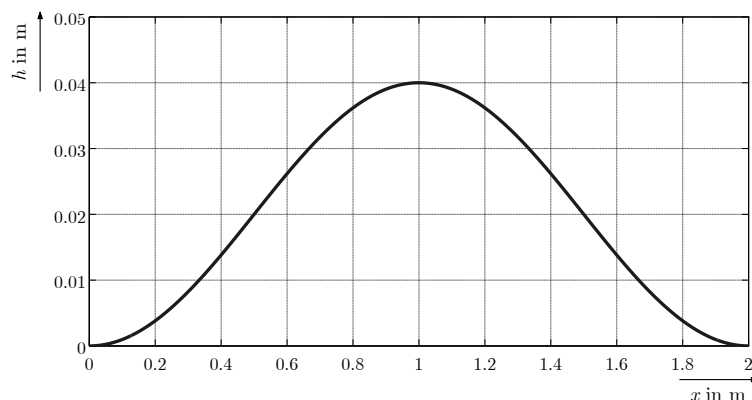


Figure 3.13: Elevation vs. longitudinal length of the cosine-shaped obstacle.

Depending on the passing velocity, the cosine waves excite the vehicle at differing frequency bands. The faster the vehicle crosses the obstacles, the higher are the excitation

⁸Reichel (2003): Untersuchungen zum Einfluss stufenlos verstellbarer Schwingungsdämpfer auf das instationäre Bremsen von Personewagen p. 48

frequencies (refer to Figure 3.14). The cosine waves are made from steel and rigidly connected to the pavement. Their driving surfaces are glued with a so called Safety Walk, which is an artificial pavement with similar properties (especially the friction coefficient) as normal asphalt pavement.

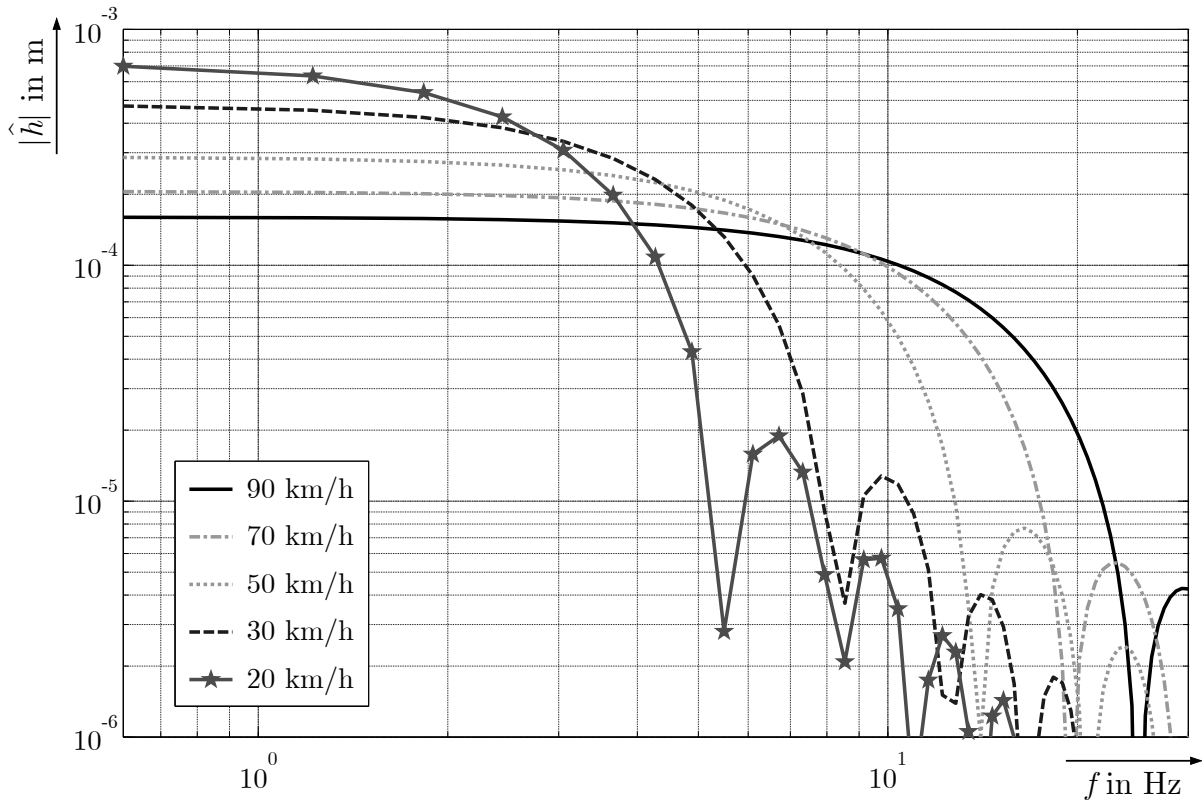


Figure 3.14: Frequency spectrum of the seismic excitation caused by passing the cosine waves for different passing velocities. Data gained by calculus⁹.

3.4.2 Test Track ‘Standard Road’

The test track ‘Standard Road’ has been chosen with the intention to get results from driving and braking on it that are comparable to the ones on a typical German Autobahn. The test track is located on a closed airfield that belongs to Technische Universität Darmstadt and can be used for test drives (August-Euler-Flugplatz in Griesheim). In Figure 3.15 this test track is shown. The white line in the picture marks the elevation profile of this test track, which has been measured (refer to Figure 3.16). This profile has a slowly increasing slope (70 cm per 100 m) and its unevenness is comparable to the one on typical highways. From inspection it can be seen that the pavement structure looks similar to the one that can be found on typical roads.

⁹Reichel (2003): Untersuchungen zum Einfluss stufenlos verstellbarer Schwingungsdämpfer auf das instationäre Bremsen von Personewagen p. 61



Figure 3.15: Test track ‘Standard Road’ (an airfield) on which part of the braking tests are executed with the testing vehicle during a braking procedure.

To make this inspection more quantifiable two measurands are chosen which allow to compare the test track to other roads:

The unevenness U_P and the Delta Spring Displacement Δ_{S_S} . It is assumed that the power spectral density of the pavement overdriven shows a linear behavior in the double-logarithmic frequency domain. The unevenness U_P values the elevation profile of the pavement in the frequency domain. The Delta Spring Displacement Δ_{S_S} provides with information about the overall power of the excitation due to driving over a given pavement. As is shown in section 4.4.2, this quantity is based on the self-leveling effect of active shock absorbers. It measures the change in vertical level of the vehicle’s body for different shock absorber configurations and is the higher, the stronger the seismic excitation, the more power is put into the system due to the pavement’s vertical unevenness. Δ_{S_S} measures therefore the overall unevenness. U_P provides with information about how the power of the pavement is distributed in the frequency domain. U_P is the negative slope of the elevation profile plotted vs. the wave number.

Figure 3.16 shows the elevation profile of a 100-m-part of the airfield which is used to execute braking procedures. The data is gained from own measuring with a laser distance instrument. Besides the determination of the slope, which can be seen in the figure, the measurement of the elevation profile was undertaken to determine the roughness of the pavement.

Figure 3.17 shows the frequency spectrum of the elevation profile of the test tracks that are used for the braking procedures. It can be seen that the unevenness $U_P \approx 1 \pm 0.1$ on the chosen track. For typical highways $U_P \approx 1$ as well (refer to Mitschke¹⁰)¹¹. This means that the chosen test track is similar to a typical German highway with respect to the

¹⁰Mitschke/Wallentowitz (2004): Dynamik der Kraftfahrzeuge p. 298.

¹¹The unevenness W in relevant literature is often defined as the slope of the power spectral density (PSD) of the pavement. Here U_P is the slope of the elevation profile and has therefore values that are by the factor two smaller than the ones that are calculated from using the PSD.

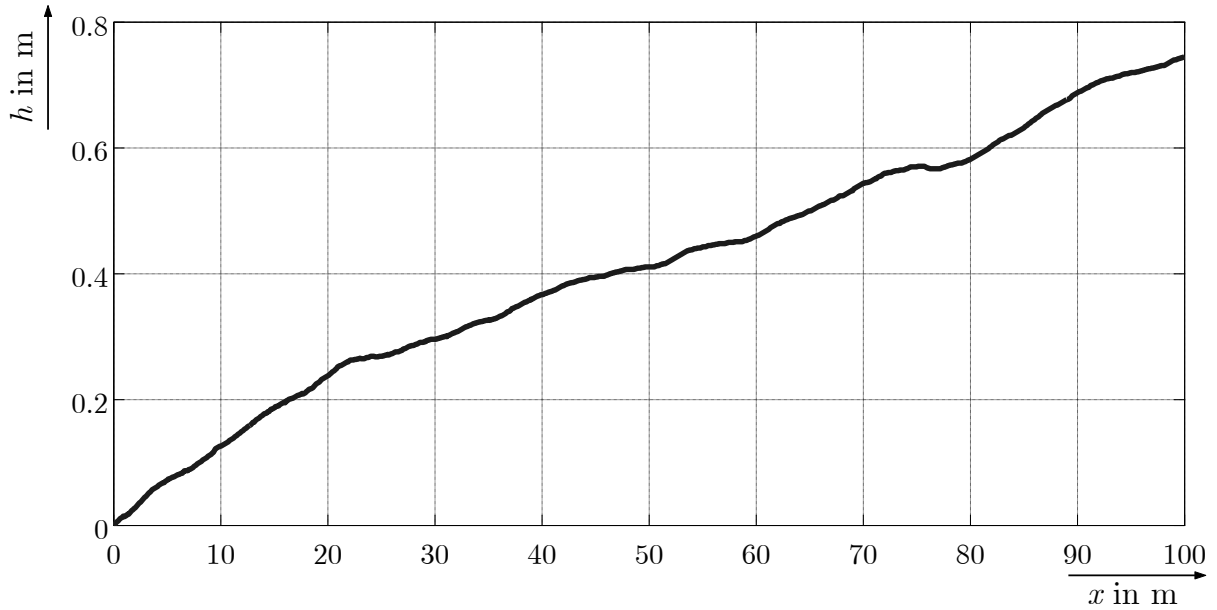


Figure 3.16: Longitudinal elevation profile of the test track ‘Standard Road’ that is used for braking tests mainly.

measurand U_P . For such a typical road the amplitudes of elevation decrease approximately with f^{-1} , same as the amplitudes on the test track ‘Standard Road’ do.

For the test track ‘Standard Road’ the same testing procedure as explained in section 4.5 is executed. The value for the Delta Spring Displacement at the front right wheel for this testing track at a vehicle’s speed of 85 km/h and for switching from $F_{z,\text{req}} = +1$ to $F_{z,\text{req}} = -1$ or vice versa is

$$\Delta_{S_S,\text{fr}} = 2.8 \text{ mm.} \quad (3.14)$$

Comparing this value with the ones from a typical German Autobahn, which are presented in Figure 4.17, shows that the test track chosen is comparable to those typical roads. This is for two reasons: First of all, because the frequency spectrum of the test track chosen is similar to the one that can be found on ordinary highways. Secondly, the newly introduced measurand Δ_{S_S} , which measures the possible effect strength on a given pavement, is also comparable to the ones found in reality. Thus, the test drives executed on the test track chosen are assumed to be representative for such typical highways as the ones shown in Figure 4.14. For those kinds of pavement, that is for stochastic pavements which feature a linear decreasing elevation profile in the double-logarithmic wave-number plot, the frequency spectrum of the excitation is independent of the driving velocity. With increasing velocity it is only the magnitude that increases, but the distribution of excitation over the frequency spectrum remains constant.

Thus, results which are gained on such a test track for the case when the only excitation is the seismic excitation (no braking, acceleration, or curve-driving), can be assumed to have the same quality, no matter at which driving speed they are gained. If hard damping is better with respect to lowering the RMS on wheel load on a given stochastic road at one constant velocity, it should be better for every constant velocity.

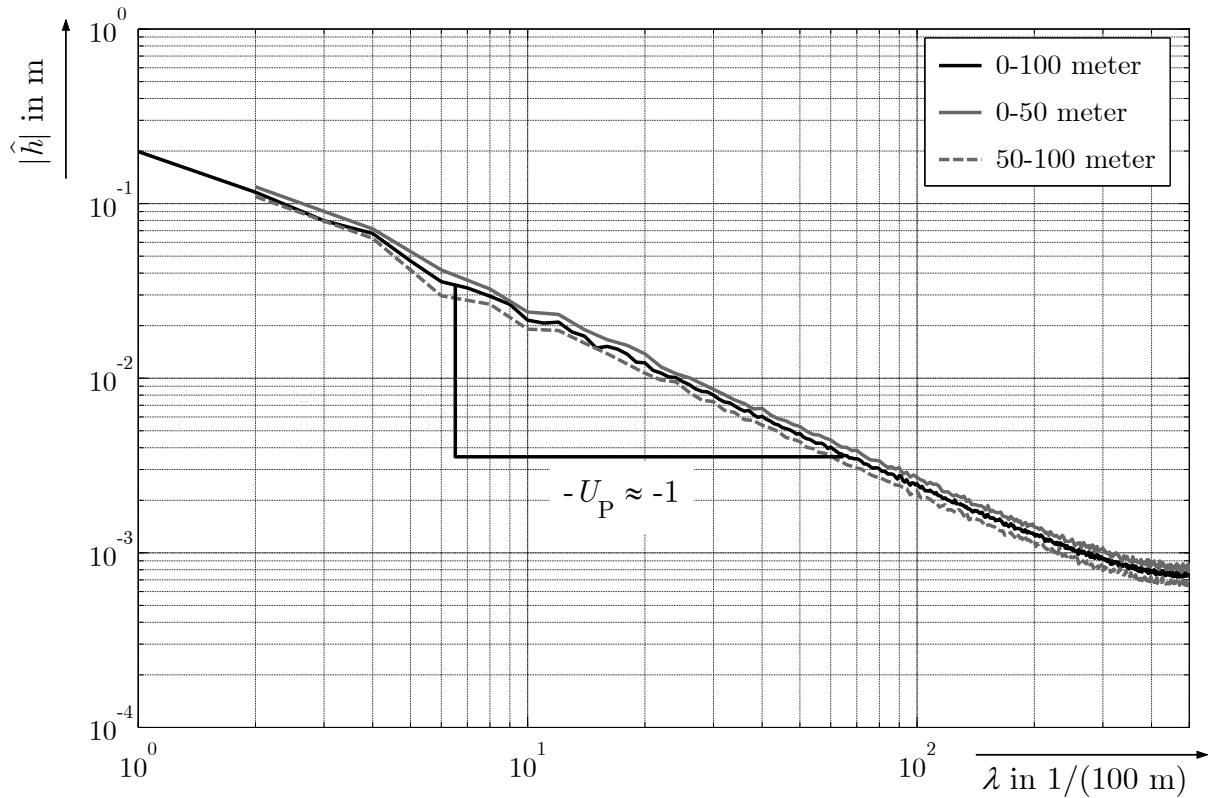


Figure 3.17: Spectrum in the distance domain of the test track that was used to execute braking procedures on an ordinary road. The longitudinal elevation profile of a distance of 100 meters was measured. The spectrum for the total 100 meters, the first 50 meters and the last 50 meters are shown. λ is the so called wave number that measures the number of waves per 100 meters. $\lambda = 10/(100 \text{ m})$ means that there are 10 full wavelengths per 100 meters at the given pavement.

3.5 Conclusions

In this chapter the testing tools have been presented. The active shock absorbers which are used as actuators in this thesis and the terms spreading and rebound/compression ratio have been introduced. Both are essential parameters for the effect which an active shock absorber can have on the vertical dynamics. The testing vehicle is chosen such that it covers a wide range of vehicles that can be found on German streets. A braking machine is used to guarantee that the initial slope of braking pressure is reproducible from one braking procedure to another.

Most of the physical quantities that ought to be determined to value the braking performance can be measured by means of sensors whose signal is directly connected to the respective physical quantity. Some measurands, however, have to be determined indirectly. The most important representatives for those are the dynamic wheel load, the wheel load integral, and the damper velocity. The former are calculated from accelerometer signals, the latter is calculated from the signals of displacement sensors.

The testing tools used include ones that are meant to investigate the vertical dynamics of the testing vehicle, ones that allow to investigate the coupling between vertical and longitudinal dynamics, and ones that are chosen to determine the braking distance.

The first purpose is fulfilled by a 4-post test rig which is used for vertical excitations of the testing vehicle, for the second purpose defined, cosine-shaped obstacles are used, and for the latter purpose a test track that is comparable to a German highway is chosen. This test track is selected such that a representative statement about the potential to reduce the braking distance by means of active shock absorber control is possible.

The parameters which influence the braking distance have been identified and distributed in two dimensions over three categories each. There are parameters which can be controlled and measured, and these are the ones which are indeed kept constant during the braking procedures in order to make them comparable. All parameters which cannot be controlled must be treated as random errors to the results of the determination of the braking distance.

Summarizing, it can be stated that the testing tools are chosen such that the braking distance can be determined in the precision which is required to measure the effect which the vertical dynamics has on the longitudinal dynamics. Furthermore, all testing tools are chosen such that the expected conclusions are representative for real-life applications.

4 Vertical Dynamics

In this chapter the vertical dynamics of the testing vehicle are investigated in a quarter-car simulation model, in test-rig trials, and in test drives. The objective is to find the connection between the switching of the shock absorber from one constant line to the other (hard to soft or vice versa) and the course of wheel load in the time and the magnitude domain. To do this it is necessary to define references to which the course of wheel load after switching the shock absorber can be compared. Thus, experiments with a high reproducibility of the course of wheel load are designed in order to be able to compare the course of wheel load with and without switching the shock absorber.

After introducing a couple of definitions in section 4.1, in section 4.2 the general possibility to have an influence on wheel load by means of active shock absorbers is explained. The focus lies on the transient behavior of the wheel load, the behavior in the long run does not play a role here.

The quarter-car model which is used for numerical investigations of the vertical dynamics is introduced in section 4.3. This model is a seismic excited non-linear oscillator with two degrees of freedom. It is also in this section that fundamental thoughts about the frequency range in which the use of a shock absorber controller makes sense are developed. For those thoughts the quarter-car model is partly linearized by using constant but differing damping coefficients for rebound and compression.

Based on those fundamentals, the core controller with which the wheel load is controlled is introduced in section 4.4. It is called MiniMax-controller, for it is a control logic which switches between hard and soft damping. The possibility to continuously adjust the vehicle's damping is not made use of. The controller works individually for each wheel and has two inputs: the actual damper velocity v_D and the actual request of wheel load $F_{z,\text{req}} \in \{-1, +1\}$ at the respective wheel. The one and only output is the damper current $I_D \in \{0 \text{ A}, 1.6 \text{ A}\}$. With this core controller artificial characteristic lines for the shock absorbers can be generated, depending on the request of wheel load. These lead to a lowering/lifting of the body, whose effect is discussed in section 4.4, too.

The complex source of the request of wheel load which is applied to reduce the braking distance—an essential part of the overall controller—is not discussed in this chapter, but in chapter 5, where the longitudinal dynamics are addressed.

In the following section 4.5 the testing vehicle is set on a real road and the lifting and lowering effect of the MiniMax-controller is used to determine the roughness of standard southwestern German highways. The results of these measuring are taken to compare the actual testing track 'Standard Road' with a typical Autobahn in order to make the braking results transferable.

In section 4.6 in test rig experiments three steps are undertaken: First of all, the effect which the switching of the shock absorber has on wheel load is determined in its time and magnitude frame for a real car—the testing vehicle described in section 3.2. Secondly, the effect is compared for different excitation scenarios to determine if the places where the seismic excitation is applied affect the results. Finally, the numerical results from

investigations with the quarter-car model are compared with the results from the test rig.

4.1 Definitions

First of all, a couple of definitions shall be introduced for the vertical dynamics of a passenger car.

Wheel Load F_z

The wheel load F_z is the part of the force in the contact zone of tire and ground which acts in z -, meaning in vertical direction. This force is counted positive if it acts in upward direction with respect to the tire. In the scales measured in the given context the wheel load can never have values below zero, because at value zero the wheel loses its contact to the ground.

Static Wheel Load $F_{z,\text{stat}}$

The term static wheel load describes the force $F_{z,\text{stat}}$ in the contact zone of tire and ground that acts in the static case (the car is not moving and standing on a horizontal plane) in z -direction. It only depends on the total mass of the car and on the mass distribution and is assumed to be time-invariant during a driving cycle. Obviously the static wheel load always has positive values.

Body Induced Wheel Load $F_{z,\text{bi}}$

Body induced wheel load shall be defined as static wheel load which changes its value due to the deceleration $-\ddot{x}_V$ during the braking process and is reflecting the weight transfer. At the rear axle wheel load is decreasing while at the front axle it is increasing during braking due to forces acting below the vehicle's center of gravity h_{CG} . This part cannot be controlled and therefore must not be controlled. The body induced wheel load is defined as follows:

$$F_{z,\text{bi},\text{f}}(t) = F_{z,\text{stat},\text{f}} + \Delta F_{z,\text{bi}} \quad (4.1)$$

for a wheel at the front axle and

$$F_{z,\text{bi},\text{r}}(t) = F_{z,\text{stat},\text{r}} - \Delta F_{z,\text{bi}} \quad (4.2)$$

for a wheel at the rear axle, with

$$\Delta F_{z,\text{bi}} = \frac{1}{2} m_V (-\ddot{x}_V(t)) \frac{h_{\text{CG}}}{l} \quad (4.3)$$

as the difference of wheel load between braking and non-braking situation due to weight transfer which leads to a greater (smaller) stationary wheel load. h_{CG} is the height of the center of gravity of the whole vehicle, measuring from the ground, l is the wheel base—the distance from one axle to the other—, m_V is the total mass of the vehicle and \ddot{x}_V the longitudinal acceleration of the vehicle. \ddot{x}_V is negativ for braking. The same holds true for weight transfer from right to left lane when a lateral force acts on the vehicle below

h_{CG} . Since in this thesis only test drives moving straight ahead are undertaken, this kind of weight transfer does not play a role in the given context.

Dynamic Wheel Load $F_{z,dyn}$

The dynamic wheel load $F_{z,dyn}$ is the difference of the actual wheel load and the body induced wheel load. Without any longitudinal forces on another elevation than h_{CG} acting on the vehicle, this is equal to the difference of actual wheel load and static wheel load. The dynamic wheel load describes the oscillation of wheel load and by this it has positive and negative values.

$$F_{z,dyn}(t) = F_z(t) - F_{z,bi}(t) \quad (4.4)$$

Wheel Load Integral FI

The integral of the dynamic wheel load FI is defined as

$$FI(t) = \int_{t_0}^t F_{z,dyn}(\tau) \, d\tau. \quad (4.5)$$

Its benefit is explained in detail in section 5.3. Here it should just be introduced and defined analytically. The mean value of the wheel load integral is always zero in the long run, for the dynamic wheel load's mean value always equals zero in the long run. Thus, the wheel load integral cannot drift away and is therefore bounded within the limits of the maximum oscillations of the dynamic wheel load.

RMS on Dynamic Wheel Load $\text{RMS}(F_{z,dyn}) = F_{z,dyn}^{\text{eff}}$

The RMS on dynamic wheel load between times t_0 and t_1 is defined as follows:

$$\text{RMS}(F_{z,dyn}) = F_{z,dyn}^{\text{eff}} = \sqrt{\frac{1}{t_1 - t_0} \int_{t_0}^{t_1} F_{z,dyn}^2 \, dt} \quad (4.6)$$

The same definition holds true for every variable X .

$$\text{RMS}(X) = X^{\text{eff}} = \sqrt{\frac{1}{t_1 - t_0} \int_{t_0}^{t_1} X^2 \, dt} \quad (4.7)$$

4.2 Possibilities to Influence Wheel Load

As it was shown in section 2.3.2, the braking force can not only be controlled by a system which acts on the braking torque—as the ABS does—, but it can also be influenced by acting on the wheel load. Principally speaking, both ways are suitable for the given purpose in the same manner. Here the wheel load is influenced by controlling the active shock absorbers to finally influence the braking force and the braking slip. But how can

the wheel load be influenced by an active shock absorber? How does the causal direction look like? To answer these questions a simple switching from hard to soft damping is investigated in more detail. For hard damping, the damper force is greater than for soft damping, constant damper velocity provided.

In Figure 4.1 a part of a quarter-car model is shown which only includes the damper force. The force of the spring can be neglected for the following thoughts. The damper is considered to be in rebound at a constant velocity $v_D = v_B - v_W = \text{const} > 0$. In rebound the damper force points upwards with respect to the wheel and downwards with respect to the body. This means that during rebound the damper force reduces the wheel load. If the damper force was not there, the wheel would not be pulled upwards and therefore the wheel load would be greater than it is with the damper force being present. But what happens if the damper is switched from hard to soft damping at a given velocity in rebound? The damper force will decrease, the wheel will be pulled upwards less and the wheel load will therefore increase.

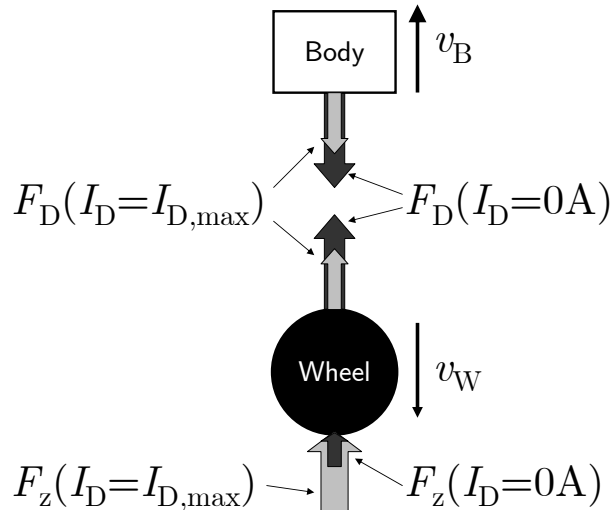


Figure 4.1: Damper force for hard and soft damping in rebound and its effect on wheel load¹.

Similar considerations can be made for every possible state of damper movement and finally one ends up with a quite simple matrix which is called the Wheel Load Influence Matrix (refer to Table 4.1). It ought to be read in the following manner—exemplarily for the upper right corner: If the damper is switched from hard to soft in rebound, this will lead to an increase in wheel load. The switching must be thought of in the following manner: By changing the system-immanent parameter k_B , one ends up with a system with a new set of parameters. Compared are then the two courses of wheel load for those two systems, starting from the same initial conditions. Those initial conditions are the actual system states at time of switching the shock absorber in both cases.

¹If the damper is in rebound and it is switched from hard to soft, the damper force will decrease and since it acts upwards with respect to the wheel the wheel load will increase.

Table 4.1: Wheel Load Influence Matrix

Shock abs. stage Switching of shock abs.	Compression	Rebound
Hard to soft	Decrease in wheel load	Increase in wheel load
Soft to hard	Increase in wheel load	Decrease in wheel load

4.3 Quarter-Car Model and Simulation

A quarter-car model is used to investigate the vertical dynamics of the testing vehicle. The model is shown in Figure 4.2. The model has two degrees of freedom, body deflection z_B and wheel deflection z_W , and is forced by a seismic excitation z_0 . It consists of two point masses which represent the part of the total body mass m_B that acts on the respective wheel and the wheel's mass m_W . Furthermore, it contains a linear spring and a linear damper for the wheel's vertical stiffness c_W and damping k_W . Both wheel parameters are of course dominated by the tire parameters. The rim does not contribute to the overall wheel's stiffness and damping in the investigated frequency band from 0–30 Hz. The vertical body spring stiffness c_B is modeled by a linear spring. The model does neither represent the braking process of the car nor its rolling behavior. Nevertheless this model can be used to investigate the vertical dynamics of the car, as will be seen in section 4.6.3.

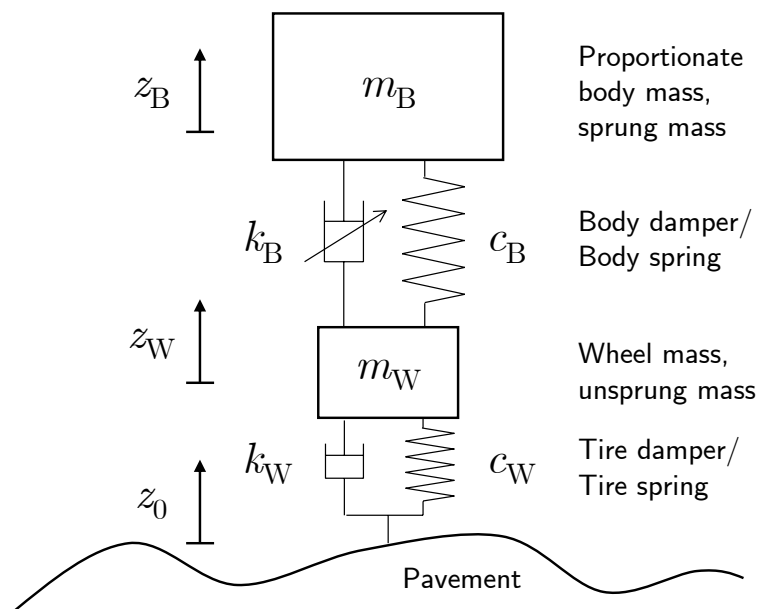


Figure 4.2: Mathematical model, used for simulation of the vertical dynamics of the testing vehicle.

The model is governed in analytical form by the following system of equations.

$$\begin{aligned} \begin{bmatrix} m_B & 0 \\ 0 & m_W \end{bmatrix} \begin{bmatrix} \ddot{z}_B \\ \ddot{z}_W \end{bmatrix} + \begin{bmatrix} k_B(v_D, I_D) & -k_B(v_D, I_D) \\ -k_B(v_D, I_D) & k_B(v_D, I_D) + k_W \end{bmatrix} \begin{bmatrix} \dot{z}_B \\ \dot{z}_W \end{bmatrix} \\ + \begin{bmatrix} c_B & -c_B \\ -c_B & c_B + c_W \end{bmatrix} \begin{bmatrix} z_B \\ z_W \end{bmatrix} = \begin{bmatrix} 0 \\ k_W \dot{z}_0 + c_W z_0 \end{bmatrix} \end{aligned} \quad (4.8)$$

The gravitational acceleration is not included, for the origin of the coordinates is set to the static equilibrium. The static wheel load in this model therefore has the value zero. The dynamic wheel load is determined by the sum of tire damper and tire spring force.

$$F_{z,\text{dyn}}(t) = k_W [\dot{z}_0(t) - \dot{z}_W(t)] + c_W [z_0(t) - z_W(t)] = -(F_{k_W}(t) + F_{c_W}(t)) \quad (4.9)$$

The principle of linear momentum for the body and the wheel writes down as:

$$m_B \ddot{z}_B = -(F_{k_B} + F_{c_B}), \quad (4.10)$$

where the body damper force F_{k_B} plus the body spring force F_{c_B} —provided that they are positive—cause a downward acceleration of the body. The principle of linear momentum for the wheel writes:

$$m_W \ddot{z}_W = F_{k_B} + F_{c_B} - (F_{k_W} + F_{c_W}), \quad (4.11)$$

where the body damper force F_{k_B} plus the body spring force F_{c_B} —provided that they are positive—cause an upward acceleration of the wheel and the wheel damper force F_{k_W} plus the wheel spring force F_{c_W} cause a downward acceleration of the wheel. Both the wheel damper force F_{k_W} and the wheel spring force F_{c_W} sum up to the negative of the dynamic wheel load (refer to equation 4.9). Thus, the dynamic wheel load can also be written as:

$$F_{z,\text{dyn}} = m_W \ddot{z}_W - (F_{k_B} + F_{c_B}) \quad (4.12)$$

Together with equation 4.10 this leads to:

$$F_{z,\text{dyn}} = m_W \ddot{z}_W + m_B \ddot{z}_B \quad (4.13)$$

This means that the dynamic wheel load of a quarter-car model can be calculated by summing up the vertical wheel acceleration and the vertical body acceleration, weighted with the wheel and the body mass respectively. This is the so called Aachen procedure to calculate the dynamic wheel load (refer to section 3.2.4).

Furthermore, it should be mentioned that the system of equations is nonlinear, since the damping factor k_B of the active shock absorber is a function of the damper velocity and of the damper current: $k_B = k_B(v_D, I_D)$, where the damper velocity v_D is defined as the difference between vertical body velocity \dot{z}_B and vertical wheel velocity \dot{z}_W .

$$v_D(t) = \dot{z}_B(t) - \dot{z}_W(t) \quad (4.14)$$

The damping factor k_B depends on the damper current I_D , because this is how the desired damper characteristic is adjusted. For a given damper velocity an indefinite number of different k_B can be set by choosing $I_D \in [I_{D,\text{min}}, I_{D,\text{max}}]$. Neither the setpoint for the damper

current nor the setpoint for the damping factor are met immediately after switching the damper from one state to another. These time delays are implemented in the model by means of first order low-pass filters, where the damper force is filtered.

The damping factor vs. the damper velocity is shown in Figure 4.3 and in Figure 4.4. These data are related to the front and the rear left damper of the testing vehicle and have been obtained on a test rig at and by ZF Sachs AG. The actual damping ratio depends not only on the damper velocity but also on the parameter damper current I_D . In the figure only the two extrema of this dependency are shown. The real damper can adopt any value of damper current between 0 and 1.6 A.

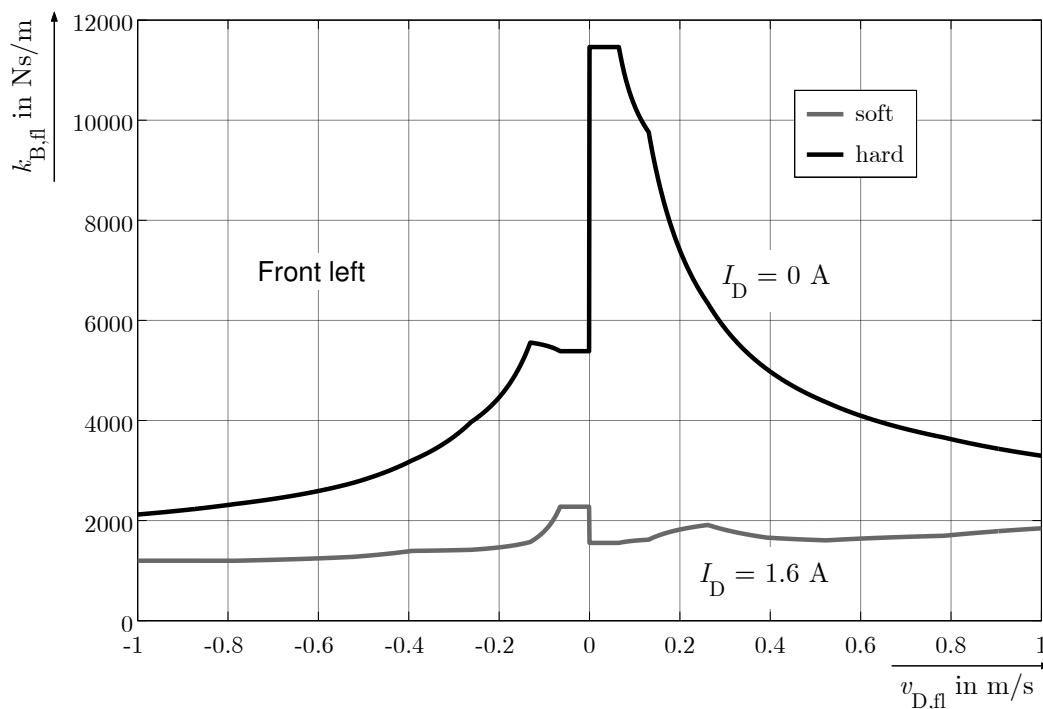


Figure 4.3: Damping factors used in the quarter-car model, gained from experiments with the front left damper of the testing vehicle, source: ZF Sachs AG.

The parameters of the quarter-car model are shown in Table 4.2. As for the tire damping k_W it must be mentioned that this value is a rough approximation of the values measured, which lay between 200 and 1,000 Ns/m, depending on and decreasing with the excitation frequency. But the actual value of the tire damping factor is not that important, because it is very small compared to the body damping factor. It is only important that there is a tire damping at all, because it is responsible for a phase shift in the wheel load which is measured by summing up vertical tire spring and damper force.

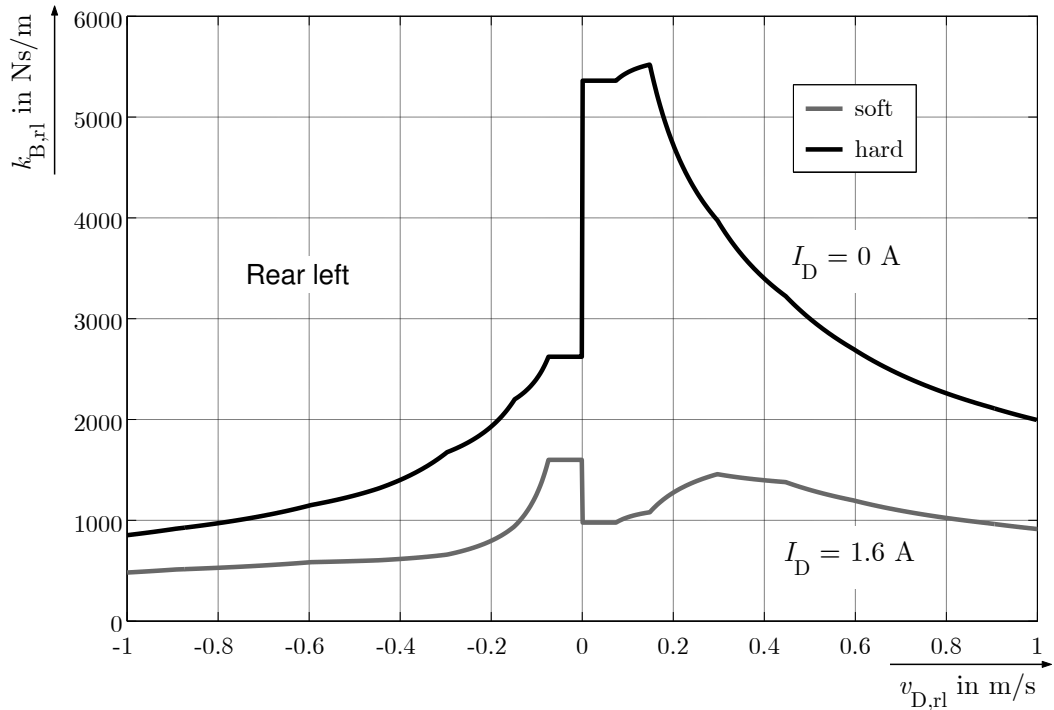


Figure 4.4: Damping factors used in the quarter-car model, gained from experiments with the rear left damper of the testing vehicle, source: ZF Sachs AG.

Table 4.2: Parameters of the quarter-car model

Parameter	Value		Source
	front left	rear left	
m_B	380 kg	290 kg	own measuring: calculated from static wheel load
m_W	31 kg	22 kg	own measuring: weight measuring with damper and coil spring dismantled
c_B	29 N/mm	28.6 N/mm	own measuring: hydraulic press and lifting platform
c_W	228 N/mm	228 N/mm	own measuring: hydraulic shaker
k_B	as shown in Figures 4.3 and 4.4		ZF Sachs AG
$k_{B,\text{lin}}(I_D = 1.6 \text{ A})$	1500 Ns/m	1200 Ns/m	calculated from characteristic diagram
$k_{B,\text{lin}}(I_D = 0 \text{ A})$	6000 Ns/m	4000 Ns/m	
k_W	400 Ns/m	400 Ns/m	own measuring: hydraulic shaker
First undamped eigenfrequency f_{e1}	1.3 Hz	1.5 Hz	calculated from the given parameters
Second undamped eigenfrequency f_{e2}	14.4 Hz	17.2 Hz	calculated from the given parameters

Linearized Quarter-Car Model

For the following investigations the quarter-car model is linearized in the sense that the damping coefficients for hard and soft damping are set to the values given in Table 4.2. This is done because otherwise it is impossible to solve the governing equations of motion analytically. These equations of motion write as:

$$\mathbf{M} \ddot{\mathbf{z}}_{\text{lin}} + \mathbf{K} \dot{\mathbf{z}}_{\text{lin}} + \mathbf{C} \mathbf{z}_{\text{lin}} = \mathbf{f} = \begin{bmatrix} 0 \\ k_{\text{W}} \dot{z}_0 + c_{\text{W}} z_0 \end{bmatrix} \quad (4.15)$$

The eigenfrequencies for the undamped linearized system can be found in Table 4.2. Now if $z_0(t)$ is assumed to be of the form:

$$z_0(t) = \hat{z}_0 e^{j\Omega t}, \quad (4.16)$$

the particular solution for the system of forced differential equations can be found with the following approach:

$$\mathbf{z}_{\text{lin}} = \hat{\mathbf{z}} e^{j\Omega t} \quad (4.17)$$

applied to equation 4.15 yields to:

$$-\Omega^2 \mathbf{M} \hat{\mathbf{z}} e^{j\Omega t} + j\Omega \mathbf{K} \hat{\mathbf{z}} e^{j\Omega t} + \mathbf{C} \hat{\mathbf{z}} e^{j\Omega t} = \begin{bmatrix} 0 \\ j\Omega k_{\text{W}} + c_{\text{W}} \end{bmatrix} \hat{z}_0 e^{j\Omega t} \quad (4.18)$$

$$[\mathbf{C} - \Omega^2 \mathbf{M} + j\Omega \mathbf{K}] \hat{\mathbf{z}} = \begin{bmatrix} 0 \\ j\Omega k_{\text{W}} + c_{\text{W}} \end{bmatrix} \hat{z}_0 \quad (4.19)$$

The complex vector of amplitudes is thus given by:

$$\hat{\mathbf{z}}(\Omega) = [\mathbf{C} - \Omega^2 \mathbf{M} + j\Omega \mathbf{K}]^{-1} \begin{bmatrix} 0 \\ j\Omega k_{\text{W}} + c_{\text{W}} \end{bmatrix} \hat{z}_0 \quad (4.20)$$

$$\frac{\hat{\mathbf{z}}(\Omega)}{\hat{z}_0} = \begin{bmatrix} \hat{z}_{\text{B}}(\Omega) \\ \hat{z}_{\text{W}}(\Omega) \end{bmatrix} \frac{1}{\hat{z}_0} = [\mathbf{C} - \Omega^2 \mathbf{M} + j\Omega \mathbf{K}]^{-1} \begin{bmatrix} 0 \\ j\Omega k_{\text{W}} + c_{\text{W}} \end{bmatrix} \quad (4.21)$$

According to equation 4.13 the amplitude of the dynamic wheel load can be calculated as:

$$\hat{F}_{z,\text{dyn}}(\Omega) = m_{\text{B}} \hat{z}_{\text{B}}(\Omega) + m_{\text{W}} \hat{z}_{\text{W}}(\Omega), \quad (4.22)$$

where $\hat{\mathbf{z}}(\Omega) = -\Omega^2 \hat{\mathbf{z}}(\Omega)$. Both $\hat{\mathbf{z}}$ and $\hat{F}_{z,\text{dyn}}$ are complex quantities. The part of dynamic wheel load which causes a movement of the car's body and the one which causes the car's wheel to oscillate can be separately written as:

$$\hat{F}_{z,\text{dyn},\text{B}}(\Omega) = m_{\text{B}} \hat{z}_{\text{B}}(\Omega) \quad (4.23)$$

$$\hat{F}_{z,\text{dyn},\text{W}}(\Omega) = m_{\text{W}} \hat{z}_{\text{W}}(\Omega) \quad (4.24)$$

This means that part of the dynamic wheel load is responsible and therefore measurable in terms of vertical body acceleration, another part is measurable in terms of vertical wheel

acceleration. The question is, to which amount do those two parts combine to the total dynamic wheel load? This question needs to be answered in order to be able to determine in which frequency range the relevant oscillations will take place and in order to decide if either the body or the wheel oscillations are more relevant in the given context.

In Figure 4.5 the dynamic wheel load response vs. the excitation frequency of a seismic excitation is plotted. For frequencies well below 10 Hz, for both hard and soft damping the main part of dynamic wheel load results in an oscillation of the vehicle's body. This is because at those low frequencies the wheel is almost not moving with respect to the seismic excitation. It just moves up and down with the same phase as the seismic excitation and transfers the dynamic wheel load to body spring and damper forces which then excite the vehicle's body. One can see that for hard damping the dynamic wheel load almost only consists of the part that results in body oscillations over the whole frequency bandwidth. It is only at 30 Hz that the two parts, body and wheel part, contribute with the same amount to the dynamic wheel load's effect.

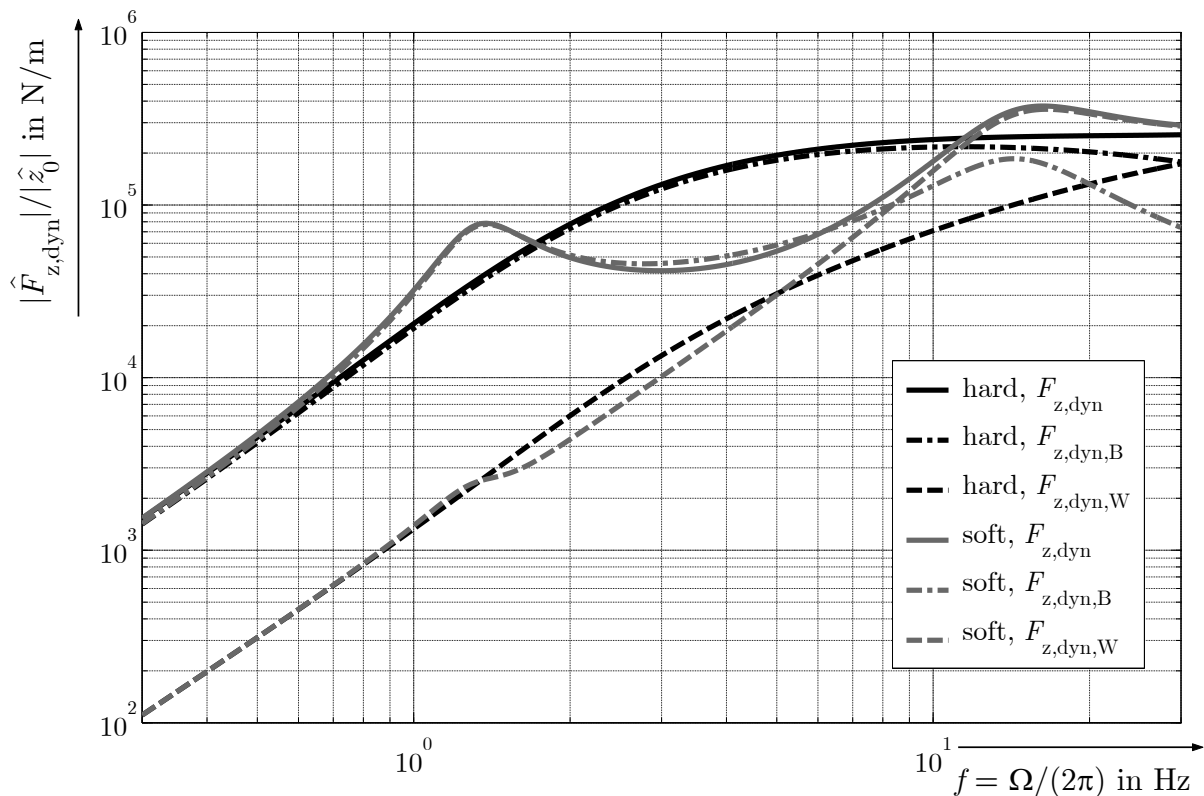


Figure 4.5: Amplitude of dynamic wheel load per amplitude of seismic excitation vs. frequency. Data gained from the linearized quarter-car model for the front left wheel.

For soft damping the picture is slightly different. Here it is already below 10 Hz that the wheel part exceeds the body part. This is because for soft damping the wheel and the body are less dynamically connected than for hard damping. Thus, the wheel can oscillate in its eigenfrequency at around 15 Hz without affecting the body. So due to the seismic excitation and by this due to the dynamic wheel load oscillation the wheel can oscillate without transferring vibrational energy to the body. This is why in case of soft dampers and at higher frequencies the dynamic wheel load is almost only reflected in wheel oscillations. If the damping coefficient is rather high, this means that the wheel oscillation

is strongly connected to the body's oscillation and via the wheel the dynamic wheel load is directly translated into body oscillation.

Furthermore, one can see that the amplification of dynamic wheel load at higher frequencies is approximately by factor five higher than at low frequencies. For soft damping the local maximum between 1 and 2 Hz has a value of 80 kN/m, whereas the local maximum between 10 and 20 Hz has a value of almost 400 kN/m. For hard damping there are no distinguished maxima, but still the dimension of ratio for amplifications at high and low frequencies is roughly the same as for soft damping. This gives a picture of what to expect in terms of frequency spectrum when exciting one of the wheels with the same amplitude of seismic excitation at every frequency—i. e. with a white noise on displacement level.

The response of the integral of dynamic wheel load FI —a quantity which will be introduced and used in more detail in section 4.6.1—to a seismic excitation is also determined by means of the linearized quarter-car model. The complex amplitude of the integral of dynamic wheel load can be determined by simply dividing the complex amplitude of the dynamic wheel load by the excitation frequency $j\Omega$.

$$\hat{FI}(\Omega) = \frac{\hat{F}_{z,\text{dyn}}(\Omega)}{j\Omega} \quad (4.25)$$

In Figure 4.6 the response of the integral of dynamic wheel load to a seismic excitation is plotted vs. the excitation frequency. The integral of dynamic wheel load is investigated because it establishes the connection between vertical and longitudinal dynamics. The detailed explanation of why this is the case can be found in section 5.3.

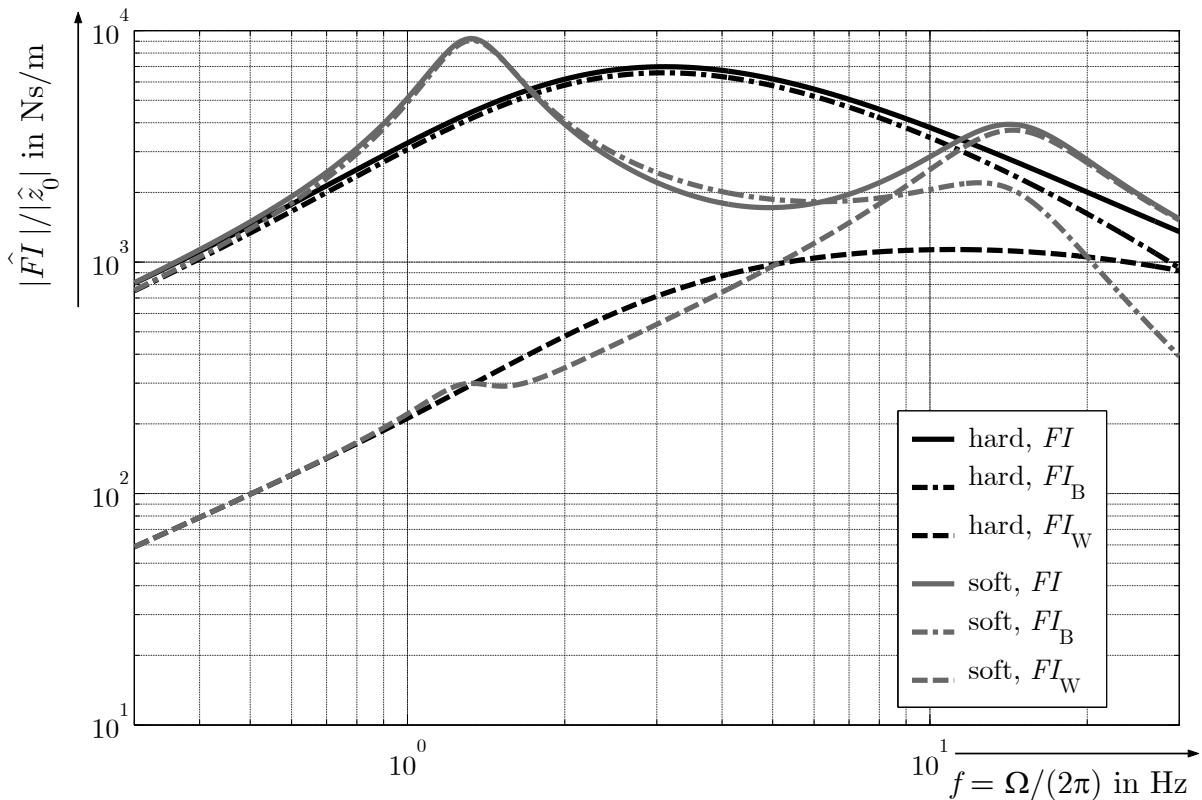


Figure 4.6: Amplitude of the integral of dynamic wheel load per amplitude of seismic excitation vs. frequency. Data gained from the linearized quarter-car model for the front left wheel.

Now for this integral, the distribution over frequencies differs from the one for pure dynamic wheel load. Since the integral has a lowpass-filtering behavior, the lower frequencies are weighted stronger now. For hard damping the maximum of the integral of wheel load appears at 3 Hz, whereas for soft damping it lies between 1–2 Hz. For both hard and soft damping the amplitudes of the integral of dynamic wheel load are by a factor 2–3 smaller for high frequencies above 10 Hz than for low frequencies below 10 Hz. This means that with respect to the integral of dynamic wheel load the oscillations of the body are more relevant than the oscillations of the wheel. This has two reasons: First, because the part of dynamic wheel load which causes body oscillations is greater for lower frequencies and second, because the magnification of the integral of dynamic wheel load is smaller for high frequencies than for low frequencies. Both reasons cause that the control algorithm for longitudinal purposes is most needed at lower frequencies.

In Figure 4.7 the amplitude of the integral of dynamic wheel load per amplitude of seismic excitation, divided by the excitation frequency is shown.

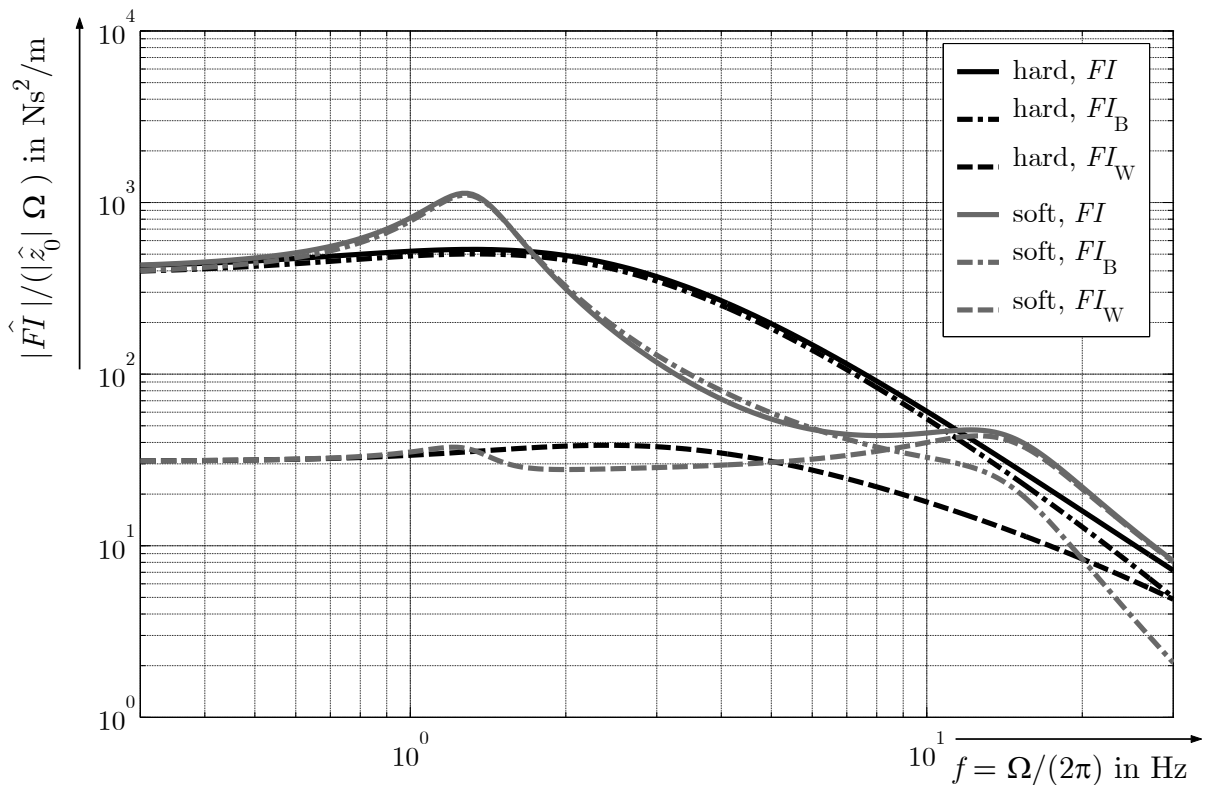


Figure 4.7: Amplitude of dynamic wheel load per amplitude of seismic excitation divided by Ω vs. frequency. Data gained from the linearized quarter-car model for the front left wheel.

Why is this division by the frequency done? Looking back at section 3.4.2, it becomes clear why. On a road with a standard roughness the amplitude of vertical excitation decreases with the wave number (for a constant velocity this is comparable to a frequency in the time domain) to the power of minus one. Translated into a time-based frequency this means that driving at a constant speed the amplitude of the vertical excitation also decreases with the frequency to the power of minus one. Thus, driving on an ordinary road, the excitation by the pavement causes the integral of dynamic wheel load to behave in the way shown in Figure 4.7 with respect to frequency. The necessity to control the dynamic

wheel load and its integral therefore lies at lower rather than at higher frequencies. In case of braking, the quarter-car is not only excited by the seismic excitation but also by the additional (subtracted) wheel load at the front (rear) wheel due to weight transfer (refer to section 2.2). This kind of excitation holds very low frequencies, assuming that the braking force and with it the weight transfer is applied constantly and immediately. It therefore can be neglected in the thoughts just made, because it does not hold a noteworthy proportion of high frequencies and therefore does not change the quality of conclusions just drawn.

Looking at the response of the integral of dynamic wheel load to a seismic excitation gives an idea of the frequency bandwidth within which the wheel-load controller needs to work. But this is only one part of the whole inspection, it is the demand part. The second question which needs to be answered is the supply question. In which frequency band is it possible to actually influence the wheel load? To answer this question, in Figure 4.8 the amplitude of damper velocity $\hat{v}_D = \hat{z}_B - \hat{z}_W$ per amplitude of seismic excitation is plotted vs. frequency. It can be seen that the amplitude of damper velocity oscillations increases with increasing frequency. For the same amplitude of seismic excitation the amplitude of damper velocity is higher at higher frequencies than at lower frequencies. Since the damper velocity delivers a direct connection to the possible strength of the effect a wheel-load controller can have (refer to section 4.6.2), this implies that the possible effect of the controller is highest at high frequencies. This is correct for a white noise excitation on the displacement level. But again, in reality the seismic excitation is comparable to a white noise on velocity level rather than on displacement level.

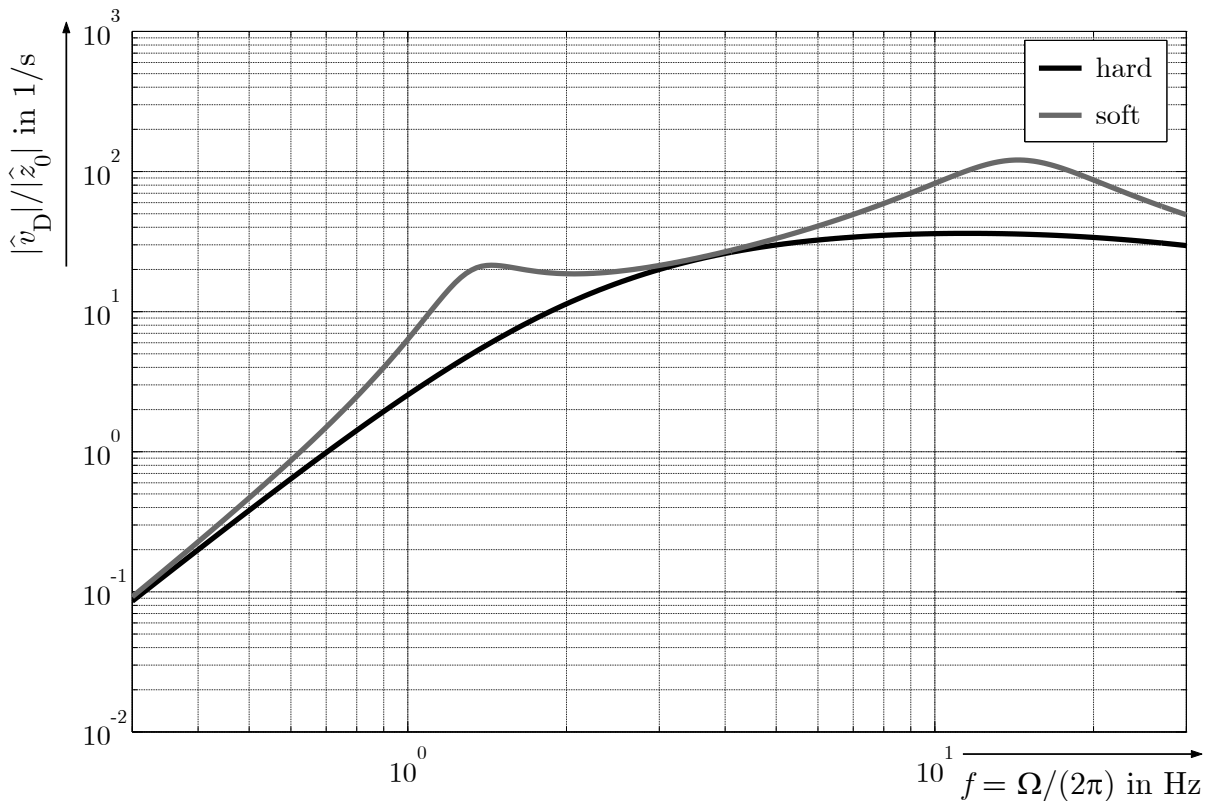


Figure 4.8: Amplitude of damper velocity per amplitude of seismic excitation vs. frequency. Data gained from the linearized quarter-car model for the front left wheel.

That is why, similar to the thoughts formed for the integral of dynamic wheel load,

in Figure 4.9 the amplitude of the damper velocity per seismic excitation is plotted vs. frequency and divided by the frequency. It can be seen that now the amplitude of damper velocity decreases with the excitation frequency from 1–3 Hz on. The maximum of damper velocity is reached for both hard and soft damping at approximately 1–4 Hz.

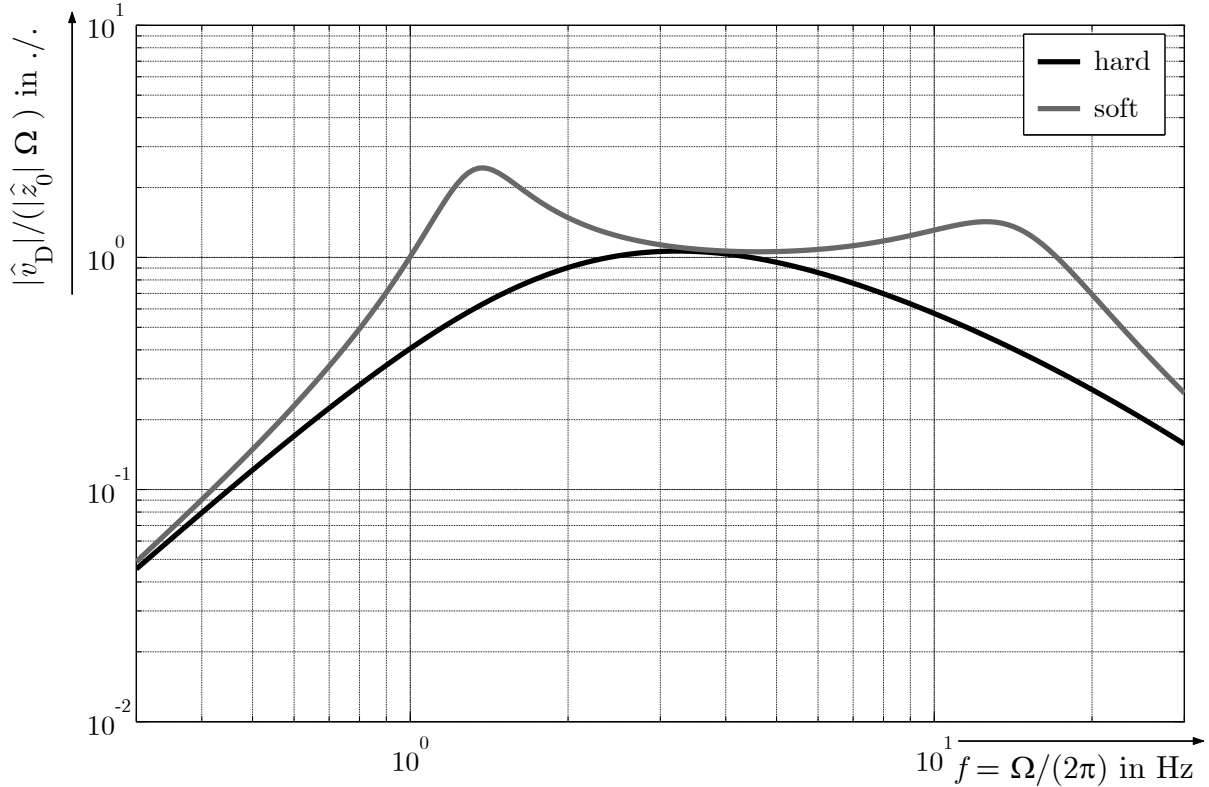


Figure 4.9: Amplitude of damper velocity per amplitude of seismic excitation divided by Ω vs. frequency. Data gained from the linearized quarter-car model for the front left wheel.

Comparing Figure 4.7 with Figure 4.9 it can be seen that the demand on the wheel-load controller in terms of operation frequency band is quite similar to the supply a wheel-load controller can deliver. The correlation between integral of dynamic wheel load and the damper velocity is high. In Figure 4.10 the integral of dynamic wheel load is plotted vs. the damper velocity for a road-like excitation. Only frequencies between 1 and 30 Hz are looked at. It can be seen that, simplifying speaking, the greater the damper velocity, the greater the integral of dynamic wheel load. This shows once again that for the given purpose—braking on a road with a normal roughness—the supply and the demand side of the problem overlap very well. If the oscillation of the integral of dynamic wheel load took place at frequencies above, let's say, 20 Hz and at those frequencies there was not any oscillation of the shock absorber, it would not be possible to purposefully influence the course of the integral of dynamic wheel load by means of active shock absorbers. The supply and the demand side of the problem would not match. But, since the wheel load integral and the damper velocity are influenced on the same level of physical quantities (the wheel load integral is on velocity level—due to the integration of the acceleration signals, and the damper velocity obviously is on velocity level as well) and their distribution in the frequency domain is similar, the supply and the demand side of the problem fit.

Comparing the results from the quarter-car simulation model in Figure 4.9 with the ones

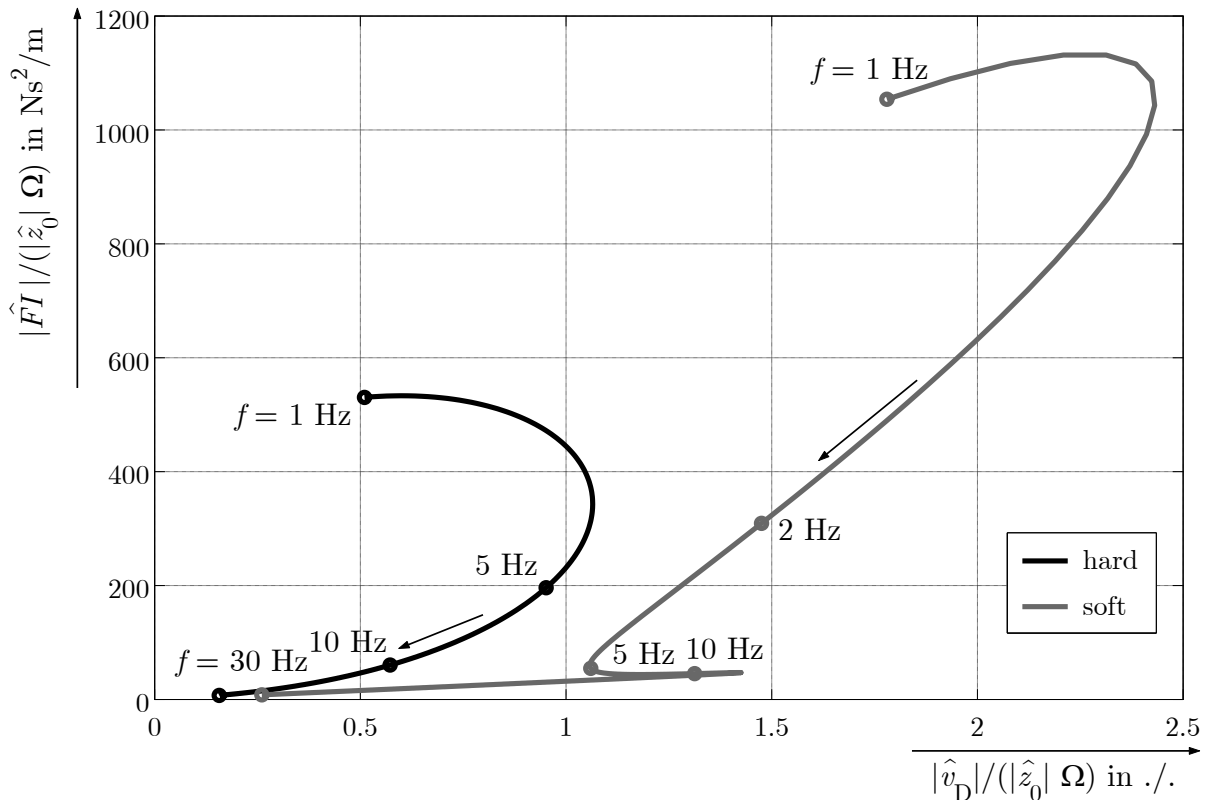


Figure 4.10: Amplitude of integral of dynamic wheel load per amplitude of seismic excitation divided by Ω vs. amplitude of damper velocity per amplitude of seismic excitation divided by Ω . Data gained from the linearized quarter-car model for the front left wheel.

from a real braking procedure in Figure 5.9 on page 132 it can be seen that the qualitative course of the frequency spectrum is comparable for the simulation and the real world. Those two figures are comparable because the simulation is made for an excitation that decreases with f^{-1} and the real-world test drives are executed on the ‘Standard Road’, whose elevation profile decreases with f^{-1} , too. In both cases the maximum amplitude of damper velocity occurs between frequencies of 1–2 Hz for soft damping. For hard damping the maximum amplitude lies at a slightly higher frequency for the simulation (3–4 Hz), whereas in the real world the maximum for hard damping lies at 2 Hz. For both hard and soft damping the amplitudes of damper velocity decrease from their low-frequency maxima on. The higher amplitudes at very low frequencies below 1 Hz in the real-world plot can be explained by the fact that there the system is not only excited by the seismic excitation alone, but also by the additional wheel load caused by the weight transfer during braking.

4.4 Wheel Load-Controller—MiniMax-Controller

In section 4.2 the Wheel Load Influence Matrix was introduced (refer to Table 4.1 on page 64). This matrix shows that it is possible to purposefully influence the course of wheel load. This knowledge about the effect of switching the shock absorber can be implemented into a switching logic. This logic chooses between the two characteristic lines ‘soft’ and ‘hard’, depending on the inputs ‘damper velocity’ and ‘request of wheel load’,

and is therefore called MiniMax-Controller. It is only the two extrema that are selectable states for the MiniMax-Controller for the following reason:

It is assumed that most of the time the shock absorber cannot provide the damper force which is requested. The requested damper force is either too large or it has a sign that would make an active element necessary. Reichel² used a controller to reduce the oscillations of dynamic wheel load which made use of the whole spectrum of characteristic lines of the active shock absorber. His results showed that even though there was the possibility to set the damper current to an intermediate level, it was almost at all times that the output of his controller was either ‘hard’ or ‘soft’. This in connection with the fact that after setting the damper current two first order low-pass filter apply before the actual damper force is set (with respect to the damper current and with respect to the damper force) leads to the construction of the MiniMax-controller. Both low-pass filter smooth the course of damper force and bring a time delay to the system. Thus, if the request at a given time is to increase the wheel load, this request should be followed by the controller as quickly and as strongly as possible to partly compensate the effect of the filters. If the dimension of change in damper force was much greater than it actually is, this MiniMax-strategy ought to be reconsidered. But for the given system it is suitable.

Another advantage is that the MiniMax-controller is independent of the actual characteristic lines of the shock absorber. Furthermore, it is only the sign of the damper velocity that is necessary as input. Those are two implementation reasons which make the MiniMax-controller more feasible for close to reality applications.

The damper velocity v_D , or better, the sign of the damper velocity $\text{sign}(v_D)$ provides with information about the direction into which the shock absorber is moving—compression or rebound. The request of wheel load $F_{z,\text{req}}$ has values of either one (increase wheel load) or minus one (decrease wheel load). This request can come from any top-level controller which might be in service. It can either be a global-chassis-management controller or, like in this context, a more specific controller, namely the one whose final purpose is to reduce the braking distance. This top-level controller which delivers the request of wheel load is described in section 5.3. For now it is not of any interest where the request of wheel load comes from. It is just either one or minus one.

In Figure 4.11 the principle function of the MiniMax-controller is shown. Depending on the inputs v_D and $F_{z,\text{req}}$ the damper current I_D is switched to either 0 or 1.6 A (hard or soft shock absorbers). This means if either the request of wheel load or the damper velocity changes its sign, the active shock absorber will be switched from hard to soft or vice versa. The change in the course of wheel load is not caused by the fact that either hard or soft damping is present itself. It is caused by the fact that the shock absorber is switched. Without switching, the course of wheel load might be good or bad in the sense of small oscillations, but the transient change which is used as a tool by the MiniMax-controller only occurs when switching the shock absorber.

Furthermore, since the damping factor changes its value from hard to soft or vice versa every time v_D passes zero, it is possible to establish artificial characteristic lines for the active shock absorbers by means of the MiniMax-controller. As it is described in section 3.1, shock absorbers in general have a stronger rebound than compression stage, the damper forces in rebound are greater than in compression for the same absolute value of damper

²Reichel (2003): Untersuchungen zum Einfluss stufenlos verstellbarer Schwingungsdämpfer auf das instationäre Bremsen von Personenzugmaschinen.

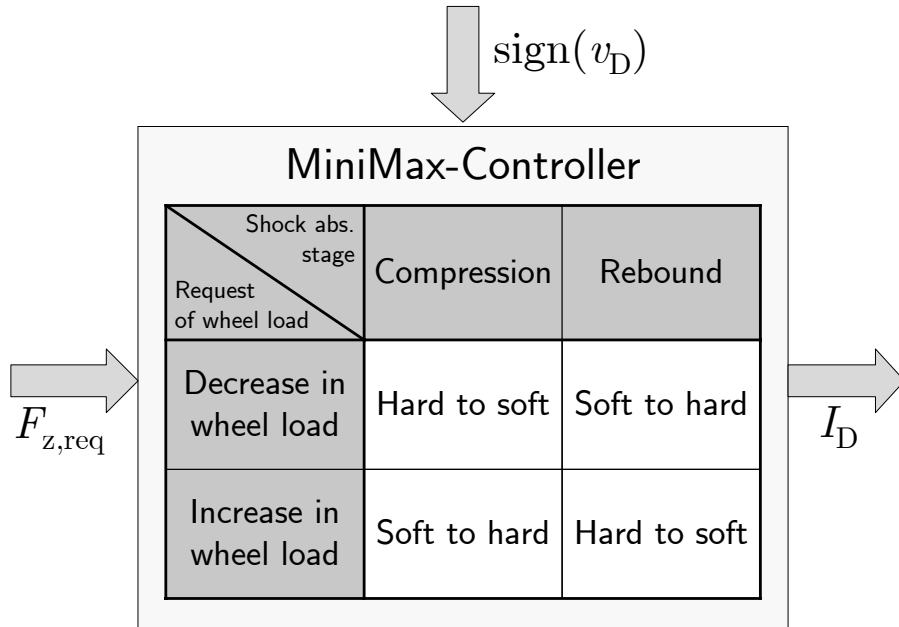


Figure 4.11: MiniMax-controller.

velocity. With the active shock absorber for both rebound and compression the damping can be set to either soft or hard. If the request of wheel load stays constant at ‘increase wheel load’ (‘decrease wheel load’) during time, this leads to a soft (hard) shock absorber in rebound and to a hard (soft) shock absorber in compression. Thus, those artificial characteristic lines lead to a smaller rebound/compression ratio³ s_{RC} (refer to equation 3.1 on page 37) of the shock absorber characteristic for ‘increase wheel load’ and to a greater spreading for ‘decrease wheel load’.

4.4.1 Artificial Characteristic Lines

By means of the MiniMax-controller the active shock absorber can be operated in characteristic lines which it does not really possess by construction. Figure 4.12 shows those artificial characteristic lines for the shock absorber of the testing vehicle at the front left wheel. If the request of wheel load $F_{z,req}$ is kept constant at e.g. +1, the shock absorber will be switched from hard to soft or vice versa every time the damper velocity passes the value zero. Thus, for this example the artificial characteristic line in Figure 4.12 which is marked with circles will establish. The rebound/compression ratio s_{RC} is much smaller than it is for the standard characteristic lines ‘hard’ or ‘soft’. In fact, for the given shock absorber $s_{RC}|_{F_{z,req}=+1} \approx 1$. If the request of wheel load is kept constant at -1 , this ratio for the then establishing characteristic line $s_{RC}|_{F_{z,req}=-1} \approx 3...5$, depending on the damper velocity’s magnitude.

The wheel load which can be gained at the i -th wheel by switching the active shock absorber from one setting to another (hard to soft or $F_{z,req} = -1$ to $F_{z,req} = +1$, this does not matter in the short run, it is basically the same in the short run) equals the difference of the damper force $\Delta F_{D,i}$ between hard and soft damping for a given damper velocity

³Ratio between the average damping coefficient in rebound and the average damping coefficient in compression.

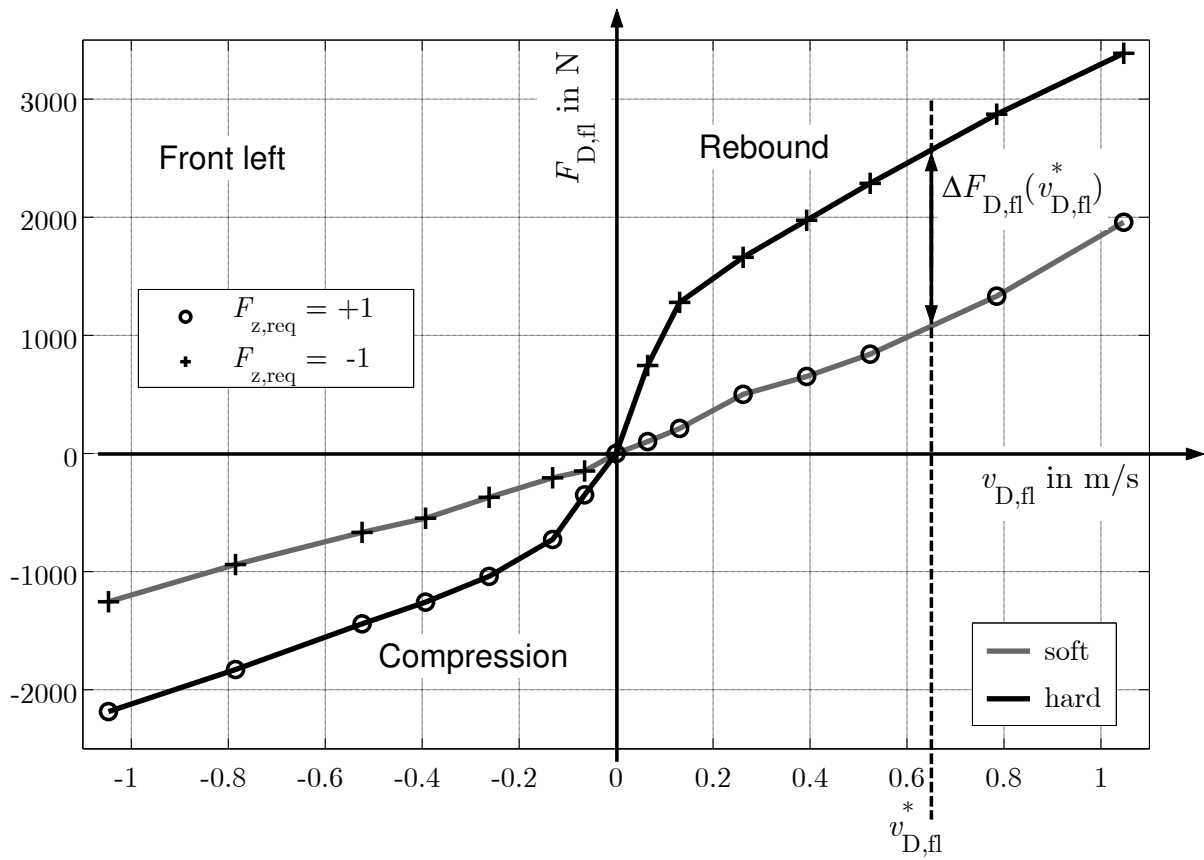


Figure 4.12: Characteristic lines of the active shock absorber mantled at the front left wheel of the testing vehicle.

$v_{D,i}^*$. Thus, the greater the spreading s_{hs} between the hard and the soft characteristic line, the greater the possible effect on wheel load. But it must be kept in mind that the wheel load effect which goes into the desired direction is always followed by a wheel load effect in the opposite direction. This is because wheel load can neither be increased nor decreased in the long run. The mean value of dynamic wheel load is always zero in the long run.

4.4.2 Lowering and Lifting of the Vehicle's Body

The difference between damping coefficient in rebound and compression leads to a self-leveling effect. This means that the vehicle's body is lowered if the average damper force is smaller in compression than in rebound. In a quarter-car model the only forces which act on the vehicle's body are the body damper and the body spring force. Thus, during one oscillation cycle in stationary condition these forces must sum up to zero. Figure 4.13 shows the principle of the effect which leads to a lowering and lifting of the vehicle's body.

- a) In the static case where no oscillations are present, the spring's displacement $s_S = z_B - z_W$ is equal to $s_{S,static}$.
- b) The active shock absorber is operated such that the artificial characteristic line is maximum hard in rebound ($I_D = 0 A$ for $v_D \geq 0$) and minimum soft in compression ($I_D = 1.6 A$ for $v_D < 0$). This is equivalent to the case where the request of wheel load $F_{z,req} = -1$. For a ratio $s_{RC} > 1$ this leads to a lowered body and the mean spring displacement with respect to time is equal to $s_{S,1} < s_{S,static}$.
- c) The shock absorber is now operated such that the artificial characteristic line is minimum soft in rebound ($I_D = 1.6 A$ for $v_D \geq 0$) and maximum hard in compression ($I_D = 0 A$ for $v_D < 0$). This is equivalent to the case where the request of wheel load $F_{z,req} = +1$. Now due to the increased damper force in compression and the lowered damper force in rebound the wheel load will increase and cause the body to accelerate upwards as long as due to the increasing spring force the vehicle's body will at a point be accelerated downwards again. This is the point in time when the wheel load is not increased anymore but the Delta Wheel Load is equal to zero. Afterwards the wheel load is decreased as long as it takes for the body to reach its new stationary position.
- d) The active shock absorber is now still operated such that the request of wheel load $F_{z,req} = -1$. The vehicle's body is now in stationary position again. For a ratio $s_{RC} < 1$ this leads to a lifted body and the mean spring displacement with respect to time is equal to $s_{S,2} > s_{S,static}$.

The amount of lifting and lowering of the vehicle's body can also be calculated in an analytical way. The spring and the damper force are calculated by multiplying the body spring stiffness respectively the body damping coefficient with the spring displacement respectively the damper velocity (equations 4.26 and 4.27).

$$F_{c_B}(t) = c_B [z_B(t) - z_W(t)] = c_B s_S(t) \quad (4.26)$$

$$F_{k_B}(t) = k_B [\dot{z}_B(t) - \dot{z}_W(t)] = k_B \dot{s}_S(t) = k_B v_D(t) \quad (4.27)$$

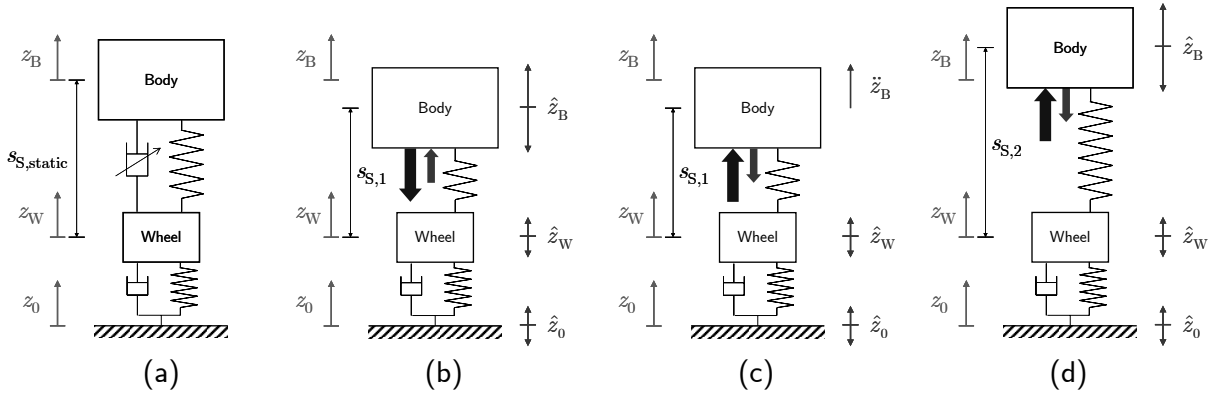


Figure 4.13: A quarter-car model describes the vertical movement of the vehicles body when a seismic excitation causes it to oscillate. The amplitudes of the oscillations of body z_B , wheel z_W and seismic excitation z_0 are referred to as \hat{z}_B , \hat{z}_W and \hat{z}_0 . The upwards and downwards pointing arrow right of the model demonstrates the oscillation of the respective degree of freedom.

If the quarter-car is in a stationary, periodic mode due to a seismic, periodic excitation, the spring and the damper force must sum up to zero over one time period. This is because those are the two forces which move the vehicle's body either up or down. If the oscillation is stationary, there is no long-term movement of the body. If it is additionally periodic, the forces—which cause an acceleration of the body—must sum up to zero over a time period.

$$\oint F_{c_B}(t) + F_{k_B}(t) dt = 0 \quad (4.28)$$

For the following thoughts the damping coefficient k_B is assumed to be constant in rebound and compression but differs with the sign of damper velocity.

$$k_B = \begin{cases} k_{B,R} & \text{for } \dot{s}_S = v_D \geq 0 \\ k_{B,C} & \text{for } \dot{s}_S = v_D < 0 \end{cases}, \quad (4.29)$$

where $k_{B,R}$ stands for the damping coefficient in rebound and $k_{B,C}$ for the one in compression. The ratio of damping coefficient in rebound and the one in compression is called s_{RC} (refer to section 3.1). For the testing vehicle, s_{RC} can have values between approximately 1 and 3...5 for the front and the rear axle, depending on the damper velocity and the damper setting—hard and soft, or $F_{z,req} = -1$ and $F_{z,req} = +1$.

$$\frac{k_{B,R}}{k_{B,C}} = s_{RC} \quad (4.30)$$

Now the oscillation of the spring displacement caused by a seismic excitation is assumed to be not only periodic but harmonic plus a constant displacement $s_{S,mean}$. This displacement in stationary mode, which describes a lowering or lifting of the body, is to be determined in the following steps.

$$s_S(t) = s_{S,mean} + \hat{s}_S \cos(\omega t) \quad (4.31)$$

This assumption also leads to a harmonic oscillation of the damper velocity $v_D(t) = \dot{s}_S(t)$:

$$\dot{s}_S(t) = -\omega \hat{s}_S \sin(\omega t) \quad (4.32)$$

Applying equations 4.26, 4.27, 4.31, and 4.32 to equation 4.28 and integrating over one time period of the assumed periodic oscillation leads to:

$$\int_0^{\frac{2\pi}{\omega}} c_B (s_{S,\text{mean}} + \hat{s}_S \cos(\omega t)) - k_B \omega \hat{s}_S \sin(\omega t) dt = 0 \quad (4.33)$$

$$c_B s_{S,\text{mean}} \frac{2\pi}{\omega} - \left[\int_0^{\frac{\pi}{\omega}} k_{B,C} \omega \hat{s}_S \sin(\omega t) dt + \int_{\frac{\pi}{\omega}}^{\frac{2\pi}{\omega}} k_{B,R} \omega \hat{s}_S \sin(\omega t) dt \right] = 0 \quad (4.34)$$

$$c_B s_{S,\text{mean}} \frac{2\pi}{\omega} + [k_{B,C} \hat{s}_S \cos(\omega t)]_0^{\frac{\pi}{\omega}} + [k_{B,R} \hat{s}_S \cos(\omega t)]_{\frac{\pi}{\omega}}^{\frac{2\pi}{\omega}} = 0 \quad (4.35)$$

$$c_B s_{S,\text{mean}} \frac{2\pi}{\omega} = 2 k_{B,C} \hat{s}_S - 2 k_{B,R} \hat{s}_S \quad (4.36)$$

$$s_{S,\text{mean}} = \frac{\omega \hat{s}_S}{\pi c_B} (k_{B,C} - k_{B,R}) \quad (4.37)$$

Applying equation 4.30 and substituting $\omega \hat{s}_S$ with \hat{v}_D finally leads to:

$$s_{S,\text{mean}} = -k_{B,C} (s_{RC} - 1) \frac{\hat{v}_D}{\pi c_B} \quad (4.38)$$

From equation 4.37 derives that the self-leveling effect is proportional to the difference of linearized damping coefficients for rebound and compression, $k_{B,R} - k_{B,C}$, and to the amplitude of the damper velocity \hat{v}_D of a given harmonic oscillation. From equation 4.38 derives that the self-leveling effect is proportional to $(s_{RC} - 1)$, to the linearized damping coefficient in compression $k_{B,C}$, and again to the amplitude of the damper velocity \hat{v}_D of a given harmonic oscillation. It is reciprocal to the body spring stiffness. It can also be seen that for a spreading greater than one (damping coefficient in rebound is greater than in compression) an oscillation leads to a negative value for $s_{S,\text{mean}}$, which means that the body is lowered. If the spreading is equal to one (equal damping coefficient for rebound and compression), no self-leveling effect will occur at all.

As can be seen in equation 4.13 on page 65, the dynamic wheel load can be measured in terms of the sum of vertical body and vertical wheel acceleration. If the damper is switched in such a way that the changing damping force leads to an upwards acceleration of the vehicle's body, this therefore means that the wheel load is increasing, otherwise the body would not be accelerated upwards. Of course, at the same time the wheel will be accelerated downwards, which would indicate a decreasing wheel load. But since the mass of the wheel is by factor 8...13 smaller than the mass of the body (22...47 kg compared to 290...380 kg), this downwards pointing acceleration is 8...13 times greater than the upwards acceleration of the body. This in combination with the fact that the maximum deflection of the tire spring is by factor 10 smaller than the one of the body spring (can be measured

in terms of stiffness: 288 kN/m compared to 28.6...29 kN/m) leads to the conclusion that the downwards acceleration of the wheel will last 80...130 times shorter than the upwards acceleration of the body does. Thus, the part of the effect which leads to an acceleration of the wheel will disappear very quickly, whereas the acceleration of the body will last longer and contribute to the main part of the effect.

Delta Spring Displacement Δs_S

As has been shown in the previous sections, switching from one artificial characteristic line to another not only increases or decreases the wheel load, but it also leads to a lowering or lifting of the vehicle's body. The amount of this change in spring displacement can be calculated analytically if the course of damper velocity is harmonic and if it is assumed that the damping coefficients for rebound and compression are constant. To measure the self-leveling effect in reality, where those assumptions do not hold true, a measurand is introduced. The spring displacement at the i -th wheel $s_{S,i}$ is defined as the difference between body and wheel displacement $z_{B,i} - z_{W,i}$, whereas Delta Spring Displacement is the difference between the mean values (with respect to time) of the $s_{S,i}$ of the two stationary states for different damping characteristics $k_{D,1}(v_D)$ and $k_{D,2}(v_D)$. Since for a given seismic excitation not equal to zero the spring displacement varies with the characteristic of the active shock absorber, there is always a lifting respectively lowering of the vehicle's body if the active shock absorber is switched from one artificial characteristic line to another. This lifting or lowering is measured with the Delta Spring Displacement quantity.

$$\Delta s_{S,i,1 \rightarrow 2} = \frac{1}{t_2 - t_s} \int_{t_s}^{t_2} s_{S,i} dt - \frac{1}{t_s - t_1} \int_{t_1}^{t_s} s_{S,i} dt \quad (4.39)$$

for $t_1 \ll t_s$ and $t_2 \gg t_s$, $F_{z,\text{req}} = \text{req}_1$ for $t \in [t_1; t_s]$ and $F_{z,\text{req}} = \text{req}_2$ for $t \in [t_s; t_2]$. The shock absorber is switched from characteristic line 1 to characteristic line 2 and the quantity measures the difference in spring displacement for the long-run average before and after switching the shock absorber.

4.5 Test Drives on a Typical German Autobahn

In test drives two details of the vertical dynamics are investigated which cannot be investigated in test rig trials. Firstly, the effect of switching the shock absorber on the course of wheel load is identified in real test drives. The difference to test rig trials is the spinning wheel, the type of oscillation of wheel load, and the incoherent excitation at left and right wheel. For reproducibility reasons those test drives are executed on the 'Defined Obstacles' test track (refer to section 3.4.1). Since it is not only the vertical but also the longitudinal dynamics which are investigated in this kind of test drives, those test drives are covered in section 5.2.2.

Secondly, the amount of lowering and lifting of the vehicle's body is determined in test drives on German highways. The question which needs to be answered is if the amount of lowering and lifting is similar to the one that can be found on the test track 'Standard Road', which is used for executing the full-braking test drives. Besides that those highway

test drives should deliver the time constant of the vertical movement of the vehicle's body. How long does it take for the body to be lowered or lifted?

To determine how big the self-leveling effect is on an ordinary road, test drives on 400 km of southwestern German Autobahn are executed. Besides the purpose to determine the strength of the self-leveling effect there is yet another objective which ought to be achieved by those Autobahn test drives: All braking procedures executed in chapter 5 are executed on the test track 'Standard Road', which is the pavement of an old airfield that belongs to Technische Universität Darmstadt (refer to section 3.4.2). To determine if this pavement is representative for a typical German Autobahn the Δ_{SS} measured at the airfield is compared to the one measured on the Autobahn track. This comparison already was made in section 3.4.2. Here the method to actually determine the Delta Spring Displacement is explained.

The test drives to determine the Delta Spring Displacement which occurs when driving on an ordinary road were executed on the route shown in Figure 4.14.

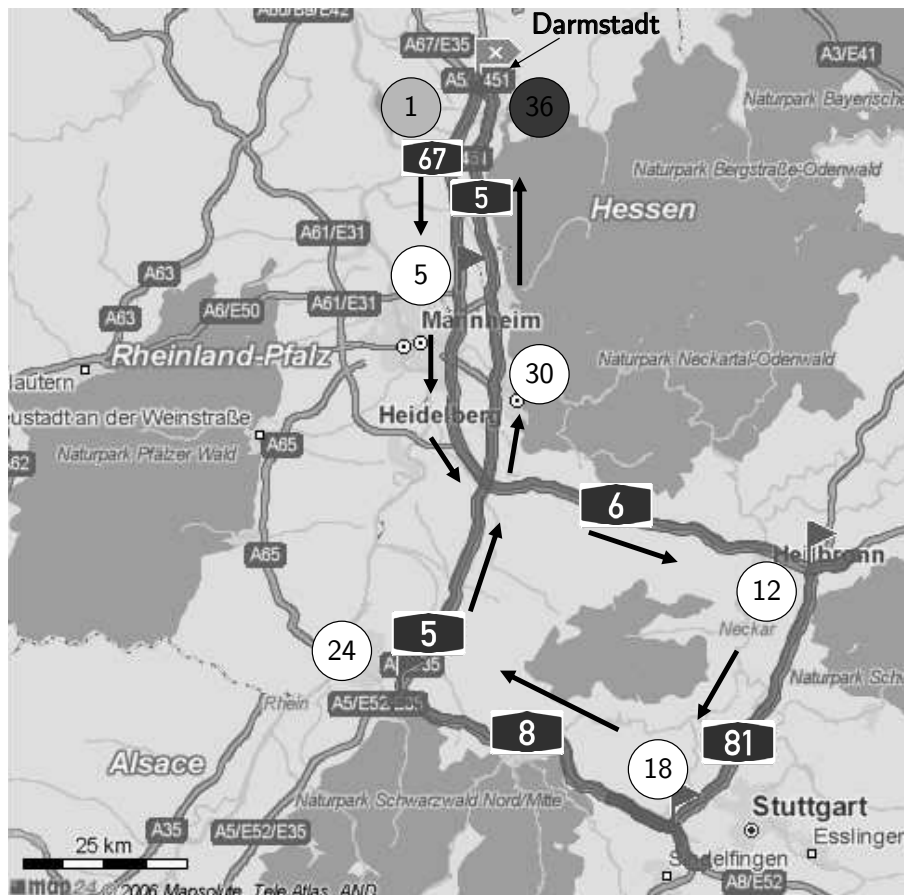


Figure 4.14: Routing of the track that is measured with respect to its unevenness by making use of the self-leveling effect⁴. The numbers give the number of the road section that starts at the given position. The overall length of the testing track is approximately 400 km.

The vehicle's velocity is kept constant at 85 km/h during the test drives. On all highways it is the very right lane which is driven on. There it is possible to drive in between the trucks, which are lining up on the right lane in Germany, and therefore adopt to their

⁴N.N. (2006b): Website – map 24

constant velocity. Parts of the test drive in which the velocity could not be kept constant due to traffic or other reasons are not analyzed. The testing procedure is as follows: The strategy to decrease (increase) the wheel load is pursued in each case for fifteen seconds. This leads to a lowering (lifting) of the vehicle's body. After switching the strategy to 'increase' ('decrease'), the vehicle's body is lifted (lowered). The mean value of the spring displacement of the front right wheel for the time after switching the strategy minus the mean value of spring displacement before switching the strategy gives the Delta Spring Displacement of the actual switching process. The principle of this procedure is explained in Figure 4.15.

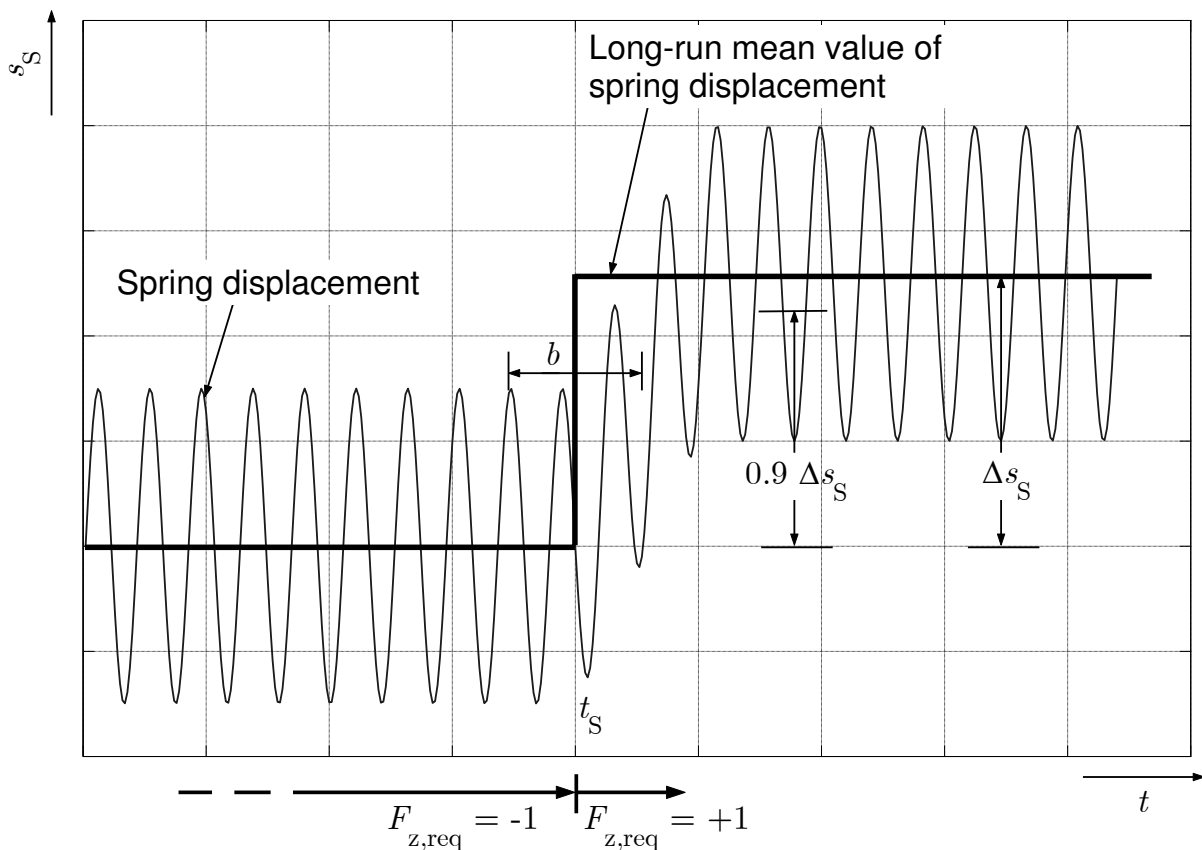


Figure 4.15: Method that is used to determine the Delta Spring Displacement due to switching the control of the active shock absorbers from $F_{z,\text{req}} = -1$ to $F_{z,\text{req}} = +1$ on an ordinary road.

Since the body needs time to establish its new position after switching the strategy, in each case the first five seconds after t_S are not counted to determine the mean value of spring displacement. The Delta Spring Displacement Δs_S provides information about the power which is put into the oscillation system 'vehicle' by passing the pavement. It is the bigger the faster the vehicle drives. In the given context, Δs_S furthermore provides information about how strong the switching effect of the shock absorbers will be and for how long it will last.

It is not only the Delta Spring Displacement Δs_S which is determined in the Autobahn test drives, but also the time the vehicle's body needs to establish its new stationary elevation after a switching of the strategy ('increase wheel load' to 'decrease wheel load' or vice versa). This time $t_{90\%}$ is defined as the time at which 90% of the total Delta Spring

Displacement is reached after a strategy change. Since the pure spring displacement signal is noisy, it is not the spring displacement itself which is observed to find $t_{90\%}$, but the floating mean value of the spring displacement. For the calculation of the floating mean value of s_S at a given time, $b = 2.5$ s of the signal are averaged (1.25 s backwards and 1.25 s forwards). Those 2.5 s were determined as the best suitable value by analyzing how many seconds during a stationary period need to be averaged such that this mean value is equal to the long run mean value for every window b . Figure 4.16 shows the described quantities exemplarily for two strategy switchings at the front right wheel on part of the Autobahn.

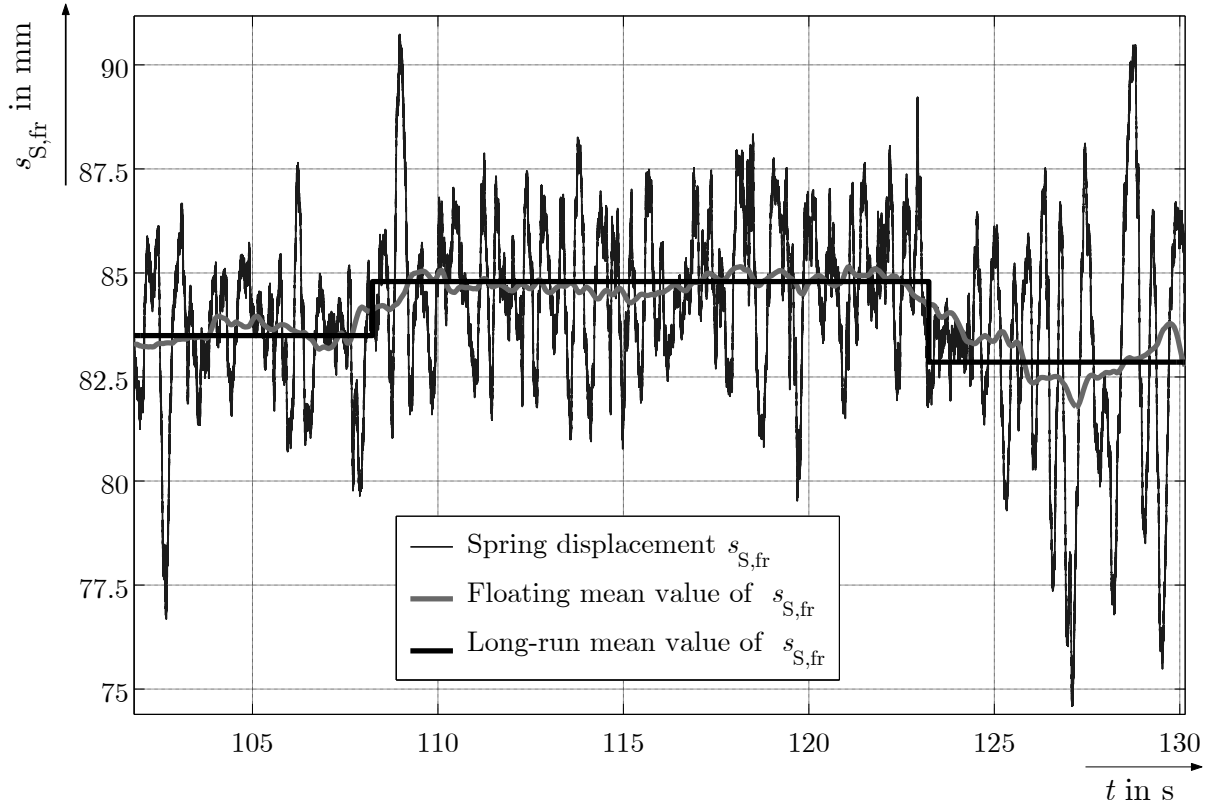


Figure 4.16: Result from a switching the control of the active shock absorbers from $F_{z,\text{req}} = -1$ to $F_{z,\text{req}} = +1$ and vice versa on an ordinary road.

For the front right wheel the time $t_{90\%}$ has mean values for 200 switchings each of:

$$F_{z,\text{req}} = -1 \text{ to } F_{z,\text{req}} = +1: t_{90\%} = 1.1 \text{ s}$$

$$F_{z,\text{req}} = +1 \text{ to } F_{z,\text{req}} = -1: t_{90\%} = 0.85 \text{ s}$$

Those values give a rough impression of how long it takes for the vehicle's body to establish the new stationary condition after switching the strategy. They strongly depend on the value for b and can therefore not deliver information of how long the vehicle's body is accelerated upwards or downwards after switching the strategy. But still, the values determined for $t_{90\%}$ help to determine the time it takes for a strategy change to have its full effect on the lifting or lowering of the body.

In Figure 4.17 the results of determining the front right Delta Spring Displacement $\Delta s_{S,\text{fr}}$ for the chosen highways are shown. The averaged values of $\Delta s_{S,\text{fr}}$ for every road section

are plotted versus the number of the respective road section (for the numbering refer to Figure 4.14). For each road section there are approximately 10–12 switching processes, 5–6 in each direction ('increase' to 'decrease' and vice versa). It can be seen that the Delta Spring Displacement varies in a range from 2–4 mm in both directions—either switching from 'increase' to 'decrease' or vice versa. Figure 4.17 shows that there are some sections which are worse than other sections in the sense that the pavement is rougher. Numbers 6, 7, 20, 22, and 28, 29 have a higher mean value of Delta Spring Displacement than the other sections. Those are road sections which follow close behind the city of Stuttgart on the Autobahn no.8 and sections close behind the Kreuz Walldorf on Autobahn no.5. Those parts of the highway system are known to be in a poor condition. Several bumps and short waves follow each other there. Beside those sections the results of the other parts of all Autobahn sections overdriven lie in a band of $\Delta s_{S,fr} \approx 2\text{--}3\text{ mm}$. Since the result for the Delta Spring Displacement of the chosen test track 'Standard Road' also lies within this band, this test track is assumed to be representative for those southwestern German highways (refer to section 3.4.2).

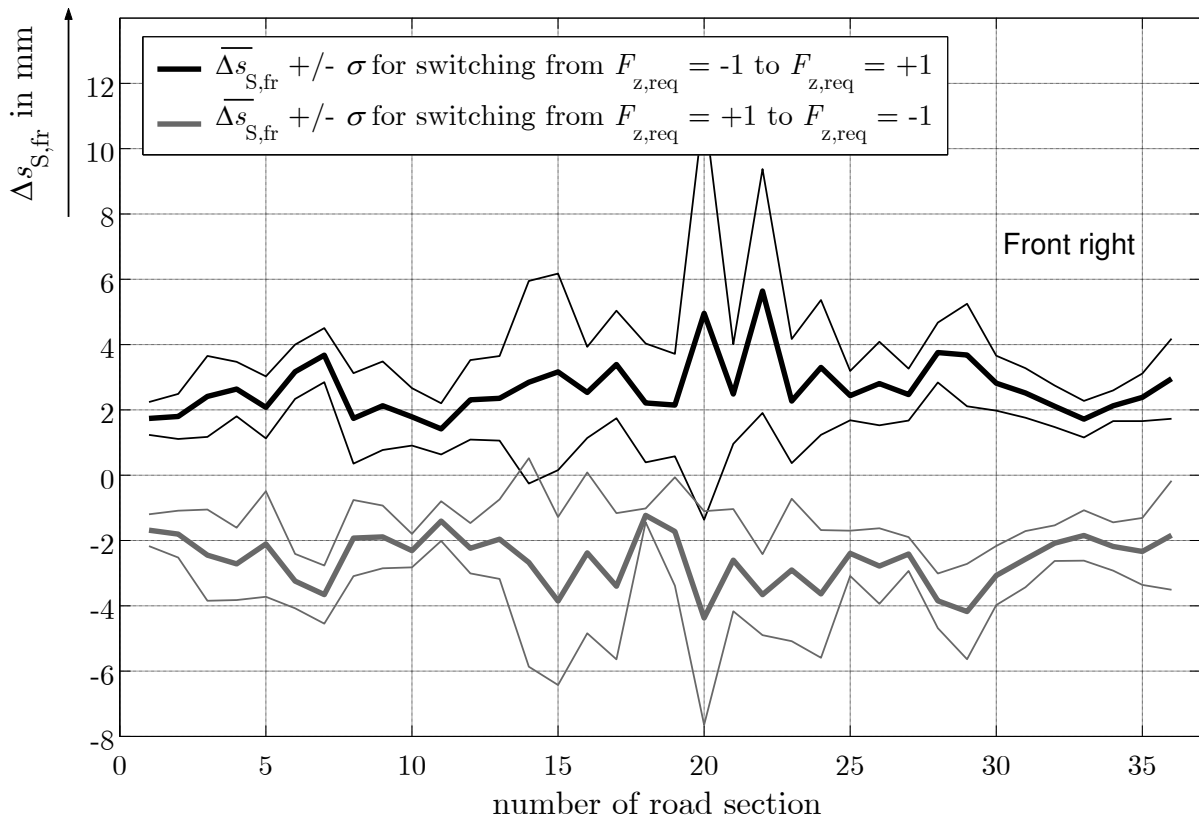


Figure 4.17: Mean values of the Delta Vertical Displacement $\Delta s_{S,fr}$ of the front right wheel which occurs when switching from one request of wheel load (e. g. 'decrease wheel load') to another (e. g. 'increase wheel load').

4.6 Test Rig Experiments

Test rig trials are executed to validate the Wheel Load Influence Matrix (refer to Table 4.1 on page 64) and the assumptions of the quarter-car model described in section 4.3. The hypothesis is formed that the wheel load can be influenced purposefully in a desired direction. But it is not only this question of the direction of the effect which needs to be answered. In fact, the time behavior and the absolute values by which the wheel load can be influenced must be determined in order to be able to decide if the active shock absorber and its switching can affect the vertical dynamics heavily enough to finally increase the braking performance. In section 4.3 it could be shown that the damping velocity is highest at low frequencies when driving on a road with a typical unevenness. The next question which needs to be answered is: How is the damper velocity connected to the effect which the active shock absorber can have on the course of wheel load?

4.6.1 Method

To answer these questions a testing procedure was developed which allows to measure the influence of switching the shock absorber from one constant characteristic line to another, e.g. from hard to soft damping or vice versa. During this procedure the testing vehicle is put on a 4-post test rig (for a detailed description of this test rig refer to section 3.3) and stimulated by seismic excitations on either all wheels, only one wheel, one axle, or one side. No matter where the seismic excitation is applied, it always is applied as a sinusoidal oscillation at one constant frequency during one trial. The frequencies applied range from 0.5 Hz up to 30 Hz, in order to cover the whole spectrum of relevant vertical oscillations of the vehicle. The amplitude \hat{s}_P with which the testing vehicle is excited depends on the given frequency. It is the reciprocal of the excitation frequency f_e times a constant $\hat{s}_{P,1\text{ Hz}} = 50\text{ mm}$.

$$\hat{s}_P(f_e) = \frac{1}{f_e} \hat{s}_{P,1\text{ Hz}} \quad (4.40)$$

or on velocity level:

$$\hat{s}_P = 2\pi \cdot 50\text{ mm/s} \approx 0.314\text{ m/s} = \text{const.} \quad (4.41)$$

The periodic seismic excitation eventually leads to a periodic response of the whole system. This means that once the whole system oscillates in a stationary condition, the course of every single quantity is periodic. Thus, it is possible to measure the effect of switching the active shock absorber at a wheel. Changing any parameter of the oscillating system leads to a transient reaction of the system and finally to a new stationary situation. Now that it is known what would have happened if the shock absorber had not been switched (because the courses of all measurands are periodic), the difference between the actual course of any measurand after switching the shock absorber and the proposed course which would have established if the shock absorber had not been switched gives information about how the switching process affects the system. For all tests whose results are shown here the standard inflation pressure of $p_T = 2.3\text{ bar}$ is used.

Before the detailed description of the developed testing method starts, some definitions shall be introduced. The quantities which are essential for the measuring process are the following ones.

Switching Time t_s

The switching time t_s is the time at which the damper is switched from one constant damper setting to another. For all following definitions the time scale is set such that $t_s = 0$ s. I. e. the time starts to count at the time of switching the shock absorber.

Delta Wheel Load ΔF_z

The difference of the dynamic wheel load after switching the shock absorber and the dynamic wheel load which would have established if the shock absorber had not been switched is called Delta Wheel Load ΔF_z .

$$\Delta F_z(t) = F_{z,\text{dyn}}^w - F_{z,\text{dyn}}^{w/o} \quad (4.42)$$

For a time period $t \in [t_s; t_s + t_{\text{search}}]$ it is defined as:

$$\Delta F_z(t) = \begin{cases} F_{z,\text{dyn}}(t) - F_{z,\text{dyn}}(t - T) & \text{for } t \in [t_s; t_s + T) \\ F_{z,\text{dyn}}(t) - F_{z,\text{dyn}}(t - 2T) & \text{for } t \in [t_s; t_s + 2T) \\ \dots & \dots \\ F_{z,\text{dyn}}(t) - F_{z,\text{dyn}}(t - nT) & \text{for } t \in [t_s; t_s + t_{\text{search}}) \end{cases}, \quad (4.43)$$

where T is the time period $T = \frac{1}{f_e}$ of the respective seismic oscillation. The time period for which an effect is searched after switching the shock absorber is $t_{\text{search}} = 200$ ms. It is chosen such that every effect lies within this time period. The Delta Wheel Load always refers to the course of wheel load one period before the switching takes place, no matter how many periods after the switching are searched for an effect. That means it always refers to what would have happened if the shock absorber had not been switched.

Delta Wheel Load Integral ΔFI

The integral of the difference of the wheel load values with switching and without switching, ΔFI , is defined for the same time period $t \in [t_s; t_s + t_{\text{search}}]$ as:

$$\Delta FI(t) = \int_{t_s}^t \Delta F_z(\tau) d\tau \quad (4.44)$$

Effect Time t_e

The Effect Time t_e is defined as the time at which the absolute value of Delta Wheel Load Integral crosses a given boundary FI^{bound} for the first time after switching the shock absorber.

$$t_e = \min \left(t \in [t_s; t_s + t_{\text{search}}] \mid |\Delta FI(t)| > FI^{\text{bound}} \right) \quad (4.45)$$

Total Effect Time $t_{e,tot}$

The Total Effect Time $t_{e,tot}$ is the time at which the effect caused by switching the shock absorber vanishes, meaning that ΔF_z crosses zero for the first time after t_e .

$$t_{e,tot} = \min (t \in [t_e; t_s + t_{search}] \mid |\Delta F_z(t)| = 0) \quad (4.46)$$

Effect Magnitude A_e

The Effect Magnitude A_e is defined as the Delta Wheel Load Integral ΔFI , counted from t_s to $t_s + \Delta t_e$. In this thesis and for the given testing vehicle $\Delta t_e = 50$ ms. The value of this time period mainly depends on the dynamics of the active shock absorber and on the vertical dynamics of the vehicle. It is chosen in such a way that for the given experimental setup the mean value of the Total Effect Time $t_{e,tot}$ is greater or equal to Δt_e for every excitation frequency.

$$A_e = \Delta FI(t_s + \Delta t_e) \quad (4.47)$$

Total Effect Magnitude $A_{e,tot}$

The Total Effect Magnitude $A_{e,tot}$ is defined as the Delta Wheel Load Integral ΔFI counted from t_s to $t_{e,tot}$. After $t > t_{e,tot}$ the Delta Wheel Load ΔF_z changes its sign and therefore the Delta Wheel Load Integral's absolute value decreases. Thus, by the Total Effect Magnitude the maximum positive effect of a switching of the active shock absorber from hard to soft or vice versa is measured. The Total Effect Magnitude is not the maximum effect that can be achieved by switching the shock absorber from 'decrease' to 'increase' or vice versa. But it still gives an impression of how much effect can be gained by only switching the shock absorber from one constant characteristic line to another.

$$A_{e,tot} = \Delta FI(t_{e,tot}) \quad (4.48)$$

In Figure 4.18 the method which is used on the test rig is described. It shows the course of dynamic wheel load vs. time for one wheel which stands exemplary for all wheels. At time t_s the active shock absorber at the respective wheel is switched from one constant setting to another. Selectable settings are soft ($I_D = I_{D,max} = 1.6$ A), middle ($I_D = I_{D,middle} = 0.8$ A) and hard ($I_D = I_{D,min} = 0$ A).

Long before the switching of the shock absorber (approximately five time periods) the whole system has reached its stationary mode. Once the shock absorber is switched, the course of dynamic wheel load changes with respect to the course one time period before. The integral of the difference between the dashed line and the solid line between $t_s - T$ and t_s measures this change. There is a dead time between switching the shock absorber and its first measurable effect on dynamic wheel load in which the course of dynamic wheel load remains similar to the one a period before. Until t_e it is not possible to notice that the shock absorber has been switched at all, only by looking at the wheel load.

To investigate the switching process means to investigate the transient behavior of the system, shifting from one stationary state to another. The switching of the shock absorber changes the governing equations of the system. It can be interpreted in such a way that

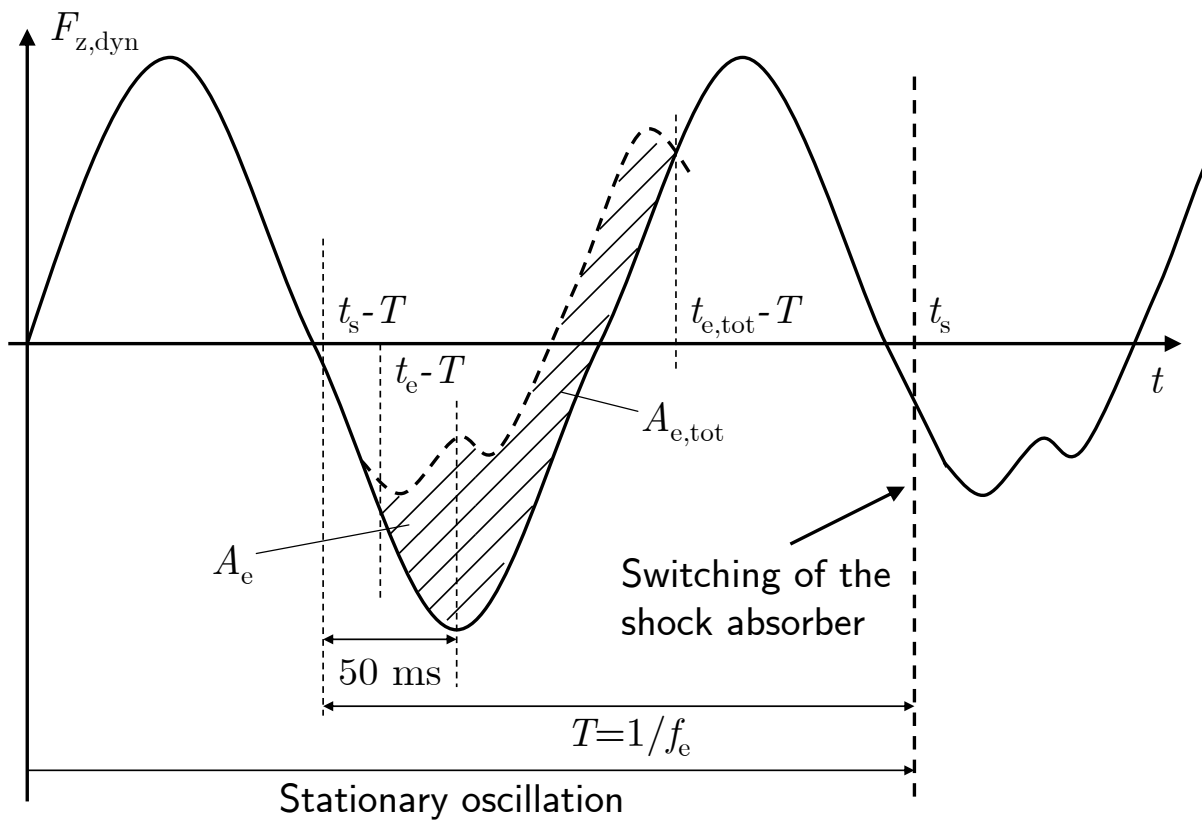


Figure 4.18: Principle of the test rig experiment that has been developed to measure the effect of a switching of the active shock absorber on the dynamic wheel load in both the time and the magnitude frame. The integral of the difference of dynamic wheel load after the switching and a time period before gives information about the strength of the switching effect and the time that it needs for the effect to take place.

two systems (hard and soft) are started at the same initial conditions. It is then the two different courses of wheel load which are compared.

Besides determining the effect of switching the shock absorber, the test rig trials are also valid to verify the use of the quarter-car model. Figure 4.19 shows the strategy to verify the usage of a quarter-car model in order to model the transient behavior after a switching process. The vehicle is put on the test rig and excited in the previously described manner. It is not only an excitation at every four wheels (a) which is applied, but also an excitation at only the front axle (b), only the front left wheel (c), and only one track (d). The assumption is that the kind of excitation (a–d) does not influence the switching effect dramatically in both magnitude and time frame.

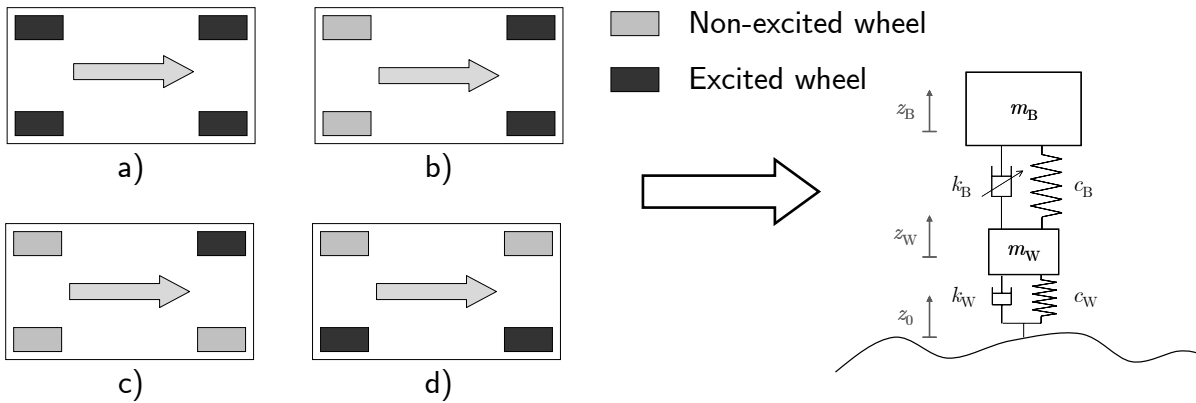


Figure 4.19: Validation strategy to prove the correctness of use of a quarter-car model.

To assure that this assumption holds true, the null hypothesis H_0 and its alternative hypothesis H_1 are formed:

H_0 : The results of the switching procedure with respect to Effect Time and Effect Magnitude for a wheel vary with the type of seismic excitation—whether it is only applied at this wheel or at other wheels at the same time as well.

H_1 : The results of the switching procedure with respect to Effect Time and Effect Magnitude for a wheel are the same, no matter if the seismic excitation is applied only at the switched wheel or at other wheels at the same time as well.

It must be tested if by applying a ‘worst case’ scenario (excitation b–d), which is valid for falsifying the hypothesis H_0 , it can actually be falsified. If this is the case, the opposite of the hypothesis (the results are independent of the existence of seismic excitation at other than the inspected wheel) is assumed to be true. If this again is the case, if the measured results of a switching process depend only on the measurands of this wheel, a quarter-car model is suitable to model the switching process.

Even if it can be shown that the effect of switching the shock absorber at a wheel is independent of the places of excitation, it does not necessarily mean that switching the shock absorber at a wheel does not influence the course of wheel load at other wheels. But this is another aspect, and even if there is this effect on other wheels, modeling the switching at a wheel by a quarter-car model is still valid. The effect that switching the shock absorber on one wheel has on another wheel cannot be implemented in a controller, because

the effect on other wheels depends on the actual damper velocity of those. Depending on the damper velocity at the non-switched shock absorber, it can either be a positive or a negative effect which is caused by the switched shock absorber at the non-switched wheel. But since the effect of switching is greater at the switched wheel than at the non-switched wheel, it is always better to switch the shock absorber if this is the output of the wheel-load controller at the wheel which ought to be switched than to retain the switching due to the damper velocity situation of the non-switched wheel.

Summarizing, if the effect at a wheel mainly depends only on the oscillations at this wheel, this means that for the wheel-load controller it is admissible to use an individual controller for every wheel.

4.6.2 Results

The experiments previously described are undertaken for excitation frequencies between 0.5 and 30 Hz. The location of excitation varies from excitation at all four wheels to excitation at only one wheel over only one track, and one axle. At those wheels where no excitation takes place the shock absorbers are set to their hardest damping.

In Figure 4.20 the measured effect is exemplarily shown for an all-wheel excitation at a frequency of $f_e = 2$ Hz for the front left wheel. The dynamic wheel load with and without switching, the damper velocity, and the damper current are shown. At time t_s the shock absorber is switched from hard to soft. The damper velocity $v_D(t_s)$ at time of switching is negative, which means that the shock absorber is in compression. Therefore what is expected (referred to the wheel load influence matrix in Table 4.1 on page 64) is the lowering of wheel load. And this is in fact what happens: At $t_e \approx 20$ ms after switching the shock absorber the course of wheel load $F_{z,\text{dyn}}^w(t)$ is significantly below the course of wheel load $F_{z,\text{dyn}}^{w/o}(t)$. The wheel load with switching is at the maximum approximately 800 N lower than for the course without switching the shock absorber.

Furthermore, Figure 4.20 shows that the effect is reversed after the Total Effect Time $t_{e,\text{tot}}$ is reached. It is starting from there that the until then negative wheel load integral becomes more positive, because the Delta Wheel Load is also positive from $t_{e,\text{tot}}$ on. It is approximately at the time when the damper velocity changes its sign that the effect becomes negative. This makes sense in the way that it is due to the damper velocity that a damper force is present at all. The change of this damper force is the change in wheel load which can be measured and used for controller purposes.

If now the damper velocity changes its direction, the effect will not go into the desired direction anymore. It will rather be the opposite of what was desired when switching the shock absorber, when the damper velocity had a different sign. When applying the switching of the shock absorber into a controller this fact needs to be remembered. The first effect caused by the switching is ‘positive’ in the sense that it points in the direction which was requested when switching the shock absorber. But between 30 and 200 ms later the desired effect is over and from then on it is ‘negative’ in the sense that the Delta Wheel Load now points in the undesired direction. It depends mainly on the excitation frequency when this point of return will be reached, but it will be reached eventually in every case.

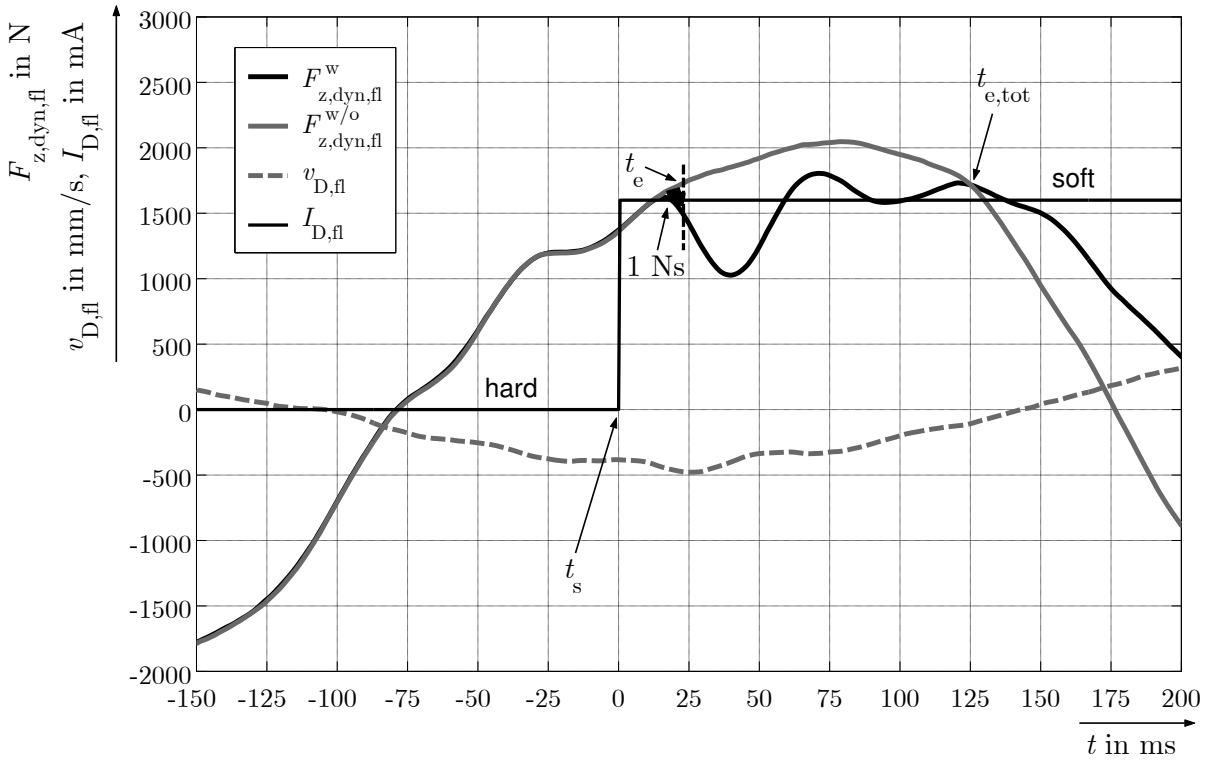


Figure 4.20: Test rig experiment: Effect of switching the shock absorber at the front left wheel at an excitation frequency of $f_e = 2$ Hz. Excitation on all four wheels.

Time Frame

The plot in Figure 4.20 shows the results of only one switching process exemplarily. To make a switching process comparable to one another, the previously described quantities Effect Time and Effect Magnitude were introduced. In this section the effect of switching the shock absorber in the time frame is analyzed. In Figure 4.21 the Total Effect Time and the Effect Time are plotted vs. the excitation frequency for the front left wheel. The same is shown in Figure 4.22 for the rear right wheel.

In both cases it can be seen that the average Effect Time is approximately constant for every excitation frequency. At the rear axle it takes slightly longer for the effect to get to the tire contact zone. This is probably because the shock absorbers at the rear axle are not mounted directly to the axle. There the damper force acts via a lever arm on the axle, and this lever arm is suspended in a rubber mounting, which could lead to a time delay in the transmission path of damper force to wheel load. The Total Effect Time decreases with an increasing excitation frequency. This is due to the fact that switching the shock absorber has a positive effect on the course of the wheel load only as long as the damper velocity has the same sign as it had at the time of switching.

Furthermore, it can be seen that the direction in which the shock absorber is switched (hard to soft or soft to hard) effects neither the Effect Time nor the Total Effect Time strongly.

This means: First of all, assuming that superposition can be done, the average time that it takes for the switching of the shock absorber to have an effect on the wheel load is independent of the type of excitation, may it be a noise, a periodic or any other transient

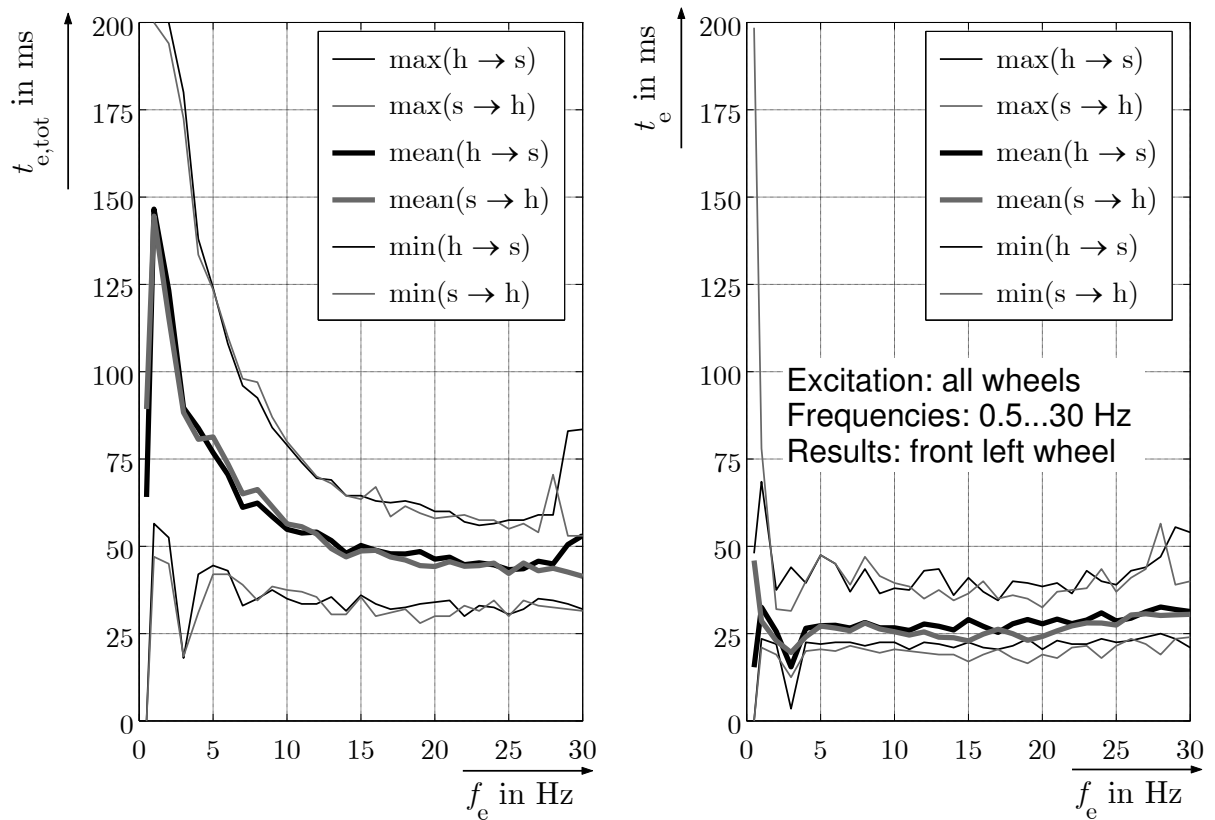


Figure 4.21: Total Effect Time and Effect Time vs. excitation frequency for front left wheel and seismic excitation at all four wheels equally.

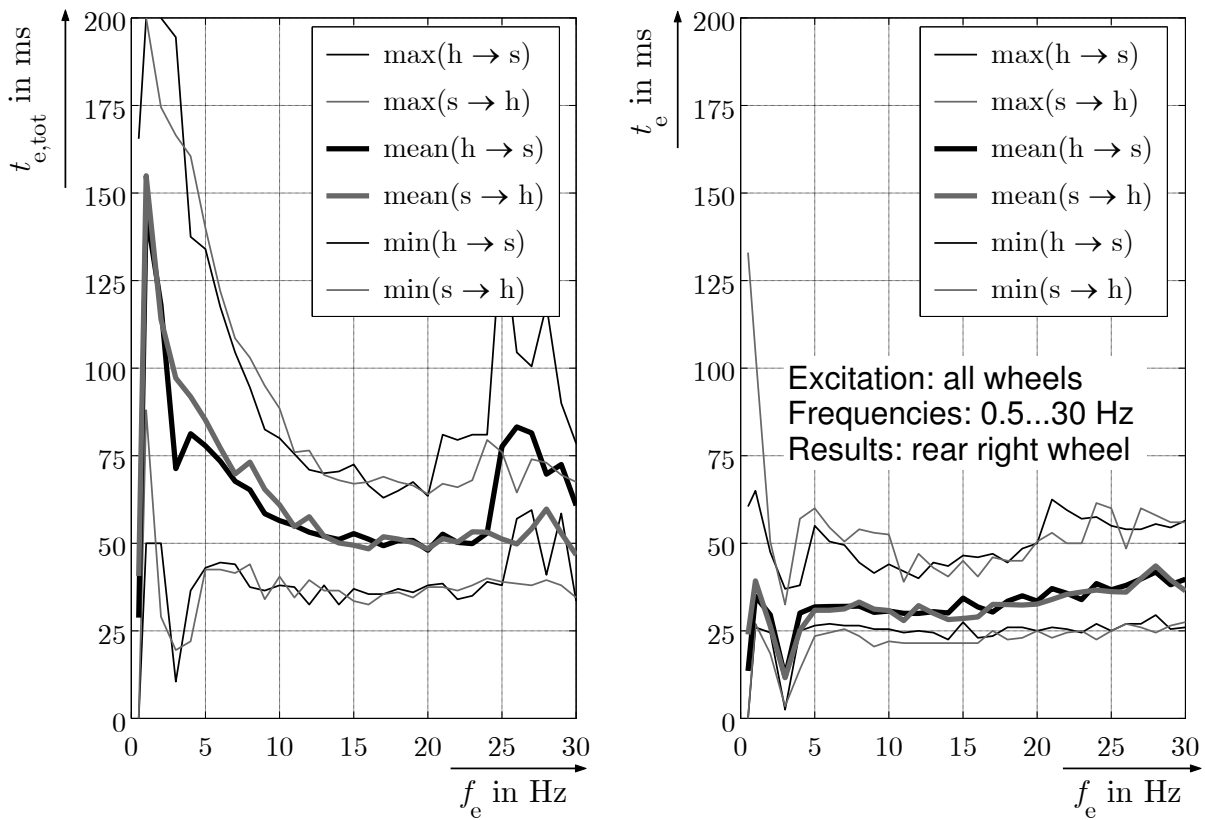


Figure 4.22: Total Effect Time and Effect Time vs. excitation frequency for rear right wheel and seismic excitation at all four wheels equally.

type of seismic excitation. It only depends on the velocity of the shock absorber at time of switching $v_{D,s} = v_D(t_s)$ and on the switching direction (refer to Figure 4.23).

One main part of this time delay comes from the fact that the electromagnetic valve within the shock absorber has to change its opening condition and that the hydraulic pressure within the shock absorber has to change. The second main part comes from the fact that the tire first has to be deformed in order to transfer the damper force into wheel load. Yi has also shown this effect by applying a sudden change of shock absorber setting (soft to hard) to an active shock absorber at constant damper velocity⁵.

The second conclusion from Figure 4.21 is that the duration of the effect and with this its positiveness is longer the lower the excitation frequency. Hence, superposition cannot be done in this case. The duration of the effect of switching the shock absorber strongly depends on the frequencies with which the vehicle is excited.

In Figure 4.21 it can furthermore be seen that it takes approximately an average time of 26 ms for the effect to take place at the front left wheel and 32 ms for the rear right wheel. Due to symmetry the same holds true for the front right and the rear left wheel, so that in this sense the front left wheel stands exemplary for the front axle and the rear right wheel for the rear axle. Just above the body eigenfrequency, at 3 Hz, the effect takes place at an average time of 18 ms respectively 12 ms. This has two reasons:

Firstly, because here the body and the wheel movement are out of phase, the amplitudes are rather large, and the pitching and the vertical eigenfrequency of the vehicle's body interfere. Those facts are the reason that the reproducibility of the course of wheel load from one time period to another is slightly smaller here than at other frequencies. This is why the band of 1Ns for the Delta Wheel Load Integral can be crossed earlier for the oscillations at this frequency.

Secondly, between 3 and 4 Hz the difference for hard and soft damping of the magnification of the transfer function from seismic excitation to dynamic wheel load is greatest (refer to Figure 4.5 on page 69). This means that—dynamically seen—a switching from hard to soft causes a greater difference in wheel load here than at other frequencies. Therefore, the transient transmission from the stationary condition for hard (soft) to soft (hard) damping is stronger than at other frequencies and the threshold FT^{bound} of 1Ns is reached faster.

Furthermore, it can be seen that the duration of the effect varies between mean values of approximately 150 and 50 ms. The longest effect duration is achieved at low frequencies of 1 Hz. Above 10 Hz there is almost no difference in the effect duration anymore for the different frequencies. This shows that at higher frequencies the effect is not very useful, it has its highest effectiveness at frequencies below 5 Hz. This corresponds very well with the fact that the frequency spectrum of damper velocity for driving on an ordinary road has its maximum at the exact same frequencies (refer to Figure 4.9 on page 73 for simulation results on this topic and to Figure 5.9 on page 132 for experimental results). So the supply and demand fits together: The maximum effect is supplied by the system at frequencies below 5 Hz and the maximum effect is demanded at the same frequencies.

In Figure 4.23 the Effect Time is plotted vs. the damper velocity at the time of switching of the shock absorber for the most relevant frequencies between 0.5 and 5 Hz. It can be seen that there is a tendency for the Effect Time to be smaller the greater the damper velocity at time of switching. It can also be seen that in most of the cases the Effect Time lies at approximately 25 ms. This means it takes 25 ms for the switching of the shock

⁵Yi/Wargelin/Hedrick (1992): Dynamic Tire Force Control by Semi-Active Suspensions.

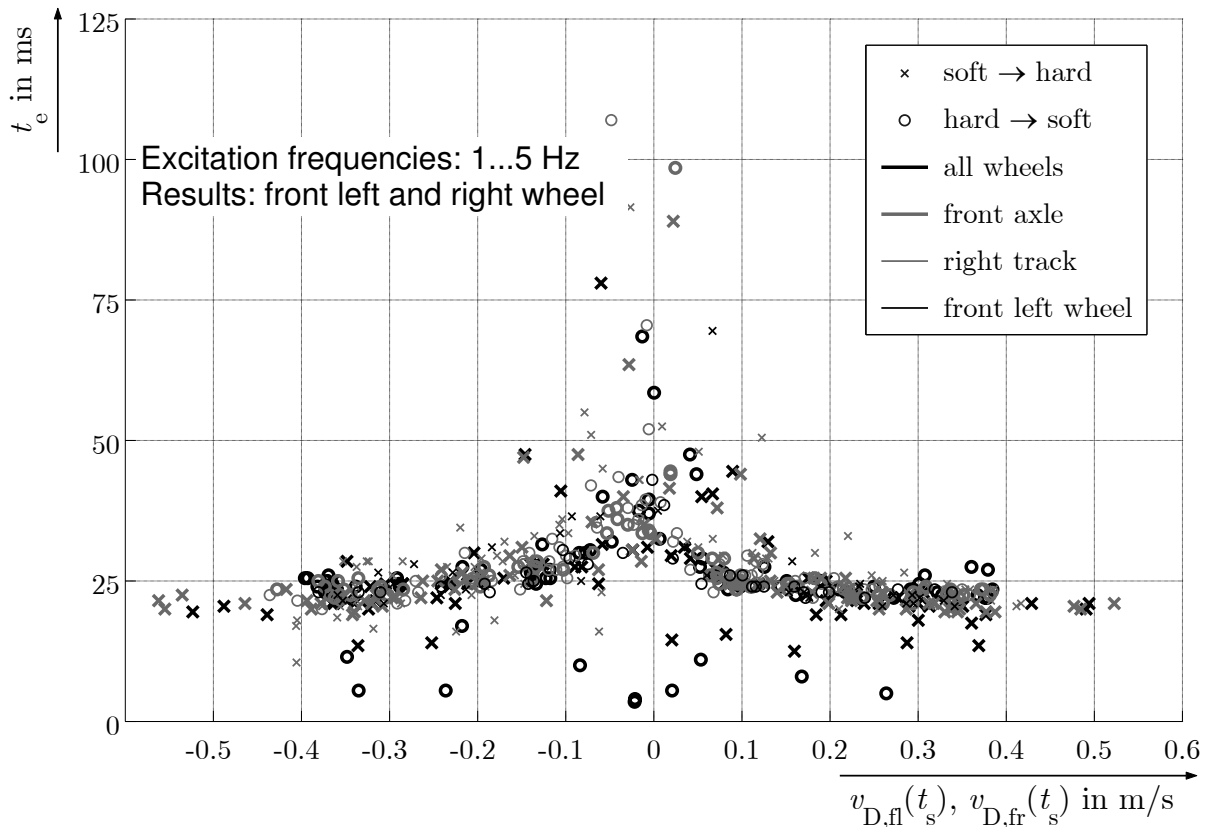


Figure 4.23: Effect Time vs. damper velocity at time of switching the shock absorber for front left and front right wheel and seismic excitation at different wheels. Results are gained from test rig experiments.

absorber to have an effect on the course of wheel load. In some cases this time is shorter, in some it is much longer. The cases in which it takes very long for the effect to take place (from 50 up to 100 ms) are those in which the damper velocity at the time of switching is low ($|v_D| < 0.1$ m/s). At those low velocities the shock absorber is either at the upper or at the lower turning point, and it takes time before the full damper force—and with it the full measurable effect—has established from there on.

Another thing that Figure 4.23 shows are the results for the Effect Time for different types of excitation. The vehicle is either excited at only the front left wheel, the front axle, the right track, or at all four wheels. It can be seen that the principle behavior of the Effect Time does not vary, no matter what type of excitation is used. There is always the tendency for the Effect Time to decrease with increasing damper velocity at time of switching. It is also always that the mean value of t_e for most switching processes lies at around 25 ms. The shorter Effect Times for excitation at all wheels which occur in some cases can be explained again by the fact that those appear at 3 Hz excitation frequency where the course of wheel load is not as reproducible as at other frequencies.

The important conclusion for falsifying hypothesis H_0 on page 90 is that the variance of Effect Time for the same type of excitation and all other parameters being constant is in the same dimension as the variance of Effect Time for a differing type of excitation *ceteris paribus*⁶. This means that when switching the shock absorber at a given damper velocity,

⁶“Ceteris paribus is a Latin phrase, literally translated as ‘with other things being the same,’ and usually

the output in terms of Effect Time cannot be predicted more precisely, no matter if the type of excitation is only at one wheel, one axle, one track, or all wheels. Thus, the effect that the type of excitation has on the Effect Time—if present at all—is smaller than other random effects. The hypothesis H_0 on page 90 is therefore falsified in the time domain and hypothesis H_1 is presumed to be true.

Another essential thing to mention is the following: Even though the effect of switching the active shock absorbers in most cases points into the expected direction, that is, if switching from hard to soft in compression, the wheel load will decrease for example, the effect always becomes negative after a while. This means that it is only for a restricted amount of time that a positive effect, meaning in the desired direction, can be obtained.

After this time, which is measured by $t_{e,tot}$, the wheel load will take a course which is the opposite of what was desired when switching the shock absorber. The wheel load will be smaller than without switching, even though the request of wheel load was to increase and vice versa. This is because wheel load can never be increased or decreased as a whole. The times of positiveness and negativeness of dynamic wheel load can only be shifted from a bad distribution to a better distribution.

Since the relevant frequency band is the one from 1 to 5 Hz, the Effect Time in general is short enough for the given purpose to influence the wheel load goal-oriented. Even at the highest relevant frequency of 5 Hz the Effect Time corresponds only to a phase shift of approximately $25 \text{ ms} \cdot 5 \text{ Hz} \cdot 2\pi = 1/8 \cdot 2\pi = \frac{\pi}{4}$, which means that for every fourth switching case the damper velocity has changed its sign before the effect appears in the wheel load. I. e. the majority of 75 % of all switching processes will lead to a change in wheel load in the desired direction, even for an excitation frequency of 5 Hz. At lower frequencies this percentage is even higher. At 1 Hz it lies at roughly 95 % ($25 \text{ ms} \cdot 1 \text{ Hz} \cdot 2\pi = \frac{\pi}{20}$).

For any excitation frequency the fraction of switching processes which will lead to a change of wheel load in the desired direction g_{switch} can be calculated by equation 4.49.

$$g_{\text{switch}} = 1 - 2 t_e f_e \quad (4.49)$$

The fact that the values of g_{switch} for low frequencies—which are the relevant ones in the given context—lie between 75 and 95 % implies that with respect to the time frame the active shock absorbers can be used to purposefully influence the wheel load. But this only answers the question if the effect of switching the shock absorber will point into the desired direction. Another question is if the effect will take place fast enough for the given control purpose. Since to answer this question the longitudinal dynamics (which is discussed in chapter 5) needs to be taken into account, it is covered in section 5.3.1 on page 126. Nevertheless, the answer shall be anticipated: The switching of the shock absorber is admissible to influence the lateral dynamics of a passenger car purposefully with respect to the time frame.

Magnitude Frame

In the previous section the switching effect was investigated in the time frame and it was shown that with respect to time the effect is feasible for a goal-oriented influence on the course of wheel load.

rendered in English as ‘all other things being equal.’ ” Source: Wikipedia

In Figure 4.24 the total effect magnitude and the Effect Magnitude are plotted vs. the excitation frequency for the front left wheel. Here it can be seen that both the average total effect and the average effect are stronger the lower the excitation frequency. This has two reasons: First, it is due to the longer Total Effect Time for lower frequencies which leads to a greater Delta Wheel Load Integral. Second, it is due to the greater amplitude of the Delta Wheel Load.

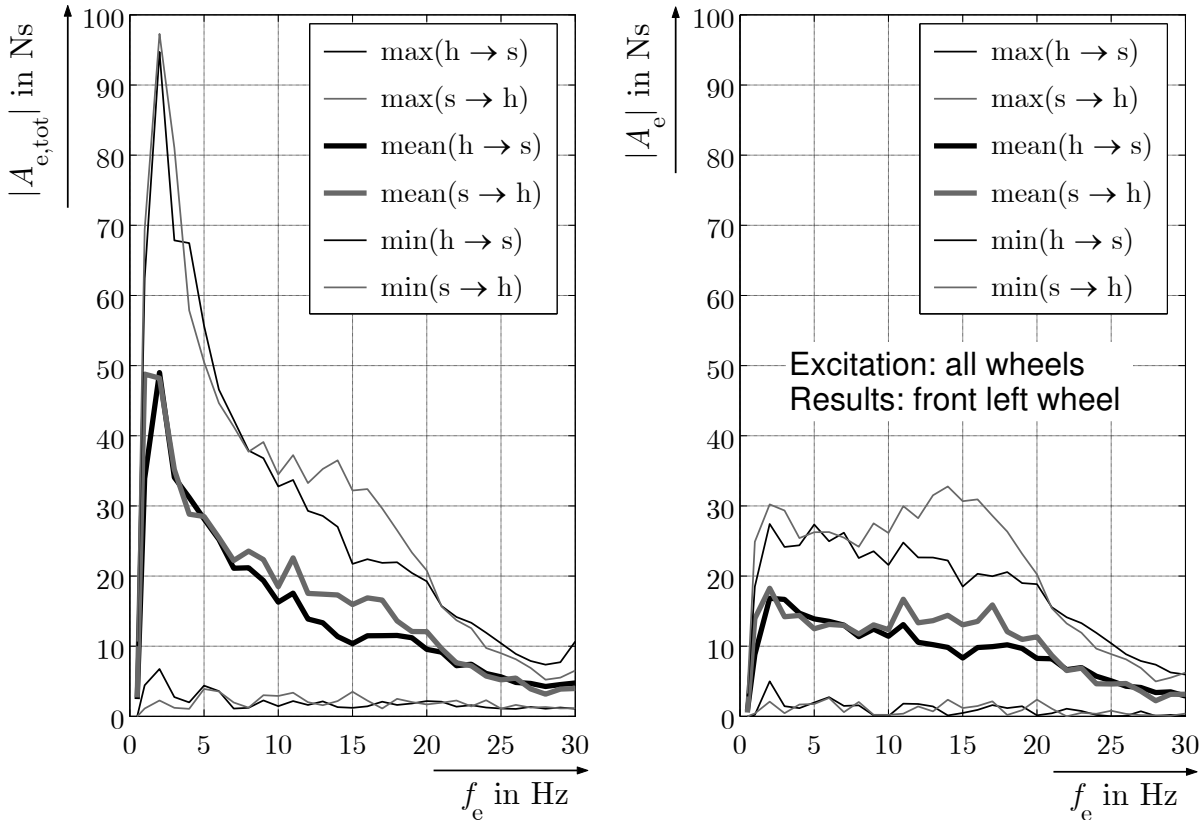


Figure 4.24: Total Effect Magnitude and Effect Magnitude vs. excitation frequency for front left wheel and seismic excitation at all four wheels equally. Results are gained from test rig experiments.

Again, a superposition is not allowed to do, because the effect is not independent of the excitation frequency at which it is measured. But it can be seen that for frequencies between 1 and 5 Hz the total effect is greatest. Again, those are the frequencies at which both the supply and the demand side have the highest amplitudes.

The same holds true for the rear axle. The only difference is that there the Effect Magnitude is by factor two smaller than it is at the front axle. This is because the spreading at the front axle is by approximately factor two greater than the spreading at the rear axle (refer to Figures 4.3 and 4.4 on page 66). The Delta Damper Forces are therefore also by factor two greater. Thus, the switching effect is twice as strong at the front as it is at the rear axle.

Since the relevant frequencies are low ones, in Figure 4.25 both the Total Effect Magnitude $A_{e,tot}$ and the Effect Magnitude A_e are plotted vs. the damper velocity at time of switching for excitation frequencies between 1 and 5 Hz only. This figure shows that A_e in the given frequency band strongly depends on the absolute value of damper velocity at

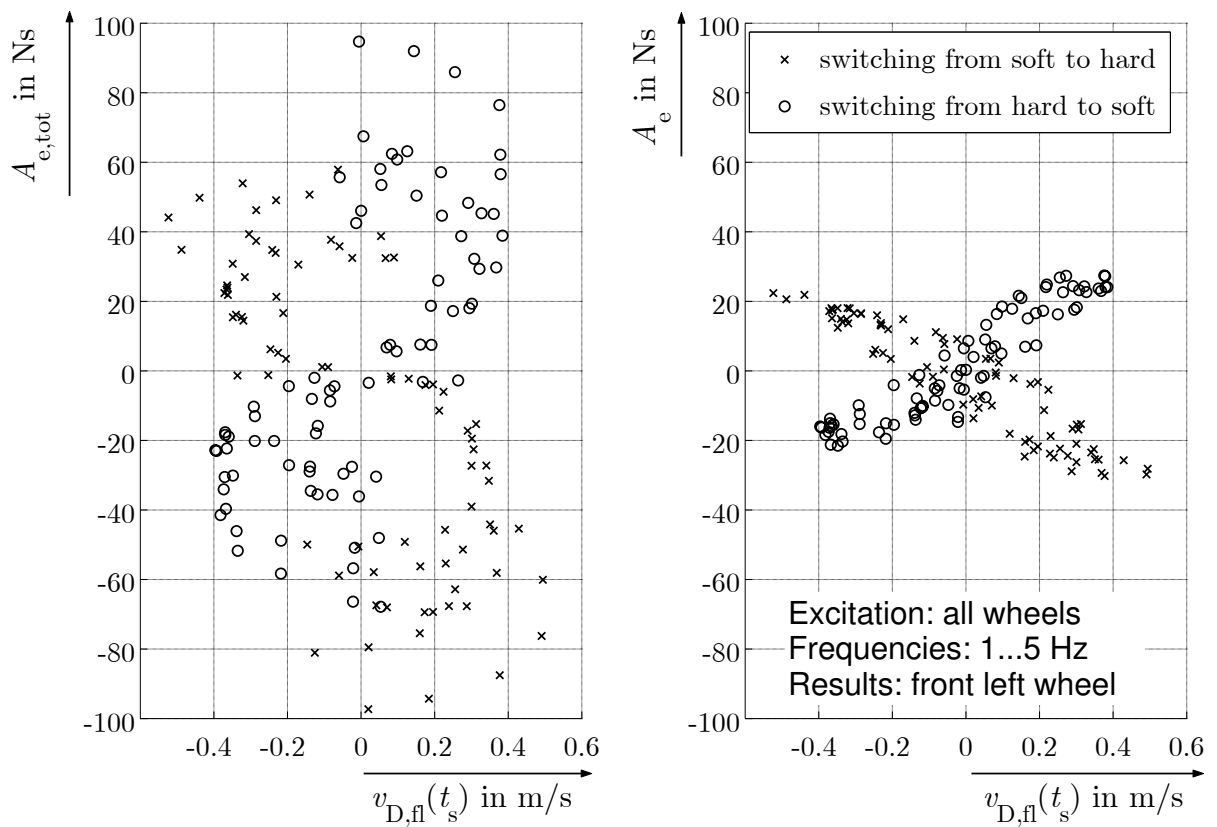


Figure 4.25: Total Effect Magnitude and Effect Magnitude vs. damper velocity at time of switching the shock absorber for front left wheel and seismic excitation at all four wheels equally. Results are gained from test rig experiments.

time of switching. The greater this velocity, the greater the effect magnitude.

It can also be seen that the effect leads to the requested change of wheel load in most of the cases. It is only in rare cases at low damper velocities that the Effect Magnitude has an other than the expected sign. In general it holds true that the Effect Magnitude is positive for switching the shock absorber from soft to hard in compression and from hard to soft in rebound, and vice versa. As for the Total Effect Magnitude $A_{e,tot}$, the values are more stretched than they are in the case of A_e . How strong $A_{e,tot}$ will be depends on the system's states at time of switching.

In the same manner as it was done in the time frame, it is now checked if the hypothesis H_0 formed on page 90 can be falsified in the magnitude frame as well. If this was the case, a quarter-car model could be used to predict the measurand Effect Time.

Figure 4.26 shows the effect magnitude for the wheel's of the front axle for different types of seismic excitation vs. the damper velocity at time of switching. It is either all wheels which are excited, only the front axle, the right track, or the front left wheel. It can be seen that the effect magnitude is almost not affected by the type of excitation. The variance of Effect Magnitude for a given damper velocity lies in the same dimension as the variance between the different types of excitations.

For all types of excitations it holds true that most of the switching processes lead to a change in wheel load in the desired direction (results in the I. and III. quadrant for switching from hard to soft and in the II. and IV. quadrant for switching from soft to hard).

Thus, from Figure 4.26 the conclusion can be drawn that the strength of the effect and its sign are independent of the type of excitation—at least, the dependency is smaller than the system-inherent variance. Hypothesis H_0 is therefore falsified, the alternative hypothesis H_1 is assumed to be true. It is furthermore assumed that the switching effect can be modeled by means of a quarter-car model in the magnitude frame, too. Thus, the use of the quarter-car model is validated for modeling the switching effect on the wheel load.

The given values of Total Effect Magnitude and effect magnitude can directly be translated into change of braking slip. For doing this please refer to equation 5.23, where the connection between vertical forces (wheel load) and braking slip is drawn.

The averaged Effect Magnitudes shown in Figure 4.24 lead to changes in braking slip at a wheel of the front axle of approximately $|\Delta\lambda_B| = 0.8\text{--}4\%$, assumed that the gear box is in second gear, the vehicle speed $v_x = 70\text{ km/h}$, and the actual friction factor $\mu = 1$.

In third or higher gears or in neutral position the change in braking slip is even greater (*ceteris paribus*) due to the reduced effective mass moment of inertia of the front axle's wheels. There it is approximately $|\Delta\lambda_B| = 1.5\text{--}7.5\%$ (third gear) and $|\Delta\lambda_B| = 1.9\text{--}9.5\%$ (neutral position) which can be achieved by a change in wheel load of the dimension given in Figure 4.24. The detailed description how to calculate those values can be found in equation 5.23 on page 117. Another numerical example is given on page 121. Here these values shall only be mentioned without calculation to show how strongly a simple switching of the active shock absorbers from hard to soft or vice versa can influence the braking slip.

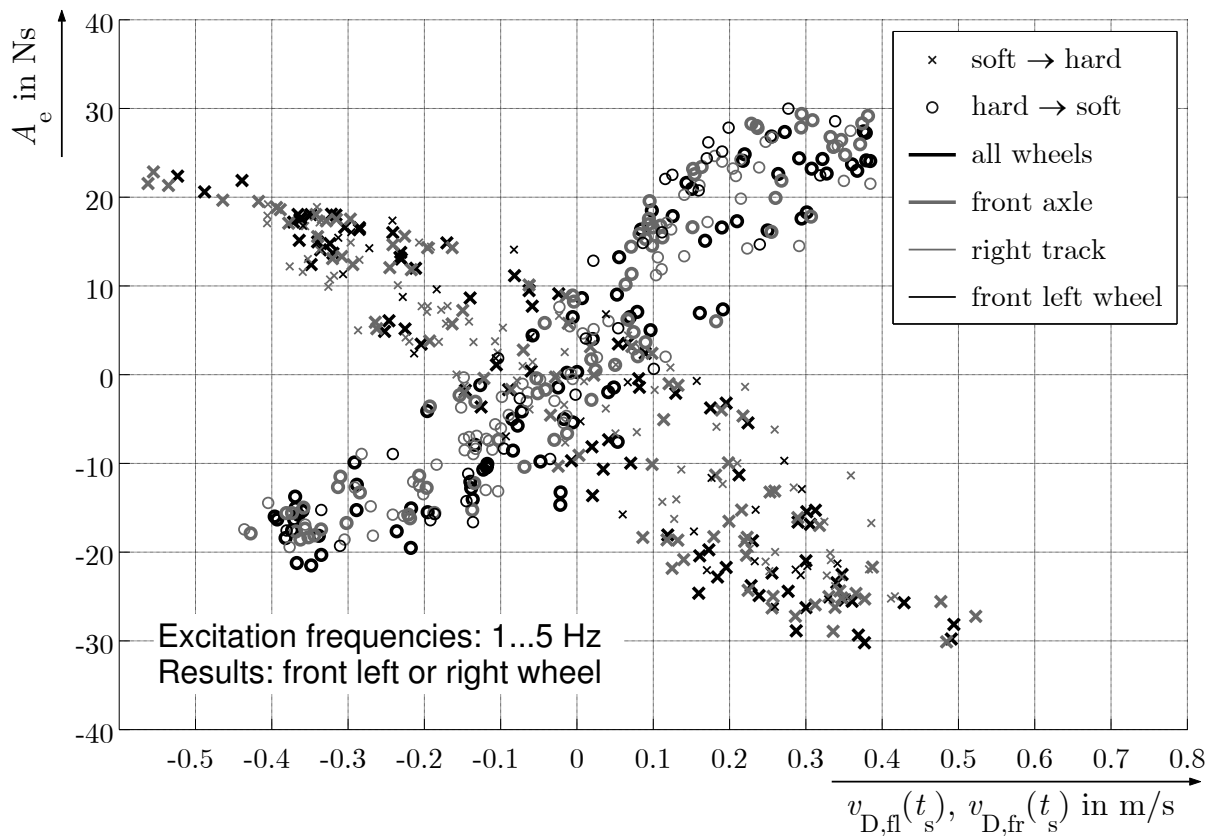


Figure 4.26: Effect Magnitude vs. excitation frequency for the front left respectively the front right wheel and seismic excitation at all four wheels, front axle, right track, and front left wheel only. Excitation frequencies lie between 1 and 5 Hz.

4.6.3 Comparison of Simulation and Experiment

The simulation model introduced in section 4.3 is used to make the results gained from the test rig experiments independent of the specific testing vehicle investigated in this thesis. In the former section it was shown that using a quarter-car model is suitable for modeling the switching effect of the shock absorbers, because the effect has a negligible amount of dependency on the form of excitation. Now it needs to be determined how well the model maps the values gained from real experiments into the simulation world. In Figure 4.27 the Effect Time for applying the same seismic excitation to the quarter-car model as was applied to the real car at the front left wheel is shown. It can be seen that the Effect Time is reproduced by the quarter-car model very well. It is only at higher frequencies above 20 Hz that there is a relevant deviation from the Effect Times measured in the test rig experiments. Since the relevant frequencies lie below 5 Hz, this deviation does not negatively influence the use of the model.

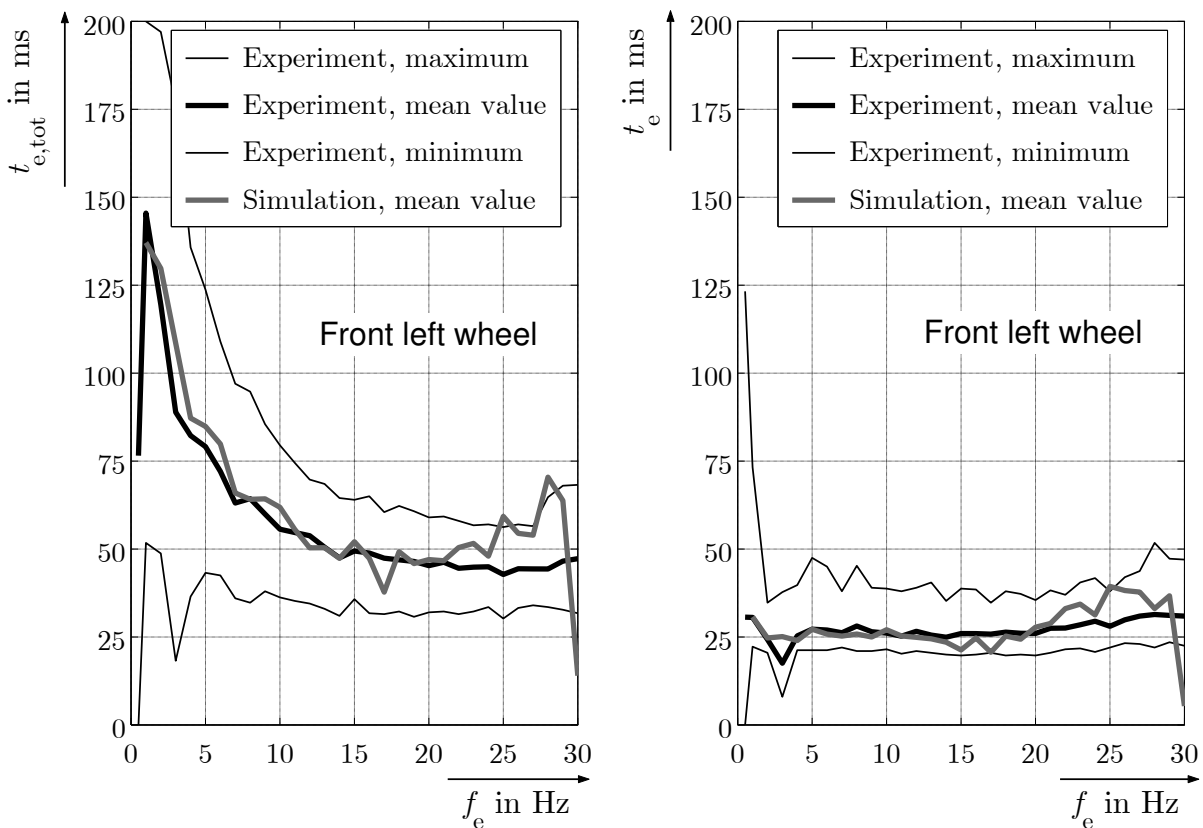


Figure 4.27: Total Effect Time and Effect Time vs. excitation frequency. Results are gained for the front left wheel from test rig experiments and from the quarter-car simulation model described in section 4.3.

In Figure 4.28 the result from the same simulation is shown. Now the Total Effect Magnitude is plotted vs. the excitation frequency. It can be seen that the quarter-car model maps the Total Effect Magnitude which can be found in reality in a good manner into the simulation world. Not only the principle behavior—a decreasing Total Effect Magnitude with increasing excitation frequency—but also the numerical values of Total Effect Magnitude in simulation and experiment match.

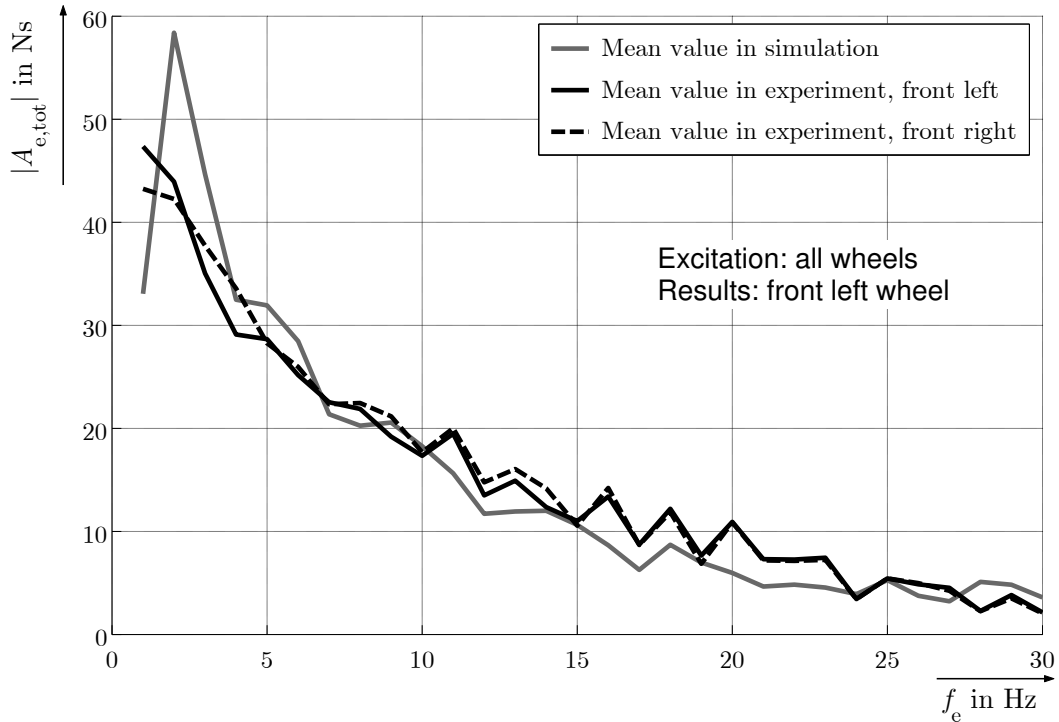


Figure 4.28: Total Effect Magnitude vs. excitation frequency. Results are gained for the front left wheel from test rig experiments and from the quarter-car simulation model described in section 4.3.

Parameter Variation

First of all, a parameter variation in the real car shall be undertaken: As it was explained in section 4.2, the difference in damper force between soft and hard at a given damper velocity leads to a change in wheel load if the shock absorber is switched. Thus, the change in wheel load should depend on this difference in damper force—it should depend linearly on the spreading s_{hs} .

In Figure 4.29 the mean values of the Total Effect Magnitude and the Effect Magnitude are shown for switching the shock absorber at the front left wheel from soft to hard or vice versa, and in addition both for switching from medium damping ($I_D = 0.8 \text{ A}$) to hard or to soft damping. In case of medium damping the values for both spreadings s_{hm} or s_{ms} are approximately half of the original hard/soft spreading s_{hs} . As can be seen in Figure 4.29, this leads to half the values in both Total Effect Magnitude and effect magnitude, compared to the original values.

Thus, interpolation with respect to the spreading of the shock absorber is admissible. This also lets expect extrapolation to be feasible at least in small ranges. What happens to the switching process if the spreading of the shock absorber is increased? This question cannot be answered with the actual real shock absorbers, for their spreading cannot be increased any further than s_{hs} . But here the simulation model can help. Using the model, parameter variations can be undertaken to check on the dependency of the results on those parameters.

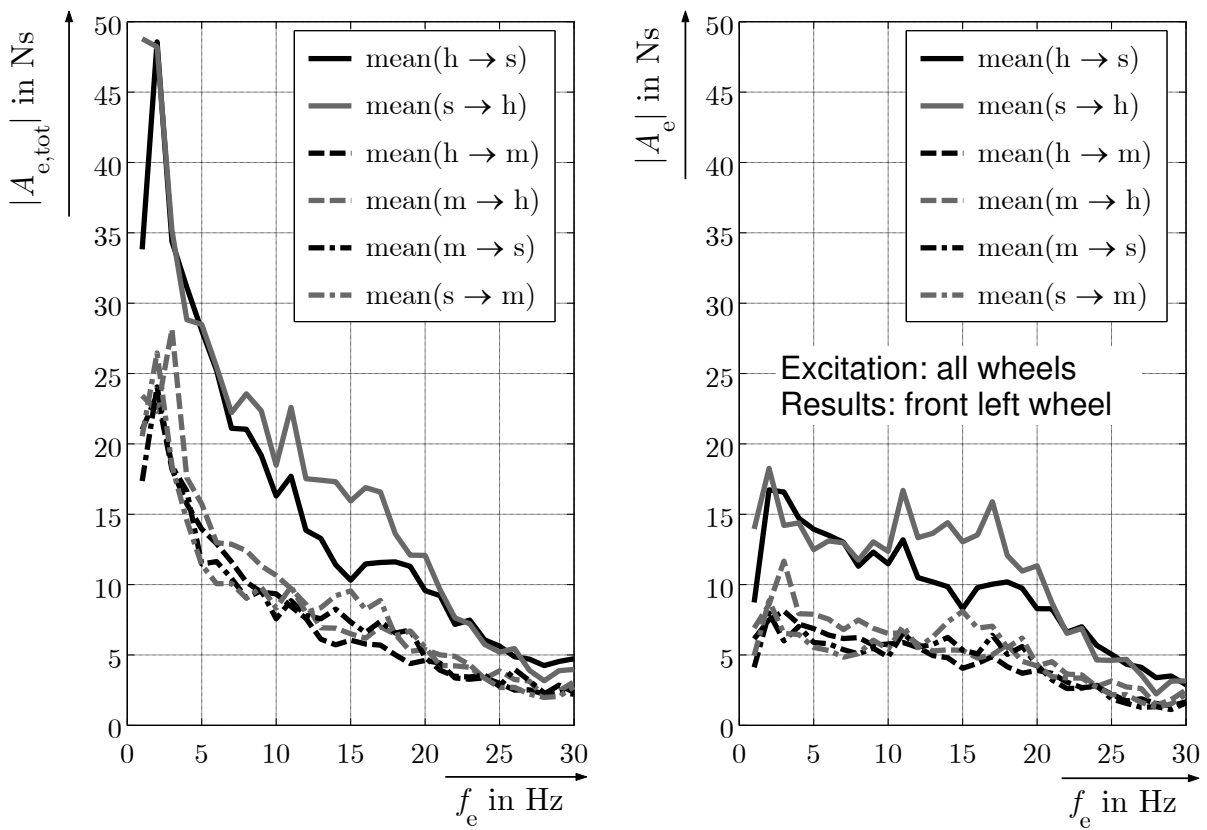


Figure 4.29: Total Effect Magnitude and Effect Magnitude for differing switching procedures vs. excitation frequency. Results are gained for the front left wheel from test rig experiments.

Figures 4.30 and 4.31 show the effect of a variation of the parameters by which the system behavior of the quarter-car model is determined. The data in both figures are gained from a simulation experiment where the quarter-car model is excited with a pseudo-noise seismic excitation. Within the simulation it is possible to determine the effect of switching the shock absorber even for such a seismic excitation where the course of wheel load is unpredictable. If the experiment was executed in the real world, the course of wheel load for a noise-type seismic excitation would not be reproducible. For the simulation model this is different, because for given initial conditions a simulation experiment always leads to the same output.

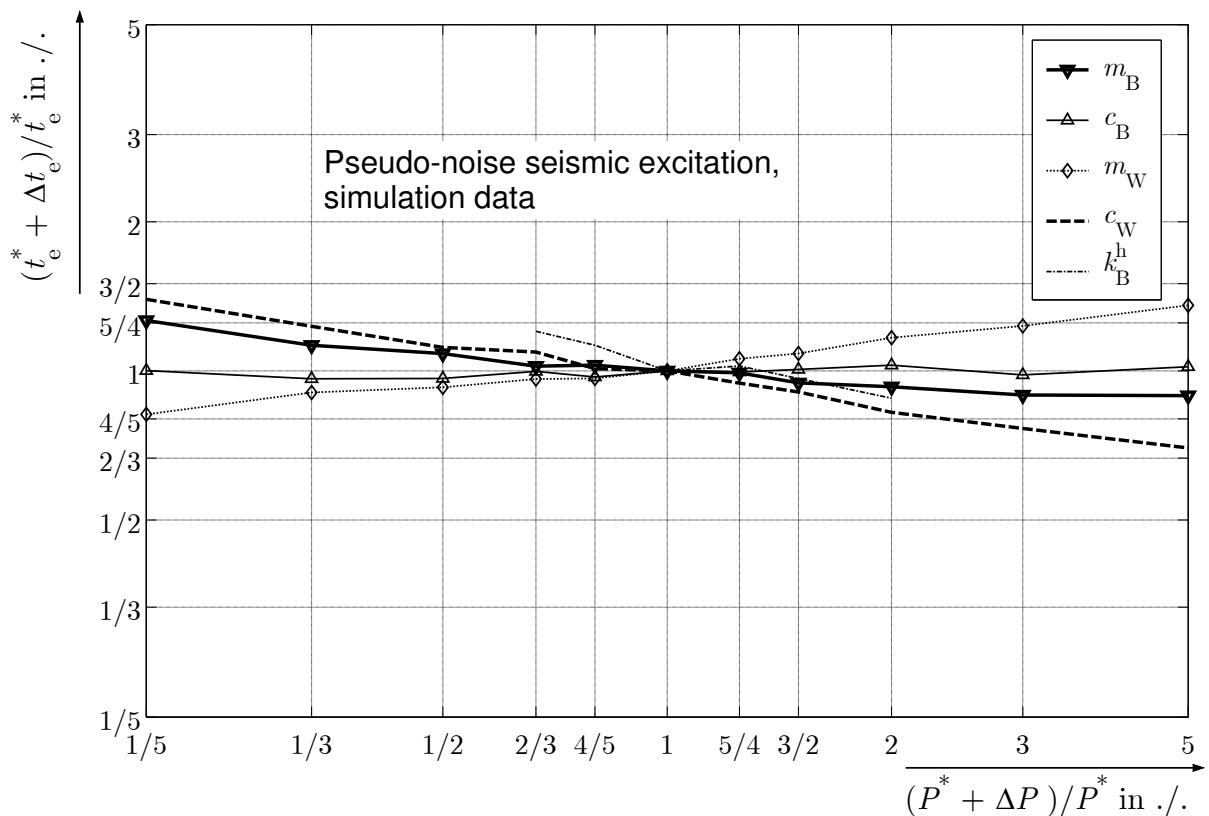


Figure 4.30: Parameter variations and their effect on the Effect Time t_e . Data gained from simulation with the quarter-car model of section 4.3 for the front left wheel and a pseudo-noise seismic excitation.

Thus, the course of wheel load after switching the shock absorber is compared with the course of wheel load without switching. For each fixed set of parameters 200 switching processes from hard to soft and 200 for soft to hard are investigated. The pseudo-noise seismic excitation starts with a randomly chosen seed. The values calculated for the parameter variation are the mean values for those 400 switching processes per set of parameters.

In both Figure 4.30 and Figure 4.31 on the abscissa the relative variation of the respective parameter from its original value—which is listed in Table 4.2 on page 67—is shown. A value of one means that there is no variation at all, whereas a value of 3/2 means that the original value is increased by 50%. On the ordinate the relative change in Effect Time respectively Total Effect Magnitude with respect to those values which establish when using the original set of parameters is shown.

Figure 4.30 shows that the Effect Time is almost not influenced by the stiffness of the body spring c_B . Recalling that the switching effect is caused by the change in damper force and is therefore independent of the parallelly acting spring force, this result is plausible. The Effect Time is slightly influenced by the body mass m_B . The greater this parameter, the shorter the Effect Time.

But the most interesting part to see is the effect that a change of one of the wheel parameters or of the hardest characteristic line of the shock absorber has on t_e , because there the effect is most intense. An increase in wheel spring stiffness or a decrease in wheel mass both lead to a shortening of the Effect Time. This is because the change in wheel load only establishes if the tire is either additionally compressed or additionally released. In case of a reduced wheel mass, compressing or releasing the tire happens faster because of the reduced mass moment of inertia. In case of a raised tire spring stiffness the same amount of tire deflection leads to higher changes in wheel load—which again lets t_e decrease.

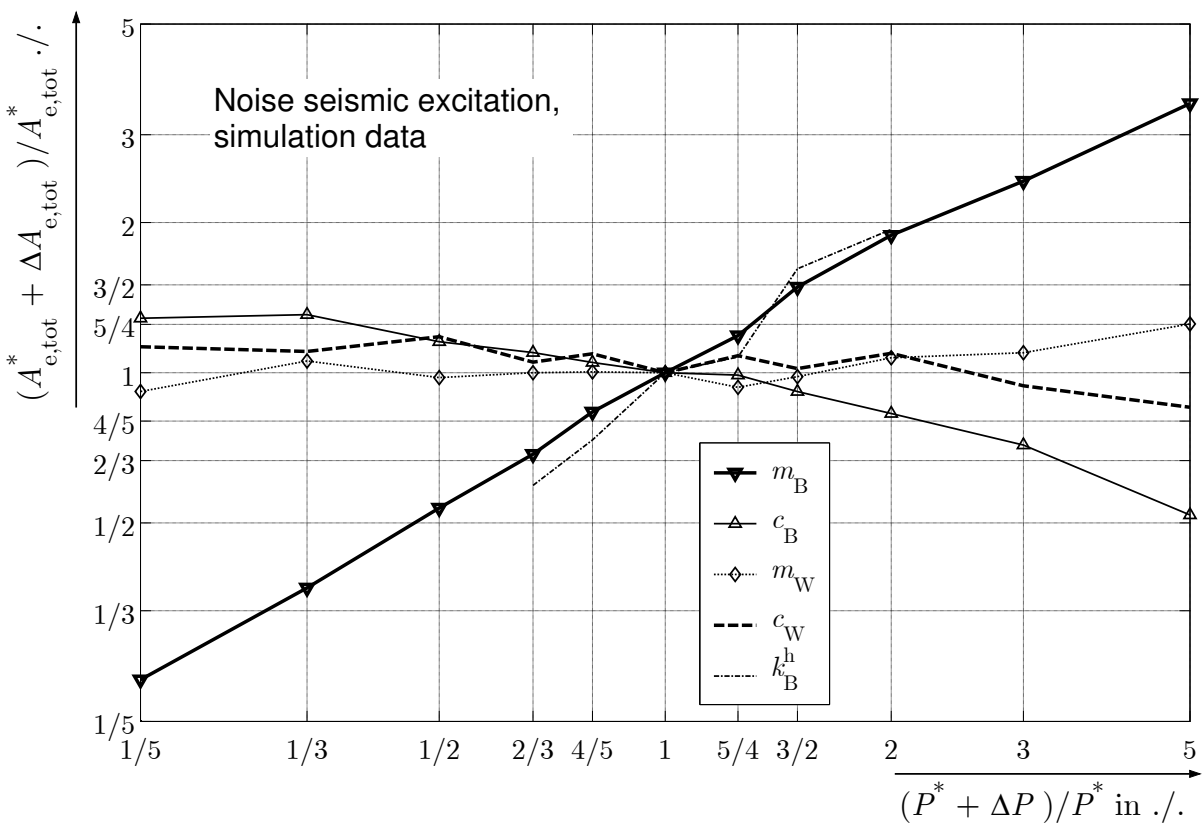


Figure 4.31: Parameter variations and their effect on the Total Effect Magnitude $A_{e,tot}$. Data gained from simulation with the quarter-car model of section 4.3 for the front left wheel and a pseudo-noise seismic excitation.

The spreading s_{hs} of the shock absorber, which is varied by multiplying the damper forces of the hardest characteristic line of the shock absorber with a factor, also has a strong influence on the Effect Time. The greater the spreading, the shorter the Effect Time. This is simply because the change in damper force is the greater, the greater the spreading. And the greater the change in damper force, the faster the measurable effect on the wheel load occurs, because the speed of tire deflection depends on the force that

is applied to the wheel/tire. Nevertheless, for all those parameter variations the change in Effect Time is rather small compared to the change in the respective parameter. This means that with respect to the Effect Time the results are not sensitive to failures in the determination of parameters or to a change of the testing vehicle.

Figure 4.31 shows that the Total Effect Magnitude mainly depends on the spreading s_{hs} and on the mass of the body. For both parameters an increase leads to an increasing Total Effect Magnitude. For the parameter ‘body mass’ it is an almost one to one dependency. This means that for a heavier car the Total Effect Magnitude is bigger by almost the same factor as the vehicle’s mass is bigger.

Thus, the Effect Magnitude per mass almost remains constant, no matter how great the value of the body mass will be (in the given dimensions from 0.2 to 5 times the original value). Taking into account that the heavier a car, the more braking force is needed to decelerate it, it does not improve the overall performance of the switching effect to increase the body mass.

For the spreading this looks slightly different. The spreading can be changed without changing the mass of the vehicle. Increasing the spreading alone therefore leads to an improvement in the sense that the magnitude on the supply side can be increased without changing any other parameters that might lead to an increase in magnitude on the demand side.

4.7 Conclusions

In this chapter the relevant frequency band for a shock absorber controller was determined by means of a linearized quarter-car model. The wheel load integral as well as the damper velocity have the maximum amplitudes at frequencies below 5 Hz for a seismic excitation which decreases with f^{-1} , which is typical for a road with a typical unevenness. The wheel load integral here represents the demand side of the problem and the damper velocity the supply side. Both sides match with respect to the frequency spectrum.

It was shown that the switching of the active shock absorber can be used to influence the course of wheel load in a directed way. The wheel load influence matrix was introduced, which describes the direction of the switching effect. Derived from this matrix, a controller, the so called MiniMax-controller, was introduced. With this controller artificial characteristic lines for the active shock absorbers can be established.

These artificial lines can be used to lift and lower the body of the vehicle, given that a seismic excitation is present. Switching from one artificial line to another changes the governing equations which describe the vehicle’s vertical motions. This again leads to an increase or decrease in wheel load—depending on the direction of switching and the sign of damper velocity at time of switching.

It was shown that the increase or decrease of wheel load always leads to a lifting or lowering of the vehicle’s body. The part of Delta Wheel Load which acts on the vertical wheel motion is not as relevant for the switching effect as the body motion, because due to the limited tire deflection and the low wheel mass the acceleration of the wheel will end up to 100 times faster than the one of the body. Thus, the effect of switching is longer and stronger the larger the maximal spring deflection of the body spring.

A testing procedure was developed to measure the effect of switching the shock absorber in both the time and the magnitude domain. In test rig experiments the Effect Time

and the Effect Magnitude for the given testing vehicle were determined. The Effect Time and the Effect Magnitude at a wheel are independent of the places at which the seismic excitation is applied. Exciting only the front axle, only one track, or all four wheels at a time leads to the same dimension of Effect Time and Effect Magnitude. Thus, with respect to those two quantities, the coupling between the wheels can be neglected and a quarter-car model is sufficient for modeling them. The simulation model was validated, such that the results with respect to the vertical dynamics are transferable to every passenger car which is characterized by the properties which a quarter-car model represents.

The wheel load influence matrix as well as the MiniMax-controller are parameter-independent and therefore hold true for every passenger car which is equipped with an active shock absorber. In fact, the conclusion actually holds true for every land-based vehicle which has an adjustable suspension parameter. The parameter which is switched does not necessarily have to be the damping coefficient. It can also be the spring stiffness or—very unusual, but theoretically possible—the mass of the wheel or the body. Parameter variations undertaken with a quarter-car showed that the Total Effect Magnitude can be increased by increasing the spreading of the shock absorber.

The MiniMax-controller developed was furthermore implemented in a real car and used to determine the roughness of some 400 km of southwestern German highways in order to compare those results with the test track ‘Standard Road’. Those test drives have also shown that lifting and lowering of the vehicle’s body are not only a theoretical construct, but can also be measured with a real car on a real road, no extreme or special kind of excitation needed.

With the results from this chapter a tool is provided which allows to increase or decrease the course wheel load purposefully. It is now also known for how long a change of wheel load in the desired direction is achievable by switching the shock absorber and how strong it is. The Total Effect Magnitude can be even higher if the shock absorber is not only switched from one constant to another constant characteristic line but from the artificial characteristic line ‘increase wheel load’ to ‘decrease wheel load’ or vice versa. Up to the point in time when the damper velocity changes its sign after switching the shock absorber, there is no difference between switching from one constant passive line to the other and switching from one artificial line to the other.

There are two reasons why switching the active shock absorber causes an increase or decrease in wheel load. At first, due to the difference in damper force at a given damper velocity for hard and soft damping the switching of the damper causes a Delta Damper Force which can directly be translated into a Delta Wheel Load. This means, if the damper force is decreased by switching the damper this will lead to an increasing/decreasing in wheel load, depending on the damper stage at the time of switching. Secondly, due to the difference of damping coefficient for rebound and compression—which can purposefully be increased by controlling the dampers—the body is lowering or lifting, depending on the direction of control. While the body is accelerated upwards, the wheel load is increasing and vice versa. Thus, the greater the difference of spring displacement for the lower and the upper state of the body, the longer the switching effect will continue.

5 Longitudinal Dynamics

In this chapter the MiniMax-controller developed in section 4.4 is applied to the longitudinal dynamics of the vehicle. The MiniMax-controller is used as the core for a slip controller which is meant to lead to an enhanced braking performance. The controller is investigated in real test drives.

After preliminary definitions in section 5.1, in section 5.2 the connection between vertical dynamics and longitudinal dynamics is established. It is shown that it is not the wheel load itself but rather the integral of this quantity which affects the longitudinal dynamics, namely the braking slip.

With this knowledge, in section 5.3 a slip controller is developed. The braking slip is meant to be the control variable. But it cannot be controlled directly, because if the braking slip is increasing by a high amount, the ABS-controller will act on this and it is therefore too late for an intervention in the vertical dynamics to reduce the braking slip. It is thus that the wheel load integral is used as the substitute control variable.

In section 5.4 the slip controller developed is implemented in a real car and test drives are executed with it. The objective is to reduce the braking distance. For this purpose first of all a testing procedure is defined which allows to make braking procedures such reproducible that a possible enhancement of braking performance due to the shock-absorber controller—if present—can be measured.

5.1 Definitions

The following definitions make one braking process comparable to another. Since a braking process is influenced by many variables (refer to section 2.2), to be able to gain reliable information about the effect of the shock-absorber controller, it is an important factor to keep as many influencing factors under control as possible. As will be seen in later sections, even though all those controllable parameters are kept constant, the variance of braking distance is still such large that it needs to be analyzed statistically. But if the parameters which are controllable were not kept constant, the variance would be such large that the number of test drives to be undertaken would be too large to realize.

In real test drives a light barrier—which is attached to the rear bumper of the vehicle—is used for several purposes. Passing the light barrier reflectors—which are fixed in the pavement coordinate system—beside other purposes initiates both measuring an braking.

Initiation of Braking t_{BI}

The time of initiation of the braking process t_{BI} is defined as the time at which the braking machine used is triggered to pull the braking pedal. This signal depends on passing a light barrier reflector.

Initial Velocity $v_{x,0}$

The initial velocity $v_{x,0}$ of the vehicle is defined as the average longitudinal velocity v_x which the vehicle occupies between passing the first and the second light barrier reflector, L_0 and L_1 .

$$v_{x,0} = \frac{1}{t_{L_1} - t_{L_0}} \int_{t_{L_0}}^{t_{L_1}} v_x(t) dt \quad (5.1)$$

Begin of Braking Process t_{BB}

Especially the beginning of the braking process highly influences the measured result. Since the vehicle holds its highest velocity at the beginning of the braking process, every measuring error at the beginning of the braking procedure will lead to a higher total error than an error at the end of the braking procedure. This is why a braking machine is used to map out the initial part of the braking procedure as reproducible as possible. But still, a starting point for the braking needs to be defined. The braking pressure of the front left wheel's braking cylinder $p_{B,fl}(t)$ is used as measurand. Once it crosses a predefined threshold $p_{B,BB}$, the full-braking procedure is defined as started.

$$t_{BB} = \min(t \mid p_{B,fl}(t) > p_{B,BB}) \quad (5.2)$$

The threshold is defined such that it lies close to the maximum braking pressure, but not too close such that the small gradient in braking pressure shortly before the maximum braking pressure is reached would cause strongly differing results from one braking procedure to the other. For braking on the test track 'Standard Road' the threshold lies at $p_{B,BB} = 60$ bar.

End of Braking Process t_{BE}

The end of the braking process is defined via a threshold of the longitudinal velocity v_x . For measuring reasons it should not be waited until the vehicle completely stands still for the braking process to be defined as finished. The end of the braking process is assumed to be at the time when the longitudinal velocity passes a given threshold from above for the first time.

$$t_{BE} = \min(t \in [t_{BB}; \infty) \mid v_x(t) < v_{x,BE}) \quad (5.3)$$

Since it is difficult to determine exactly the longitudinal velocity being equal to zero, it is better to assume the braking process to have ended at a time still driving with a small velocity than to have to deal with wide spreadings due to measuring failures. This would be the case if the exact time of standing still was measured. The threshold for the velocity to be passed is set to $v_{x,BE} = 3$ km/h. At this speed the remaining braking distance on a typical road with $\mu_{\max} \approx 1$ is only 3.5 cm. Assuming that the braking distance could be shortened by 10% (a very optimistic assumption) by the shock absorber controller, the failure in comparing damper-controlled and damper-uncontrolled test drives due to assuming the braking procedure has finished at 3 km/h is a maximum of 0.35 cm. This is way below the measuring accuracy and can therefore be neglected.

Braking Distance d_B

The braking distance for a given braking procedure is measured by means of the integral of longitudinal velocity of the vehicle. Integrating this measurand from the time at which the braking procedure has started to the time at which the braking procedure has ended gives the distance which has been traveled between those two points in time.

$$d_B = \int_{t_{BB}}^{t_{BE}} v_x(t) dt \quad (5.4)$$

The longitudinal velocity of the vehicle v_x is measured by an optical sensor in high precision. The correctness of the determination of the braking distance is double checked with the signals from light barrier reflectors. The reproducibility of the results is even more important than the absolute correctness, since the braking distances for different damper settings are to be compared. The absolute value is of less interest than the ranking of braking distances for different damper settings to each other.

The random error of the determination of the braking distance is 0.25 %. It corresponds to an absolute random error of approximately 5 cm for a braking procedure with an initial velocity of 70 km/h. This error was determined with the signals of the light barrier which is attached to the vehicle. By passing light barrier reflectors which are positioned in defined distances and comparing the result of integrating the signal of the longitudinal velocity with the actual traveled distance, measured by the light barrier signal, allows to determine this random error (for the setting refer to Figure 5.7 on page 128).

The braking distance is one out of two overall integrating measurands that give final information about how good the braking procedure was in the given context. All other measurands help to understand why the braking procedure is good or not that good, but the braking distance is the one measurand that represents the main objective of the whole controller.

Corrected Braking Distance $d_{B,corr}$

The braking distance measured by integrating the longitudinal velocity of the vehicle gives the correct information about the actual braking distance which was obtained for the given initial velocity. The problem is that, even though the cruise control is used to recover the same initial velocity for every braking procedure, there may be differences in the actual initial velocities of $+/- 1$ km/h. This might seem to be a small value, but recalling that the expected shortening of braking distance is in the range of a couple of percent, a deviation of 1 km/h for an initial velocity of 70 km/h is not acceptable. This problem is solved by correcting the actual, measured braking distance d_B . The correction goes like this: Assuming that the mean value of deceleration of the vehicle is the same for a given test drive, no matter if it starts at an initial velocity $v_{x,0}^A$ or at an initial velocity $v_{x,0}^B$, given that

$$\left| \frac{v_{x,0}^A - v_{x,0}^B}{v_{x,0}^B} \right| \ll 1, \quad (5.5)$$

then the corrected braking distance, the braking distance that would have established if the vehicle's speed at the starting of the braking procedure had been the desired value

$v_{x,0}^{\text{des}}$, can be calculated by:

$$d_{\text{B,corr}} = d_{\text{B}} \left(\frac{v_{x,0}^{\text{des}}}{v_{x,0}} \right)^2 \quad (5.6)$$

This corrected braking distance is the one that is used for all comparisons of hard, soft, and controlled damping. If only ‘braking distance’ is mentioned in the following sections, it is always referred to this corrected braking distance, unless otherwise noted.

Integral of the Square of Vehicle Speed With Respect to the Traveled Distance *VI*

The braking distance d_{B} gives information about how good the braking procedure was in the sense of making the vehicle stop as early (measured in distance) as possible. This is a useful measurand if the vehicle will eventually stop before a crash happens. Still there might be cases in real life when a full-braking procedure is initiated by the driver and a crash cannot be prevented anymore. For those cases the braking distance alone is not sufficient to value the quality of the braking procedure.

In case of a collision with any kind of obstacle, the lower the kinetic energy of the vehicle at the time of the crash, the better for car and driver. The kinetic energy is proportional to the square of the vehicle’s speed. For a given position s_x^* , the objective is therefore to minimize the kinetic energy which the vehicle holds when it reaches this position. I. e., the integral of the square of the vehicle’s speed with respect to the traveled distance, given by

$$VI = \int_{s_x(t_{\text{BB}})}^{s_x(t_{\text{BE}})} v_x^2(s_x) ds_x \quad (5.7)$$

is a valid measurand to value the course of vehicle speed during a braking procedure—something that the braking distance itself cannot provide. The smaller *VI*, the better is the braking procedure in the sense that the probability of holding a high kinetic energy at the time of a possible collision is smallest, given that the exact position of the obstacle is unknown.

Cumulative Percentage g_{CP}

The cumulative percentage is a tool from the field of statistics. It is widely used especially in Economics. In the given context it is introduced because with its help it is possible to get a quick impression of how the braking distances of different shock absorber settings compare to each other. The definition of the cumulative percentage can be found e. g. in Bley Müller¹. Treating the results of braking procedures due to the uncertainties in the parameters which influence the braking distance as random variables, the cumulative percentage gives information of how many braking procedures in percentage of all considered braking procedures with a fixed parameter setting led to braking distances below a given distance in meters.

¹Bley Müller/Gehlert/Gülicher (1996): Statistik für Wirtschaftswissenschaftler p. 8.

$$g_{\text{CP}}^i(d) = \begin{cases} 0 & \text{for } d < d_{\text{B},1}^i \\ g_n & \text{for } d_{\text{B},n}^i \leq d < d_{\text{B},n+1}^i \\ 1 & \text{for } d \geq d_{\text{B},N}^i \end{cases}, \quad (5.8)$$

where $i \in \{\text{h, s, c}\}$, n is the counting index which arranges the braking distances d_{B} in an ascending order, and g_n is the percentage of braking procedures which have shorter or equal braking distances than $d_{\text{B},n}^i$. The same definition holds true for every quantity. Here it is shown exemplary for the absolute braking distance d_{B} .

Velocity Difference v_{diff}

The velocity difference v_{diff} at a wheel is the difference between the speed of the vehicle v_{x} and the speed of the respective wheel v_{W} , where the speed of the wheel is defined as the effective radius of the wheel times its angular velocity $v_{\text{W}} = \omega_{\text{W}}(t) r_{\text{eff}}$. If the wheel locks, the velocity difference equals v_{x} . If the wheel is completely free spinning, the velocity difference equals zero.

$$v_{\text{diff}}(t) = v_{\text{x}}(t) - v_{\text{W}}(t) = v_{\text{x}}(t) - \omega_{\text{W}}(t) r_{\text{eff}} \quad (5.9)$$

The velocity difference can be interpreted as the braking slip, weighted with the actual longitudinal velocity v_{x} . The only difference to other measurands which are weighted with v_{x} is that it is not divided by the mean value of longitudinal velocity.

Averaged Values for all Wheels

For every braking procedure the braking distance is a measurand which gives information about the braking performance with one single value. Other measurands which are calculated for every wheel individually, but should be compared with the braking distance, must therefore be added together to one single value as well. When braking, the wheel load at the front axle and with it the braking force there is increasing due to the weight transfer. Assuming that the wheel load and the braking force are connected via a constant factor μ , the ratio between braking force/wheel load at the front and the rear axle is given by:

$$e_{\text{f/r}}(\mu) = \frac{F_{\text{z,f}}(\mu)}{F_{\text{z,r}}(\mu)} = \frac{F_{\text{B,f}}(\mu)}{F_{\text{B,r}}(\mu)} = \frac{l_{\text{r}} + \mu h_{\text{CG}}}{l_{\text{f}} - \mu h_{\text{CG}}} \quad (5.10)$$

The ratio of wheel load at the front axle per total wheel load is given by:

$$e_{\text{f}}(\mu) = \frac{F_{\text{z,f}}(\mu)}{F_{\text{z,tot}}(\mu)} = \frac{F_{\text{B,f}}(\mu)}{F_{\text{B,tot}}(\mu)} = \frac{l_{\text{r}} + \mu h_{\text{CG}}}{l}, \quad (5.11)$$

and analog for the rear axle:

$$e_{\text{r}}(\mu) = \frac{F_{\text{z,r}}(\mu)}{F_{\text{z,tot}}(\mu)} = \frac{F_{\text{B,r}}(\mu)}{F_{\text{B,tot}}(\mu)} = \frac{l_{\text{f}} - \mu h_{\text{CG}}}{l} \quad (5.12)$$

Thus, every deviation at the front axle weights by $e_{\text{f/r}}$ stronger than a deviation at the rear axle. This is why for any quantity X which is transferred from four individual wheel

values into a single value, the quantities of front and rear axle are weighted as shown in the following equation:

$$X_{\text{tot}} = \frac{e_f(\mu)}{2} (X_{\text{fl}} + X_{\text{fr}}) + \frac{e_r(\mu)}{2} (X_{\text{rl}} + X_{\text{rr}}) \quad (5.13)$$

For test drives executed on the test track ‘Standard Road’, $\mu \approx 1.04$ and therefore the factors $e_f \approx 0.77$ and $e_r \approx 0.23$. Thus, the total braking force of the front axle is by the factor 3.3 greater than the total braking force of the rear axle.

5.2 Connecting Wheel Load and Braking Slip/Braking Force

In section 4.4 the controller for the vertical dynamics was introduced and explained. Now this control logic is used to be a part of a controller of the longitudinal dynamics. First of all, the connection between wheel load and braking force needs to be established. How does the change of wheel load and the change of wheel load integral due to switching the active shock absorbers influence the braking force and the braking slip? This question will be answered in the following section.

5.2.1 Theoretical Approach

In Figure 5.1 the effect which a change in wheel load has on the braking force and the braking slip is described principally. The different states which should be described are labeled from A–D. The explanation for the states and what happens from the transition from one state to the other goes as follows:

- A** The wheel is in an arbitrary steady state at a given braking slip $\lambda_{\text{B}}|_{\text{A}}$ and a given braking force $F_{\text{B}}|_{\text{A}}$, close to the maximum of the μ -slip curve. Then a change in wheel load $\Delta F_z = F_z|_{\text{B}} - F_z|_{\text{A}} > 0$ is applied.
- B** The change in wheel load causes the braking force to increase immediately by $\Delta F_{\text{B}} = F_{\text{B}}|_{\text{B}} - F_{\text{B}}|_{\text{A}} > 0$, whereas the braking slip remains at its level due to the mass moment of inertia of the wheel. The braking force has to be integrated first before it leads to a change in braking slip (refer to equation 5.22).
- C** Assuming that the braking torque applied to the wheel remains constant during the process described, the needed braking force for a stationary condition is still at the level $F_{\text{B}}|_{\text{C}} = F_{\text{B}}|_{\text{A}}$. With the new wheel load $F_z|_{\text{B}}$ present, the braking slip $\lambda_{\text{B}}|_{\text{C}}$ which is needed to establish the braking force $F_{\text{B}}|_{\text{C}}$ is smaller than $\lambda_{\text{B}}|_{\text{A}}$. Thus, the braking slip and with it the braking force will decrease until it reaches the level $\lambda_{\text{B}}|_{\text{C}}$.
- D** An increase in wheel load is always followed by a decrease in wheel load which will go further down than the initial level of wheel load was. This is because the overall mean value of wheel load must remain constant. If the wheel load decreases from $F_z|_{\text{C}}$ by $2\Delta F_z$ to the level $F_z|_{\text{D}}$, the braking force will again decrease immediately by $\Delta \tilde{F}_{\text{B}}$ from $F_{\text{B}}|_{\text{C}}$ to $F_{\text{B}}|_{\text{D}}$. Since the braking force needed still is $F_{\text{B}}|_{\text{C}} = F_{\text{B}}|_{\text{A}}$, the sudden drop in wheel load and braking force is followed by the braking slip, which

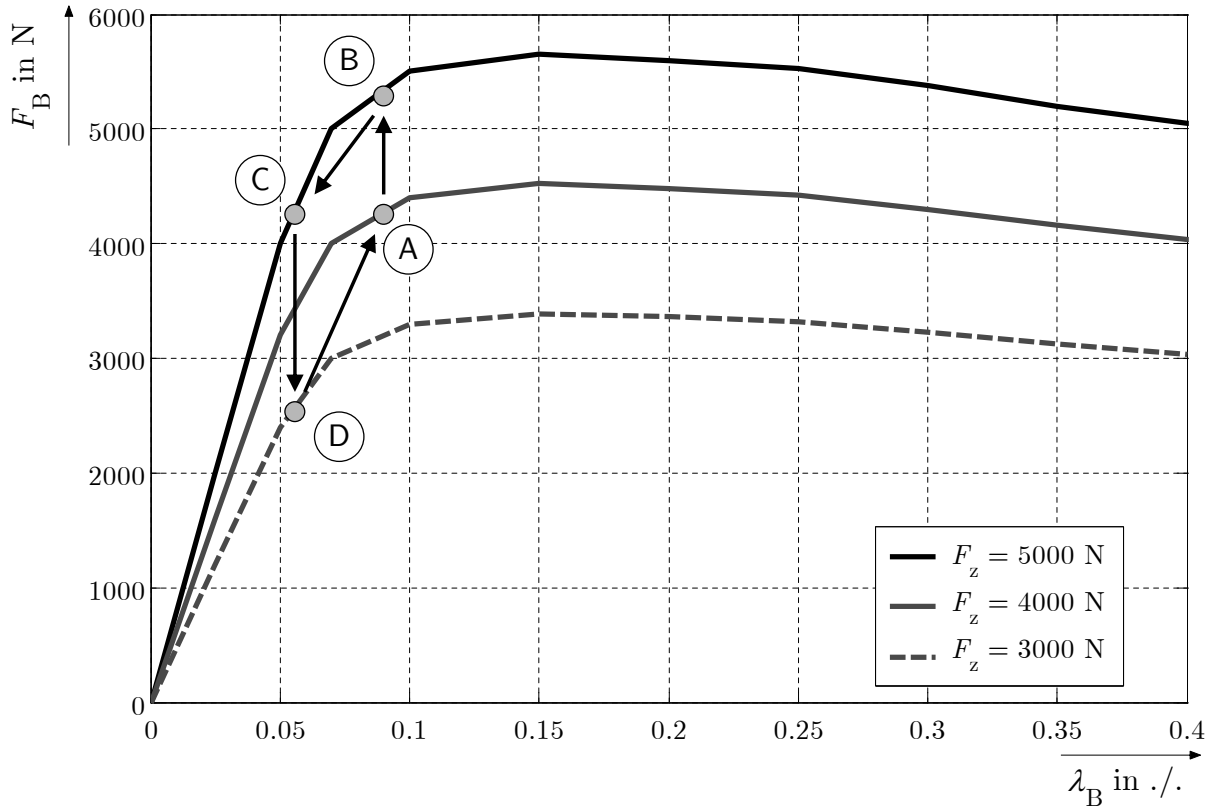


Figure 5.1: Braking force F_B vs. braking slip λ_B . Change in braking force and braking slip due to a change in wheel load, assuming that the braking torque and the μ -slip curve are constant. A typical μ -slip curve for a summer tire on a typical road is used. Values for wheel load are chosen in accordance to the ones found in the testing vehicle, but besides that they are chosen arbitrary.

will increase from $\lambda_{B|D}$ back to $\lambda_{B|A}$, because the value of braking force is too low to keep the braking slip at level $\lambda_{B|D}$.

A Finally, the wheel load, the braking force, and the braking slip will have established their initial values in point A again.

The process described is one for an initially increasing wheel load. Now what happens if this time, starting from B, the wheel load decreases? The braking force will also decrease by ΔF_B from $F_{B|B}$ to $F_{B|A}$. Again, assuming that the braking torque is kept constant, the braking force desired for the wheel to be in equilibrium is at the level of $F_{B|B}$. This level cannot be achieved on the line of low wheel load $F_{z|A}$. Thus, in this case the braking slip will increase dramatically until either the wheel load is increasing again, the braking torque is lowered, or the wheel locks.

The question arises how the vertical dynamics and the longitudinal dynamics are connected with each other such that it can be used for controller purposes and how the previous thoughts can be implemented in a more analytical sense. In section 4.3 the quantity ‘wheel load integral’ was already introduced. By use of this quantity higher frequencies in the oscillation of the vertical tire force are neglected. Why is this useful? Looking at the principle of angular momentum for a wheel, it becomes clear that the wheel’s speed is

influenced by both the braking force and the braking torque. Both are quantities acting in the longitudinal direction.

$$J_W \ddot{\varphi}_W = F_B r_{\text{eff}} - M_B \quad (5.14)$$

Assuming that the braking force and the braking torque are constant, a sudden change in only the braking force by ΔF_B will lead to also a sudden change in the wheel's rotational acceleration $\Delta \ddot{\varphi}_W$:

$$J_W \Delta \ddot{\varphi}_W = \Delta F_B r_{\text{eff}} \quad (5.15)$$

Integrating this equation leads to:

$$\Delta \dot{\varphi}_W = \Delta \omega_W = \frac{r_{\text{eff}}}{J_W} \int \Delta F_B dt \quad (5.16)$$

Multiplying with the effective wheel radius r_{eff} leads to the wheel's speed at the left hand side of the equation:

$$\Delta v_W = \Delta \omega_W r_{\text{eff}} = \frac{r_{\text{eff}}^2}{J_W} \int \Delta F_B dt \quad (5.17)$$

This means that the wheel's speed, which is directly connected to the braking slip and with this to the longitudinal dynamics of the vehicle, is influenced by the integral of the braking force. Changing the braking force by ΔF_B leads to a change in wheel speed by Δv_W which is proportional to the integral of the braking force. This implies that if the braking force is oscillating with rather high frequencies, this does not affect the wheel speed.

Recalling that the braking slip is defined as

$$\lambda_B = 1 - \frac{\omega_W r_{\text{eff}}}{v_x} \quad (5.18)$$

and assuming that the vehicle's longitudinal velocity v_x changes much slower than the wheel's velocity², this leads to the following connection between the change in wheel speed Δv_W and the change in braking slip $\Delta \lambda_B$:

$$\Delta \lambda_B = \lambda_B(t_2) - \lambda_B(t_1) = \left[1 - \frac{\omega_W(t_2) r_{\text{eff}}}{v_x(t_2)} \right] - \left[1 - \frac{\omega_W(t_1) r_{\text{eff}}}{v_x(t_1)} \right] \quad (5.19)$$

With

$$v_x(t_1) \approx v_x(t_2) = v_x \quad (5.20)$$

this leads to

$$\Delta \lambda_B = -\frac{\Delta \omega_W r_{\text{eff}}}{v_x} = -\frac{\Delta v_W}{v_x} \quad (5.21)$$

²The longitudinal acceleration of a vehicle on a normal pavement with standard tires is approximately 10 m/s² max. The acceleration of the wheel can be up to 10 times higher. This is due to the large braking torque which can be applied to brake down the wheel.

Applying equation 5.17 to equation 5.21 leads to

$$\Delta\lambda_B = -\frac{r_{\text{eff}}^2}{J_W v_x} \int \Delta F_B dt \quad (5.22)$$

Thus, the braking slip is connected to the braking force via the braking force's integral with respect to time. If a sudden change in braking force is applied, it will be followed by a change in braking slip with a phase shift of $\pi/2$.

Now yet another assumption is made: Assuming that a change in wheel load ΔF_z will lead to a change in braking force of the amount $\Delta F_B = \mu \Delta F_z$, where μ is the actual ratio between braking force and wheel load, and assuming furthermore that μ does not change, equation 5.22 becomes

$$\Delta\lambda_B = -\frac{\mu r_{\text{eff}}^2}{J_W v_x} \int \Delta F_z dt \quad (5.23)$$

In the same manner equation 5.17 becomes

$$\Delta v_W = \Delta\omega_W r_{\text{eff}} = \frac{\mu r_{\text{eff}}^2}{J_W} \int \Delta F_z dt \quad (5.24)$$

Thus, both the braking slip and the wheel speed, which are quantities of the vehicle's longitudinal dynamics, are connected with the vertical dynamics via the integral of wheel load. This implies that high frequencies in wheel load oscillations do not effect the braking slip as much as low frequencies do. In Figure 4.6 on page 70 it is shown that for the quarter-car model of the testing vehicle the integral of wheel load is higher at frequencies around the body eigenfrequency than at frequencies around the wheel eigenfrequency.

Having this in mind and looking again at equations 5.23 and 5.24, it becomes clear that the braking slip and the wheel speed are mainly influenced at lower frequencies. This already holds true if driving on a road with a white noise elevation profile. If the elevation profile is a more realistic one and decreases with approximately f^{-1} , the influence of low frequencies on the braking slip and the wheel speed is even more important (refer to Figure 4.7 on page 71).

In the same manner as it is done in equation 5.23, where Delta Wheel Load is connected with a change in braking slip, Delta Braking Torque ΔM_B can be connected with the change in braking slip as well. Applying the same method as before, it derives that

$$\Delta\lambda_B = \frac{r_{\text{eff}}}{J_W v_x} \int \Delta M_B dt \quad (5.25)$$

5.2.2 Test Drives to Validate the Connection Between Wheel Load and Braking Force/Braking Slip

Test drives are executed to determine to which amount and in which time frame the switching of the active shock absorber influences the wheel load and the braking force/braking slip in real test drives on a real road. The test drives are comparable in their objective to the test rig trials, where it was also the objective to determine those effects of the switching in the context of the vertical dynamics (refer to section 4.6).

In the same manner as in the experiments on the test rig, the vertical dynamics are investigated by switching the active shock absorber and comparing what would have happened if it had not been switched with the actual course of wheel load after switching the shock absorber. The test drives are also meant to determine if equation 5.23 can be verified with numerical values.

Method and Experimental Setting

To determine those effects it is necessary to produce courses of wheel load, braking force, and braking slip which are reproducible enough to detect the change in those measurands caused by switching the shock absorber. That is why the cosine-shaped obstacles introduced in section 3.4.1 are passed, because by passing these obstacles the excitation is well defined and much stronger than the unforeseeable random excitations from a real pavement.

The dampers are not controlled by the MiniMax-controller in those test drives, but rather switched at a defined time from soft to hard and hard to soft respectively, to determine to which amount and in which time frame the switching of the damper affects the braking slip and the braking force. It is assumed that an increasing wheel load leads to an increasing braking force and to a decreasing braking slip, and vice versa.

Figure 5.2 shows the experimental setting for the experiments. The initial velocity is set to $v_{x,0} = 50$ km/h, the gearbox is in second gear. The braking procedure is executed with a rather low braking pressure of $p_{B,MC} \approx 24$ bar. This is far below the usual critical braking pressure at which the ABS starts to control on standard pavement of $p_{B,fl} \approx 80$ –100 bar. The braking pressure is chosen to be such low because an intervention of the ABS during the test drives would lead to a course of braking force and braking slip which would not be reproducible anymore, for the ABS—if it controls—does not control at the same time for every test drive.

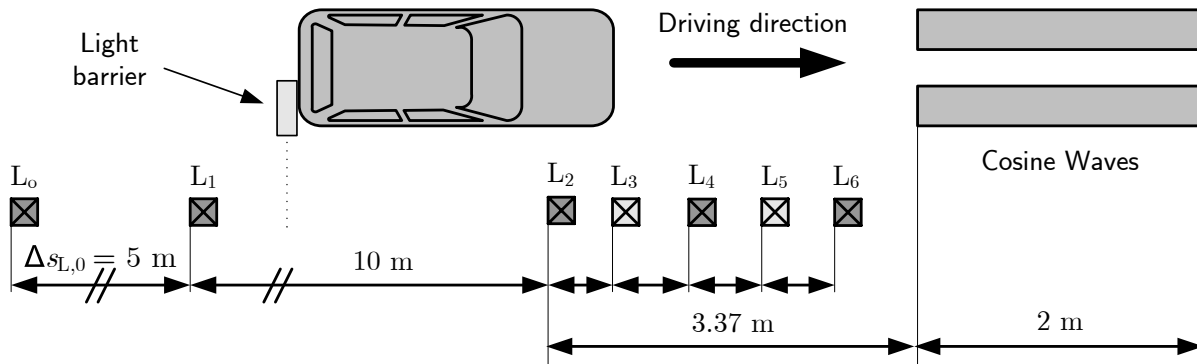


Figure 5.2: Experimental setting for test drives to investigate the switching effect on the wheel load, on the braking slip and on the braking force. Initial velocity $v_{x,0} = 50$ km/h.

I. e., the braking force as well as the braking slip are at a rather low level. But still the effect of switching the shock absorber can be measured with the experimental setting described. At the light barrier reflector L_0 the measuring starts, at L_1 the braking procedure is initiated, at L_2 the front wheels of the vehicle touch the cosine wave for the first time, at L_4 the front wheels are on top of the cosine waves, and at L_6 the front wheels leave the cosine waves.

The switching of the shock absorbers of the front axle is set to a point at which they are either clearly in compression or clearly in rebound. This is shortly after touching the cosine waves for the first time and shortly after leaving the summit of the cosine waves. Passing the light barrier reflector L_3 makes the shock absorbers of the front axle switch when they are in compression, and passing L_5 initiates a switching within rebound. The shock absorbers of the rear axle are set to hard for all of those test drives.

Braking force and wheel load are measured by means of the measuring rim described in section 3.2.3.

Results

Figure 5.3 shows the effect of switching the active shock absorber of the front left wheel on the braking slip, the braking force, and on the wheel load. The same stages as theoretically described in section 5.2.1 can be seen in this time plot of real test drives.

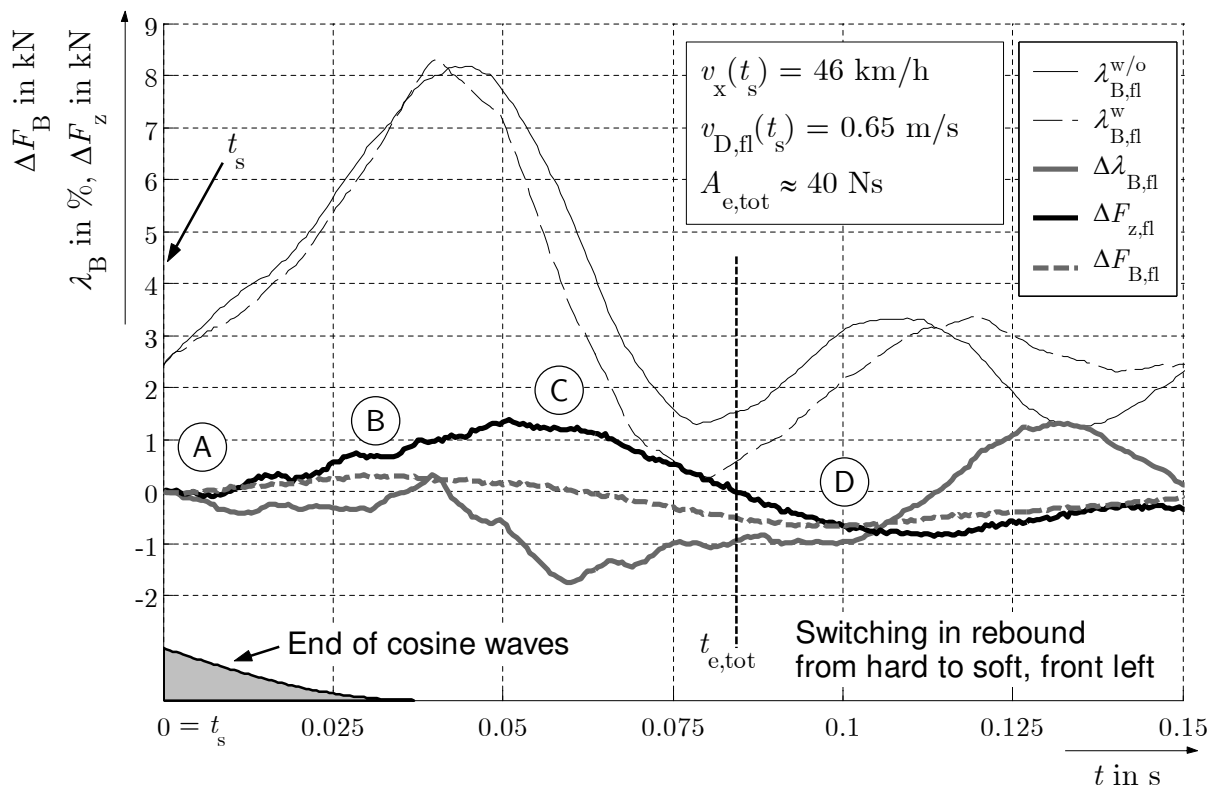


Figure 5.3: Course of Delta Braking Slip, Delta Braking Force, and Delta Wheel Load due to switching the shock absorber of the front axle in rebound from hard to soft when passing the cosine waves.

In point A the wheel load starts to increase because of the switching from hard to soft in rebound. The braking force follows at the same time. At first nothing happens to the braking slip, it stays constant (Delta Braking Slip $\Delta \lambda_{B,fl}$ approximately zero).

It is at point B, where the Delta Braking Force reaches its maximum, that the braking slip starts to decrease until point C is reached.

At point C the braking force finds back to its initial value, the Delta Braking Force is zero. Recalling the argumentation of section 5.2.1 shows that this is exactly what is

expected to happen. It is first the braking force which changes before the braking slip follows. Between points C and D the braking force decreases while the braking slip stays approximately constant.

In point D, after passing the Total Effect Time $t_{e,tot}$, when the Delta Wheel Load is actually negative, the slip starts to increase again. This is the behavior which was predicted by the theoretical considerations.

The change in braking slip is rather small, because in the experiment given the braking pressure is applied at a low level. At the maximum of the μ -slip curve the same amount of change in wheel load leads to greater changes in braking slip, because there the slope of the μ -slip curve is smaller.

Similar to the Effect Time, the Total Effect Time, and the Total Effect Magnitude, which were defined in equations 4.45, 4.46, and 4.48 on page 87, those quantities can be calculated for the given experimental setting as well. In Table 5.1 those quantities are given for all four possibilities of switching, referring to the wheel load influence matrix in Table 4.1 on page 64. Beside the measurand $A_{e,tot}$ which values the vertical dynamics, the measurand $E_{e,tot}$ is introduced. This measurand is the integral of Delta Braking Force with respect to time from the time of switching the shock absorber t_s to the time when Delta Braking Force is zero again. The definition of $E_{e,tot}$ is therefore similar to the one of $A_{e,tot}$, but it is a measurand of the longitudinal dynamics.

Table 5.1: Effect Time, Total Effect Time, and Total Effect Magnitude for passing the cosine waves and switching the shock absorber.

	Compression				Rebound			
	t_e	$t_{e,tot}$	$A_{e,tot}$	$E_{e,tot}$	t_e	$t_{e,tot}$	$A_{e,tot}$	$E_{e,tot}$
hard to soft	14 ms	65 ms	-23 Ns	-8 Ns	12 ms	85 ms	+40 Ns	+10 Ns
soft to hard	11 ms	61 ms	+19 Ns	+6 Ns	11 ms	89 ms	-41 Ns	-11 Ns

Comparing Table 5.1 with the results in section 4.6, it can be seen that the Effect Time t_e is shorter in the given experimental setting than it is in the test rig experiments described in section 4.6. An explanation for this behavior could be that the wheel load here is measured by means of the 6-component measuring rim, whereas in the test rig experiments the wheel load was measured directly in the tire contact zone. Since the damper force acts directly at the measuring rim, but needs to be transferred by the tire into actual wheel load, in the very beginning of the switching process it is supposably more the damper force than the wheel load which the measuring rim measures.

As was shown in section 3.2.3, the time delay $\Delta\tau_{F_z}$ between force measured by the measuring rim, $F_{z,rim}$, and the actual wheel load F_z is approximately 5 ms. Thus, part of the shorter Effect Time can be explained by this time delay. The other part of the shorter Effect Time can be explained by the fact that the damper velocity at the time of switching is rather high. There is a tendency that a higher damper velocity at time of switching leads to a shorter Effect Time (refer to Figure 4.23 on page 96).

Comparing the results shown in Figure 5.3 to values that can be calculated from the theoretical approach in section 5.2.1 shows that the main assumption, that the change in braking slip is connected to the integral of wheel load, holds true—not only qualitative but also quantitative. Applying the parameters from Table 3.1 on page 40 to equation 5.23, taking the value for the Delta Wheel Load Integral as the Total Effect Magnitude $A_{e,tot}$ from

Table 5.1, and realizing that the friction factor $\mu \approx 0.37$ (this value can be approximated best by looking at Figure 5.5) for the test drives looked at leads to:

$$\Delta\lambda_B \approx -\frac{0.37 \cdot (0.304 \text{ m})^2}{6.3 \text{ kg m}^2 \cdot 46 \text{ km/h}} 40 \text{ Ns} \approx -1.7 \% \quad (5.26)$$

This value of $\Delta\lambda_B \approx -1.7\%$, determined by rough calculation, reflects well what actually can be measured in reality. The course of Delta Braking Slip starts to decrease at point C and reaches minimum values between approximately -1% and -1.7% . Thus, the theoretical thoughts which have been made with respect to the connection of change in wheel load and following change in braking slip can be justified.

Doing the same calculus using directly the Effect Magnitude of the Delta Braking Force $E_{e,\text{tot}}$ (refer to Table 5.1) by making use of equation 5.22 on page 117 leads to:

$$\Delta\lambda_B \approx -\frac{(0.304 \text{ m})^2}{6.3 \text{ kg m}^2 \cdot 46 \text{ km/h}} 10 \text{ Ns} \approx -1.1 \%, \quad (5.27)$$

which is a good approximation of the quasi-stationary value for the braking slip around time $t_{e,\text{tot}}$ in Figure 5.3.

In Figure 5.4 the courses of Delta Braking Slip, Delta Braking Force, and Delta Wheel Load are shown which establish after switching the shock absorber of the front left in rebound from soft to hard. Switching the shock absorber from soft to hard in rebound leads to a decrease in wheel load.

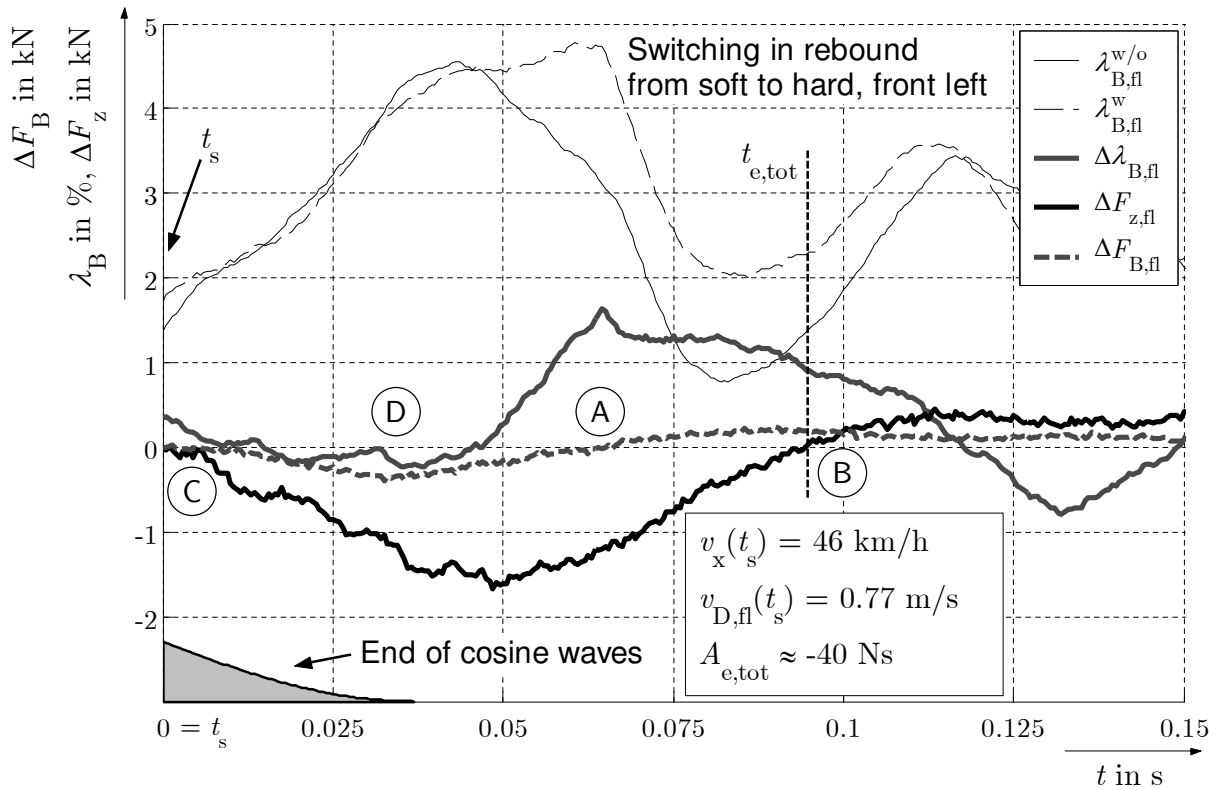


Figure 5.4: Course of Delta Braking Slip, Delta Braking Force, and Delta Wheel Load due to switching the shock absorber of the front axle in rebound from soft to hard when passing the cosine waves.

Thus, the chronology of events starts at point C shown in Figure 5.1. When the wheel load starts to decrease in point C, the braking force also decreases with almost no time delay, the braking slip remains unchanged. In point D the braking force is at its minimum and starts to increase again. In point A it reaches its old value again. This is what could be seen by theoretical considerations as well. Between points D and A the braking slip increases because the same amount of braking force is needed as it was before the switching occurred, but with less wheel load provided. The then following increase in wheel load also lets the braking force increase until point B is reached. Between points A and B the braking slip remains approximately constant—as predicted by theoretical thoughts.

Again, comparing the numerical values of this switching process—which are basically the same as in the previously described switching process shown in Figure 5.3—shows that the change in braking slip can be predicted by numerical analysis (numerical $\Delta\lambda_B \approx +1.7\%$ for wheel load integral analysis and $\Delta\lambda_B \approx +1.3\%$ for braking force analysis, measuring between $+1\%$ and $+1.7\%$).

Both Figure 5.3 and Figure 5.4 show that the switching of the shock absorber not only influences the wheel load in a way which can be used for a controller, but also influences the braking slip and the braking force such that it can be made use of, because the course of those quantities can be predicted.

Furthermore, the assumption that the change in braking slip is connected to the integral of the change in wheel load can be verified. Applying numerical values shows that the values for the calculated and the measured braking slip lie in the same dimension.

Figure 5.5 shows the change in braking force ΔF_B vs. the change in wheel load ΔF_z for all four sections of the Wheel Load Influence Matrix. It can be seen that increasing the wheel load leads to an increasing braking force and vice versa. It can furthermore be seen that the braking force follows the wheel load with almost no time delay. Furthermore, the ratio between ΔF_B and ΔF_z , which is defined as the friction coefficient μ , is approximately constant in the first couple of milliseconds after switching the shock absorber. The value for the friction coefficient can be estimated from the given figure. E. g., for switching from hard to soft in rebound, the Delta Braking Force after 30 ms is approximately 300 N, whereas the Delta Wheel Load at this time has a value of 800 N. Thus, the friction coefficient in this situation is $\mu \approx 300/800 = 0.375$.

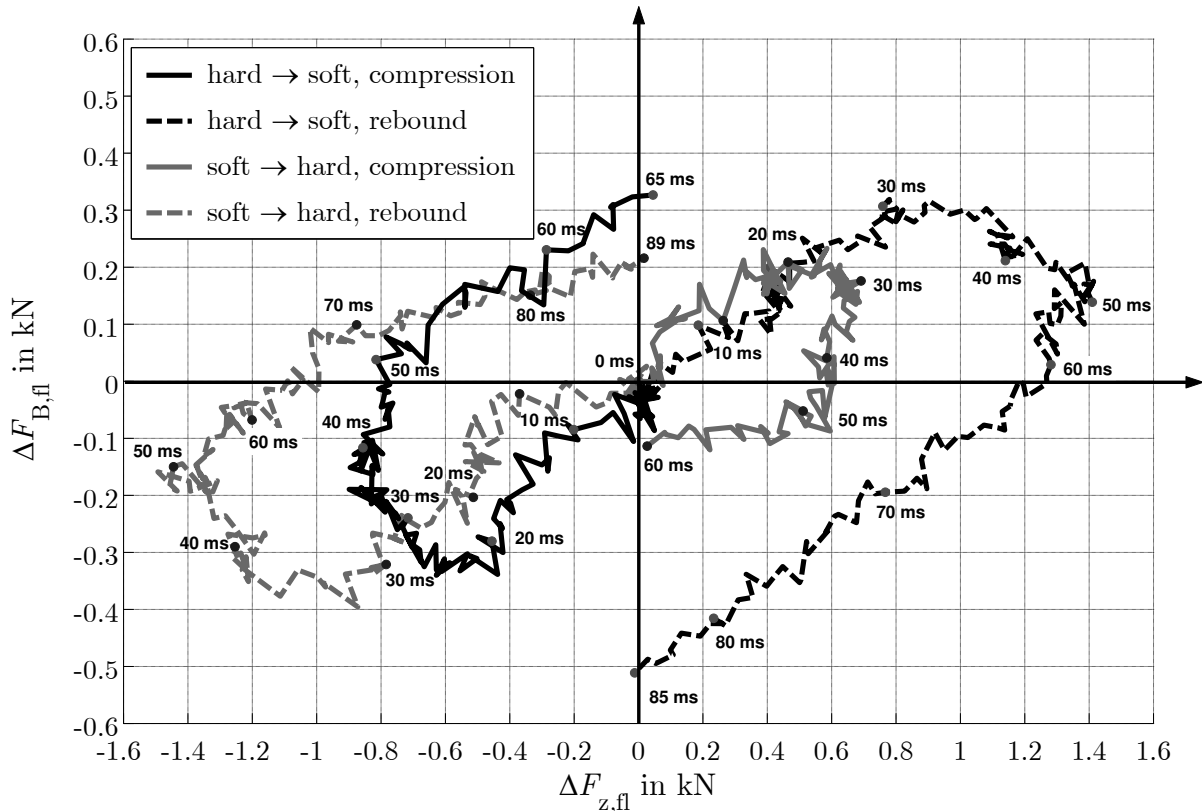


Figure 5.5: Delta Braking Force vs. Delta Wheel Load at the front left wheel, switching the shock absorbers when passing the cosine waves. Measuring executed with the 6-component measuring rim.

5.3 Slip Controller

Designing the control mechanism for the active shock absorbers to reduce the braking distance, three questions need to be answered: Due to the fact that the braking distance d_B in its dependency on the vertical dynamics of a vehicle cannot be written down in a closed form and therefore cannot be determined analytically, the quantity which ought to be influenced by the control of the active shock absorbers needs to be defined. It must be a quantity of which one knows that influencing it will also influence the braking distance in the wished manner. So the question is: Which quantity should be controlled in order to reduce the braking distance? The second question deals with measuring the control variable. Assuming that it cannot be measured directly, which quantity should then be taken to act as measurand? The third and last question deals with the means that should be used to influence the quantity previously described. In this thesis the means are the vertical dynamics of the car, more precisely active shock absorbers. Are active shock absorbers capable of fulfilling the control objective in terms of time behavior and in terms of magnitude of the influence they have on the control variable?

The first question was already answered implicitly in section 2.2 when braking at the optimal braking slip was detected as one crucial aspect in order to reduce the braking distance. Thus, the braking slip is the variable which serves as control variable. Keeping it at its optimal value throughout the braking procedure will shorten the braking distance.

The problem with the braking slip is the following: Once it reaches values which should be controlled, i.e. if the braking slip exceeds a given threshold, it is usually already too late to control the braking slip, because the ABS-controller will have reacted on the high slip value by then. But once the ABS-controller decreases the braking pressure, it does not make much sense to increase the wheel load in order to reduce the braking slip anymore.

The wheel-load controller should increase wheel load if and only if braking slip increases induced by values of wheel load that are too small. If braking slip increases induced by a braking torque which is too large, the wheel-load controller should not act, because such shoots in braking slip cannot be prevented by the vertical dynamics anyway.

This is why a substitute control variable is needed. The connection between wheel load integral and braking slip has already been established in section 5.2. There it is shown that a change in wheel load integral will eventually lead to a change in braking slip. This was also verified in test drives on the cosine waves in section 5.2.2. Thus, the wheel load integral is used as measurand and as substitute control variable. It serves as input for the controller. If it is too negative, the braking slip is assumed to increase soon. In this case the request of wheel load would be to increase wheel load.

This leads to the answer of the third question: The means by which the control variable—or better, the substitute control variable—shall be influenced is the MiniMax-controller with which wheel load can be increased or decreased purposefully.

The controller works independently for each wheel. A connection between the oscillations of two wheels at an axle or between front and rear axle is not implemented in the controller. For the axles this is because a switching process at the rear axle has a very low influence on the wheel load at the front axle and vice versa. This has been investigated in test rig experiments. Thus, it is not necessary to use oscillation information of one axle to control the other.

Now even though switching the shock absorbers at one track changes the course of wheel load at the other track, still there is no connection implemented in the controller. Why not? The problem with this interaction of one side and the other is, that it is quite arbitrary. One never knows what will happen at for example the left side if a shock absorber of the right side is switched. It can either cause an increase or a decrease in wheel load, depending on the current damper velocity of the non-switched side and on the course which the following damper velocity will take. This again depends strongly on the pavement which cannot be foreseen. This holds true for the switched side as well, but there the decision to switch or not to switch is based on the damper velocity and on a threshold for the damper velocity. So one can be quite sure that the wheel load actually will do what it is supposed to do: either increase or decrease, depending on $F_{z,\text{req}}$.

Figure 5.6 shows the principle of the controller which is implemented in the testing vehicle. The dynamic wheel load is integrated, and divided by the longitudinal velocity v_x it delivers the decision basis for the request of wheel load. By dividing with v_x the wheel load integral is brought from the level of braking slip λ_B to the level of velocity difference v_{diff} .

For the reasoning of the previous sections a negative wheel load is assumed to cause an increase in braking slip respectively in velocity difference. This increase again should be prevented by increasing wheel load ($F_{z,\text{req}} = +1$).

Thus, a threshold a is introduced such that the request of wheel load $F_{z,\text{req}} = -1$ if the wheel load integral divided by the longitudinal velocity $FI/v_x \geq a$, and $F_{z,\text{req}} = +1$ if $FI/v_x < a$. This threshold is chosen to be negative, because a strongly negative wheel

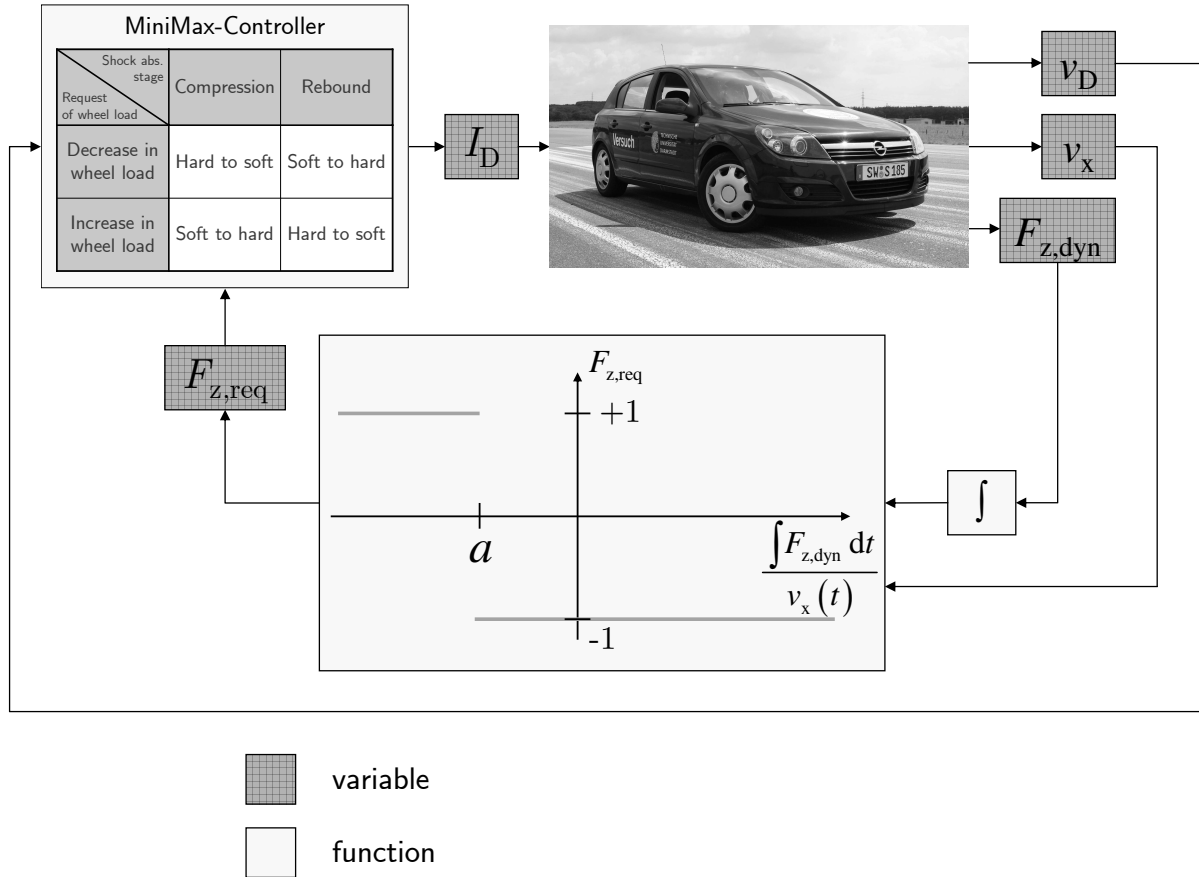


Figure 5.6: Principle of the controller used to reduce the braking distance.

load integral leads to a strong increase in braking slip. On the contrary, if the wheel load integral is strongly positiv, it does not cause a decrease in braking slip by the same amount, since the lower limit for the braking slip lies at value zero and the optimal braking slip is closer to zero than to one. Starting from e. g. 10 %, the braking slip can be increased by e. g. 30 %, but it cannot be decreased by this amount. Caused by this fact the function from which the request of wheel load derives looks asymmetrical ($a \neq 0$).

Furthermore, by choosing $a < 0$ it is prevented that the controller's output changes between $F_{z,req} = -1$ and $F_{z,req} = +1$ rapidly if the wheel load integral oscillates around zero. Only if the wheel load integral is strongly negative an intervention should follow. For all other values of FI , where $FI/v_x \geq a$, the request of wheel load is $F_{z,req} = -1$, since by using this artificial characteristic line, potential to increase wheel load is established. Due to the lowering of the vehicle's body if $F_{z,req} = -1$, the effect on the course of wheel load when switching to $F_{z,req} = +1$ will be greater if there is a harsh transition from $F_{z,req} = -1$ to $F_{z,req} = +1$ and if it is switched only if really needed, i. e. if the wheel load integral is strongly negative.

The analytical representation of a is the following:

$$a = -\frac{J_W \Delta \lambda_B}{\mu r_{\text{eff}}^2} \quad (5.28)$$

The best value for a was determined empirically in preliminary tests. In second gear and

for a wheel of the front axle it has a numerical value of $a_f = -1.9$ kg. For a wheel of the rear axle $a_r = -0.3$ kg. Both values correspond to a Delta Braking Slip of approximately 3 %.

5.3.1 Demands on the Actuator in the Time Frame

There are two aspects in which demands on the controller derive from the previously described aspects: The effect on wheel load needs to establish fast enough and its magnitude needs to be high enough to be able to influence the rotational dynamics of the wheel noticeably. To determine the actual values for both the demand on time and on magnitude level, calculations for a worst-case scenario shall be executed.

Assuming that the vehicle drives at a given speed v_x and is braked such that the braking torque M_B and braking force times the effective radius $F_B r_{\text{eff}}$ at a wheel are in balance (a situation which cannot occur stationary, but nevertheless shall be used for a thought experiment), which means that this wheel is not decelerated. Assuming furthermore that the wheel load and with it the braking force will drop from its given value to zero from one time step to the other for whatever reason, the wheel will then be decelerated with the torque $-M_B = F_B r_{\text{eff}}$. The time it would take for the wheel to lock if this worst case happened is defined as t_{lock} .

With

$$\dot{\varphi}_{W,0} = \frac{v_x}{r_{\text{eff}}} \quad (5.29)$$

and using equation 5.14 on page 116 this braking down of the wheel is governed by the following equation.

$$\dot{\varphi}_W(t) = \dot{\varphi}_{W,0} - \frac{F_B r_{\text{eff}}}{J_W} t \quad (5.30)$$

At time $t = t_{\text{lock}}$ the wheel locks, the angular velocity $\dot{\varphi}_W(t = t_{\text{lock}})$ is therefore zero, which leads to:

$$t_{\text{lock}} = \frac{\dot{\varphi}_{W,0} J_W}{F_B r_{\text{eff}}} = \frac{v_x J_W}{F_B r_{\text{eff}}^2} \quad (5.31)$$

Assuming that the vehicle is braking at $v_x = 70$ km/h or $v_x = 100$ km/h, that $F_B \approx F_z \approx 5000$ N for $\mu = 1$, and using the set of parameters from Table 3.1 on page 40 for the front left wheel leads to the values for t_{lock} that are shown in Table 5.2.

Table 5.2: Time t_{lock} that it takes for the wheel to lock in the worst case.

	Gear		
	neutral	third	second
$v_x = 70$ km/h	$t_{\text{lock}} = 55$ ms	$t_{\text{lock}} = 130$ ms	$t_{\text{lock}} = 265$ ms
$v_x = 100$ km/h	$t_{\text{lock}} = 78$ ms	$t_{\text{lock}} = 185$ ms	$t_{\text{lock}} = 380$ ms

Comparing those times for the wheel to lock in the worst case with the Effect Times in Figure 4.23 on page 96 shows that the proposed approach to use the switching effect of the shock absorber to influence the course of wheel load is admissible in the sense that

the effect in the most cases comes at least by a factor two earlier than in the worst case it would take for the wheel to lock. The effect is therefore suitable to prevent the wheel from locking.

5.3.2 Demands on the Actuator in the Magnitude Frame

It infers from the test rig experiments of section 4.6 and from the test drives of section 5.2.2 that the MiniMax-controller is capable of influencing the wheel load in the proper magnitude frame. The average Total Effect Magnitude of approximately 40 Ns at low frequencies (refer to Figure 4.24) applied at a wheel of the front axle at 70 km/h and in second gear leads to a slip change of approximately 3 %. For the rear axle, where the mass moment of inertia of the wheel and the Effect Magnitude are smaller, this value lies at approximately 10 %. The smaller the velocity of the car, the bigger the change in braking slip which can be caused by switching the shock absorber. Both values show that the shock absorbers are capable of acting as actuator in this context for the following reasoning:

If the ABS-controller is active and $p_{\text{ABS}} = -1$ because the braking slip is too high, the braking pressure usually decreases with $\Delta p_{\text{B}} \approx -20$ bar (refer to Figure 5.8) and is held at the lower level between 50–200 ms. This means that, applying the values from Table 3.1 on page 40 to equation 5.25 on page 117, such an intervention by the ABS at 70 km/h in second gear and for standard conditions leads to a change in braking slip for a wheel at the front axle of approximately 12 %. For the rear axle this value is approximately 33 %. Both values are calculated for a persistence of braking pressure reduction of 100 ms, because the average Total Effect Time $\bar{t}_{\text{e,tot}}$ at low frequencies lies at approximately 100 ms as well.

Thus, for the given states, the intervention in the vertical dynamics by switching the active shock absorbers causes a quarter to a third of the effect which the intervention in the longitudinal dynamics by the ABS has. Considering that the effect of switching the shock absorber can even be increased by switching from one artificial line to another, this implies that the shock absorber controller is capable of significantly supporting the ABS.

5.4 Reducing the Braking Distance

In this section the experiments which are executed to determine if it is possible to reduce the braking distance by means of active shock absorbers are described. The hypothesis H_0 ought to be falsified if it was possible to reduce the braking distance. This hypothesis H_0 and its alternative hypothesis H_1 are:

H_0 : It is not possible to reduce the braking distance significantly by means of control of active shock absorbers compared to the best passive damper setting out of hard or soft.

H_1 : It is possible to reduce the braking distance significantly by means of control of active shock absorbers compared to the best passive damper setting out of hard or soft.

5.4.1 Experimental Setting

The experimental setting for the test drives which are meant to determine the reduction of braking distance by means of the active shock absorbers is the following: There are always at least two light barrier reflectors, one of which initiates the measuring of the test drive, the other one initiates the braking procedure. Those two reflectors (L_0 and L_1 in Figure 5.7) stand in a distance of $\Delta s_{L,0} = 5$ m. By having them positioned in a defined distance, it is possible to verify the signal of the Correvit-sensor (refer to Table 3.2 on page 43) which measures the longitudinal velocity. The integral of the velocity signal between L_0 and L_1 must be five meters. If it is not, the velocity signal is corrected by an correction factor.

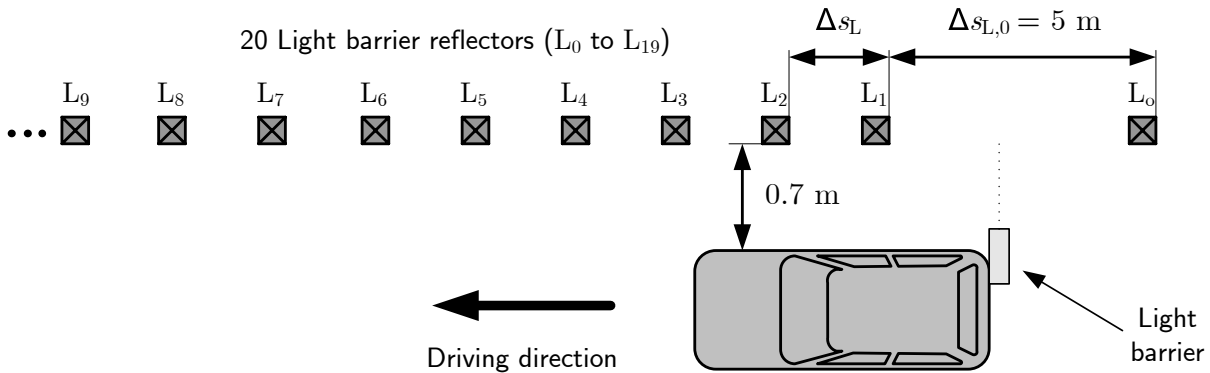


Figure 5.7: Test setup for determining the braking distance. The ABS-braking process is initiated by passing either of the light barrier reflectors from L_1 or higher. It takes approximately 200 ms for the braking machine used to increase the braking pressure to its maximum level. Passing L_0 starts the measuring system.

The light barrier reflectors are used for three reasons: First of all, to be able to calibrate the Correvit-sensor off-line.

Secondly, to initiate the braking procedure by the braking machine. This automat reaches the threshold $p_{B,BB}$ with a maximal deviation of $+/- 5$ ms. This ensures that the braking distance is not influenced by the differing application of braking pressure from braking procedure to braking procedure by a human being.

Thirdly, the reflectors are used to make sure the braking process will take place at the same pavement for every test drive which should be compared. Since the elevation profile at which the braking is executed has a strong impact on the braking distance, this is an important point to determine if and how strongly braking distances are reproducible if every parameter which can be kept constant is kept constant. Two test drives which are executed at two completely different places (e.g. a pothole and a bump) can hardly be compared with each other.

However, even braking at the very same position does not make the braking procedure such reproducible that the variance of braking distances for test drives with the same parameters is smaller than the expected braking distance reduction. The braking distances are distributed stochastically, even if every parameter which can be kept constant is in fact kept constant.

Thus, to be able to gain information about the quality of the shock absorber controller, following method is used: Test drives whose results should be compared are always the

ones which are executed for as many constant parameters as possible. Furthermore, they are executed within a short time frame of only a couple of hours, such that the effect of slowly varying parameters (refer to section 2.2.2) can be neglected.

Comparable test drives are always executed in a defined order: hard–soft–controlled1–controlled2–controlled3. This means that it is always a test drive with hard damping, followed by one with soft damping, followed by a maximum of three test drives with differing controller settings. Within such a block of comparison all long run varying parameters (refer to Table 2.1) are constant, the ones that vary in the short run and the ones that vary in the medium-term run are kept as constant as possible. To illustrate how it is made to actually keep the parameters constant, a checklist of a braking procedure is shown:

- 1 Second gear for $v_{x,0}^{\text{des}} = 70 \text{ km/h}$
- 2 Placing the light barrier reflectors
- 3 Adjusting the cruise control to $v_{x,0}^{\text{des}}$
- 4 Warming-up braking procedures with $v_{x,0}^{\text{des}}$ until $T_{\text{B}}(t_{\text{BI}})$ is constant
- 5 Starting the real, measurable braking procedures
- 6 Decoupling the clutch at an engine speed of 1,000 rpm by foot
- 7 After each braking procedure the same route is taken to start the next procedure in order to always have the same amount of cooling down of the tires and brakes
- 8 Frequency of test drives execution is constant, no breaks in between the braking procedures

Standard Setting

The standard setting for all test drives is the following:

- ‘Standard Road’
- Tire inflation pressure: $p_{\text{T}} = 2.3 \text{ bar}$
- Road condition: dry
- Initial velocity: $v_{x,0}^{\text{des}} = 70 \text{ km/h}$

5.4.2 Results for Uncontrolled Shock Absorbers

In Figure 5.8 a braking procedure is shown for soft shock absorbers exemplarily. The measurands which are presented are the ones that are most relevant for the braking procedure, either because they are inputs to the controller or because they explain the braking behavior.

The begin and the end of braking t_{BB} and t_{BE} are marked in every plot via circles.

It can be seen that there are three major drops in wheel speed during the braking procedure, which correspond to shoots in both braking slip and velocity difference. The

ABS-controller handles these shoots in braking slip with adjusting the braking pressure of the front left wheel to a level at which the braking slip does not increase anymore.

Especially for the third shoot in braking slip it can be seen that there is a close connection between wheel load integral and braking slip. It is at $t \approx 1$ s that the braking slip starts to increase even though the braking pressure is decreasing. This is caused by the fact that the wheel load integral is strongly negative at this point in time.

The braking pressure of the main cylinder $p_{B,MC}$ is increasing after the braking machine is triggered. The braking pressure of the front left wheel $p_{B,fl}$ follows and is limited by the ABS if the braking slip becomes too high. The main cylinder's braking pressure is kept between 100 and 160 bar during the whole braking procedure by the braking machine, while the front wheels' braking pressure never exceeds 120 bar.

Furthermore, the figure shows that the wheel load integral strongly correlates with the pitching movement of the vehicle. Every time the vehicle pitches forward (the spring displacement $s_{S,fl}$ of the front left wheel is negative), the wheel load integral is positive. On the contrary, if the vehicle pitches backwards ($s_{S,fl} > 0$), the wheel load integral is negative. This shows once again that the low-frequency body movements have the strongest influence on the wheel load integral. High-frequency wheel oscillations can be found in its signal, but they do not affect its positiveness or negativeness. For a strongly positive wheel load integral (which occurs two times), the braking slip is decreased down close to zero.

The boolean signals damper current I_D , ABS-signal $p_{ABS,fl}$, and request of wheel load $F_{z,req,fl}$ are also shown in Figure 5.8. The damper current is set to a constant value of $I_{D,i} = 1.6$ A, for the test drive shown is executed with soft damping. Thus, $F_{z,req,fl}$ does not influence the damper current as it does in the controlled case. Nevertheless, $F_{z,req,fl}$ is the same as it would be if the shock absorber was controlled.

The course of $F_{z,req,fl}$ demonstrates the principle function of the controller. Shortly after the initiation of the braking procedure the wheel load integral increases and the request of wheel load is set to $F_{z,req,fl} = -1$. The first shoot in braking slip is thus not caused by a wheel load integral which is too negative, but it is rather caused by the braking pressure which is above the level that can be supported by the braking force. The request of wheel load to decrease leads to a lowering of the vehicle's body which produces the potential to increase wheel load at the right time.

Around $t = 1$ s, the wheel load integral decreases, mainly due to the fact that the vehicle's body is pitching backwards. It is there that the request of wheel load is switched from 'decrease' to 'increase' to prevent a strong shoot in braking slip caused by the too negative wheel load integral. When the wheel load integral rises again, the request of wheel load is switched back to 'decrease' to generate the potential of a sudden increase in wheel load again.

Summarizing, from Figure 5.8 infers that there is a strong correlation between pitching and wheel load integral, and via this between pitching and braking slip. Similar to the explanation given in chapter 4, this is the demand side of the problem. The wheel load integral and with it the braking slip are the quantities which ought to be controlled, and they are influenced mainly by low-frequency oscillations of the vehicle's body.

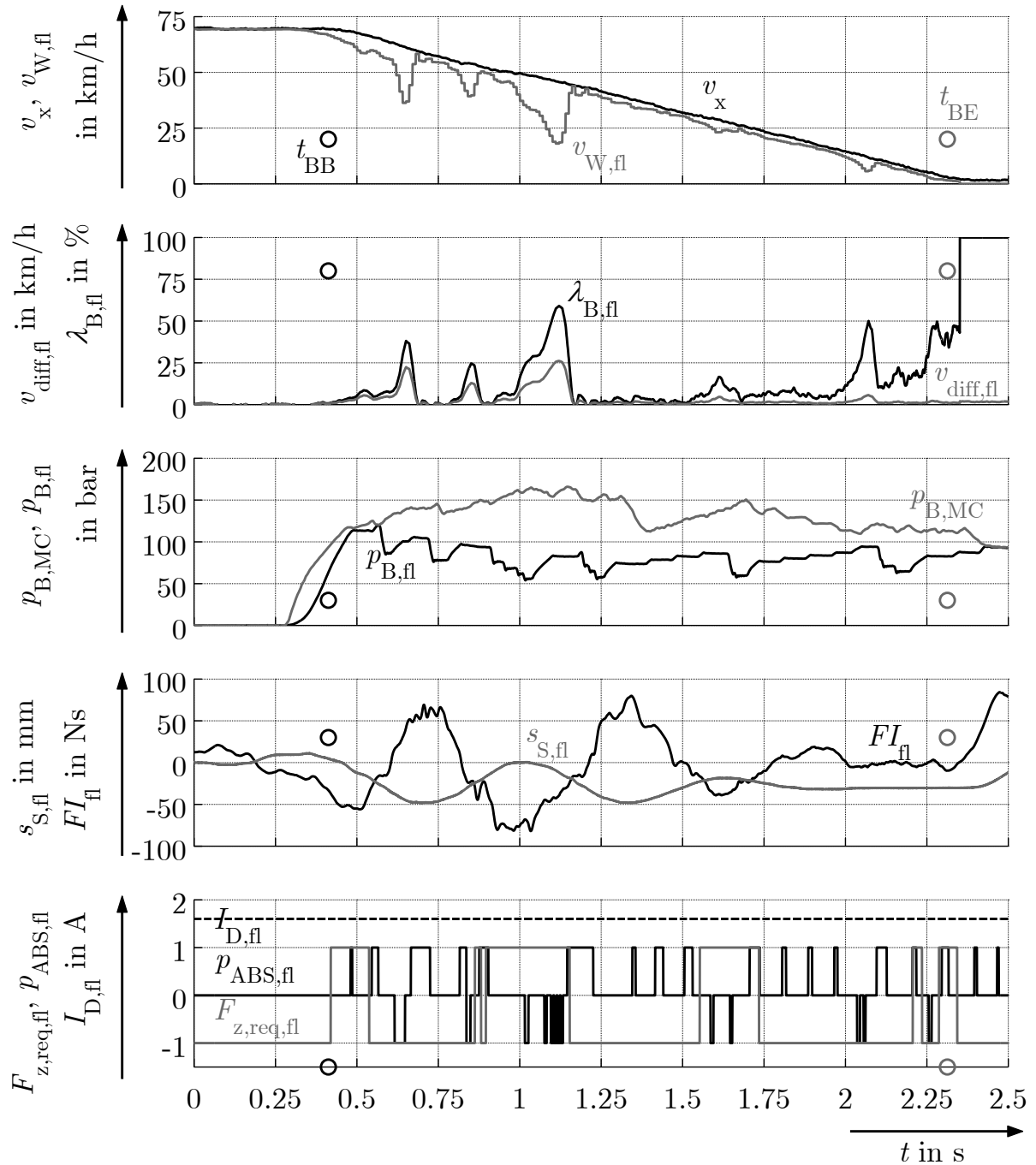


Figure 5.8: Braking procedure for soft shock absorbers. Initial velocity $v_{x,0}^{des} = 70$ km/h, test drive executed on the first part of the test track 'Standard Road'.

Frequency Analysis

In Figure 5.9 the frequency spectrum of the damper velocity for hard and soft damping during full braking out of an initial velocity of 70 km/h is shown. It can be seen that the highest amplitudes of the damper velocity lie at frequencies below approximately 5 Hz. Higher frequencies do not play a role when the car is braking, because the pitching of the body dominates all other excitations. With respect to the movement of the shock absorbers the excitations from the wheels, which happen at frequencies above 10 Hz, are not as relevant as the low-frequency body movements.

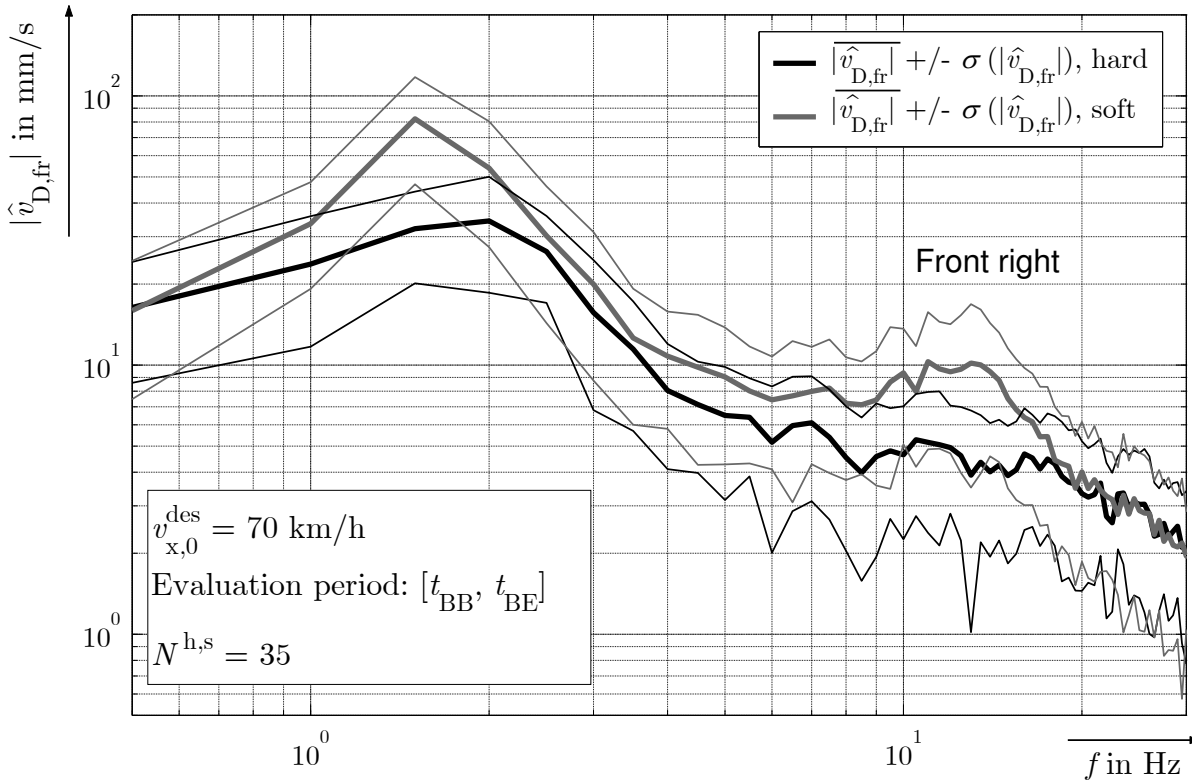


Figure 5.9: Full-braking procedures for initial velocity $v_{x,0}^{\text{des}} = 70$ km/h. Frequency spectrum of the damper velocity for 35 test drives with hard damping and 35 test drives with soft damping respectively. Test drives executed on several different spots of the 'Standard Road'.

The dimension of amplitudes is lower for hard than for soft damping, but the conclusion that the wheel oscillations are not as relevant as the body oscillations is the same for both. Figure 5.9 shows the supply side of the problem. The shock absorber can only have a strong effect on the course of wheel load if the damper velocity is high. Thus, it is at frequencies below approximately 5 Hz that the largest effect can be gained. This is the same frequency-band which infers from the demand side derived from Figure 5.8. Again, the supply and the demand side fit together with respect to their frequency-bands.

5.4.3 Results for Controlled Shock Absorbers

A total of three times 35 test drives (35 hard, 35 soft, 35 controlled) were executed with the standard settings which can be compared with respect to the braking distances. The

number of test drives was chosen such that even facing a high deviation a statistical ensured conclusion can be drawn.

To demonstrate the stochastic distribution of braking distances, Figure 5.10 shows the results for three times 15 test drives. Those were executed in the order shown in the figure on the same day. For every block of three braking distances ('hard', 'soft', and 'controlled') the braking procedures were executed at the very same initial braking position and on the same pavement. It can be seen that even in this case, where all possible parameters are kept constant, there is a high deviation of braking distances. There is no specific order of hard, soft, and controlled damping visible. But it can be seen that the average braking distance for controlled damping is smaller than for both passive damper settings. Computing the average value shows that it is almost by 2 % that the braking distance is shortened by the control of the active shock absorbers.

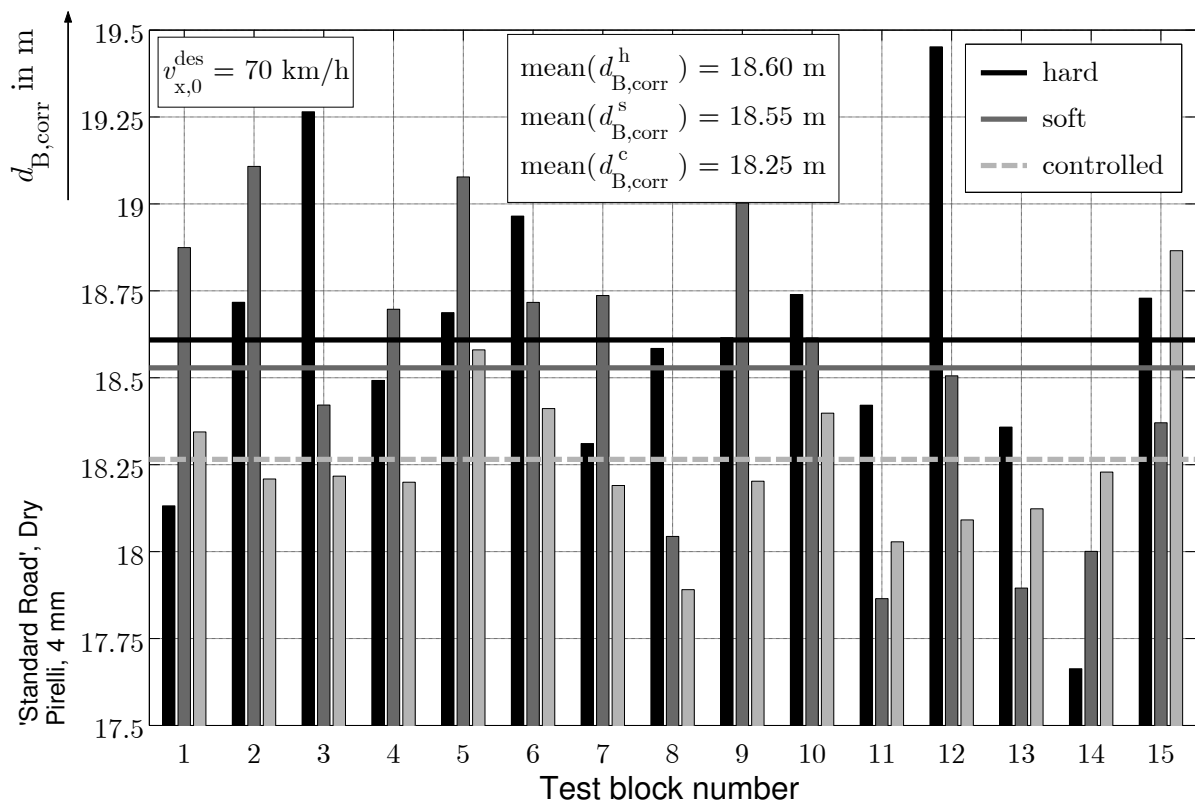


Figure 5.10: Braking distances for hard, soft, and controlled damping for an initial velocity of $v_{x,0}^{des} = 70$ km/h, test drives executed on a dry pavement with a standard roughness.

In Figure 5.11 the results of braking tests are shown which are executed on randomly chosen parts of the airfield where the testing track 'Standard Road' is located. The pavement structure and the unevenness is comparable to the one described in section 3.4.2. The plot shows the cumulative percentage of braking distances and ought to be read exemplarily for controlled damping in the following manner: In 45 % of all controlled braking procedures the braking distance is 18.25 m or shorter. The figure shows that the average braking distance which is obtained with the controlled damping is shorter than the ones for hard and soft damping. The average is shorter by 0.25 m. This means that on an averaging level the braking distance can be reduced by the given controller by 1.3 %.

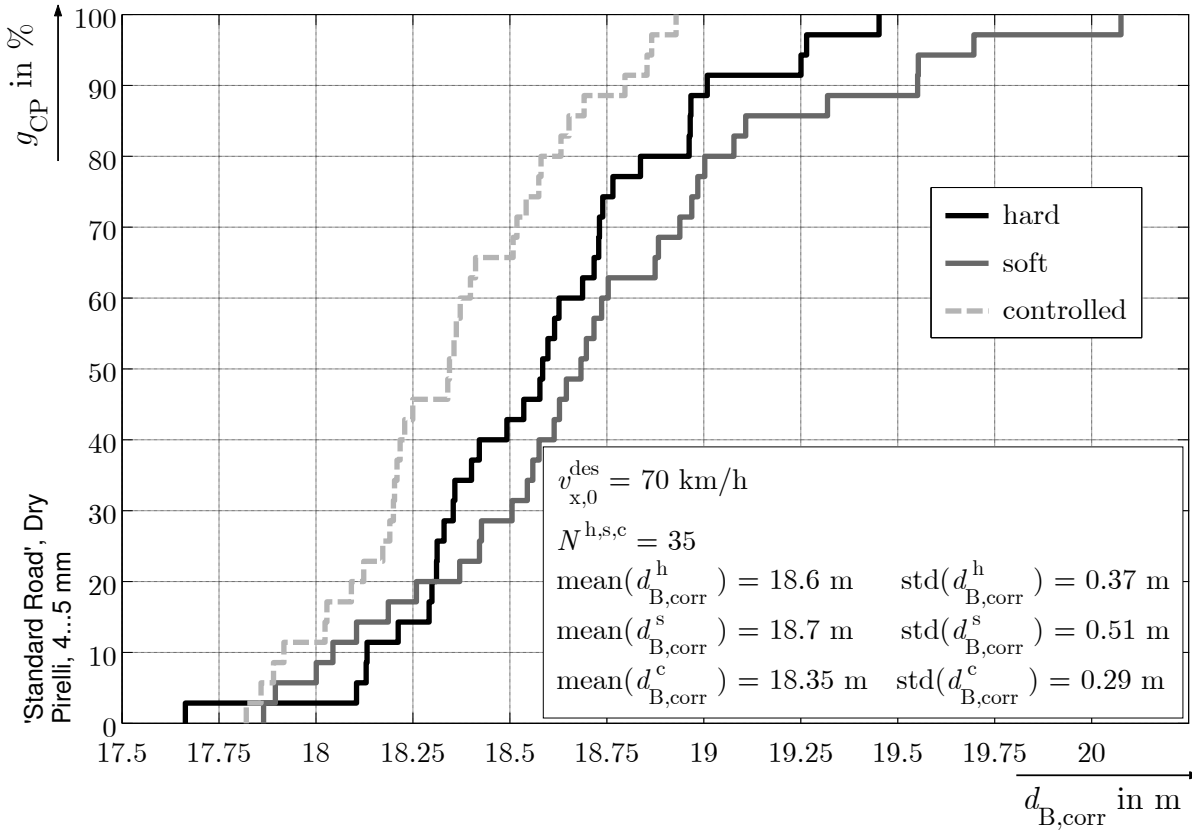


Figure 5.11: Braking distances for hard, soft, and controlled damping for an initial velocity of $v_{x,0}^{\text{des}} = 70 \text{ km/h}$, test drives executed on a dry pavement with a standard roughness.

Furthermore, the standard deviation of braking distance for the controlled test drives is smaller than for the two passive damper settings. There is no outlier in case of controlled damping as it is the case for both hard and soft damping. This means that not only the braking distance is shorter, but also the predictability of the braking distance is better for controlled shock absorbers. This could be due to the fact that in case of controlled shock absorbers those can adapt to changing pavement conditions, whereas the two passive damper settings cannot.

Figure 5.12 shows the cumulative percentage of VI for the three times 35 braking procedures described previously. Recalling that the lower VI , the lower a possible damage in case of an unpreventable crash, it can be seen that soft and controlled damping both lead to better results than hard damping. On an averaged level controlled dampers are even slightly better than soft dampers. In addition to the results with respect to the braking distance this shows another positive aspect of the shock absorber controller. It does not only decrease the braking distance d_{B} , but it also improves the quality of the braking distance in terms of a lower VI .

The benefit of the shock absorber controller lies in the fact that it combines the advantages of both hard and soft damping. Even though hard damping leads to a shorter braking distance, soft damping is better in terms of VI . If one of the two passive settings must be chosen, it first has to be decided if a shorter braking distance or a lower VI is the goal. For controlled damping, this trade-off does not need to be handled. Here the controlled damper lead to the best result with respect to both measurands, d_{B} and VI .

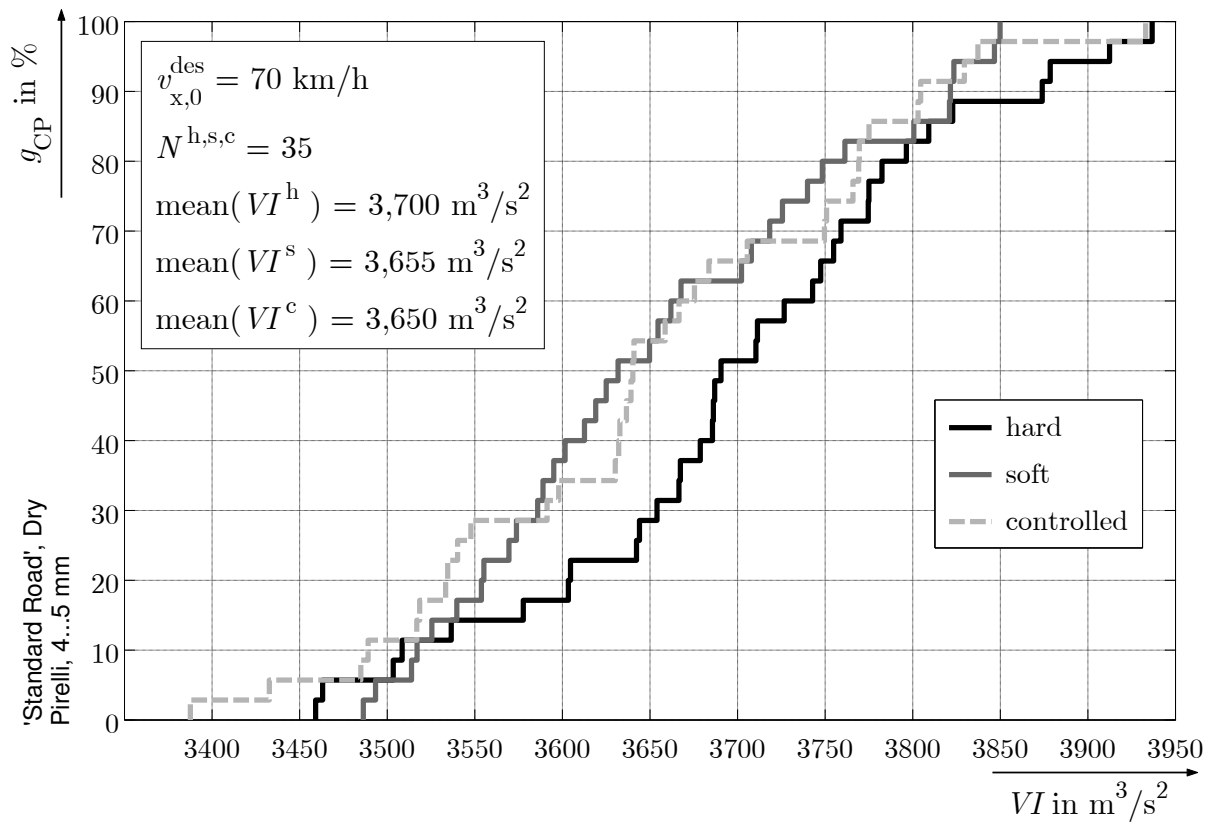


Figure 5.12: Integral of the square of the longitudinal velocity with respect to the travel distance VI for hard, soft, and controlled damping for an initial velocity of $v_{x,0}^{\text{des}} = 70 \text{ km/h}$, test drives executed on a dry pavement with a standard roughness.

Test on Normal Distribution of the Braking Distance

In order to be able to apply tools from statistics, most of the time it is necessary, or at least it makes considerations easier, if a standard distribution of the main population can be assumed. Figure 5.13 contains the same results as Figure 5.11, but here they are plotted in a slightly different way. They are plotted such that if the respective quantity follows a normal distribution, it lies on a straight line. This optimal line is also shown in the figure for every damper setting. Already by inspection it can be seen that for every damper setting the respective sample seems to follow a normal distribution very well. To make this inspection more quantifiable, a so called chi-square test to check for normal distribution is executed³.

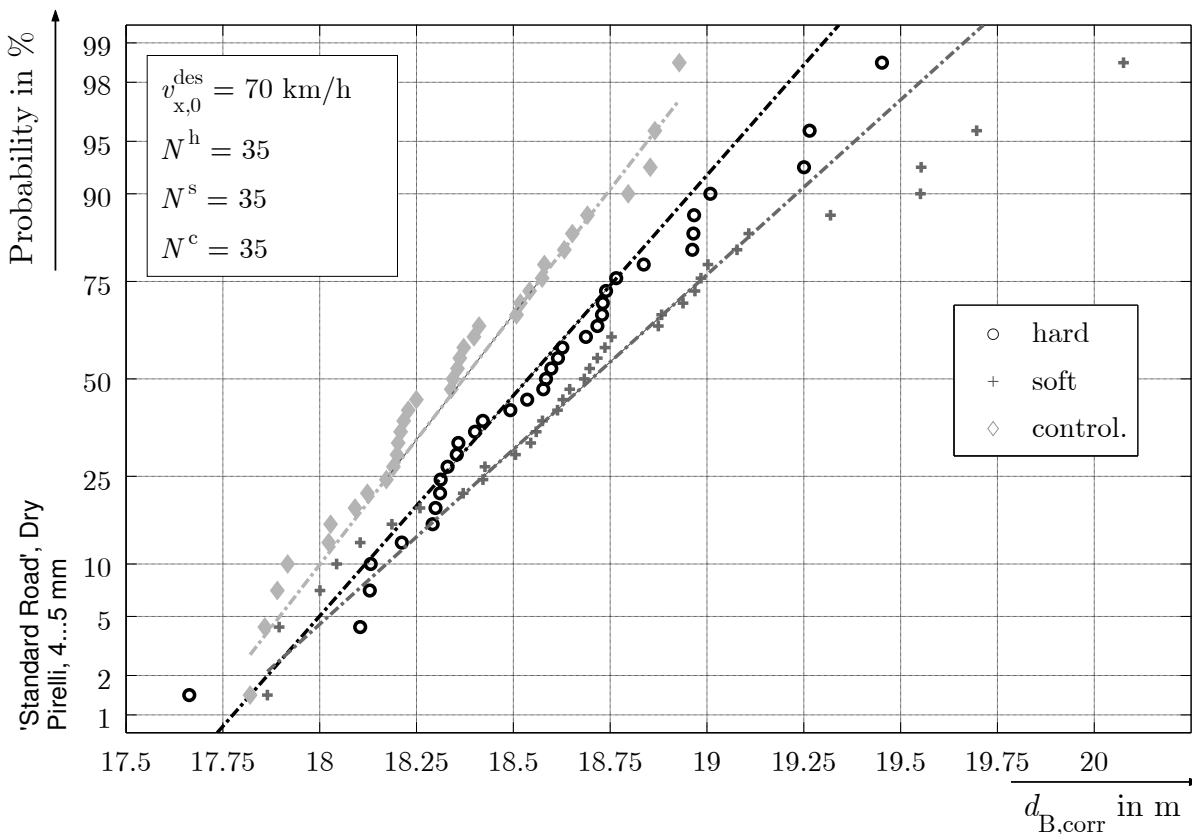


Figure 5.13: Test on Gaussian distribution for hard, soft, and controlled damping.

This chi-square test leads to the result that for all three damper settings on a level of significance of $\alpha_s = 0.05$ the hypothesis of a normal distribution cannot be abolished. It is thus assumed that for every braking procedure with the maximum number of parameters kept constant a normal distribution establishes for the braking distances.

Test on Equality of Expected Values of the Braking Distance

Now that the three braking distance samples 'hard', 'soft', and 'controlled' are statistically verified to be normal distributed, they can be tested on the equality of their expected

³Schwarze/Fusková/Kunitz (2004): Statistik – Grundkurs, Kurseinheit 12: Spezielle Testverfahren pp. 38–40.

values⁴. In one form of this test the hypothesis is formed that the expected value of one main population is greater than the expected value of another main population. It is then tried to falsify this hypothesis by the test procedure. In the given case, the hypothesis is that the expected value of braking distance for hard (soft) damping is smaller or equal than the expected value for controlled damping. This hypothesis can be falsified on a level of significance of $\alpha = 0.005$ for the comparison of hard and controlled damping. For soft and controlled damping it can be falsified on a level of significance of even $\alpha = 0.001$.

These numbers mean that with a probability of 99.5 % the expected value of braking distance for controlled damping is smaller than the one for hard damping, and with a probability of 99.9 % it is smaller than the one for soft damping.

The same test can be undertaken not only to check on equality of expected values but to check on the difference in expected values. Doing this leads to the following result:

On a level of significance of $\alpha = 0.05$, this means with a probability of 95 %, the braking distance for controlled damping is by at least 10 cm shorter than for hard damping, and by at least 20 cm shorter than for soft damping. Both results are statistically significant. Thus, it could be shown that it is indeed possible to shorten the braking by means of active shock absorbers. The hypothesis H_0 on page 127 is therefore falsified and the alternative hypothesis H_1 is assumed to be true. Even though the reduction in braking distance is shown for only one standard setting, it is sufficient to falsify the hypothesis H_0 . It is possible that by choosing another kind of seismic excitation the reduction will not be significant anymore. It is also possible that it is even more significant on other pavements. However, the fact that a reduction of braking distance is possible by means of active shock absorbers has been proven with the method described. It is the first time that this has been done and published on experimental level.

Explanatory Approach

In Figure 5.14 the cumulative percentage is plotted for different values of the longitudinal velocity. Thus, the development of ‘local braking distances’ during the braking procedure can be followed. Snapshots of traveled distances at given longitudinal velocities are taken. The figure reads in the following manner: When the given velocity of e. g. 50 km/h is reached, the average traveled distance is smallest for soft damping, followed by controlled and hard damping. This advantage of soft dampers at the beginning of the braking procedure is lost from there on until at $v_x = 3$ km/h the braking procedure is defined to be finished. Here the cumulative percentage is the same as the one shown in Figure 5.11.

In Figure 5.15 a similar plot is shown. The difference is that here snapshots of longitudinal velocity at given traveled distances are taken. E. g. it infers from the figure that at 8 m after the initiation of the braking procedure the lowest average longitudinal velocity is reached for soft dampers. Four meters later, at 12 m, the controlled setting has already passed the soft one.

It infers from Figures 5.14 and 5.15 that soft shock absorbers lead to better results during the beginning of the braking procedure, but that this advantage is overcompensated in the middle and at the end of the braking procedure, such that soft damping leads to the worst results with respect to the braking distance.

This also explains why the measurand VI is better for soft than for hard damping. If the

⁴Weber (1992): Einführung in die Wahrscheinlichkeitsrechnung und Statistik für Ingenieure pp. 305–312.

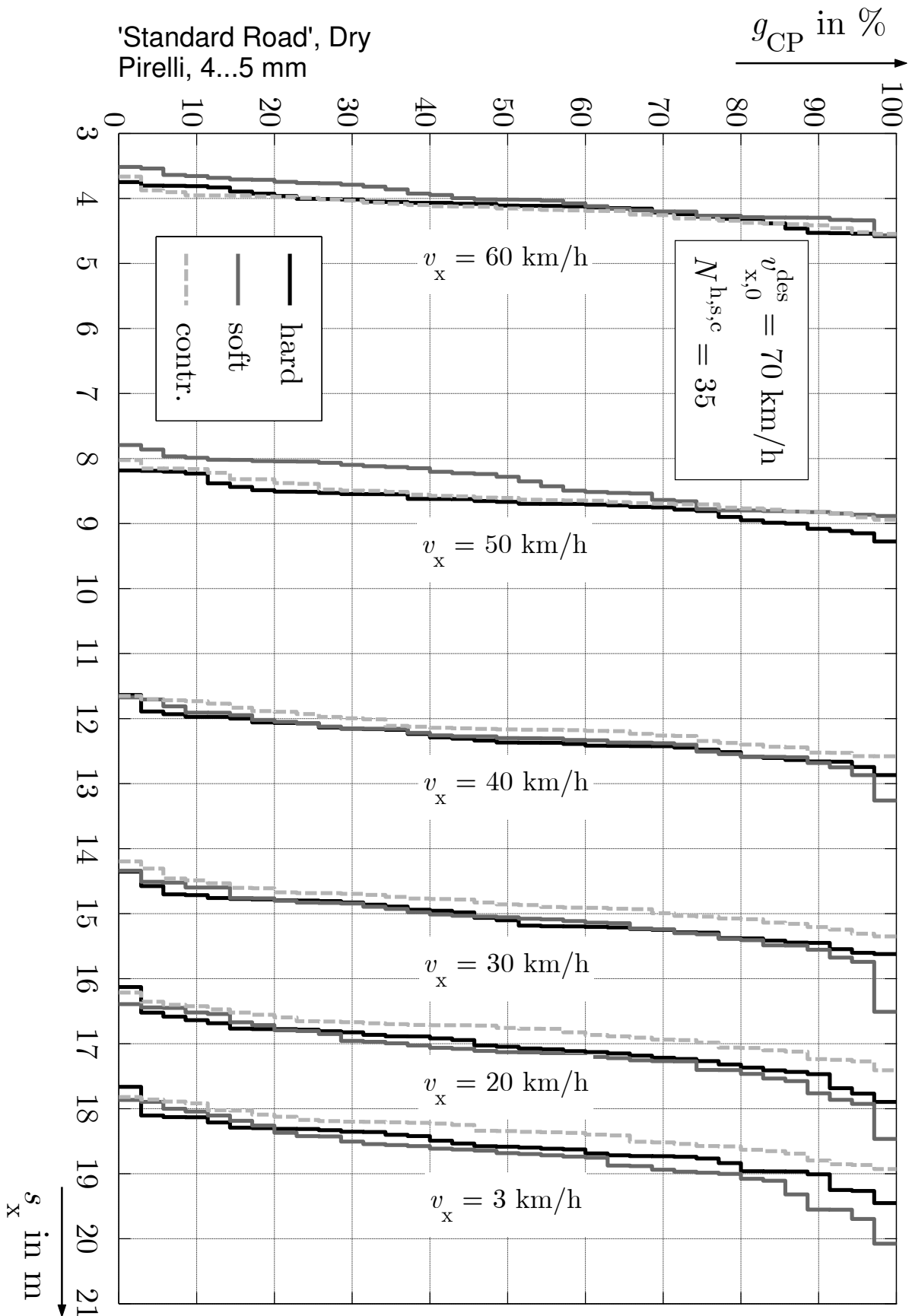


Figure 5.14: Course of longitudinal velocity for braking procedures for hard, soft, and controlled shock absorbers. Initial velocity $v_{x,0}^{des} = 70$ km/h.

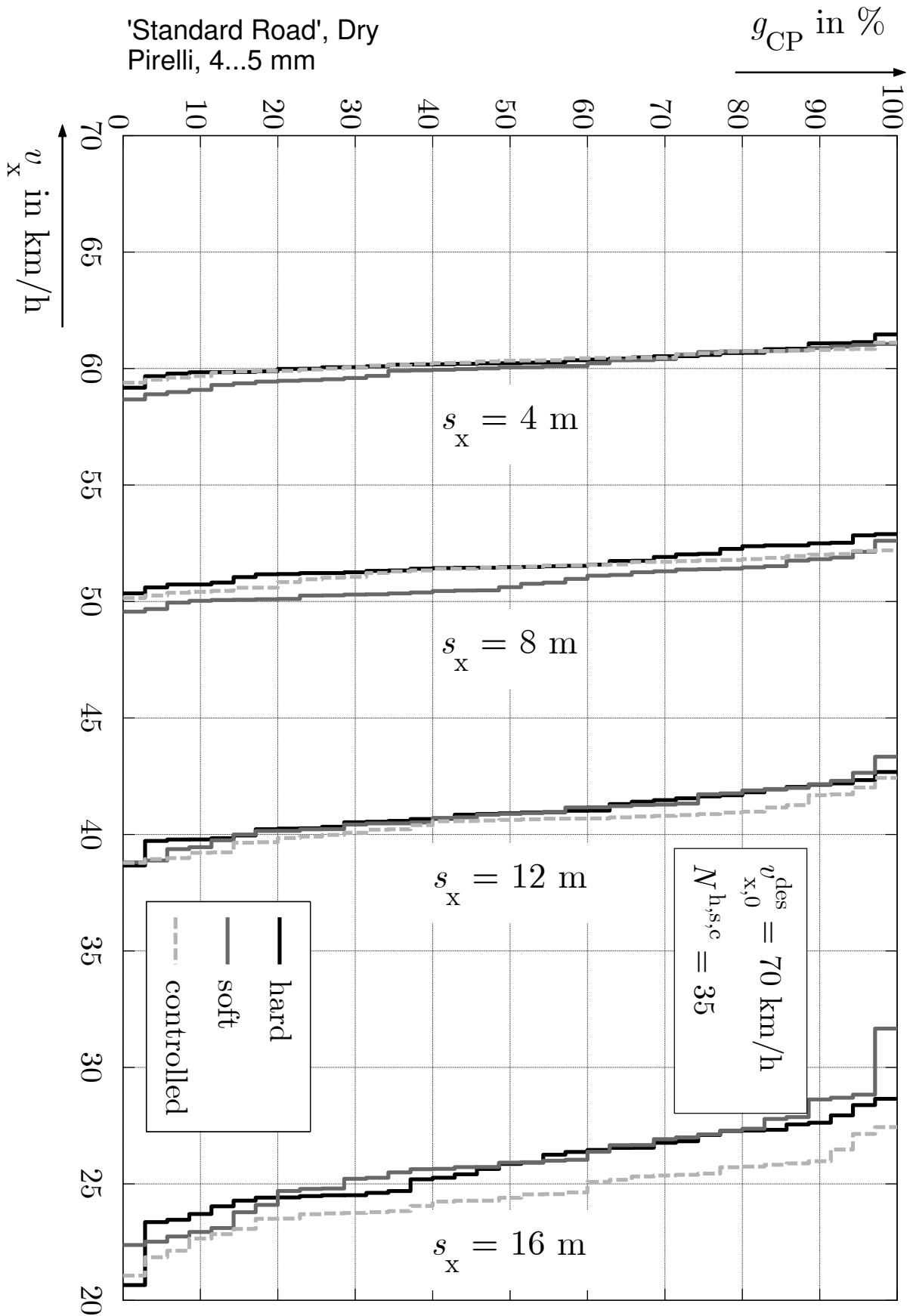


Figure 5.15: Course of traveled distance for braking procedures for hard, soft, and controlled shock absorbers. Initial velocity $v_{x,0}^{des} = 70$ km/h.

braking procedure is good in the sense of a large amount of dissipated kinetic energy, it is also good in the sense of a lowered VI . A decreased velocity during the beginning of the braking procedure is therefore valued highly when calculating VI , and thus soft damping is better here than hard damping.

But why is it that for soft damping the kinetic energy is dissipated by a great amount at the beginning of the braking procedure, but at later times this advantage of the beginning is even overcompensated? It is caused by the fact that for soft damping the first pitching of the vehicle's body is much stronger than for hard damping. Thus, the wheel load integral is also more positive for soft damping in the beginning of the braking procedure. And an increased wheel load integral again causes higher longitudinal forces—namely braking forces—which decelerate the vehicle.

This overshoot in wheel load integral for soft damping at the beginning of the braking procedure is shown in Figure 5.16. Here the courses of wheel load integral for hard, soft, and controlled damping have been averaged for 15 braking procedures each. It can be seen that between 0.2 and 0.4 s after the begin of braking the wheel load integral for soft damping is much larger than for hard damping. This is also the time during which the dissipation of kinetic energy works better for soft then for hard damping. The overshoot in wheel load integral during the beginning of the braking has to be 'paid' with a strong drop between 0.4 and 0.8 ms. This drop leads to the worsening of soft damping compared to hard and controlled in Figures 5.14 and 5.15.

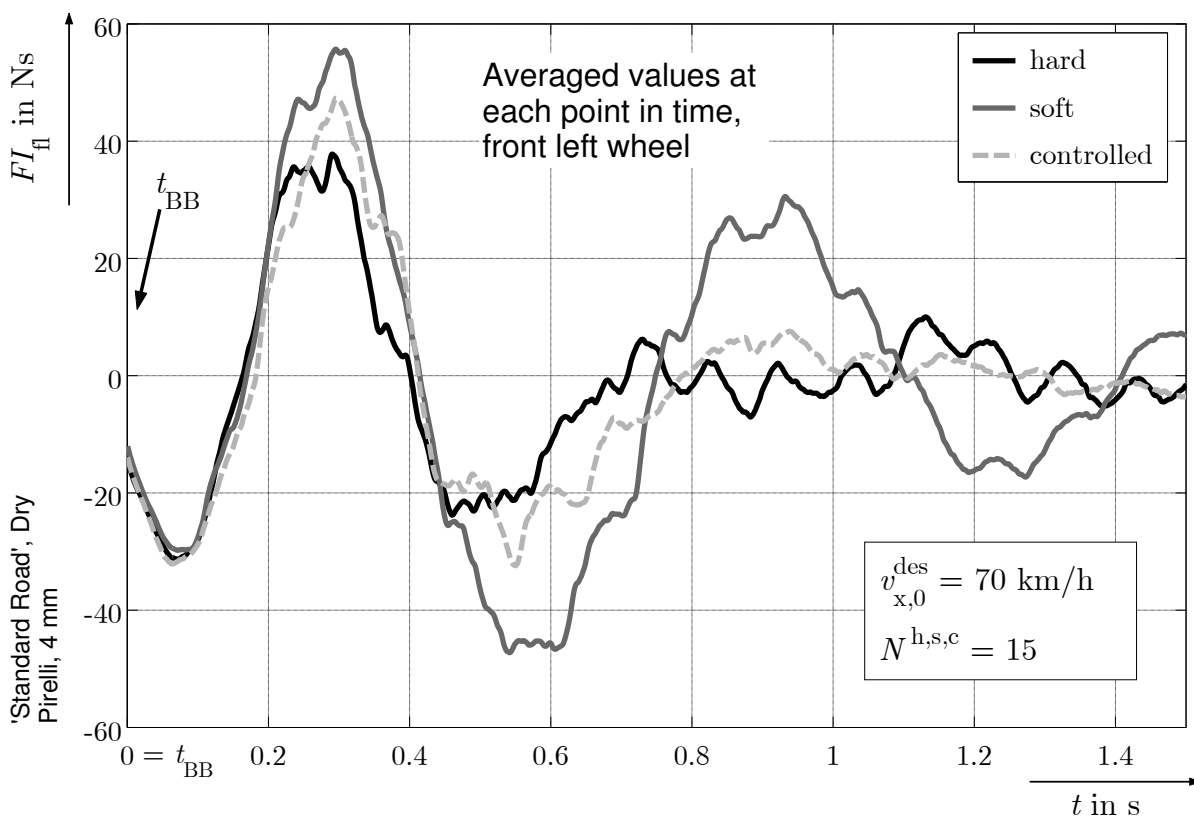


Figure 5.16: Course of averaged wheel load integral FI for hard, soft, and controlled shock absorbers with respect to time for 15 test drives each. Initial velocity $v_{x,0}^{\text{des}} = 70 \text{ km/h}$.

The controller can combine the advantages of hard and soft damping. During the beginning of the braking there is an overshoot in wheel load integral. Not as strong as for soft damping, but stronger than for hard damping. For controlled damping this overshoot does not have to be ‘paid’ with a drop in wheel load integral as drastic as for soft damping. The course of wheel load integral is smoothed by the shock absorber controller.

Correlation Between Braking Distance and Other Measurands

Table 5.3 shows the correlation coefficient for the RMS on dynamic wheel load, weighted with the vehicle speed and the braking distance, as well as the correlation coefficient for the RMS on velocity difference (which is in fact the braking slip, weighted with the vehicle speed) and the braking distance—both for all three damper settings. Surprisingly, the correlation differs for changing damping by quite a lot. In case of hard damping the correlation between RMS on wheel load and braking distance is rather high, for soft and controlled damping this does not hold true. This could be because in case of hard damping the connection between wheel and body is much stronger than for soft damping and therefore the dominating body oscillations can be found in a higher amount in the wheel and the wheel load. This is a topic for further inspection.

Table 5.3: Correlation coefficients and RMS on velocity weighted wheel load and on velocity difference for hard, soft, and controlled damping. ‘Standard road’, dry, $v_{x,0} = 70$ km/h.

Damper setting	$\rho_{F_{z,\text{eff}}^{v_x}, d_{B,\text{corr}}}$	$\rho_{v_{\text{diff},\text{eff}}, d_{B,\text{corr}}}$	$\bar{F}_{z,\text{eff}}^{v_x}$	$\bar{v}_{\text{diff},\text{eff}}$
hard	0.54	0.63	682 N	6.5 km/h
soft	0.17	0.41	776 N	6.3 km/h
controlled	0.07	0.47	687 N	5.8 km/h

It can also be seen that the correlation between braking distance and RMS on velocity difference is higher than the one between braking distance and RMS on wheel load for every damper setting. I. e., beside the RMS on wheel load the quality of the braking procedure can be measured better in terms of velocity difference. Due to the very low correlation there, especially for soft damping, the RMS on wheel load is not feasible to measure the safety.

Furthermore, a very interesting inspection: The slip controller reduces the slip oscillations. The mean value of RMS on velocity difference over all braking procedures is significantly lower for controlled damping than it is for hard or soft damping. This shows that it is indeed possible to purposefully influence the course of braking slip by a wheel-load controller which acts on the vertical dynamics.

5.5 Conclusions

In this chapter the connection between the vertical and the longitudinal dynamics was established. In a theoretical approach the integral of wheel load was determined as the connecting quantity between vertical and longitudinal dynamics. From this infers that high-frequency oscillations of the wheel load signal in the range of the wheel eigenfrequency do not affect the course of braking slip as much as low-frequency oscillations in the range of the body eigenfrequency do. Thus, the RMS on wheel load alone, which values the parts

of the wheel load signal that hold high frequencies in the same proportion as those parts that hold low frequencies, is not a sufficient measurand to determine the riding safety.

Extending the results from chapter 4, where the vertical dynamics and the effect on the course of wheel load due to controlling the shock absorbers were investigated, the effect that a switching process of the active shock absorber has on the braking force and the braking slip was determined. It was shown that the switching is capable of influencing the longitudinal dynamics in both the time and the magnitude frame good enough to act as a slip controller.

The results of the braking procedures show that there is a strong correlation between the course of the integral of dynamic wheel load and the spring deflection. Thus, the body movements are supposedly responsible by the biggest part for the outcome of a braking procedure. This means that on an ideally even road the quality of the controller should remain unchanged compared to braking procedures on the 'Standard Road' or even on a very rough road. This needs to be investigated in future test drives.

Furthermore, it is possible to reduce the braking distance by means of control of active shock absorbers. The mean value of braking distances for the controlled cases is an average of 1.3 % smaller than for the best passive damping, which is statistically significant. The integral of the square of longitudinal velocity with respect to the traveled distance, VI , can be lowered by means of active shock absorbers compared to hard damping, too. For both measurands d_B and VI the controlled damping leads to better or equal results than the respective best passive damping. Thus, the controller acts in two dimensions: It is not only the braking distance which can be decreased, but it is also the damage probability in case of a crash which is lowered by the controller.

Since the main assumptions of all model-thoughts and of the controller hold true for every land-based vehicle with adjustable suspension parameters, the results are at least transferable to other vehicles which have a suspension comparable to the one used in the testing vehicle.

6 Discussion and Outlook

6.1 Results

In this thesis the influence of the vertical dynamics of a passenger car on the longitudinal dynamics in the special case of full-braking has been investigated. The main results of this thesis are the following:

- Active shock absorbers can be operated in artificial characteristic lines which they do not hold by construction, by switching from one request of wheel load to another, rather than from hard to soft.
- It could be shown that it is possible to purposefully influence the course of wheel load by means of switching the active shock absorber from one artificial line to another.
- The effect is the longer and stronger the greater the spreading of the active shock absorber.
- It was further shown that the relevant frequencies to influence the longitudinal dynamics by means of active shock absorbers on a road with a typical unevenness lie below 5 Hz. It is mainly the oscillations of the body which are relevant in the given context.
- The connection between the vertical and the longitudinal dynamics was established by introducing the wheel load integral as the connecting measurand.
- It was shown that the effect of switching the shock absorber is feasible to influence the longitudinal dynamics both in the time and in the magnitude frame.
- A testing procedure was defined which allows to determine deviations in braking distance of 0.25 %.
- In test drives on a typical road starting from an initial velocity of 70 km/h it was shown that it is in fact possible to shorten the braking distance significantly by means of the controller developed.
- It was furthermore shown that not only the braking distance can be shortened, but at the same time the quality of the braking procedure can be enhanced by reducing the kinetic energy earlier (in the distance domain) than the hard damping does. The suggested controller thus exceeds both passive damper settings in two different disciplines independently from each other at the same time. It connects the advantages of both passive damper settings.

The results were gained by using a testing vehicle from the compact class. They ought to be discussed in the following sections.

6.2 Transferability of Results

As could be seen in section 4.6.3, switching the active shock absorber and its effect on the vertical dynamics of a passenger car can be modeled very well with a quarter-car model. The results do not depend heavily on parameter variations, which shows that they can be transferred to other passenger cars with different masses, spring stiffness, and damping coefficients easily. The main assumptions which underlie the conclusions drawn from the results of the experiments concerning only the vertical dynamics are: A heavy body mass is carried by a suspension of a kind such that it is capable of oscillations. During those oscillations, one of the system parameters is switched, which leads to a change in wheel load.

As long as a suspension system can be described in the above manner, the results of switching the shock absorber with respect to the vertical dynamics should be similar to the ones obtained in this thesis. By parameter variations in a simulation model it could furthermore be shown that an increasing spreading of the active shock absorber also lets the effect on the wheel load increase.

With regard to the connection between the vertical and the longitudinal dynamics the principle thoughts still hold true. As long as there is a wheel which is clamped between the braking torque and the braking force, it holds true that by means of the vertical dynamics via the wheel load and the braking force, the braking slip can be influenced. But here the limitations on the transferability are more strict than when looking at only the vertical dynamics. The tire and the contact between tire and pavement play major roles in the transferability, so does the mass moment of inertia of the wheels.

The tire has an influence on the transferability in several ways: Firstly, because with it the vertical stiffness of the wheel can be changed. However, if the results which suggest that the part of the dynamic wheel load causing vertical wheel oscillations is of less importance than the part causing vertical body oscillations could be found again in other vehicles, the vertical stiffness of the tire should not influence the quality of the braking distance controller by much. Secondly, because the form of the μ -slip curve has an influence on how strongly the braking slip changes due to an intervention in the vertical dynamics. Furthermore, during braking on snow or on broken stones, the maximum of the μ -slip curve lies at $\lambda_B = 1$ and therefore the controller proposed would not enhance the braking performance, because the controller objective would need to be adjusted. This point influences the whole transferability: the parameter which need to be determined for another car newly. However, the structure of the model does not change.

In the testing vehicle the mass moment of inertia of a wheel at the front axle is much higher (by factor 3–6) than the one of a wheel at the rear axle. This is due to the fact that the mass moment of inertia of the engine has to be counted at the front axle as well, because the testing vehicle is front wheel driven. If the test drives concerning the connection between vertical and longitudinal dynamics were executed with a vehicle with rear wheel drive, the mass moment of inertia would be much smaller than it was during the test drives of this thesis. It is possible that for a rear wheel driven vehicle the effect of changing slip and braking force at the front axle would be even higher than in this thesis. This already holds true if the test drives had been executed with the clutch decoupled, because then the mass moment of inertia of the engine would have been decoupled from the front axle's wheels. For experimental reasons this was not possible. Thus, it might be that even for the given testing vehicle the effect of switching the shock absorber on the

braking slip could be greater than it was in the test drives as executed.

With regard to the braking distances obtained, there is the problem that within the frame of this thesis only one set of parameters has been investigated in detail. A causal connection between the vertical and the longitudinal dynamics has been established by means of the wheel load integral. Applying this connection to the testing vehicle led to a significant reduction in braking distance. Thus, it is proved that it is in fact possible to reduce the braking distance by means of active shock absorbers in general. But still lots of parameter variations need to be undertaken to try to falsify the model built in this thesis. Only if this model stands these tests with different parameters, can it be named proven.

6.3 Relevance of Results for Other Systems

In this thesis the ABS- and the shock-absorber controller work completely independently from each other. Neither does the ABS ‘know’ of the possibility to influence wheel load, nor does it ‘know’ of wheel load induced slip oscillations. But with the wheel load integral a measurand is introduced which can support the ABS. By means of this measurand the wheel-load induced shoots in braking slip can be detected and treated separately from braking-torque induced ones. This knowledge helps to improve the control algorithms of today’s ABS-controllers.

Another industry which could make use of the knowledge gained in this thesis is the aircraft industry. The braking behavior of airplanes could also be improved by using the results of this thesis. Krüger¹ suggested this already in his thesis in 2000. Looking at the braking distance of passenger airplanes, there is also a potential to enhance the braking performance by means of semi-active suspension. An airplane today lands with a speed of approximately 250 km/h and starts to brake with reverse thrust. From approximately 100–150 km/h, depending on the situation, down to rest, the kinetic energy is dissipated by the wheel brakes—similar to a passenger car. The ABS, which is also used in airplanes, could be supported by semi-active suspension in the same manner as proposed in this thesis.

The methods can also be used for motorcycles. There they should lead to even better results, because no coupling exists between right and left track, simply because there is no right and left track. Thus, switching the shock absorber cannot influence the other side negatively. Moreover, the spring travel for motorcycles is greater than the one for cars. Thus, the Effect Time should be longer and the relative Effect Magnitude greater than for cars.

Furthermore, not only the braking performance but also the acceleration of a vehicle could be improved. Especially for very powerfully motorized vehicles with front wheel drive, the controller presented in this thesis could help to prevent wheelspin. The connection established in this case would be between the TSC and the shock absorber controller rather than between the ABS and shock absorber controller. Influencing braking or transmission slip does not make a difference for the proposed controller.

Leaving the longitudinal dynamics, the results and the conclusions of this thesis provide the other driving dynamics controller, especially the ESP, with a tool to purposefully increase or decrease the wheel load. This could help to prevent ESP-interventions when

¹Krüger (2000): Integrated Design Process for the Development of Semi-Active Landing Gears for Transport Aircraft.

driving in curves or on handling tracks. Basically, every controller which needs to have an influence on the angular velocity of a single wheel can make use of the MiniMax- and slip-controller proposed.

6.4 Outlook

In this thesis the connection between the vertical dynamics of a passenger car and its longitudinal dynamics has been established. It is now known how the vertical oscillations influence the wheel's slip, may it be the braking or the transmission slip. Furthermore, it became clear that it is the low frequency oscillations of wheel load which are responsible for changes in braking slip. This knowledge could in the long run be implemented into series applications, where right now the shock absorbers are switched to a passive damping during ABS-braking.

A crucial aspect concerning one of the controller inputs is the determination of the damper velocity. In this thesis this was done by means of spring deflection sensors. In fact, it is only the sign of the damper velocity which is needed for the proposed controller. Thus, a simpler solution to determine this controller input could be to work with switches within the shock absorber which are combined with the valves' opening condition. Since there are always valves in a shock absorber which are only opened for one direction (rebound or compression), by applying a switch to them that provides with information about the opening condition it is possible to gain a digital signal about the sign of the damper velocity.

Another solution could be to use shock absorbers which have different active valves for rebound and compression. In this case the MiniMax-controller would shrink to only two fields and only one input: the request of wheel load $F_{z,\text{req}}$. This solution would therefore provide with a tool whose only input is the request how the course of wheel load should change in the future. This would be a tool which could be mantled into a suspension system in a very modular way.

Since the results in this thesis were gained from only one set of parameters, in the first step it is necessary to confront the controller with changing parameters. The next steps here should be:

- Test drives on other types of roads, like
 - An ideally flat road to determine if the effect of shortening the braking distance still occurs there. If this was the case, it would suggest that the oscillations of wheel load due to movements of the vehicle's body have a higher influence on the braking distance than the ones due to wheel oscillations do.
 - A very rough road, again to determine how the difference in ratio between wheel and body part of wheel load oscillations affects the controller's quality. The assumption here is that the controller works not significantly worse than on a typical pavement.
 - Low- μ conditions. Here the ABS-controller has, compared to the wheel-load controller, a higher influence on the braking slip, for the wheel load has to be translated into braking torque first. This works worse for low- μ than for high- μ conditions. Yet the ABS does not face this problem. The braking torque applicable by it is independent of the tire/pavement friction conditions.

- An additional definition of the Effect Magnitude with respect to the integral of wheel load should be introduced to measure the effect until the wheel load integral passes zero.
- Not only the switching process from hard to soft and vice versa, but also the switching process from one artificial characteristic line to another should be investigated in more detail.
- Test drives with the clutch decoupled right from the beginning of the braking procedure in order to reduce the mass moment of inertia of the front axle's wheels.
- Test drives for varying initial velocities. Assuming that soft damping takes advantage of the first strong pitching right after the beginning of the braking procedure, this influence should become relatively smaller for higher initial velocities. Thus, the assumption is that soft damping should be worse compared to hard damping at higher velocities.
- Measuring of the μ -slip curve on the test track 'Standard Road' in order to determine the benchmark for the shock-absorber controller with respect to braking distance. Which amount of improvement is possible at all, measured in terms of difference between μ_{\max} and μ_{mean} ?

One aspect which was not covered in this thesis is the microscopic modeling of the force transmission in the tire contact zone. The wheel load integral shows the direction of how the connection between vertical and longitudinal tire forces looks like, but the model uncertainties are greater than the reduction in braking distance. Thus, it was not possible to reproduce the results from real test drives with a simulation model of the longitudinal dynamics. If such a model was at hand and was validated, it would save lots of experimental test effort. With the experimental data gained in this thesis it is now possible to optimize numerical models of the braking procedure.

By introducing the wheel load integral, the connection between vertical and longitudinal dynamics has been established. It is also possible to establish the connection between vertical and lateral dynamics. The side slip could be influenceable by the active shock absorbers as well. This ought to be investigated in more detail, because in lateral direction the wheel is not spinning and therefore the transfer mechanism is supposedly different and needs to be discovered.

Once the connection between the vertical and the total horizontal dynamics is drawn and fully understood, the next step can be to implement the knowledge gained into a global chassis controller (GCC). The vertical dynamics would then no longer be decoupled from a conscious connection to the horizontal dynamics. This is the next step on the way to a GCC.

7 Summary

When it comes to the design of a suspension system, a classic conflict needs to be solved: One fixed set of suspension parameters may lead to the best result with respect to handling performance for one given driving maneuver. Changing the type of maneuver, however, changes the demand on the suspension and therefore leads to a different solution for the optimal set of suspension parameters. Such a change may take place even during one single driving maneuver. To treat this conflict in a better manner, semi-active suspension systems can be used.

This thesis presents a control algorithm for a semi-active suspension system with the objective to reduce the braking distance of passenger cars. Active shock absorbers are controlled and used to influence the vertical dynamics during ABS-controlled full braking. This thesis' objective is to determine if it is possible to affect the longitudinal dynamics in an aimed way under close to reality conditions by means of controlling the vertical dynamics. Results of previous research work by Reichel¹ already suggested that this could be possible. He showed for a braking maneuver with constant velocity (front axle braking, rear axle powering) and for a specific obstacle that the longitudinal dynamics can in fact be influenced positively.

For a standard tire in standard conditions (dry or wet asphalt) the maximum braking force is applied to the ground at a braking slip level which lies between zero and one. For slip equal to zero no braking force is applied at all, for slip equal to one the braking force generally is smaller than at its maximum. Furthermore, a today's ABS-controller is not able to keep the braking slip at the optimal level during the whole braking process, because the braking slip is not only controlled by the braking torque but also by the actual wheel load—a quantity which cannot be influenced by the ABS-controller. The ABS-controller can only react on whatever happens in the wheel's vertical direction. Due to those facts there is still a gap between optimal braking distance and realized braking distance. This is why it is possible to increase the average braking force and to decrease the braking distance at all.

The approach presented in this thesis makes use of a switching control logic, called MiniMax-controller. It is named after the fact that it changes the active shock absorbers' setting only from soft to hard damping and vice versa. The damper settings between those extrema are no selectable states for the controller. In test rig trials on a 4-post test rig it is shown that by switching the shock absorber it is possible to purposefully increase or decrease the wheel load in a time and magnitude frame which is utilizable for braking procedures. The same holds true for the braking force and the braking slip. Increasing and decreasing in this context always refers to the course of the respective quantity which would have been established if the shock absorber had not been switched. Hence, the active shock absorber can be treated as a quasi-active element. The energy of those elements mostly

¹Reichel (2003): Untersuchungen zum Einfluss stufenlos verstellbarer Schwingungsdämpfer auf das instationäre Bremsen von Personenzugmaschinen p. 102.

comes from the potential energy of the body.

The effect which is caused by switching the active shock absorber takes place after a certain amount of time. The wheel load does not change its value immediately, but it rather takes approximately 25 ms for the wheel load to increase or decrease. After this period of time the wheel load changes its former value continuously. It is shown that the wheel load's integral with respect to time is connected to the braking slip. A short drop of wheel load does not affect the braking slip, because it takes time for the wheel to change its angular velocity due to its mass moment of inertia. If the drop of wheel load holds on for a longer time, which will also lead to a drop of the integral of wheel load, the braking slip will increase. At the same time a rising integral of wheel load lowers the braking slip. This is shown in braked test drives. Hence, a connection between the vertical and the longitudinal dynamics of a vehicle is established.

With this knowledge gained it is possible to control the active shock absorbers in a way that the wheel load is increased—and with it the integral of wheel load—at the right time. The right time is measured in terms of a too negative integral of wheel load. By switching the shock absorber, this integral and with it the wheel velocity is increased. Thus, the braking slip is lowered and kept at a level where the tire can transmit the maximum braking force.

Applying the switching logic to a real car and defining a setting for test drives which allows to determine the braking distance in a high accuracy, it could be shown that, generally speaking, it is possible to reduce the braking distance by affecting on the vertical dynamics of a passenger car. On a road with an unevenness like a typical German Autobahn and for an initial velocity of 70 km/h it is possible to reduce the braking distance by an average of 1.3% compared to the best passive damping. The reduction is statistically significant. Furthermore, the integral of the square of the longitudinal velocity with respect to the traveled distance, which is a measure for the probability of a high damage in case of a crash, could be reduced as well, and at the same time as the braking distance was reduced.

Uncertainties in the determination of the proper switching time in a real car cause high deviations of those results. Not for every single braking process is it possible to obtain a shorter braking distance by controlled shock absorbers than with a constant setting. But the mean value for controlled damping is smaller and the standard deviation could also be decreased. The same control algorithm as it is used in this case could be applied to other situations, as for example braking in curves or enhancing the performance of the ESP-controller.

All the results of this thesis were gained by using the longitudinal and the vertical controller—namely the ABS- and the active-shock-absorber controller—at the same time but independently from each other. Since the positive effect of the switching of the active shock absorbers is always followed by a negative effect, the full effectiveness of a controller of the vertical dynamics in terms of shorter braking distance can only be gained if the controller interacts with the ABS-controller. It is therefore essential to combine both strategies, to let the ABS know about what the active shock absorber will do in the next time step and vice versa. The results of this thesis not only let expect an improvement of braking performance but also an improvement of any other kind of controller of horizontal tire forces by a combination of vertical and horizontal control strategies—which is yet another step on the way to a global chassis control that includes every chassis control functionality.

Bibliography

- Alberti, Volker:** Möglichkeiten der adaptiven Fahrwerksdämpfung in Kraftfahrzeugen. ATZ Automobiltechnische Zeitschrift, 93 1991, Nr. 5, pp. 282–293, ISSN 0001–2785
- Alleyne, Andrew/Neuhaus, Peter D./Hedrick, Karl J.:** Application of Nonlinear Control Theory to Electronically Controlled Suspensions. In Proceedings of International Symposium on Advanced Vehicle Control, Yokohama, Japan. Society of Automotive Engineers of Japan, 14–17 September 1992, Vehicle System Dynamics 0042-3114/93/2205-0309 [⟨URL: http://mr-roboto.me.uiuc.edu/alleyne/aa_publication.html⟩](http://mr-roboto.me.uiuc.edu/alleyne/aa_publication.html), pp. 309–320
- Araki, Yoshiaki/Oya, Masahiro/Harada, Hiroshi:** Preview Control of Active Suspension Using Disturbance of Front Wheel. In **Jurgen, Ronald K. (Ed.):** Electronic Steering and Suspension Systems. Society of Automotive Engineers of Japan, October 1994, SAE Technical Paper Series 948208, ISBN 0–7680–0481–0, pp. 489–494
- Becker, Axel/Huinink, Heinrich/Rieth, Peter:** Maßnahmen zur Verkürzung des Anhaltewegs in Notbremssituationen – das 30m Auto. In Proceedings of VDA Technischer Kongress 2001, Bad Homburg, Germany. VDA, 26+27 March 2001, pp. 117–125
- Bleymüller, Josef/Gehlert, Günther/Gülicher, Herbert:** Statistik für Wirtschaftswissenschaftler. 10. edition. Verlag Franz Vahlen GmbH, München, 1996, ISBN 3–8006–2081–2
- Bokor, József et al.:** Design of Active Suspension Systems in the Presence of Physical Parameter Uncertainties. In **Jurgen, Ronald K. (Ed.):** Electronic Steering and Suspension Systems. FISITA, 1994, SAE Technical Paper Series 945062, ISBN 0–7680–0481–0, pp. 507–511
- Bose Corporation:** Bose Suspension System. [⟨URL: http://www.bose.com/pdf/technologies/bose_suspension_system.pdf⟩](http://www.bose.com/pdf/technologies/bose_suspension_system.pdf)
- Breuer, Bert:** Kraftfahrzeuge II. April 2001, Lecture notes, Chair of Automotive Engineering at Technische Universität Darmstadt
- Breuer, Bert (Ed.):** XXIII International μ Symposium—Brake Conference. VDI Verlag, Düsseldorf, 2003, Fortschritt-Berichte VDI Reihe 12 556, ISBN 3–18–355612–X
- Breuer, Bert (Ed.):** XXIV International μ Symposium—Brake Conference. VDI Verlag, Düsseldorf, 2004, Fortschritt-Berichte VDI Reihe 12 575, ISBN 3–18–357512–4

- Breuer, Bert (Ed.):** XXV International μ Symposium—Brake Conference. VDI Verlag, Düsseldorf, 2005, Fortschritt-Berichte VDI Reihe 12 597, ISBN 3-18-359712-8
- Breuer, Bert/Bill, Karlheinz (Eds.):** Bremsenhandbuch. 3. edition. Vieweg Verlag, 2006, ISBN 3-8348-0064-3
- Bussmann, Werner/Schulz, Walter/Tattermusch, Peter:** Das Fahrwerk der neuen S-Klasse Teil 1. ATZ Automobiltechnische Zeitschrift, 93 1991, Nr. 9, pp. 524-534
- Causemann, Peter:** Kraftfahrzeugstoßdämpfer. 2. edition. verlag moderne industrie, Landsberg/Lech, 2001, Die Bibliothek der Technik 185, ISBN 3-478-93210-6
- Causemann, Peter:** Moderne Schwingungsdämpfer. ATZ Automobiltechnische Zeitschrift, 105 2003, Nr. 11, pp. 1072-1079, ISSN 0001-2785
- Chadwick, Peter:** Continuum Mechanics: Concise Theory and Problems. 2. edition. Dover Publications, Inc., 1999, ISBN 0-486-40180-4
- Choi, Seung-Bok/Park, Dong-Won/Suh, Moon-Suk:** Fuzzy Sky-Ground Hook Control of a Tracked Vehicle Featuring Semi-Active Electrorheological Suspension Units. Journal of Dynamic Systems—Measurement and Control, 124 March 2002, Nr. 1, pp. 150-157 (URL: http://scitation.aip.org/journals/doc/JDSMAA-ft/vol_124/iss_1/150_1.html)
- Claar, Paul W./Vogel, Jerald M.:** A Review of Active Suspension Control for On and Off-Highway Vehicles. In Proceedings of Truck and Bus Meeting and Exposition, Charlotte, North Carolina, USA. Society of Automotive Engineers, Inc., 6-9 November 1989, SAE Technical Paper Series 892482, ISSN 0148-7191, pp. 1-12
- Crolla, David A.:** Active Suspension Control—Review of Recent Applications. Smart Vehicle, 1995, Nr. 892482, pp. 183-201
- Danesin, Davide et al.:** Vehicle Dynamics with Real Time Damper Systems. In Proceedings of 16th European ADAMS User Conference 2001, Berchtesgaden, Germany. ADAMS, 14+15 November 2001 (URL: http://www.mssoftware.com/support/library/conf/adams/euro/2001/proceedings/papers_pdf/Paper_42.pdf)
- Desai, Hiren Harshadrai/Collins, Ronald J.:** Laser Ride Height Measurement / Calibration System. In **Jurgen, Ronald K. (Ed.):** Electronic Steering and Suspension Systems. Society of Automotive Engineers, Inc., 1999, SAE Technical Paper Series 950025, ISBN 0-7680-0481-0, pp. 429-435
- Dixon, John C.:** The Shock Absorber Handbook. Society of Automotive Engineers, Inc., 1999, ISBN 0-7680-0050-5
- El-Demerdash, Samir M.:** Performance of Limited Bandwidth Active Suspension Based on a Half Car Model. In **Jurgen, Ronald K. (Ed.):** Electronic Steering and Suspension Systems. Society of Automotive Engineers, Inc., 1999, SAE Technical Paper Series 981118, ISBN 0-7680-0481-0, pp. 251-260

- El-Demerdash, Samir M./Plummer, Andrew R./Crolla, David A.:** Digital Control for Vehicle Active Suspension Systems. In **Jurgen, Ronald K. (Ed.):** Electronic Steering and Suspension Systems. Society of Automotive Engineers, Inc., 1999, SAE Technical Paper Series 964196, ISBN 0-7680-0481-0, pp. 401-408
- ElBeheiry, ElSayed Mohamed/Karnopp, Dean C.:** Optimization of Active and Passive Suspensions Based on a Full Car Model. In **Jurgen, Ronald K. (Ed.):** Electronic Steering and Suspension Systems. Society of Automotive Engineers, Inc., 1999, SAE Technical Paper Series 951063, ISBN 0-7680-0481-0, pp. 341-352
- ElBeheiry, Elsayed Mohamed et al.:** Suboptimal Control Design of Active and Passive Suspensions Based on a Full Car Model. *Vehicle System Dynamics*, 2002, Volume 26, 2002, pp. 197-222, ISSN 0042-3114
- Emura, Junichi et al.:** Development of the Semi-Active Suspension System Based on the Sky-Hook Damper Theory. In **Jurgen, Ronald K. (Ed.):** Electronic Steering and Suspension Systems. Society of Automotive Engineers, Inc., 1999, SAE Technical Paper Series 940863, ISBN 0-7680-0481-0, pp. 284-294
- Esmailzadeh, Ebrahim/Taghirad, Hamid D.:** Active Vehicle Suspensions with Optimal State-Feedback Control. *Journal of Dynamic Systems, Measurement and Control*, 123 March 2001, Nr. 1 (URL: <http://scitation.aip.org/ASMEJournals/DynamicSys/>)
- Evers, Wolfgang et al.:** Radkraft-Dynamometer (RWD/FWD) als Entwicklungswerkzeug für Felge und Radaufhängung. In *Proceedings of rad.tech 2002*, München, Germany. TÜV SÜD AG 13-14 June 2002 (URL: http://www.tuev-sued.de/uploads/images/1134986834555003080785/evers_reichel.pdf)
- Finckenstein, Karl Graf Finck von:** *Grundkurs Mathematik für Ingenieure*. 3. edition. B. G. Teubner Stuttgart, 1991, ISBN 3-519-22961-7
- Gillespie, Thomas D.:** *Fundamentals of Vehicle Dynamics*. Society of Automotive Engineers, Inc., 1992, ISBN 1-56091-199-9
- Gilsdorf, Heinz-Joachim/Heyn, Steffen/Gundermann, Frank:** Amplitudenselektive Dämpfung ASD. In *Proceedings of 13. Aachener Kolloquium Fahrzeug- und Motorradtechnik 2004*, Aachen, Germany. Ika, 4-6 October 2004 (URL: <http://www.ac-kolloquium.rwth-aachen.de/pdf/ATZ13.pdf>), pp. 649-658
- Gärtner, Andreas/Saeger, Martin:** Simulationsumgebung zur Untersuchung aktiver Wankstabilität in Verbindung mit einer Fahrdynamikregelung. In *Proceedings of Tagung - Simulation in der Fahrdynamik*, Essen, Germany. Automotive Cluster Vienne Region, 11+12 November 2003 (URL: <http://www.ika.rwth-aachen.de/forschung/veroeffentlichung/2003/11.-12.11/3sg0074.pdf>)
- Hackbusch, Wolfgang/Schwarz, Hans Rudolf/Zeidler, Eberhard; Zeidler, Eberhard (Ed.):** *Teubner-Taschenbuch der Mathematik*. B. G. Teubner Verlagsgesellschaft Leipzig, 1996, ISBN 3-8154-2001-6

- Hagedorn, Peter:** Festigkeitslehre. Band 2, Technische Mechanik. 2. edition. Verlag Harri Deutsch, Frankfurt am Main, 1995, ISBN 3-8171-1434-6
- Hagedorn, Peter:** Dynamik. Band 3, Technische Mechanik. 2. edition. Verlag Harri Deutsch, Frankfurt am Main, 1996, ISBN 3-8171-1519-9
- Hagedorn, Peter:** Statik. Band 1, Technische Mechanik. 3. edition. Verlag Harri Deutsch, Frankfurt am Main, 2001, ISBN 3-8171-1647-0
- Hennecke, Dieter/Jordan, Bernd/Ochner, Udo:** Elektronische Dämpfer Control – eine vollautomatisch adaptive Dämpfungkraftverstellung für den BMW 635 CSi. ATZ Automobiltechnische Zeitschrift, 89 1987, Nr. 9, pp.471-479
- Higashiyama, Kazuhiro et al.:** Development of the Active Damper Suspension. In **Jurgen, Ronald K. (Ed.):** Electronic Steering and Suspension Systems. Society of Automotive Engineers, Inc., 1999, SAE Technical Paper Series 948213, ISBN 0-7680-0481-0, pp.461-466
- Holtzschulze, Jens et al.:** Der Reifen – Informationsquelle zur Fahrerassistenz. In Proceedings of 13. Aachener Kolloquium Fahrzeug- und Motorradtechnik 2004, Aachen, Germany. Ika, 4-6 October 2004 (URL: <http://www.ac-kolloquium.rwth-aachen.de/pdf/ATZ13.pdf>), pp. 559-579
- Hoogterp, Francis B./Beno, Joseph H./Weeks, Damon A.:** An Energy Efficient Electromagnetic Active Suspension System. In **Jurgen, Ronald K. (Ed.):** Electronic Steering and Suspension Systems. Society of Automotive Engineers, Inc., 1997, SAE Technical Paper Series 970385, ISBN 0-7680-0481-0, pp.367-381
- Irmscher, Stephan/Hees, Eberhard/Kutsche, Thomas:** A Controlled Suspension System with Continuously Adjustable Damping Force. In **Jurgen, Ronald K. (Ed.):** Electronic Steering and Suspension Systems. Society of Automotive Engineers, Inc., 1999, SAE Technical Paper Series 9438212, ISBN 0-7680-0481-0, pp.455-460
- Isermann, Rolf:** Mechatronische Systeme. Springer-Verlag Berlin, 1999, 1. korrigierter Nachdruck, Studienausgabe, ISBN 3-540-43129-2
- Isermann, Rolf:** Regelungstechnik I. Shaker Verlag, 2002, Berichte aus der Steuerungs- und Regelungstechnik, Lecture notes, Institute of Automatic Control at Technische Universität Darmstadt, ISBN 3-8322-0605-1
- Jendritza, Daniel J./Koch, Joachim:** Piezoelektrisches Dämpfersystem zur semi-aktiven Schwingungsreduktion. ATZ Automobiltechnische Zeitschrift, 98 1996, Nr. 12, pp.656-661, ISSN 0001-2785
- Jungmann, Thomas:** So viel Continental steckt im Touareg – all4engineers. (URL: <http://www.all4engineers.com>)
- Jungmann, Thomas:** Audi magnetic ride im neuen TT – all4engineers. (URL: <http://www.all4engineers.com>)

- Keuper, Gerhard et al.:** Influence of Active Suspensions on the Handling Behaviour of Vehicles - Experimental and Theoretical Results. In **Jurgen, Ronald K. (Ed.):** Electronic Steering and Suspension Systems. Society of Automotive Engineers, Inc., 1999, SAE Technical Paper Series 945061, ISBN 0-7680-0481-0, pp. 513-522
- Klotter, Karl:** Teil B: Nichtlineare Schwingungen. Band I: Einfache Schwinger, 3. edition. Springer-Verlag New York, 1980, ISBN 0-387-09327-3
- Knaap, A. C. M. van der/Venhovens, P. J. Th./Pacejka, Hans B.:** Evaluation and Practical Implementation of a Low Power Attitude and Vibration Control System. In **Jurgen, Ronald K. (Ed.):** Electronic Steering and Suspension Systems. Society of Automotive Engineers, Inc., 1999, SAE Technical Paper Series 948211, ISBN 0-7680-0481-0, pp. 467-473
- Kojima, Hiroyoshi et al.:** Development of New Toyota Electronic Modulated Suspension—Two Concepts for Semi-Active Suspension Control. In Proceedings of Passenger Car Meeting and Exposition, Nashville, Tennessee, USA. Society of Automotive Engineers, Inc., 16-19 September 1991, SAE Technical Paper Series 911900, ISSN 0148-7191
- Konik, D. et al.:** Dynamic Drive - das neue aktive Wankstabilisierungssystem der BMW Group. In Proceedings of 9. Aachener Kolloquium, Aachen, Germany. 4-6 October 2000, pp. 471-490
- Kreyszig, Erwin:** Advanced Engineering Mathematics. 8. edition. John Wiley & Sons, Inc., 1999, ISBN 0-471-15496-2
- Krüger, Wolf:** Integrated Design Process for the Development of Semi-Active Landing Gears for Transport Aircraft. Dissertation, Universität Stuttgart, 2000, <http://elib.uni-stuttgart.de/opus/volltexte/2002/984/pdf/krueger.pdf>, Dissertation at the Institut für Flugmechanik und Flugregelung at the Universität Stuttgart
- Kutsche, Thomas/Raulf, Matthias:** Optimierte Fahrwerksdämpfung für Pkw und Nkw. In Proceedings of 7. Aachener Kolloquium Fahrzeug- und Motorradtechnik 1998, Aachen, Germany. Ika, 5-7 October 1998
- Kutsche, Thomas/Raulf, Matthias:** Optimierte Fahrwerksdämpfung für Pkw und Nkw. ATZ Automobiltechnische Zeitschrift, 103 2001, Nr. 2, pp. 130-133, ISSN 0001-2785
- Lauwerys, Christophe/Swevers, Jan/Sas, Paul:** Linear Control of Car Suspension Using Nonlinear Actuator Control. In Proceedings of ISMA 2002, International Conference on Noise & Vibration Engineering, Leuven, Belgium. ISMA, 16-18 September 2002 http://www.isma-isaac.be/publications/PMA_MOD_publications/ISMA2002/55_62.pdf, pp. 55-62

- Lauwerys, Christophe/Swevers, Jan/Sas, Paul:** Model Free Control Design for a Semi-Active Suspension of a Passenger Car. In Proceedings of ISMA 2004, International Conference on Noise & Vibration Engineering, Leuven, Belgium. ISMA, 20–22 September 2004 (URL: http://www.isma-isaac.be/publications/PMA_MOD_publications/ISMA2004/75_86.pdf), pp. 75–86
- Lieh, Junghsen:** Development of Active Suspensions Using Velocity Feedback. In **Jurgen, Ronald K. (Ed.):** Electronic Steering and Suspension Systems. Society of Automotive Engineers, Inc., 1996, SAE Technical Paper Series 960935, ISBN 0–7680–0481–0, pp. 553–557
- Meyer, W. E./Kummer, H. W.:** Mechanism of force transmission between tire and road. Society of Automotive Engineers, 1962 (620407). – Technischer Bericht
- Mühlmeier, Martin:** Bewertung von Radlastschwankungen im Hinblick auf das Fahrverhalten von Pkw. VDI Verlag, Düsseldorf, 1993, Fortschritt-Berichte VDI Reihe 12 187, Dissertation at the Institute of Automotive Engineering at Technische Universität Braunschweig, ISBN 3–18–148712–0
- Mitschke, Manfred:** Dynamik der Kraftfahrzeuge, Band B – Schwingungen. 2. edition. Springer-Verlag Berlin Heidelberg New York Tokio, 1984, ISBN 3–540–13260–0
- Mitschke, Manfred/Thesenvitz, Manfred:** Bremskraftverluste auf unebenen Fahrbahnen. VDI Verlag, Düsseldorf, 1985, Fortschritt-Berichte VDI Reihe 12 58, ISBN 3–18–145812–0
- Mitschke, Manfred/Wallentowitz, Henning:** Dynamik der Kraftfahrzeuge. 4. edition. Springer-Verlag Berlin Heidelberg New York, 2004, ISBN 3–540–42011–8
- Mittelbach, Frank/Goossens, Michel et al.:** The LATEX Companion. 2. edition. Addison-Wesley, 2004, ISBN 0–201–36299–6
- Müller, Peter et al.:** Elektronische Dämpfer Control – eine vollautomatisch adaptive Dämpfungkraftverstellung für den BMW 635 CSi. ATZ Automobiltechnische Zeitschrift, 107 2005, Nr. 10, pp. 848–857
- Mo, Changki/Sunwoo, Myoungho/Patten, W. N.:** A Bistate Control of a Semiactive Automotive Suspension. In Proceedings of Steering and Suspension Technology Symposium 1999, Detroit, Michigan, USA. Society of Automotive Engineers, Inc., 1–4 March 1999, SAE Technical Paper Series 1999-01-0725, ISSN 0148–7191, pp. 1–9
- Moline, David et al.:** Simulation and Evaluation of Semi-Active Suspensions. In **Jurgen, Ronald K. (Ed.):** Electronic Steering and Suspension Systems. Society of Automotive Engineers, Inc., 1999, SAE Technical Paper Series 940864, ISBN 0–7680–0481–0, pp. 295–305
- Moran, Antonio/Hasegawa, Tomohiro/Nagai, Masao:** Continuously Controlled Semi-Active Suspension Using Neutral Networks. In **Jurgen, Ronald K. (Ed.):** Electronic Steering and Suspension Systems. Society of Automotive Engineers, Inc., 1999, SAE Technical Paper Series 948209, ISBN 0–7680–0481–0, pp. 483–488

- Motta, Daniel S./Zampieri, Douglas E./Pereira, Allan K. A.:** Optimization of a Vehicle Suspension Using a Semi-Active Damper. In Proceedings of IX Congresso e Exposição Internacionais da Tecnologia da Mobilidade, São Paulo, Brasil. Society of Automotive Engineers, Inc., 3–5 October 2000, SAE Technical Paper Series 2000-01-3304, ISSN 0148–7191, pp. 1–10
- N.N.:** Schwingungsdämpfer mit elektrorheologischen Fluiden. ATZ Automobiltechnische Zeitschrift, 97 1995a, Nr. 4, p. 253, ISSN 0001–2785
- N.N.:** Variable Stoßdämpfer ohne Elektronik. ATZ Automobiltechnische Zeitschrift, 97 1995b, Nr. 6, p. 329, ISSN 0001–2785
- N.N.:** Website – all4engineers. \langle URL: <http://www.all4engineers.com> \rangle
- N.N.:** Website – map 24. \langle URL: <http://www.de.map24.com> \rangle
- N.N.:** Website – Opel Ireland. \langle URL: <http://www.opel.ie> \rangle
- Nordmann, Rainer/Birkhofer, Herbert:** Maschinenelemente und Mechatronik I. Shaker Verlag, 2001, Lecture notes, Technische Universität Darmstadt, ISBN 3–8265–9343–X
- Nouillant, Cédric/Moreau, Xavier/Oustaloup, Alain:** Hybrid Control of a Semi-Active Suspension System. In Proceedings of Automotive and Transportation Technology Congress and Exhibition, Barcelona, Spain. Society of Automotive Engineers, Inc., 1–3 October 2001, SAE Technical Paper Series 2001-01-3269, ISSN 0148–7191, pp. 1–8
- Ono, Eiichi/Masashi, Yamashita/Yamauchi, Yoji:** Distributed Hierarchy Control of Active Suspension System. In **Jurgen, Ronald K. (Ed.):** Electronic Steering and Suspension Systems. Society of Automotive Engineers, Inc., 1999, SAE Technical Paper Series 948220, ISBN 0–7680–0481–0, pp. 443–448
- Pacejka, Hans B.:** Tire and Vehicle Dynamics. Butterworth-Heinemann, Elsevier Science, 2002, ISBN 0–7680–1126–4
- Palmeri, Paolo S./Moschetti, Alberto/Gortan, Luigi:** H-Infinity Control of Lancia Thema Full Active Suspension System. In **Jurgen, Ronald K. (Ed.):** Electronic Steering and Suspension Systems. Society of Automotive Engineers, Inc., 1999, SAE Technical Paper Series 950583, ISBN 0–7680–0481–0, pp. 315–322
- Panagiotidis, Michael:** Einsatz von Radschwingungstilgern im Fahrwerk zur Steigerung des Schwingungskomforts und Reduktion der Radlastschwankungen. In Proceedings of 13. Aachener Kolloquium Fahrzeug- und Motorradtechnik 2004, Aachen, Germany. Ika, 4–6 October 2004 \langle URL: <http://www.ac-kolloquium.rwth-aachen.de/pdf/ATZ13.pdf> \rangle , pp. 627–647
- Petek, Nicholas K. et al.:** Demonstration of an Automotive Semi-Active Suspension Using Electrorheological Fluid. In **Jurgen, Ronald K. (Ed.):** Electronic Steering and Suspension Systems. Society of Automotive Engineers, Inc., 1999, SAE Technical Paper Series 950586, ISBN 0–7680–0481–0, pp. 323–328

- Pinkos, Andrew/Shtarkman, Emil/Fitzgerald, Thomas:** An Actively Damped Passenger Car Suspension System with Low Voltage Electro-Rheological Magnetic Fluid. In **Jurgen, Ronald K. (Ed.):** Electronic Steering and Suspension Systems. Society of Automotive Engineers, Inc., 1994, SAE Technical Paper Series 948210, ISBN 0-7680-0481-0, pp. 475-481
- Redlich, P./Wallentowitz, Henning:** Vehicle Dynamics with Adaptive or Semi-Active Suspension Systems Demands on Hardware and Software. In Proceedings of Advanced Vehicle Control (AVEC 94), Tsukuba, Japan. Society of Automotive Engineers of Japan, 24-28 November 1994
- Redlich, P./Wallentowitz, Henning:** Vehicle Dynamics with Adaptive or Semi-Active Suspension Systems Demands on Hardware and Software. In **Jurgen, Ronald K. (Ed.):** Electronic Steering and Suspension Systems. Society of Automotive Engineers, Inc., 1999, SAE Technical Paper Series 948221, ISBN 0-7680-0481-0, pp. 437-442
- Reichel, Jochen:** Untersuchungen zum Einfluss stufenlos verstellbarer Schwingungsdämpfer auf das instationäre Bremsen von Personewagen. VDI Verlag, Düsseldorf, 2003, Fortschritt-Berichte VDI Reihe 12 553, Dissertation at the Chair of Automotive Engineering at Technische Universität Darmstadt, ISBN 3-18-355312-0
- Reitze, Clemens:** Closed Loop Entwicklungsplattform für mechatronische Fahrdynamikregelsysteme. Universitätsverlag Karlsruhe, July 2004, Schriftenreihe des Instituts für Technische Mechanik \langle URL: <http://www.ubka.uni-karlsruhe.de/cgi-bin/pview?document=/2004/maschinenbau/17&search=/2004/maschinenbau/17> \rangle , Dissertation at the Institut für Technische Mechanik at Universität Karlsruhe, ISBN 3-937300-19-8
- Robert Bosch GmbH (Ed.):** Kraftfahrtechnisches Taschenbuch. 23. edition. Vieweg Verlag, 1999, ISBN 3-528-03876-4
- Robert Bosch GmbH (Ed.):** Automotive Handbook. 5. edition. SAE Society of Automotive Engineers, 2000, ISBN 0-7680-0669-4
- Roßdorf-Zimmermann, Bastian et al.:** Verbesserung der Fahrdynamik durch verstellbare Dämpfer. In Proceedings of 13. Aachener Kolloquium Fahrzeug- und Motorradtechnik 2004, Aachen, Germany. Ika, 4-6 October 2004 \langle URL: <http://www.ac-kolloquium.rwth-aachen.de/pdf/ATZ13.pdf> \rangle , pp. 667-681
- Schwarz, Ralf et al.:** ESP II – Fahrdynamik der nächsten Generation – Teil 1 – Komponenten und Funktionen. ATZ Automobiltechnische Zeitschrift, 105 2003a, Nr. 11, pp. 1062-1069, ISSN 0001-2785
- Schwarz, Ralf et al.:** ESP II – Fahrdynamik der nächsten Generation – Teil 2 – Funktionsintegration und Elektronik. ATZ Automobiltechnische Zeitschrift, 105 2003b, Nr. 12, pp. 1178-1182, ISSN 0001-2785
- Schwarz, Ralf/Rieth, Peter:** Global Chassis Control – Systemvernetzung im Fahrwerk. at – Automatisierungstechnik, 2003, Issue 7, 2003, pp. 300-312 \langle URL:

<http://www.atypon-link.com/OLD/doi/abs/10.1524/auto.51.7.300.22740>),
ISSN 0178-2312

- Schwarze, Jochen/Fusková, Lidmila/Kunitz, Harald:** Statistik – Grundkurs, Kurseinheit 12: Spezielle Testverfahren. 2004, Lecture notes, Fachbereich Wirtschaftswissenschaft at FernUniversität in Hagen
- Shutto, Shigeru/Toscano, James R.:** Magnetorheological Fluid Technology for Vehicle Applications. In Proceedings of FISITA 2006, World Automotive Congress, Yokohama, Japan. 22–27 October 2006
- Smakman, Henk:** Functional Integration of Slip Control with Active Suspension for Improved Lateral Vehicle Dynamics. Herbert Utz Verlag GmbH, 2000, Dissertation at Technische Universiteit Delft, ISBN 3-89675-704-0
- Smith, Malcolm C./Wang, Fu-Cheng:** Controller Parameterization for Disturbance Response Decoupling—Application to Vehicle Active Suspension Control. IEEE Transactions on Control Systems Technology, Volume 10, Issue 3, May 2002, pp.393–407 (URL: http://ieeexplore.ieee.org/xpl/freeabs_all.jsp?isnumber=21533&arnumber=998029&count=15&index=7), ISSN 1063-6536
- Steinauer, Bernhard/Kempkens, Eckhard/Ueckermann, Andreas:** Zustandserfassung und -bewertung der Bundesfernstraßen – Verbessertes Verfahren zur Beurteilung der Längsebenheit. Straße und Autobahn, 54 January 2003, Nr. 1, pp.29–37, ISSN 0039-2162
- Strogatz, Steven H.:** Nonlinear Dynamics and Chaos. Perseus Publishing, Cambridge, Massachusetts, 2000, ISBN 0-7382-0453-6
- Tiemann, Rüdiger:** Untersuchungen zum Bremsverhalten von Pkw mit ABS auf unebener Fahrbahn unter besonderer Berücksichtigung des Einflusses des Schwingungsdämpfers. VDI Verlag, Düsseldorf, 1994, Fortschritt-Berichte VDI Reihe 12 204, Dissertation at the Chair of Automotive Engineering at Technische Universität Darmstadt, ISBN 3-18-320412-6
- Tomizuka, Masayoshi:** Advanced Control Systems I. 1999, Lecture notes, Department of Mechanical Engineering at University of California at Berkeley
- Tongue, Benson H.:** Principles of Vibration. 2. edition. Oxford University Press, 2002, ISBN 0-19-514246-2
- Tonoli, Andrea et al.:** Electromagnetic Shock Absorbers for Automotive Suspensions: Electromechanical Design. In Proceedings of ESDA 2006, 8th Biennial ASME Conference on Engineering Systems Design and Analysis, Torino, Italy. 4–7 July 2006
- Trächtler, Ansgar:** Integrierte Fahrdynamikregelung mit ESP, aktiver Lenkung und aktivem Fahrwerk. at – Automatisierungstechnik, 2005, Nr. 1, pp.11–19 (URL: <http://www.atypon-link.com/OLD/doi/abs/10.1524/auto.53.1.11.56705?cookieSet=1&journalCode=auto>), ISSN 0178-2312

- Valàšek, Michael et al.:** Development of Semi-Active Road-Friendly Truck Suspensions. Pergamon—Control Engineering Practice, June 1998, Nr. 6, pp. 735–744, ISSN 0967–0661/98
- Valàšek, Michael/Novàk, M.:** Ground hook for semi-active damping of truck's suspension. In Proceedings of CTU Workshop 96, Engineering Mechanics, Brno, Czech Republic. January 1996, pp. 467–468
- Valàšek, Michael et al.:** Extended Ground-Hook—New Concept of Semi-Active Control of Trucks Suspension. Vehicle System Dynamics, 1997, Nr. 27, pp. 289–303, ISSN 0042–3114
- Weber, Hubert:** Einführung in die Wahrscheinlichkeitsrechnung und Statistik für Ingenieure. 3. edition. B. G. Teubner Stuttgart, 1992, ISBN 3–5190–2983–9
- Weber, Ingo:** Verbesserungspotenzial von Stabilisierungssystemen im Pkw durch eine Reibwertsensorik. Düsseldorf: VDI Verlag, 2005, Fortschritt-Berichte VDI Reihe 12 592, Dissertation at the Chair of Automotive Engineering at Technische Universität Darmstadt, ISBN 3–18–359212–6
- Winner, Hermann:** Kraftfahrzeuge II. 2006, Lecture notes, Chair of Automotive Engineering at Technische Universität Darmstadt
- Winner, Hermann et al.:** Die Bremse im mechatronischen Fahrwerk. In **Breuer, Bert/Bill, Karlheinz (Eds.):** Bremsenhandbuch. 3. edition. Vieweg Verlag, 2006, ISBN 3–8348–0064–3. – Kapitel 22, pp. 359–372
- Wölfel, Horst Peter:** Maschinendynamik. 1999, Lecture notes, Fachgebiet Maschinendynamik at Technische Universität Darmstadt
- Wolfsried, Stephan/Schiffer, W.:** Active Body Control (ABC) – das neue aktive Federungs- und Dämpfungssystem des CL-Coupés von DaimlerChrysler. In Proceedings of Reifen–Fahrwerk–Fahrbahn 1999, Hannover, Germany. VDI Verlag, Düsseldorf, 21+22 October 1999, VDI-Berichte 1494, ISBN 3–18–091494–7
- Yeh, Edge C./Lu, Shao How:** A Genetic Algorithm Based Fuzzy System for Semi-Active Suspension System Design. In **Jurgen, Ronald K. (Ed.):** Electronic Steering and Suspension Systems. Society of Automotive Engineers, Inc., 1999, SAE Technical Paper Series 94A087, ISBN 0–7680–0481–0, pp. 417–428
- Yi, Kyongsu/Hedrick, Karl J.:** Active and Semi-Active Heavy Truck Suspensions to Reduce Pavement Damage. In Proceedings of Truck and Bus Meeting and Exposition, Charlotte, North Carolina, USA. Society of Automotive Engineers, Inc., 6–9 November 1989, SAE Technical Paper Series 892486 (URL: <http://www.uctc.net/papers/027.pdf>), ISSN 0148–7191, pp. 30–37
- Yi, Kyongsu/Wargelin, Margaret/Hedrick, Karl J.:** Dynamic Tire Force Control by Semi-Active Suspensions. In Proceedings of 1992 ASME Winter Annual Meeting, November, Anaheim, California, USA. ASME, 9–13 November 1992 (URL: <http://www.uctc.net/papers/097.pdf>), pp. 1–31

- Yoshimura, Toshio/Takagi, Atsushi:** Pneumatic Active Suspension System for a One-Wheel Car Model Using Fuzzy Reasoning and a Disturbance Observer. *Journal of Zhejiang University SCIENCE*, 5 2004, Nr. 9, pp.1060–1068 (URL: <http://www.zju.edu.cn/jzus/2004/0409/040907.pdf>), ISSN 1009–3095
- Yu, Fan/Crolla, David A.:** Analysis on Benefits of an Adaptive Kalman Filter Active Vehicle Suspension. In **Jurgen, Ronald K. (Ed.):** *Electronic Steering and Suspension Systems*. Society of Automotive Engineers, Inc., 1998, SAE Technical Paper Series 981120, ISBN 0–7680–0481–0, pp. 269–275
- Zádor, Istvá/Falvy, Bence/Palkovics, László:** Electro-mechanical Suspension Actuator with Energy Recuperative Feature. In *Proceedings of FISITA 2006, World Automotive Congress, Yokohama, Japan. 22–27 October 2006*

Student Research Work Advised

Breitenbücher, Jan: Optimierung eines 2D-Nickmodells zur Abbildung eines ABS-geregelten Bremsvorgangs bei gleichzeitigem Einsatz einer Verstelldämpferregelung (Optimization of a 2D-Pitch Model for Simulation of ABS Controlled Braking with Simultaneous Control of Active Dampers). November 2006, Studienarbeit no.920/06 at the Chair of Automotive Engineering at Technische Universität Darmstadt

Brungs, Felix: Literaturrecherche zum Thema Regelung von Verstelldämpfersystemen (Literature Research Concerning Control Strategies of Active Shock Absorbers). September 2005, Studienarbeit no.885/05 at the Chair of Automotive Engineering at Technische Universität Darmstadt

Cajan, Boris: Aufbau und Parametrisierung eines Simulationsmodells eines BMWs 535i (E39) unter SIMPACK (Design and Parametrization of a Simulation Model of a BMW 535i (E39) with SIMPACK). November 2004, Diplomarbeit no.366/04 at the Chair of Automotive Engineering at Technische Universität Darmstadt

Cruces Vallejo, Pablo: Untersuchungen zur Interaktion von ABS- und Verstelldämpferregelung im Fahrversuch (Investigation of the Interaction of ABS- and Adaptive Damper Control in Test Drives). December 2005, Diplomarbeit no.387/05 at the Chair of Automotive Engineering at Technische Universität Darmstadt, accepted at Universitat Politècnica de Catalunya, Spain

Duddek, Moritz: Implementierung und Untersuchung der sogenannten MiniMax-Strategie zur Regelung von Verstelldämpfern unter realen Fahrbedingungen (Implementation and Investigation of the so called MiniMax-Strategy for the Control of Active Shock Absorbers within Close-to-Reality Test Drives). May 2006, Diplomarbeit no.396/05 at the Chair of Automotive Engineering at Technische Universität Darmstadt

Fuchs, Julian: Ermittlung der Radlast mithilfe serientauglicher Messgrößen (Determination of Wheel Load With Ready for Series Measurands). November 2004, Studienarbeit no.869/04 at the Chair of Automotive Engineering at Technische Universität Darmstadt

Fujara, Marian: Aufbau und Parametrisierung eines Simulationsmodells eines Opel Astra unter Vedyna (Design and Parametrization of a Model of an Opel Astra Within Vedyna). February 2005, Diplomarbeit no.379/04 at the Chair of Automotive Engineering at Technische Universität Darmstadt, accepted at Fachhochschule Dortmund

- Harchut, Frank:** Ermittlung der Bremsenergie am Viertelfahrzeugmodell und im Fahrversuch (Determination of Braking Energy in a Vehicle Model and in On Road Experiments). November 2004, Studienarbeit no.870/04 at the Chair of Automotive Engineering at Technische Universität Darmstadt
- Hemm, Markus:** Erstellen und Implementieren von Regelungskonzepten zur Bremswegverkürzung am 2D-Einspurmodell (Design and Implementation of Control Strategies for Braking Distance Reduction in a 2D-Single-Lane-Model). February 2005, Diplomarbeit no.372/04 at the Chair of Automotive Engineering at Technische Universität Darmstadt
- Huckauf, Felix:** Konzeption und Aufbau eines Bremsautomaten für Fahrversuche zur Verstelldämpferregelung (Design and Implementation of a Braking Machine). June 2005, Studienarbeit no. 880/04 at the Chair of Automotive Engineering at Technische Universität Darmstadt
- Koenen, Jan:** Modellidentifikation und Untersuchung der Regelstrecke in ABS-geregelten Fahrversuchen in Kombination mit einer semi-aktiven Radaufhängung (Model Identification and Investigation of the Control Path in ABS-Controlled Road Trials in Combination with Semi-Active Suspension). November 2005, Studienarbeit no.890/05 at the Chair of Automotive Engineering at Technische Universität Darmstadt
- Krpo, Kenan:** Untersuchungen zur Auswirkung des Umschaltvorgangs von Verstelldämpfern auf die Radlast und den Schlupf in gebremsten Fahrversuchen (Experimental Braking Testing to Determine the Influence of Switching of Active Dampers on Wheel Load and Slip). March 2006, Studienarbeit no.906/05 at the Chair of Automotive Engineering at Technische Universität Darmstadt
- Laketic, Radoica:** Implementierung und Untersuchung der sogenannten MiniMax-Strategie zur Regelung von Verstelldämpfern unter realen Fahrbedingungen (Implementation and Investigation of the so called MiniMax-Strategy for the Control of Active Shock Absorbers within Close-to-Reality Test Drives). June 2006, Master's Thesis no.397/05 at the Chair of Automotive Engineering at Technische Universität Darmstadt
- Luft, Mirko:** Konzeption und Durchführung von Fahrversuchen zur Validierung eines 2D-Einspurmodells (Conception and Execution of Experiments to Validate a 2D-Pitch Model). July 2004, Studienarbeit no. 864/04 at the Chair of Automotive Engineering at Technische Universität Darmstadt
- Matl, Matthias:** Untersuchung zum Zeitverzug in Regelkreisen zur Verringerung der Radlastschwankung und Erhöhung der Bremskraft im Fahrbetrieb durch Verstelldämpfer (Investigation on Time Delays in Control Circuits to Reduce the Oscillation of Wheel Force and to Increase the Brake Force by Adaptive Dampers). December 2005, Diplomarbeit no. 393/05 at the Chair of Automotive Engineering at Technische Universität Darmstadt
- Puff, Matthias:** Auswahl, Aufbau und Inbetriebnahme eines Messsystems zur Regelung adaptiver Verstelldämpfer im Pkw (Election, Assembling and Initial Operation of a

Measuring System for Automatic Control of Adaptive Shock Absorber Systems in Passenger Cars). February 2005, Studienarbeit no. 872/04 at the Chair of Automotive Engineering at Technische Universität Darmstadt

Redelbach, Martin: Konzeption, Planung und Durchführung von Experimenten zur Validierung eines 2D-Nickmodells eines Pkws (Conception, Planning and Execution of Experiments to Validate a 2D-Pitch Model of a Car). November 2006, Studienarbeit no. 921/06 at the Chair of Automotive Engineering at Technische Universität Darmstadt

Reinhard, Björn-Hendrick: Modellidentifikation und Bewertung ausgewählter Regelstrategien zur Beeinflussung der Radlastschwankung im Prüfstands- und Fahrversuch (Model Identification and Benchmarking of Selected Control Strategies for Wheel Load Impact on a Test Stand and in Road Trials). July 2005, Diplomarbeit no. 382/04 at the Chair of Automotive Engineering at Technische Universität Darmstadt

Ruiz Ortega, Manuel: Entwicklung und Implementierung einer Strategie zur Regelung von Verstelldämpfern mit dem Ziel der Bremswegverkürzung (Design and Implementation of a Control Strategy for Active Damper to Shorten the Braking Distance). December 2006, Diplomarbeit no. 407/06 at the Chair of Automotive Engineering at Technische Universität Darmstadt

Schramm, Thomas: Klassifizierung von Straßenabschnitten anhand des Höhenprofils der Fahrbahnoberfläche (Classification of Roads on Basis of the Vertical Pavement Profile). April 2005, Studienarbeit no. 878/04 at the Chair of Automotive Engineering at Technische Universität Darmstadt

Vulpius, Andreas: Potentialabschätzung zur Bremskrafteerhöhung mittels des Selbstpumpereffekts von Verstelldämpfern (Estimation of the Potential to Increase the Braking Force by Taking Advantage of the Self Pumping Effect of Adaptive Dampers). January 2006, Studienarbeit no. 901/05 at the Chair of Automotive Engineering at Technische Universität Darmstadt

Wejwoda, Matthias: Entwicklung und Validierung eines Verfahrens zur fahrzeugautonomen Bestimmung des Höhenprofils realer Fahrbahnoberflächen (Development and Validation of a Procedure for the Vehicle-Autonomous Determination of the Vertical Pavement Profile). April 2005, Studienarbeit no. 879/04 at the Chair of Automotive Engineering at Technische Universität Darmstadt

Wolf, Daniel: Implementierung von Regelstrategien zur Bremswegverkürzung durch Verstelldämpfersysteme (Implementation of Control Strategies to Combine Braking and Adaptive Damping Systems Heading to a Reduced Braking Distance). June 2005, Diplomarbeit no. 376/04 at the Chair of Automotive Engineering at Technische Universität Darmstadt, research work executed at BMW AG, Munich

Own Publications

- Niemz, Tobias et al.:** Die Bremse im mechatronischen Fahrwerk. In **Breuer, Bert/Bill, Karlheinz (Eds.):** Bremsenhandbuch. 3. edition. Vieweg Verlag, 2006, ISBN 3-8348-0064-3.– Kapitel 22, pp.359–372
- Niemz, Tobias et al.:** Verbesserung des Bremsverhaltens von Pkw durch Einsatz variabler Dämpfer. In Proceedings of chassis.tech 2007, Garching, Germany. TÜV SÜD Automotive GmbH, 1+2 March 2007
- Niemz, Tobias et al.:** QUADS – Verkehrssicherheitsaspekte einer neuen Fahrzeugart. In Proceedings of 33. Kongress der Deutschen Gesellschaft für Verkehrsmedizin e.V., Bonn, Germany. Wirtschaftsverlag NW, Verlag für neue Wissenschaft GmbH, 10–12 March 2005, BASt-Bericht M 171
- Niemz, Tobias/Winner, Hermann:** Bremswegverkürzung durch dynamische Dämpferregelung. In Proceedings of Reifen–Fahrwerk–Fahrbahn 2005, Hannover, Germany. VDI Verlag, Düsseldorf, 25+26 October 2005, VDI-Berichte 1912, ISBN 3-18-091912-4, pp. 181–197
- Niemz, Tobias/Winner, Hermann:** Reducing RMS on Wheel Load in ABS-braking Situations by Control of Semi-active Suspension. In Proceedings of ESDA 2006, 8th Biennial ASME Conference on Engineering Systems Design and Analysis, Torino, Italy. 4–7 July 2006a
- Niemz, Tobias/Winner, Hermann:** Reduction of Braking Distance by Control of Active Dampers. In Proceedings of FISITA 2006, World Automotive Congress, Yokohama, Japan. 22–27 October 2006b
- Niemz, Tobias/Winner, Hermann:** Improving Braking Performance by Control of Semi-Active Suspension. In Proceedings of EAEC 2007, 11th European Automotive Congress, Budapest, Hungary. The Scientific Society of Mechanical Engineers (GTE), 30 May – 1 June 2007

Lebenslauf

Persönliche Daten

Name: Sebastian Tobias Niemz
Geburtsdatum: 2. November 1976
Geburtsort: Frankfurt am Main
Familienstand: ledig
Staatsangehörigkeit: deutsch

Schulzeit

09/1986 – 06/1995 Altsprachliches Rudi-Stephan-Gymnasium, Worms
Leistungskurse: Gemeinschaftskunde, Mathematik, Physik
Abschluß: Allgemeine Hochschulreife am 19. Juni 1995

Zivildienst

08/1995 – 08/1996 Deutsches Rotes Kreuz, Worms
Ausbildung zum Rettungssanitäter, anschließend
tätig im Krankentransport und Rettungsdienst

Studium

10/1996 – 09/1997 Johannes Gutenberg-Universität, Mainz
Studium der Physik
10/1997 – 03/2003 Technische Universität Darmstadt
Studium des Allgemeinen Maschinenbaus
Abschluß: Diplom-Ingenieur am 31. Januar 2003
08/2000 – 05/2001 University of California at Berkeley, USA
Auslandsstudium
08/2002 – 01/2003 University of California at Berkeley, USA
Auslandsstudium und Anfertigung der Diplomarbeit
Betreuer: Prof. Benson H. Tongue
10/2003 – heute FernUniversität in Hagen
Zweitstudium der Volkswirtschaftslehre
Vordiplom: 30. September 2005

Berufstätigkeit

03/2003 – 08/2003 Technische Universität München, Garching
Wissenschaftlicher Mitarbeiter am Lehrstuhl für
Angewandte Mechanik bei Prof. Heinz Ulbrich
11/2003 – 12/2006 Technische Universität Darmstadt
Wissenschaftlicher Mitarbeiter am Fachgebiet
Fahrzeugtechnik bei Prof. Hermann Winner